NEBC
LITHIUM - FORMATION WATER DATABASE

Geoscience BC Report 2024-03

February 2024
Canadian Discovery Ltd.

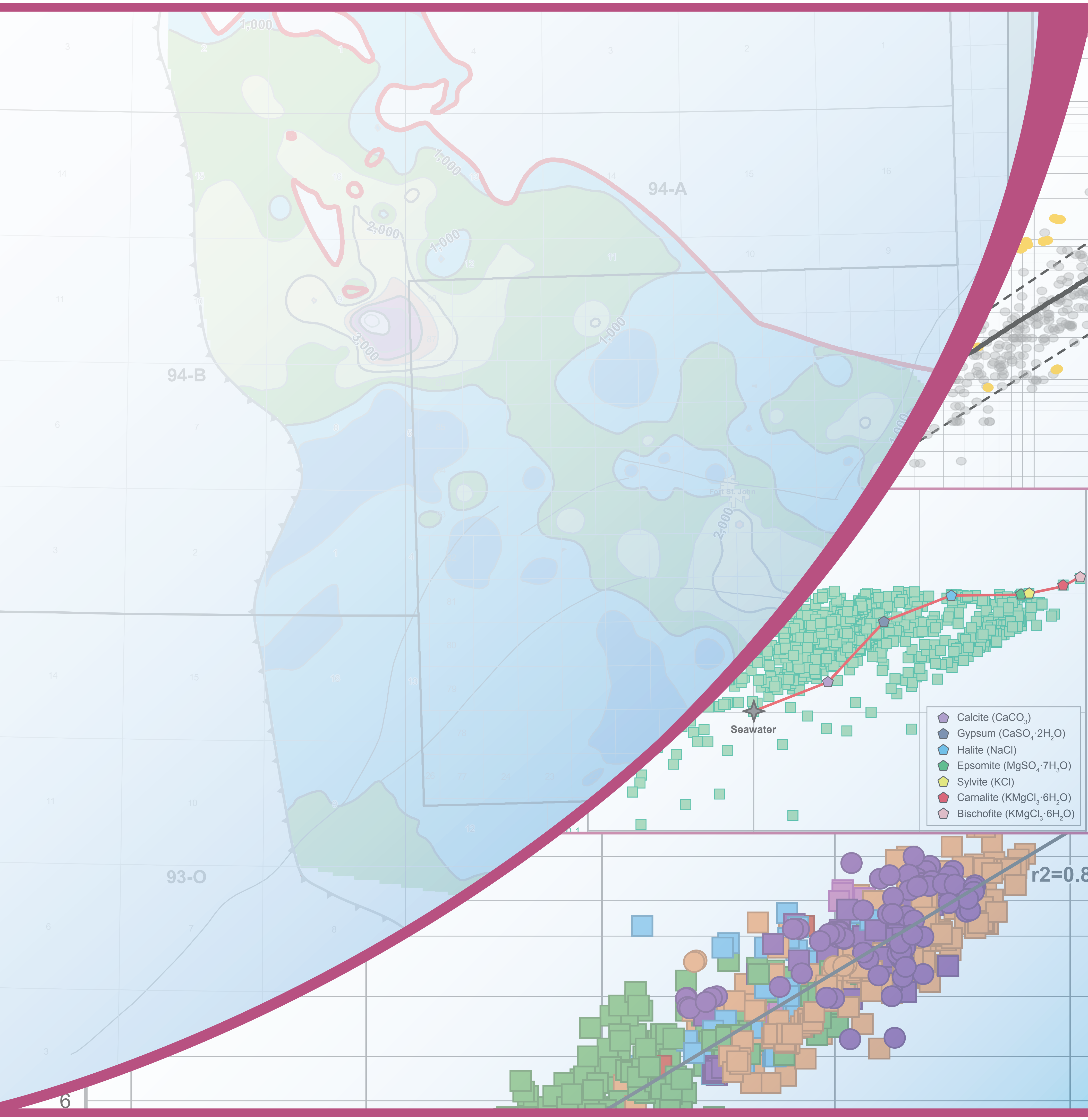

Geoscience BC
NORTHERN DEVELOPMENT
Matrix Solutions Inc. A Montrose Environmental Company
Canada
Natural Resources Canada • Geological Survey of Canada
Ressources naturelles Canada • Commission géologique du Canada
Canadian Discovery Ltd.

NEBC LITHIUM FORMATION WATER DATABASE

Canadian Discovery Ltd.

FEBRUARY 2024

PREPARED FOR:
Geoscience BC

PREPARED BY:
Canadian Discovery Ltd.
APEGA Permit No. P09364

Kaush Rakhit, MSc, P. Geol
Executive Chairman and Principal Author

MATTHEW SCORAH
ID 88726

Matthew Scorah

Matthew Scorah, PhD, P. Eng
Vice President Decarbonization

MERIDEE FOCKLER

Meridee Fockler

Meridee Fockler, P.Geol.
Technical Analysis Director

Marielle Hopf

Marielle Hopf, P. Geo
Geologist

Tessa Wilson, M.Sc., P.Geo
Geologist

PERMIT TO PRACTICE
CANADIAN DISCOVERY LTD.
RM SIGNATURE: Matthew Scorah
RM APEGA ID #: 88726
DATE: February 2, 2024
PERMIT NUMBER: P009364
The Association of Professional Engineers and Geoscientists of Alberta (APEGA)

COPYRIGHT AND DISCLAIMER

TABLE OF CONTENTS

Table of Contents

Appendices

Tables

Figures

List of figures available in *Appendix G*

NEBC Lithium Formation Water Database

EXECUTIVE SUMMARY

Introduction

Lithium is a vital mineral for the energy transition and the development of a low carbon economy. The Canadian government has identified lithium as a critical mineral, essential for energy storage and Electric Vehicle (EV) batteries along with uses in defence and security, consumer electronics, critical infrastructure and medical applications. The International Energy Agency (IEA) projects a seven-fold increase in lithium demand from 2021 to 2030 to achieve its net zero scenario (IEA, 2023). Presently, over 75% of the world's lithium production comes from Australia and Chile, with Chile holding the largest reserves in the world with 9.3 million tonnes of lithium (USGS, 2023). Natural Resources Canada reports that as of 2022, Canada produced 500 tonnes of lithium (0.4% of world supply) and has 3.6% of the world's reserves (Natural Resources Canada, 2023).

Traditional lithium extraction techniques include hard rock mining, including both surface (open-pit) or subsurface (underground) methods, and evaporative brine processing whereby the lithium is concentrated and extracted from brines using vast ponds in hot, arid climates. These methods encounter a number of challenges such as long project lead times, poor recovery rates, environmental sensitivity and geographic concentration. This has led to the evaluation of additional sources such as volcanic sediments, geothermal brines and deep saline brines. Along with the evaluation of these relatively novel sources, new extraction techniques are being developed to ensure efficient and economic recovery. The rapid development of direct lithium extraction (DLE) technologies has opened a vast, scalable and sustainable resource by extracting lithium from deep saline brines.

For context, preliminary economic assessments of the Clearwater and Sturgeon Lake lithium brine projects in Alberta (Devonian Leduc Formation) that will employ DLE have defined substantial lithium brine resources. As the developers advance these projects, these resources (or a portion thereof) could be classified as a reserve. It is important to note that a reserve is the economically mineable part of a resource taking into consideration all of the project elements (location, quantity, grade, geological characterization, etc.) as defined by the Canadian Institute of Mining, Metallurgy and Petroleum (CIM). World reserves of lithium are estimated to be approximately 26 million tonnes of lithium, while world resources, not necessarily economically viable for extraction, total 98 million tonnes of lithium. The potential scale of lithium resources within underground brines in Western Canada can be put into context when looking at E3 Lithium's Clearwater project, which currently estimates a resource of roughly 16 million tonnes of lithium carbonate equivalent (LCE) (E3 Lithium, 2023).

Given the potential for lithium resources in Western Canada, Geoscience BC and the Northern Development Initiatives Trust (NDIT) engaged Canadian Discovery Ltd. (CDL) in 2021 to identify the in situ lithium concentrations and resource potential of deep saline brines in northeast British Columbia (NEBC). The study findings would serve as a means to inform a variety of organizations and stakeholders ranging from governments looking to develop policy and regulations in the natural resource sector to Indigenous groups, local communities and private companies considering the viability of lithium extraction from deep saline brines in NEBC *(figure 1.1)*. Extracting lithium from deep saline brines provides British Columbia (BC) with an opportunity to use its extensive oil and gas industry knowledge, data and highly skilled workforce to produce this critical mineral.

The NEBC Lithium Project

A first of its kind in BC, this study extends the understanding of lithium resources of the Western Canada Sedimentary Basin from Alberta and Saskatchewan, where substantial public data and research are already available. The study was conducted in three phases:

Phase 1: initial sample collection where operators in NEBC were asked to provide water (brine) samples from currently producing oil and gas operations.

Phase 2: laboratory analysis of the brine samples for a full suite of physical and chemical parameters to produce a preliminary brine characterization dataset including metals.

Phase 3: integration and reporting of the analyzed data with water chemistry from existing datasets, the reservoir and physical geology of NEBC and published literature on the controls and distribution of lithium in saline brines.

Project Outcomes

A total of 133 samples were obtained in NEBC through the sampling program, of which 95 were unique, the remainder being test blanks and duplicates for quality and assurance. These 95 samples were supplemented by 229 samples made available from the Geological Survey of Canada. The report also relied on data from over 2,000 samples available in Alberta through the Alberta Geological Survey, Geological Survey of Canada and other sources. These combined datasets were analyzed to aid in the understanding of lithium concentrations and controls by stratigraphic zones, lithology, geography and basin evolution. The observed lithium concentration in NEBC ranges from negligible up to 100 milligrams per Litre (mg/L). Of the 362 available samples, 272 were from the Triassic Montney Formation (Montney). The poor data control in other horizons of potential interest did not provide the confidence to calculate an in situ lithium resource.

The sample data from the Montney, along with detailed geologic mapping provided by CDL, allowed the determination of an in situ lithium resource based on an estimate of the total water saturated pore volume, interpolation of the sampled lithium concentrations and other indicative data *(figure 1.2)*.

Lithium concentrations exceeding 50 mg/L are currently deemed as economically interesting by industry given the current advancements in DLE technology. Within the Montney, CDL estimates an in situ LCE resource of 9.8 million tonnes with an average concentration of 56 mg/L over an area of 32,000 km^2. The Montney within this area is a low porosity, low permeability, gas-bearing reservoir that has water saturations ranging from less than 10 to 45%.

This estimate of an in situ lithium resource within the Montney must be viewed in the appropriate context. It is widely accepted that the Montney will be the major source of natural gas in NEBC and will supply both domestic and export consumption, including LNG, for decades of future development. Due to the unconventional characteristics of the Montney reservoir, it is not economically and physically feasible to exploit for lithium brines on a standalone basis. In practical terms, lithium in brines is co-produced as a by-product of natural gas production that requires the injection of hydraulic fracturing (frac) fluids that interact with formation waters and minerals to create lithium-enriched fluids, which include the original frac fluids and producible formation fluids (brines). As such, economic lithium extraction from the Montney requires identification of areas with sufficient and sustainable fluid production (after the initial frac fluids have been produced) along with existing fluid gathering systems to economically deploy DLE technologies and infrastructure. Areas with sufficient and sustainable fluid production will reduce the risks associated with the long-term production needed to ensure a project is viable while existing fluid gathering systems will help to reduce project capital costs.

This study highlights data from areas in the Montney currently being developed and provides the fluid production data of the aggregate produced water. As an example, a gathering system producing 30,000 m^3/month of water is estimated to yield up to 86 tonnes of LCE per year based on an average lithium concentration of 56 mg/L.

Unknown Factors

The study findings are preliminary as many unknown factors remain and further investigation is recommended, including:

1. Lithium distribution in under-sampled geologic units. To further investigate this unknown factor, CDL conducted extensive multi-variate analysis of fluid composition, whole rock geochemistry and basin history. A simple and useful observation was that the majority of lithium concentrations in excess of 30 mg/L occurred when formation waters had total dissolved solids (TDS) greater than 150,000 mg/L. Based on TDS mapping used as a proxy for estimating potential lithium concentration, the project identified a number of areas and geologic horizons, such as the Devonian Keg River and Slave Point formations, the Permian Belloy Formation and Triassic Halfway and Charlie Lake formations, as zones of interest where further sampling should be conducted *(figure 1.2)*.
2. *Montney investigation*. Additional investigation is needed in the Montney to reduce the risks associated with lithium production and ensure a project's viability. Future work should focus on determining in what state the lithium occurs within the Montney and also the physical processes that lead to produced water enrichment (diffusion, water-rock interaction, free formation water flow) as well as an understanding of the primary lithium sources.
3. *Existing and future infrastructure*. As brine and, in turn, lithium are by-products of oil and gas production in NEBC, the long-term infrastructure and gathering system footprint will influence the potential for lithium production in the area. A forecast of development activities in the Montney as a gas resource will assist in determining the longevity of lithium as a co-produced by-product.

Further understanding of points 2 and 3 above is critical for moving from an in situ resource definition (similar to an original gas-in-place or OGIP calculation for gas resources) to a more defined resource estimate that will help to inform all stakeholders of lithium production in BC.

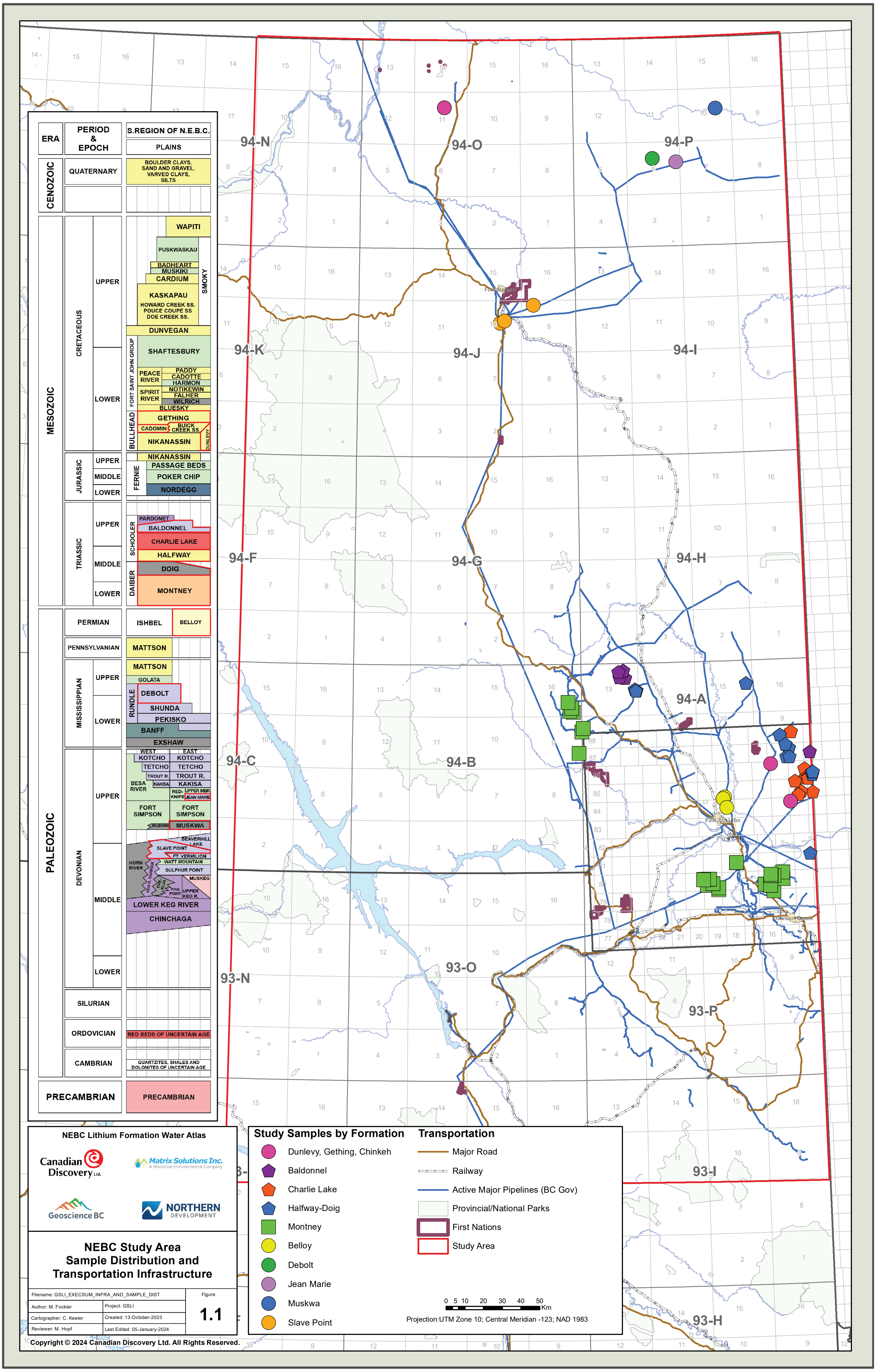

© Canadian Discovery Ltd.

Figure 1.1

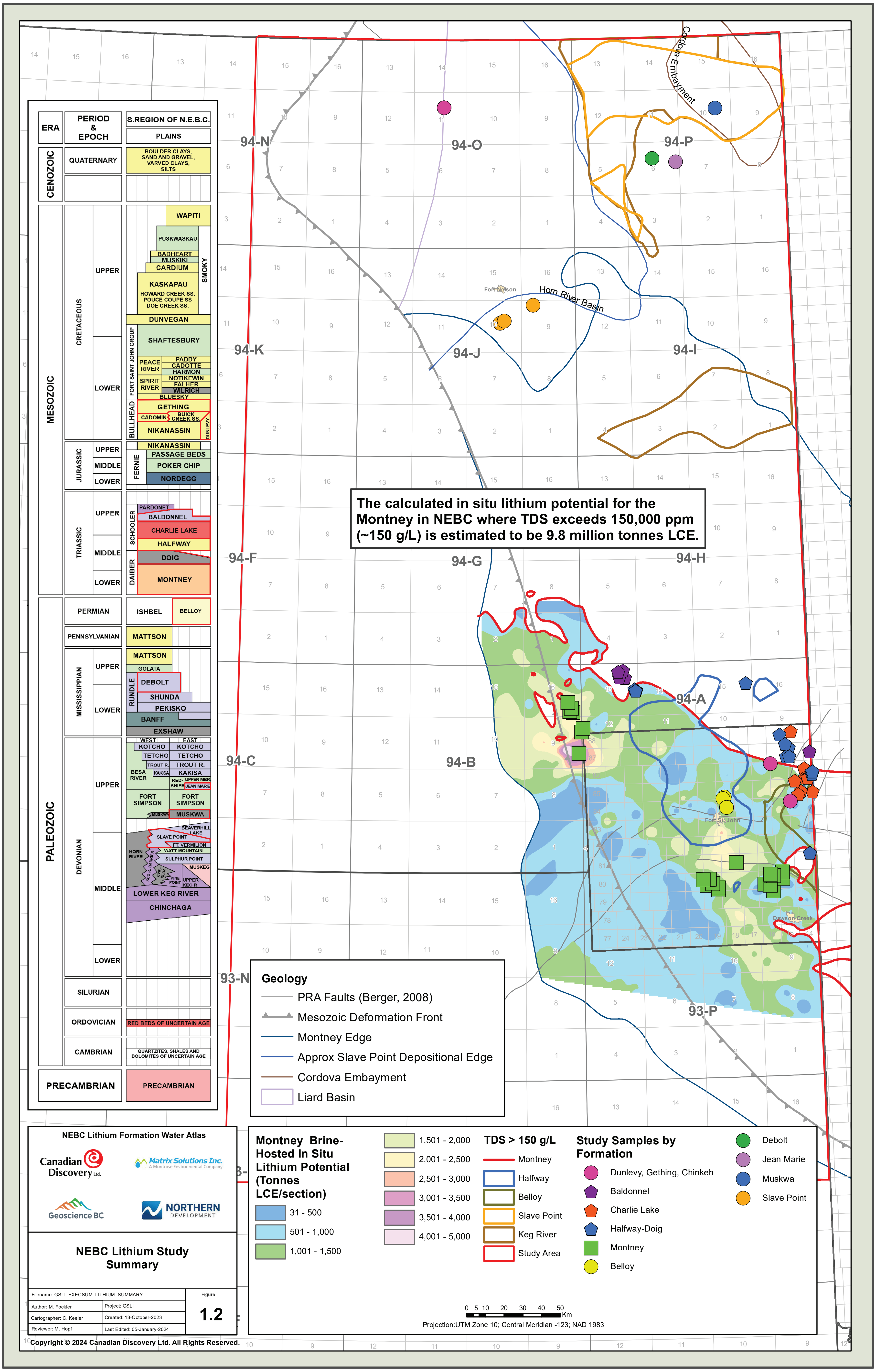

The calculated in situ lithium potential for the Montney in NEBC where TDS exceeds 150,000 ppm (~150 g/L) is estimated to be 9.8 million tonnes LCE.

© Canadian Discovery Ltd.

Figure 1.2

Acknowledgements

The project partners acknowledge that this research concerns the territory of the Treaty 8 First Nations of British Columbia. We encourage anyone considering new development or activities in their territories to engage early and engage often with appropriate Indigenous groups. The Province of British Columbia's Consultative Areas Database can be used to identify potentially impacted First Nations and their respective contacts.
(https://www2.gov.bc.ca/gov/content/data/geographic-data-services/land-use/contacts-for-first-nation-consultation-areas)

The principal author would like to thank Canadian Discovery Ltd. for its in-kind funding contribution to get this complex project over the finish line. Canadian Discovery Ltd. and Matrix Solutions thank the project partners for their support of this project, including Geoscience BC, Natural Resources Canada, LithiumBank Resources, and Northern Development Initiatives Trust. Geoscience BC is grateful to the Province of British Columbia and Northern Development for funding this project. This study had a Project Advisory Committee facilitated by Randy Hughes of Geoscience BC, and the project partners extend a sincere thank you to the anonymous peer reviewers and the following committee members for their time and valuable input.

Project Advisory Committee

Daniel Alessi	University of Alberta (Chair)
Sobhi Alhashwa	Ovintiv
Colin Frostad	Tourmaline
Eric Munson	Shell (Vice-Chair)

Canadian Discovery Ltd would like to thank the following contributors to this study:

Kaush Rakhit, MSc, P. Geol.	Executive Chairman and Principal Author
Christa Williams, P. Geol.	Vice President Business Development
Matthew Scorah, PhD, P. Eng.	Vice President Decarbonization
Meridee Fockler, P. Geol.	Senior Geologist and GIS Analyst
Allison Gibbs, P. Geol.	Senior Hydrodynamicist
David Murfitt, M.Env., P.Geo.	Senior Hydrogeologist
Eric Pelletier M.Sc. P.Geo.	Geologist
Marielle Hopf, P. Geo.	Geologist
Tessa Wilson, MSc. P. Geo.	Geologist
Paul Patton	Senior Graphic Designer
Candace Keeler	Cartographer and GIS Analyst

References

- E3 Lithium, 2023. 43-101 Technical Report: Lithium Resource Estimate, Bashaw District Project, Central Alberta (effective date March 21, 2023).

- IEA, 2023. Total demand for lithium by end use in the Net Zero Scenario, 2021-2050. https://www.iea.org/data-and-statistics/charts/total-demand-for-lithium-by-end-use-in-the-net-zero-scenario-2021-2050

- LithiumBank, 2023. LithiumBank Reports US$2.7 Billion Pre Tax NPV From Preliminary Economic Assessment on a 31,350 TPA LHM Operation at Boardwalk Lithium Brine Project, Alberta, Canada. https://www.lithiumbank.ca/news/2023/ithiumankeports27illionreaxromrelimin20230525071202#:~:text=The%20Li%2Dbrine%20resources%20were,resource%20has%20units%20of%20grams.

- Natural Resources Canada, 2023. https://natural-resources.canada.ca/our-natural-resources/minerals-mining/mining-data-statistics-and-analysis/minerals-metals-facts/lithium-facts/24009

- Standard Lithium, 2021. Standard Lithium Announces Positive Preliminary Economic Assessment and Update of Inferred Mineral Resource at South-West Arkansas Lithium Project. https://www.standardlithium.com/investors/news-events/press-releases/detail/99/standard-lithium-announces-positive-preliminary-economic

- U.S. Geological Survey. Mineral commodity summaries 2023: U.S. Geological Survey, 112 p. https://pubs.usgs.gov/periodicals/mcs2023/mcs2023.pdf

LITHIUM OVERVIEW

Lithium Overview Introduction

On December 12, 2015, 196 Parties at the UN Climate Change Conference in Paris, France signed the Paris Agreement. This legally binding agreement aims to limit the global temperature increase by 1.5°C above pre-industrial levels. To achieve this goal, anthropogenic greenhouse gas (GHG) emissions, the cause of a significant part of this temperature increase, must be reduced by 43% within 15 years (United Nations, 2023).This is a significant decrease over a short time span and requires both economic and social reforms to succeed. Canada set a Net-Zero Emissions Accountability Act law on June 29, 2021, which legislates Canada's commitment to achieving net-zero emissions by 2050 (Government of Canada, 2023). The 2030 Emissions Reduction Plan (2022) provides a guide on how Canada will meet the Paris and Net-Zero targets. These targets and agreements have sparked a new age of low-carbon intensity technologies and products. This trend is most evident within the power and transportation sector where the use of rechargeable lithium-ion batteries can play a significant role in reducing greenhouse gas emissions.

Lithium production worldwide rose approximately 25% yearly from 2015 to 2022 to meet increasing demand, primarily from the growing electric vehicle (EV) automotive industry *(table 2.1 and figures 2.1 and 2.2)* (USGS, 2023). EVs use lithium-ion batteries, which charge faster, last longer, and have a higher power density than traditional lead-acid batteries. As lithium demand continues to increase, the search continues for stable and reliable sources of this commodity. Western Canada has an important role to play in meeting that demand as lithium is available in the Western Canada Sedimentary Basin (WCSB). Here, a growing number of subsurface operators are diversifying and pursuing commodities such as lithium, which has been identified as one of Canada's 31 critical minerals *(figure 2.3)* and is available in the Western Canada Sedimentary Basin (WCSB). The recovery of lithium from oilfield brines in the WCSB has the potential to help meet the increasing demand for this unique metal (Donaldson, 2022).

Table 2.1: International Lithium Production

	Production (tonnes)							
Country	**2015**	**2016**	**2017**	**2018**	**2019**	**2020**	**2021**	**2022**
Argentina	3,600	5,800	5,700	6,400	6,300	5,900	5,970	6,200
Australia	14,100	14,000	40,000	58,800	45,000	39,700	55,300	61,000
Brazil	200	200	200	300	2,400	1,420	1,700	2,200
Canada	-	-	-	2,400	200	-	-	500
Chile	10,500	14,300	14,200	17,000	19,300	21,500	28,300	39,000
China	2,000	2,300	6,800	7,100	10,800	13,300	14,000	19,000
Portugal	200	400	800	800	900	348	900	600
Zimbabwe	900	1,000	800	1,600	1,200	417	710	800
Other countries	-	-	500	600	-	-	120	700
World total	**31,500**	**38,000**	**69,000**	**95,000**	**86,000**	**82,500**	**107,000**	**130,000**

US lithium production withheld to avoid disclosing company proprietary data. 2022 figures are estimated. World totals are rounded.

Source: USGC, 2023. https://pubs.usgs.gov/periodicals/mcs2023/mcs2023.pdf.

Table 2.1

2.1 World Lithium Production

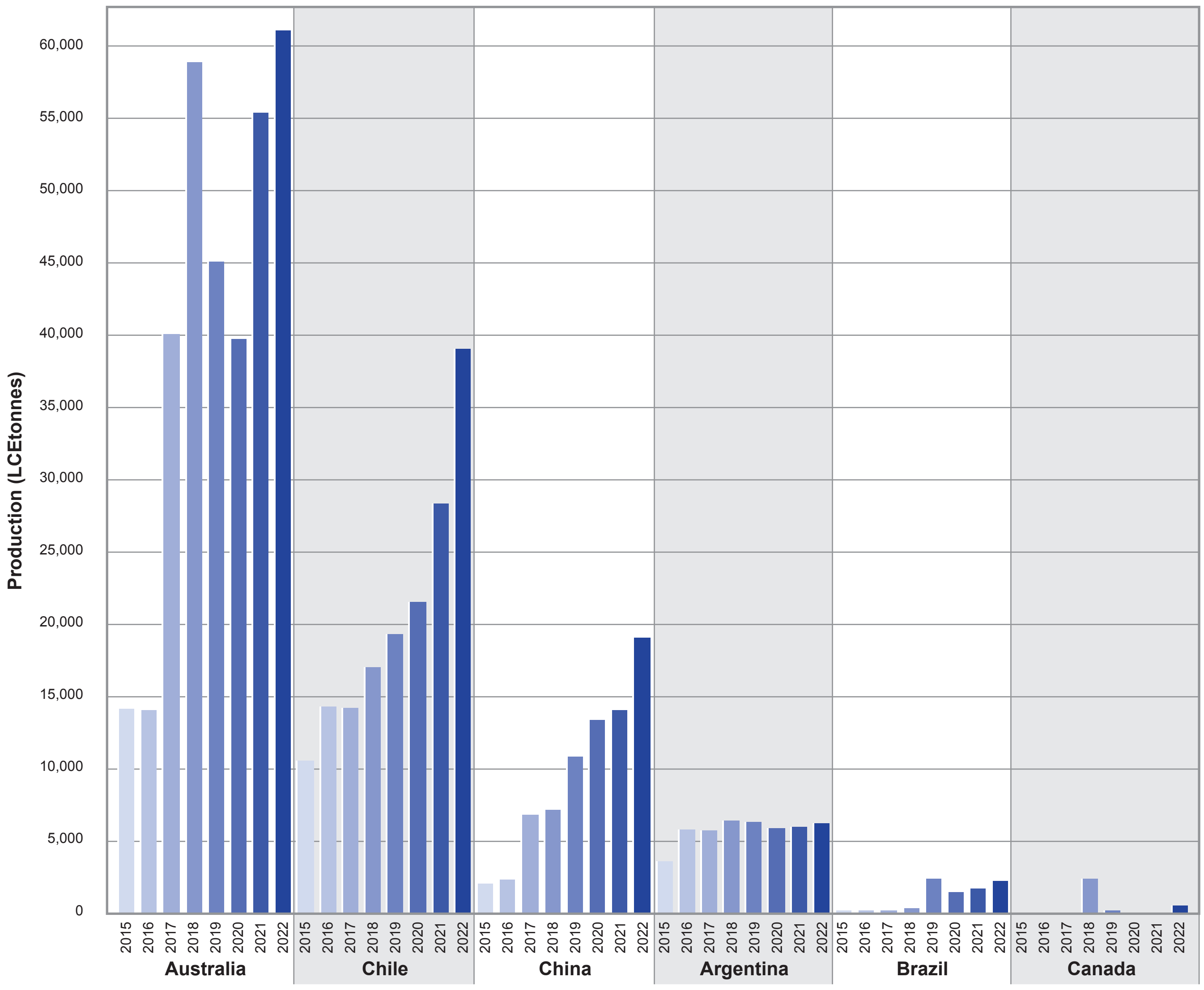

Source: *https://pubs.usgs.gov/periodicals/mcs2022/mcs2022.pdf*

© Canadian Discovery Ltd.

Figure 2.1

2.2 2022 Global Lithium End Use Markets

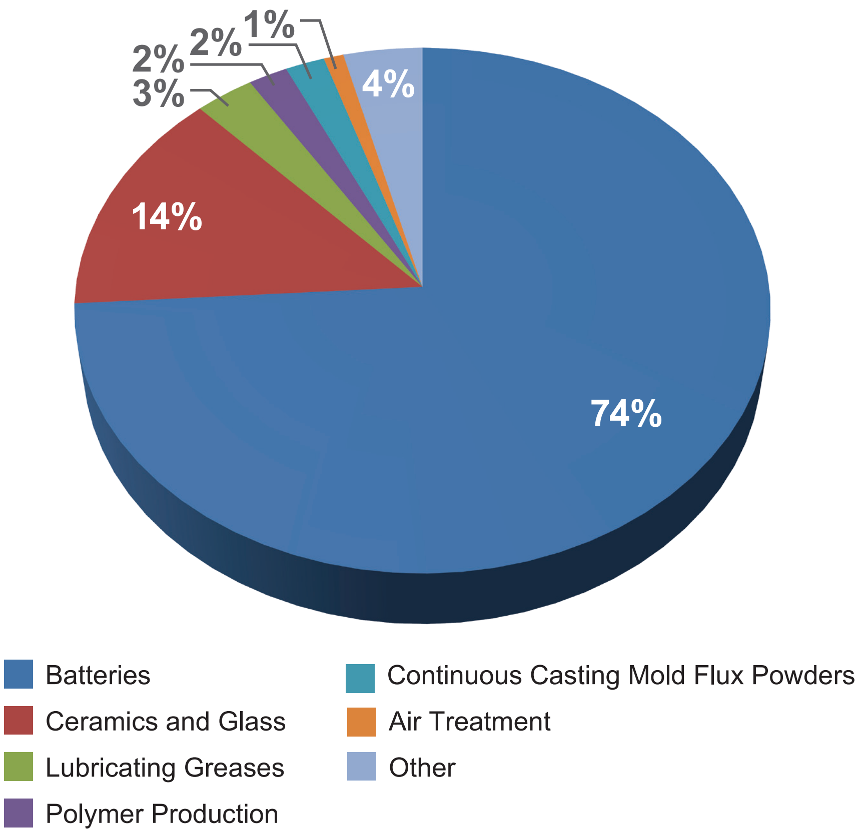

Lithium Global End Use Markets (%)	2018	2022	Difference
Batteries	46	74	28
Ceramics and Glass	27	14	-13
Lubricating Greases	7	3	-4
Polymer Production	5	2	-3
Continuous Casting Mold Flux Powders	4	2	-2
Air Treatment	2	1	-1
Other	9	4	-5

Source: *https://pubs.usgs.gov/periodicals/mcs2023/mcs2023.pdf*

© Canadian Discovery Ltd.

Figure 2.2

2.3 Canada's Critical Minerals

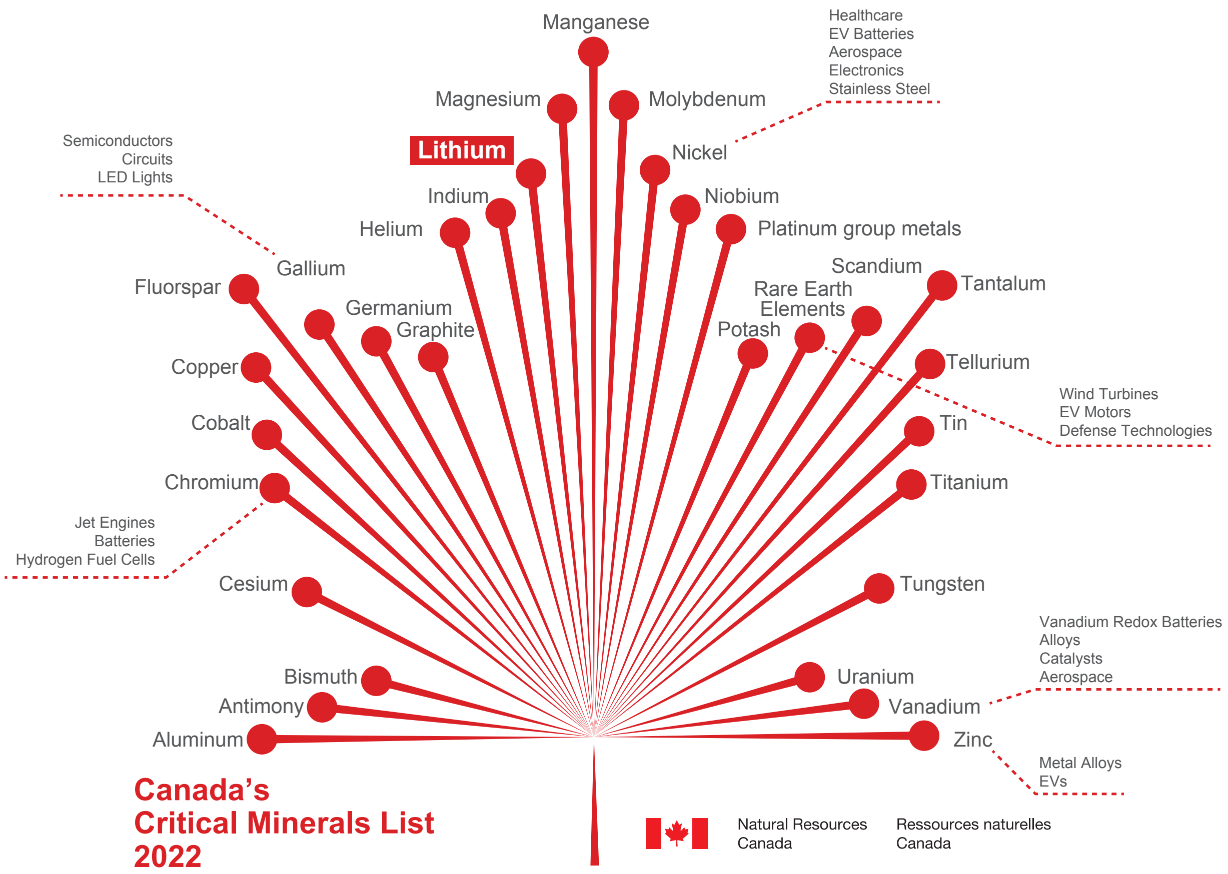

Modified from Government of Canada, 2022

© Canadian Discovery Ltd. *Figure 2.3*

Critical Minerals Defined

On March 11, 2021, Canada unveiled its Critical Minerals List comprising 31 minerals and metals, including lithium *(figure 2.3)*. Canada already produces 21 of these 31 critical minerals, with the potential for further resource development. These minerals are essential to the green and digital economies with the following general uses:

- Renewable energy production and storage
- EV batteries and motors
- Defence and security technologies
- Consumer electronics
- Critical infrastructure
- Medical applications

By building stable and reliable critical mineral supply chains, Canada can help supply its needs and that of the world with responsibly sourced products and help mitigate the risk of global supply chain disruption.

Lithium: An Interesting Element

Lithium, which is the third element on the periodic table, is classified as an alkali metal. A good conductor of heat and electricity, lithium has the highest heat capacity of any solid. It is also lightweight, with the lowest density of all the solid elements (roughly half the density of water at atmospheric conditions).

These unique properties make lithium, along with its compounds lithium hydroxide and lithium carbonate, integral to multiple industrial applications, including use in both lithium (disposable) and lithium-ion (rechargeable) batteries; in the manufacture of heat-resistant glass and ceramics; as grease lubricants; in polymer production; and as flux additives used in iron, steel, and aluminum production.

Table 2.2: Estimated Lithium Reserves and Resources

	Reserves (tonnes)	Identified Resources (tonnes)
Bolivia	-	21,000,000
Argentina	2,700,000	20,000,000
Australia	6,200,000	7,900,000
Brazil	250,000	730,000
Canada	930,000	2,900,000
Chile	9,300,000	11,000,000
China	2,000,000	6,800,000
Portugal	60,000	270,000
Zimbabwe	310,000	690,000
US	1,000,000	12,000,000
Other countries	3,300,000	14,710,000
World total	**26,050,000**	**98,000,000**

Source: USGC, 2023. https://pubs.usgs.gov/periodicals/mcs2023/mcs2023.pdf

© Canadian Discovery Ltd. *Table 2.2*

These uses consume more than 93% of current global lithium production (USGS, 2023) *(figure 2.2)*. Since there are a wide variety of lithium compounds, it is commonplace to refer to lithium content in terms of lithium carbonate equivalent (LCE) (European Lithium, 2023).

As shown in *figure 2.4* and summarized in *table 2.2*, the countries with the largest lithium resources are Bolivia, Argentina, U.S., Australia, and Chile (USGS, 2023) when considering all identified resources including brines, clays, and hard rock ores. The top five lithium producing countries are Australia, Chile, China, Argentina, and Brazil. It is important to note that U.S. production is not reported by the USGS to avoid disclosing company proprietary data.

2.4 International Lithium Production and Reserves

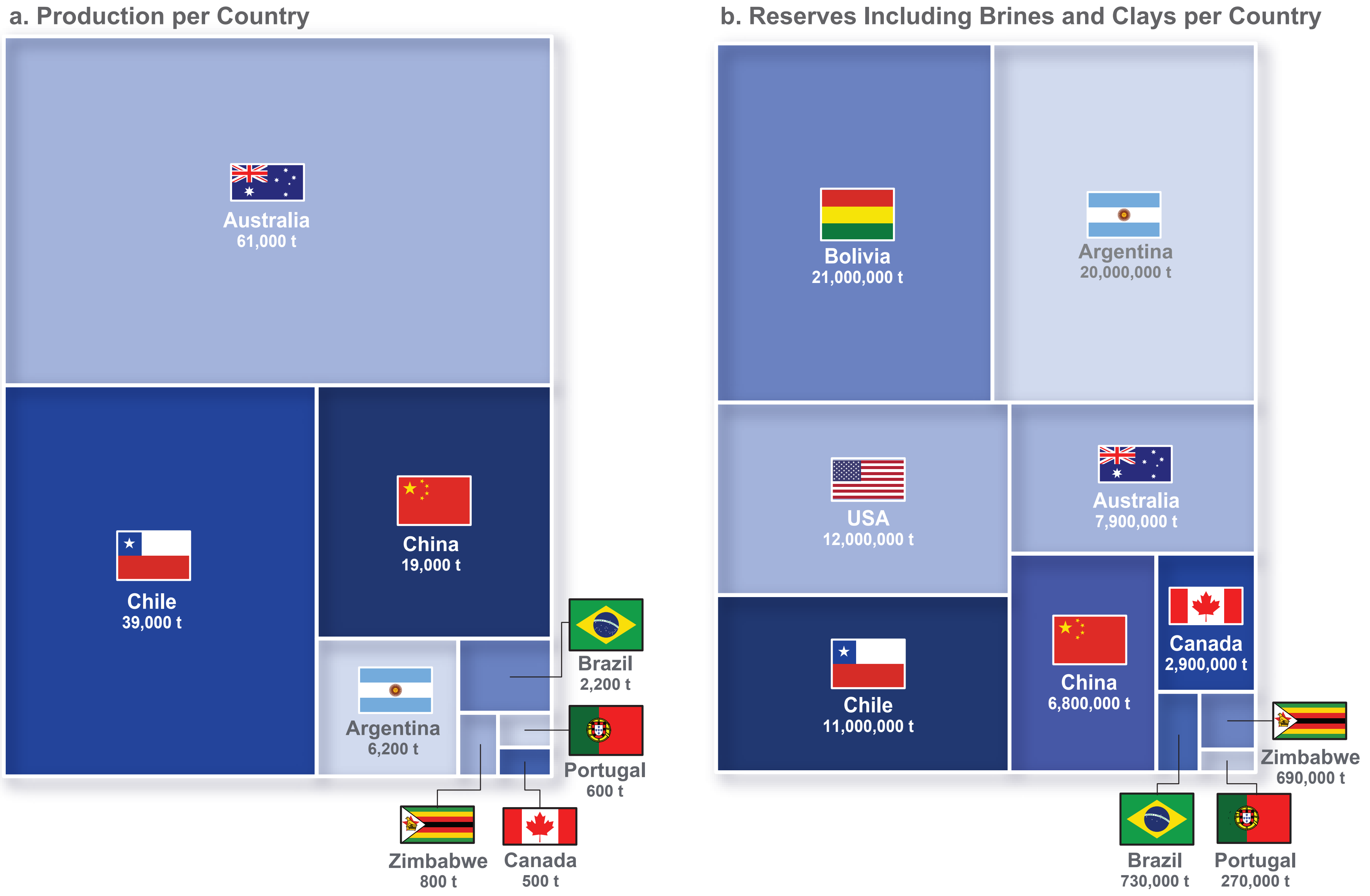

Data in metric tonnes of contained lithium unless otherwise noted

Metrics taken from https://pubs.usgs.gov/periodicals/mcs2022/mcs2022.pdf

© Canadian Discovery Ltd.

Figure 2.4

2.5 Lithium Projects in Canada

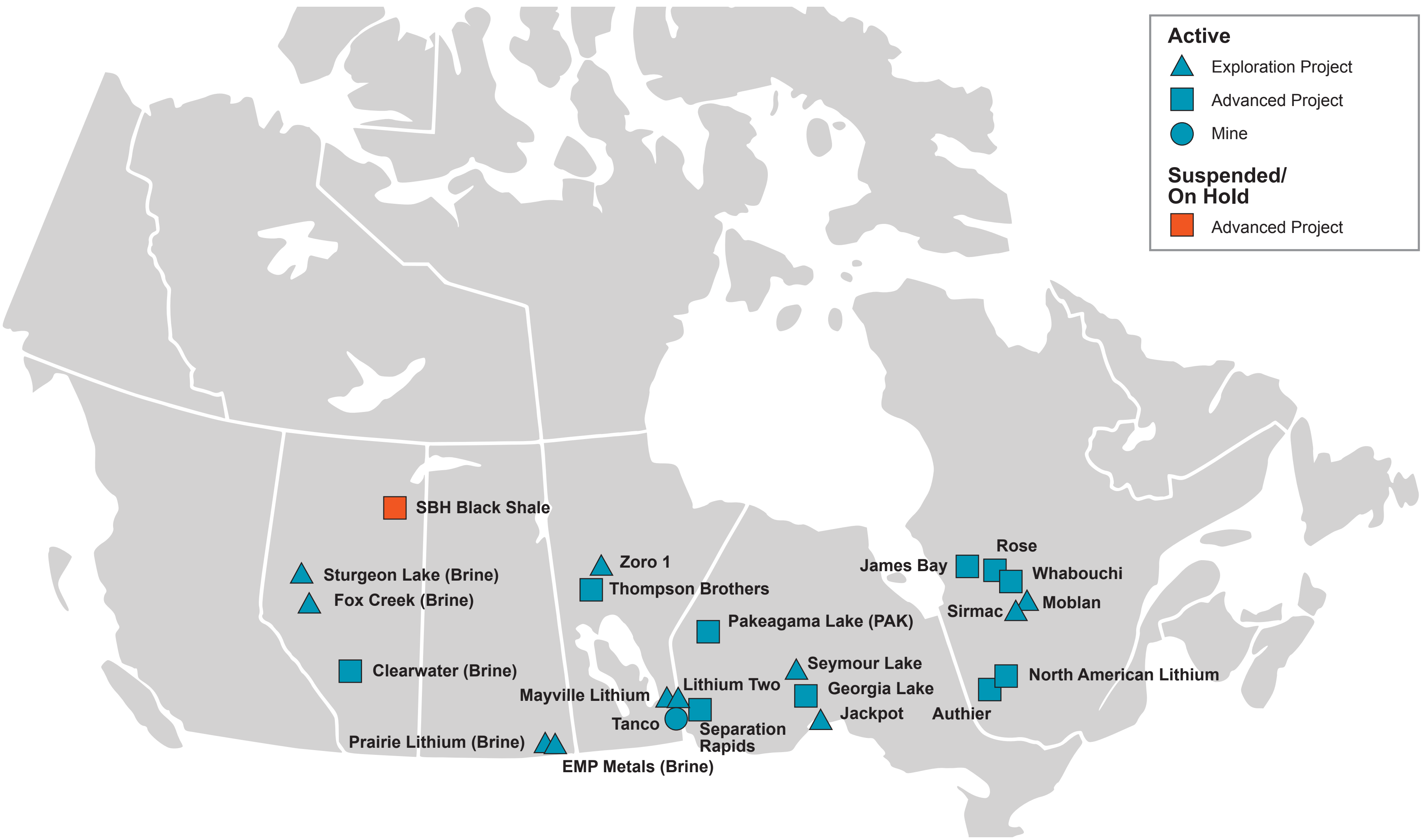

Modified from: https://natural-resources.canada.ca/our-natural-resources/minerals-mining/minerals-metals-facts/lithium-facts/24009

© Canadian Discovery Ltd.

Figure 2.5

2.6 Lithium Mobilization Model

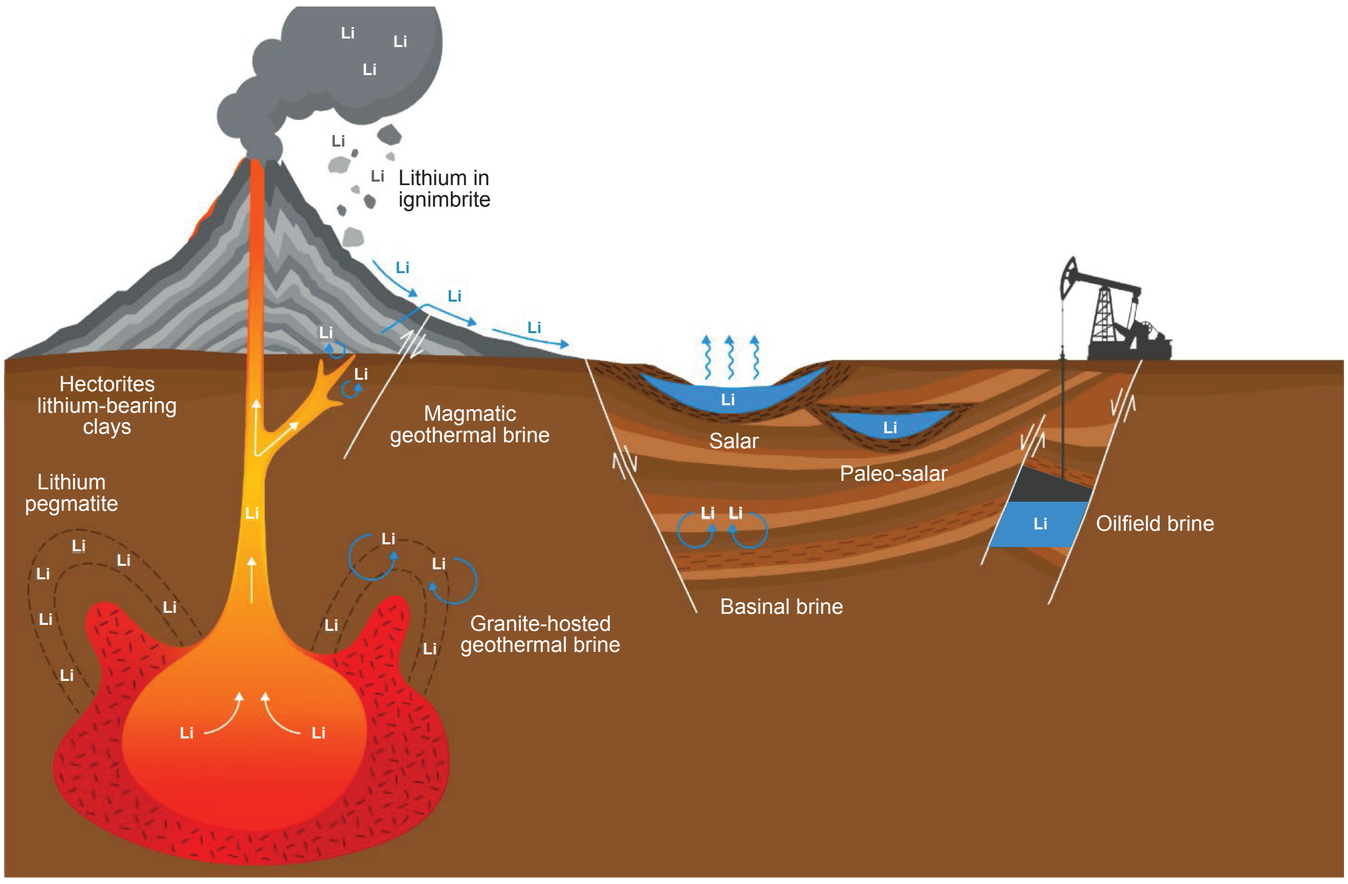

Conceptual illustration of the range of lithium (Li) deposits associated with magmatic and brine systems. These systems are connected by the flux of magma and water, which both transport Li in solution.

Modified from Bowell et al., 2020; Bradley et al., 2017

Figure 2.6

Canada has roughly 3% of the world's lithium reserves and a number of lithium projects at various levels of development, operation, or suspended operations *(figure 2.5)* (Natural Resources Canada, 2023). Various projects in Quebec reached operation but have since been put on hold due to the sharp decrease in lithium pricing. The price of lithium plunged dramatically in late 2022 because of a rise in lithium production that has not only met but has surpassed expected demand for 2023 (Reuters, 2023). Even with the price decrease in late 2022, it is still significantly higher than pricing in 2020. Depending on the end use of the lithium, prices can vary significantly. Furthermore, unlike oil and gas, the price of lithium is not listed on an index; it is set by closed contracts with the buyers. The general consensus is that lithium demand is rising worldwide and will continue to rise as Canada and other countries around the globe strive for a reduction in GHG emissions (Forbes, 2023).

Global Lithium Sources

Lithium is the 34th most abundant element in the Earth's crust with an average concentration of 20 ppm by weight (Rumble, 2023). In magmatic systems, it occurs in high-temperature aluminosilicate minerals associated with granites, granitic pegmatites, and volcanic ash. In continental systems, lithium brines occur in closed-basin sedimentary settings (salars and evaporite lakes), altered felsic volcanics and dissolved in sedimentary basin brines. Due to its reactivity, lithium does not occur in its elemental form in nature. Currently, the resources of lithium that offer economically viable production are hard rock ores and closed system brines, with the latter accounting for more than 60% of global production (Tadesse, 2019). *Figure 2.6* schematically shows the lithium cycle and displays the main sources of lithium and lithium-enrichment.

Historically, lithium was primarily sourced from hard rock mining and processing of lithium-bearing minerals. While there are more than 100 known minerals that may contain lithium, only a few are economically viable for industrial-scale lithium extraction. They include minerals found in pegmatite formations such as spodumene (3.7% Li), lepidolite (1.4–3.6% Li), and petalite (1.6–2.3% Li) (BGS, 2016). Pegmatite lithium deposits are formed during late phase felsic magma fractionation as rhyolitic magma cools and is crystallized.

Spodumene has the highest lithium content and is the primary ore for lithium production from hard rock mining. Australia is the world's largest producer of lithium sourced from spodumene. While lithium is currently extracted only from pegmatite deposits, future rock sources such as hectorite (0.53% Li) and jadarite (7.3% Li) are considered potential viable resources (Brown et al., 2016).

Given the challenges of terrestrial mining coupled with the growing demand for lithium production, the extraction of lithium from brines has expanded significantly. Brines can loosely be categorized as:

- Continental: deposits occur in contained basins where inflowing surface and sub-surface waters are moderately enriched in lithium
- Geothermal: elevated levels of lithium have been reported in geothermal areas including deep ocean thermal vents and continental hot springs
- Oilfield: waters or brines extracted during oil and gas production from underground formations that have appreciable elevated concentrations of lithium along with other critical minerals

2.7 Direct Lithium Extraction Schematic from Reservoir to Market

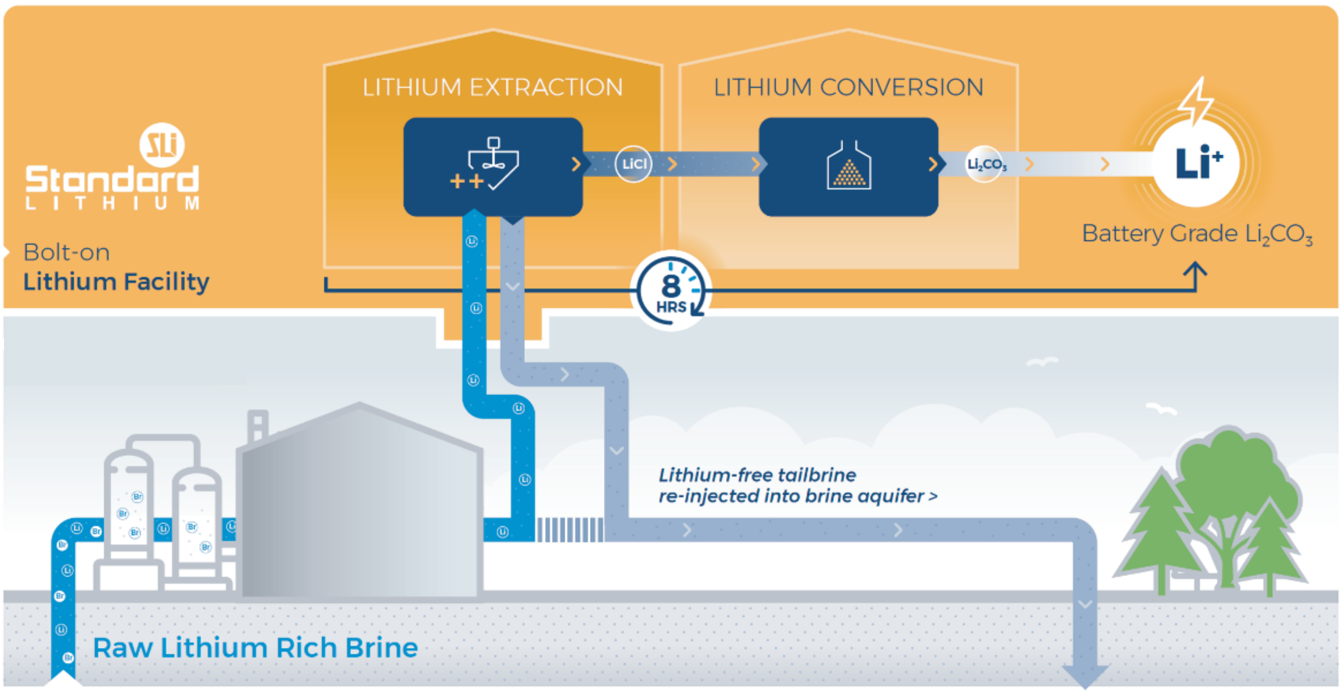

https://cleantechnica.com/2021/06/07/interview-with-standard-lithium-ceo-robert-mintak/

Figure 2.7

Presently, the extraction of lithium occurs primarily from continental brines; however, the extraction from geothermal and oilfield brines has been demonstrated and has the potential for significant growth.

Most lithium production from continental brines comes from South America's surface brines found in salars (playa lakes) within the aptly named lithium ABC triangle comprising the desert regions of Argentina, Bolivia, and Chile. Salars are seasonally flooded dry lakes that form in arid locations where annual evaporation exceeds rainfall. Key to forming the brines is a lithium source, typically high-silica volcanic rocks commonly associated with hot springs, along with sufficient subsidence to accumulate a thick sedimentary succession (Donaldson, 2022). Meteoric waters leach the lithium from the high-silica volcanic rock in which the lake is contained. For lithium production, instead of relying on surface recharge, the brines are pumped from the ground water into large holding ponds where they are left to evaporate at surface. One of the most well-known examples of lithium production from continental brines occurs from the 3,000 km^2 Salar de Atacama in Chile with an average lithium concentration of roughly 1400 mg/L or 0.14% (Investing News Network, 2023).

Petro-Lithium

Oilfield brines (saline formation waters), including geothermal brines, which represent an emerging source of lithium, are referred to as petro-lithium in North America. Lithium is extracted using proprietary technologies that are developing rapidly to allow for efficient lithium production *(figure 2.7)*. Following the separation of oil and gas, lithium chloride can be separated from the oilfield wastewater in a matter of hours, rather than months or years needed in conventional extraction methods of solar evaporation or days for hard rock mining. After lithium removal, the water can be reinjected into the reservoir to provide pressure support.

Understanding the source and distribution of lithium within oilfield and geothermal brines requires careful geochemical analysis of, and an understanding of, the lithium-enrichment process. Lithium sources and the enrichment process are discussed in detail in subsequent chapters of this study.

2.8 Western Canada Lithium Concentration Map

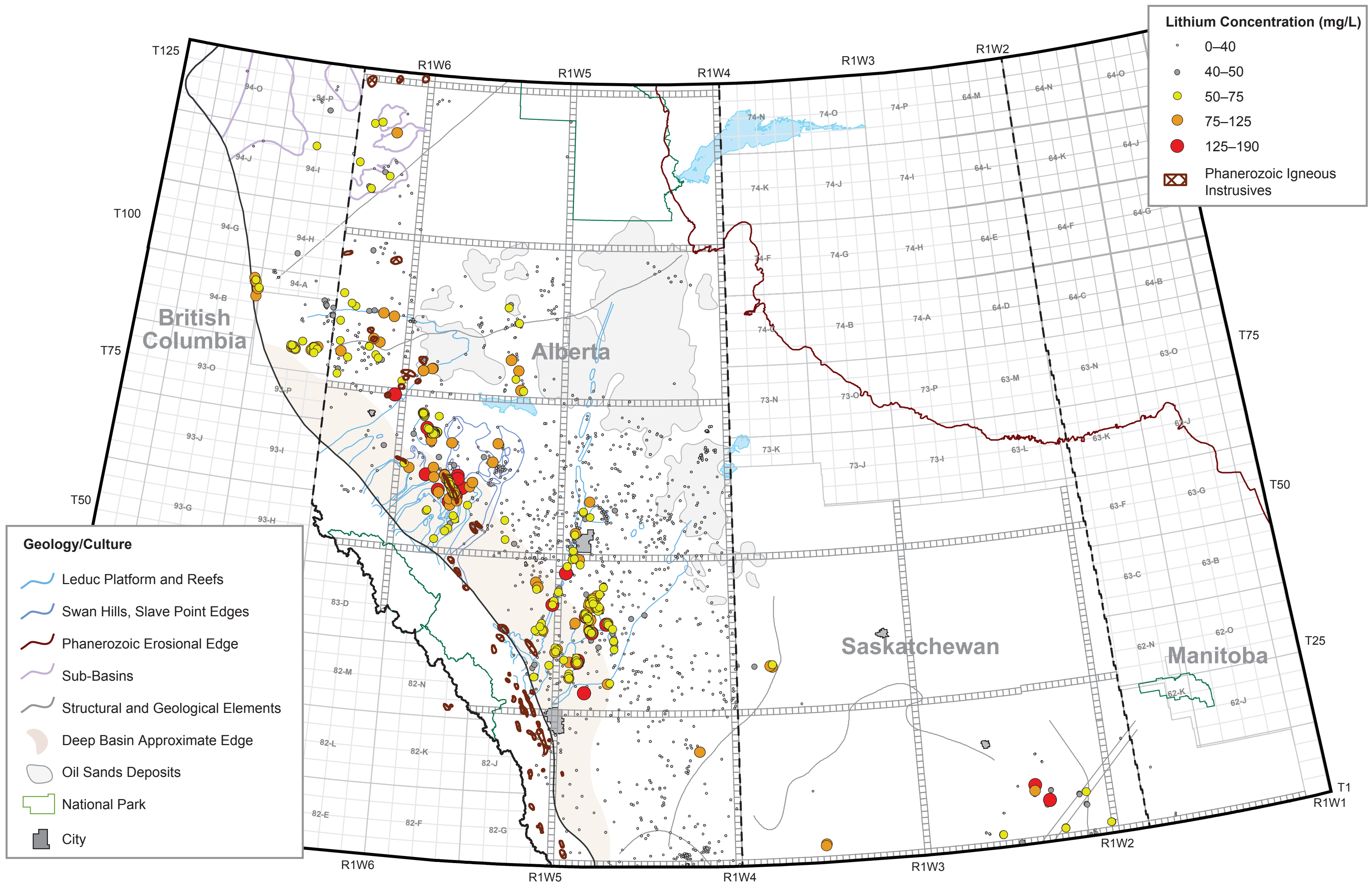

Lithium data sources from the AGS, SGS and the current study; Leduc Reefs from WCSB Atlas, 1994

Figure 2.8

Petro-Lithium in Western Canada

Starting in the 1990s and continuing to present day, provincial geological surveys have sampled formation waters in Alberta and Saskatchewan, as well as a limited number of shallow water wells and surface springs in Manitoba.

The Alberta Geological Survey (AGS) identified elevated levels of lithium and other elements in saline brines associated with oil and gas reservoirs deep in the subsurface (Hitchon et al., 1993; Eccles and Jean, 2010). The highest lithium concentrations in Alberta have been historically documented by both government and industry to occur in Devonian-age units — specifically the Beaverhill Lake (Swan Hills), Winterburn (Nisku), Woodbend (Leduc), and Wabamun groups/formations (Eccles and Berhane, 2011). Similarly, the Saskatchewan Geological Survey (SGS) identified elevated lithium values in the Devonian Duperow Formation, which is age-equivalent to the Leduc in Alberta (Jensen and Kohlruss, 2023).

The Canadian Discovery Ltd. (CDL) lithium concentration map *(figure 2.8)* across the WCSB is a compilation of all current public data. The map shows a distinct lack of samples within BC. This study focused on expanding the work done in Alberta and Saskatchewan into BC to help advance the understanding of lithium concentration, distribution and potential enrichment mechanisms in this province.

2.9 Schematic Model for Lithium Mobilization into West-Central Alberta Devonian Aquifers

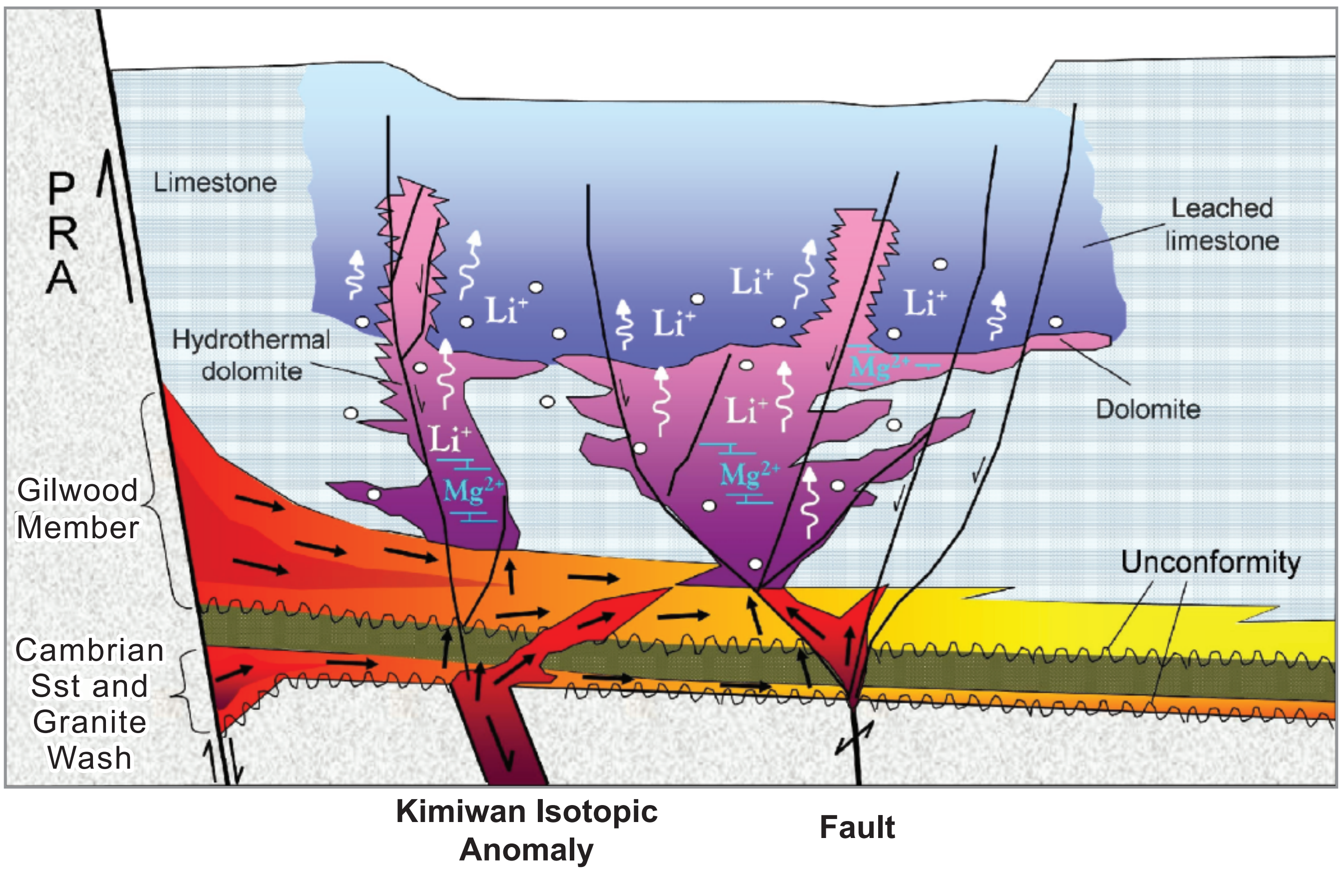

Modified from Eccles and Berhane, 2011

© Canadian Discovery Ltd. *Figure 2.9*

Sedimentary Basin Brine Evolution and Lithium-Enrichment

Understanding the processes leading to the enrichment of lithium in sedimentary basin brines is key to developing an informed exploration and development strategy. To date, the industry has relied on historical data collected through a variety of activities that were not necessarily an optimized lithium exploration strategy, possibly resulting in sampling biases and overlooked opportunities.

Work conducted by Hitchon et al., 1993; Eccles and Jean, 2010; Eccles and Berhane, 2011; Huff , 2016; Lopez et al., 2018; Lyster et al., (2022); and Rostron et al., 2022 has suggested two primary processes for the observed lithium-enrichment in Western Canada brines:

1. Enrichment through crystalline basement-derived hydrothermal processes *(figure 2.9)*
2. Evapoconcentration (subaerially evaporated seawater) primarily associated with Devonian evaporite and halite deposits *(figure 2.10)*

Recent presentations by Bishop and Robins (2023) have suggested that host rock interactions with lithium-rich clay-bearing sediments, possibly enhanced by widespread volcanism during deposition are the primary sources. Lazowski et al., (2023) suggested windblown clay particles deposited within the middle Devonian Fort Vermilion Formation represent a potentially important widespread aeolian source.

See Dugamin et al. (2023), and the thorough reference list provided by them in *Appendix E*, for a comprehensive review of lithium-enrichment processes in sedimentary formation waters. The analysis herein incorporates some of the concepts and findings published by Dugamin et al.

2.10 Cl/Br vs Na/Br

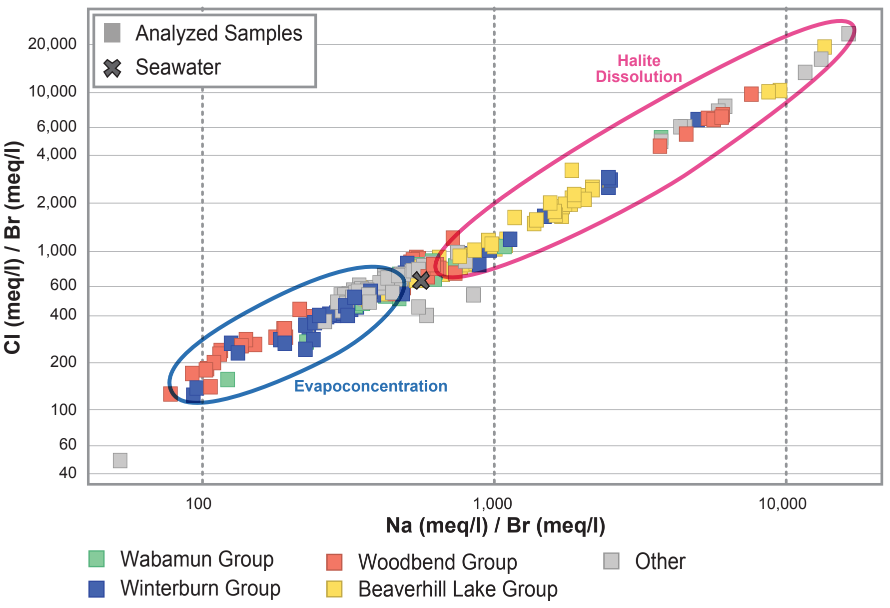

Lithium data sources Lyster et al., 2022; Eccles et al., 2011

© Canadian Discovery Ltd. *Figure 2.10*

2.11 Seawater Evaporation Process

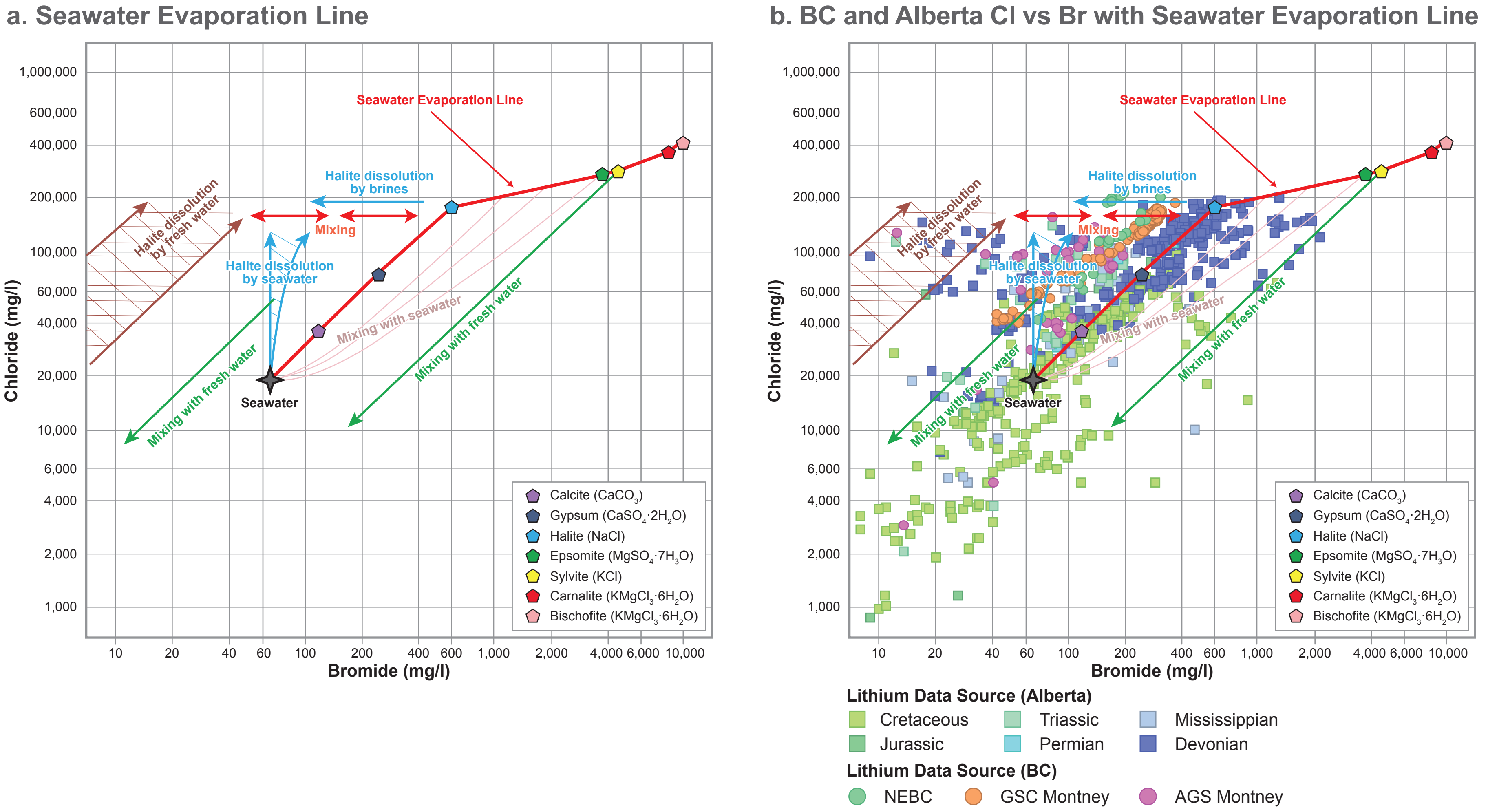

Lithium data from the AGS, GSC, geoLOGIC and the current study. Shouakar-Stash, O., 2008.

Figure 2.11

Brine Evolution and Migration

A number of ionic relationships have been used by researchers to identify the evolution of subsurface brines as it relates to primary and secondary brines. For the purpose of this discussion, "primary brines" are defined as those developed during the seawater concentration process through subaerial evaporation in sabkha environments at the sediment/water interface. The complete evapoconcentration process causes the precipitation of calcite, gypsum, halite, epsomite, sylvite, carnalite, and bischofite, and is well depicted by the relationship of chloride to bromide *(figure 2.11a)*.

Data used in this study from Alberta and BC are shown on the Cl vs Br graph in *figure 2.11b* along with their likely evolutionary trajectories. Chloride concentrations are observed to reach almost 300,000 mg/L. Bromide, a conservative ion, or an ion that preferentially stays in solution for a very long time, appears to reach a maximum concentration of 2,000 mg/L. The data suggest that Devonian formation waters reached epsomite and sylvite precipitation saturation and that the basin has undergone extensive brine migration, halite dissolution and mixing with both seawater and fresh water over its geologic history *(figure 2.11b)*. Vertical brine migration is particularly evidenced by elevated bromide levels within certain Cretaceous samples at chloride concentrations above and below seawater. The location and areal extent of the various migration and mixing paths are likely controlled by vertical and lateral hydraulic continuity and the basin's tectonic and hydrogeological history. The main mixing and dilution processes occurring within the basin are:

- Vertical and lateral brine migration
- Halite dissolution by brines and fresh waters
- Halite dissolution by seawater
- Mixing with seawater and or fresh water

Lithium-Enrichment in WCSB Brines

In *figure 2.12*, the concentrations of Br as a function of Cl and Li are plotted, normalized to their initial concentration in seawater. Chloride and bromide are enriched up to 15X and 30X respectively, whereas lithium is enriched well over 500X (to a maximum of 950X) relative to seawater. These data suggest that lithium concentration in seawater due to subaerial evaporation is an insufficient process as postulated by various other authors. The relationship of lithium as a function of the Cl/Br (mass plots) for Alberta and BC carbonates and clastics is provided in *figures 2.13a and b*. The clustering of these data provides a "brine signature" and suggests the relative contribution of primary versus secondary brines. Cretaceous reservoirs exhibit a broad dispersion (mixing) pattern versus the Jurassic and Triassic reservoirs, which exhibit the least amount of dispersion.

The Li vs Cl/Br mass ratio plots for the Illinois, Appalachia, Delaware, Louisiana Salt, Michigan, and other basins, as presented by Dugamin et al. (2023) are compared to the Alberta and BC Devonian and Triassic/Jurassic data in *figure 2.14*. In all cases, except the North German Carboniferous-Permian Mesozoic and portions of the Delaware, lithium is enriched relative to seawater evaporation trends. However, the lithium content and brine signatures between basins vary substantially, suggesting enrichment is controlled by the basin's depositional, thermal, and hydrogeological history.

2.12 Normalized Lithium Concentration Graph

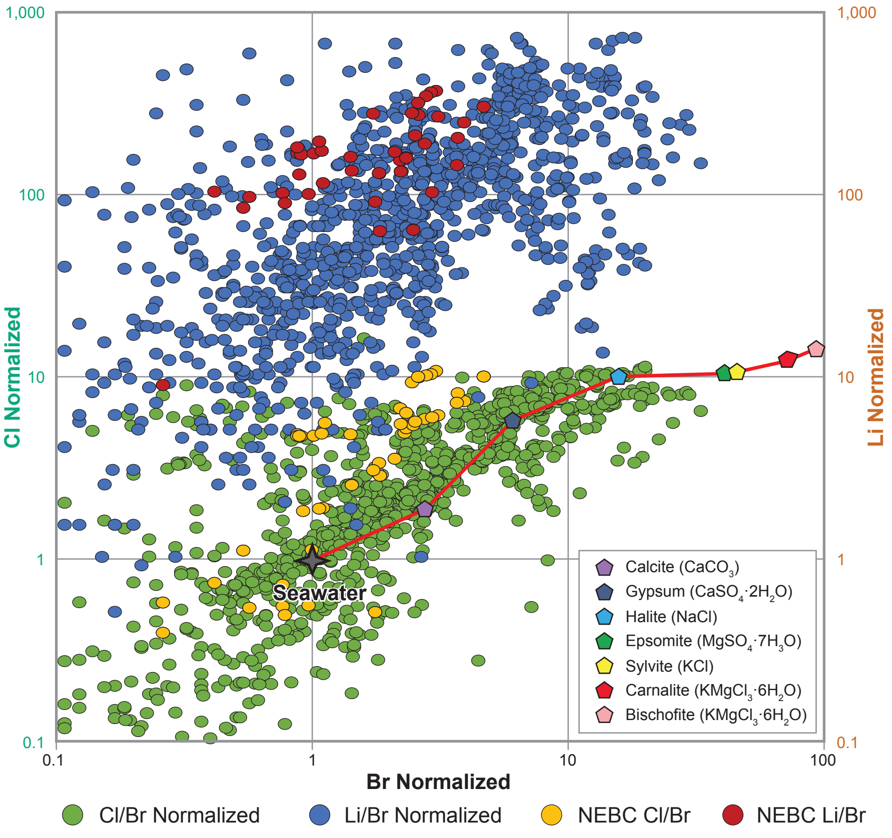

Lithium data from the AGS, GSC, geoLOGIC and the current study.
Shouakar-Stash, O., 2008.

© Canadian Discovery Ltd. *Figure 2.12*

2.13 Li vs Cl/Br Mass Ratio

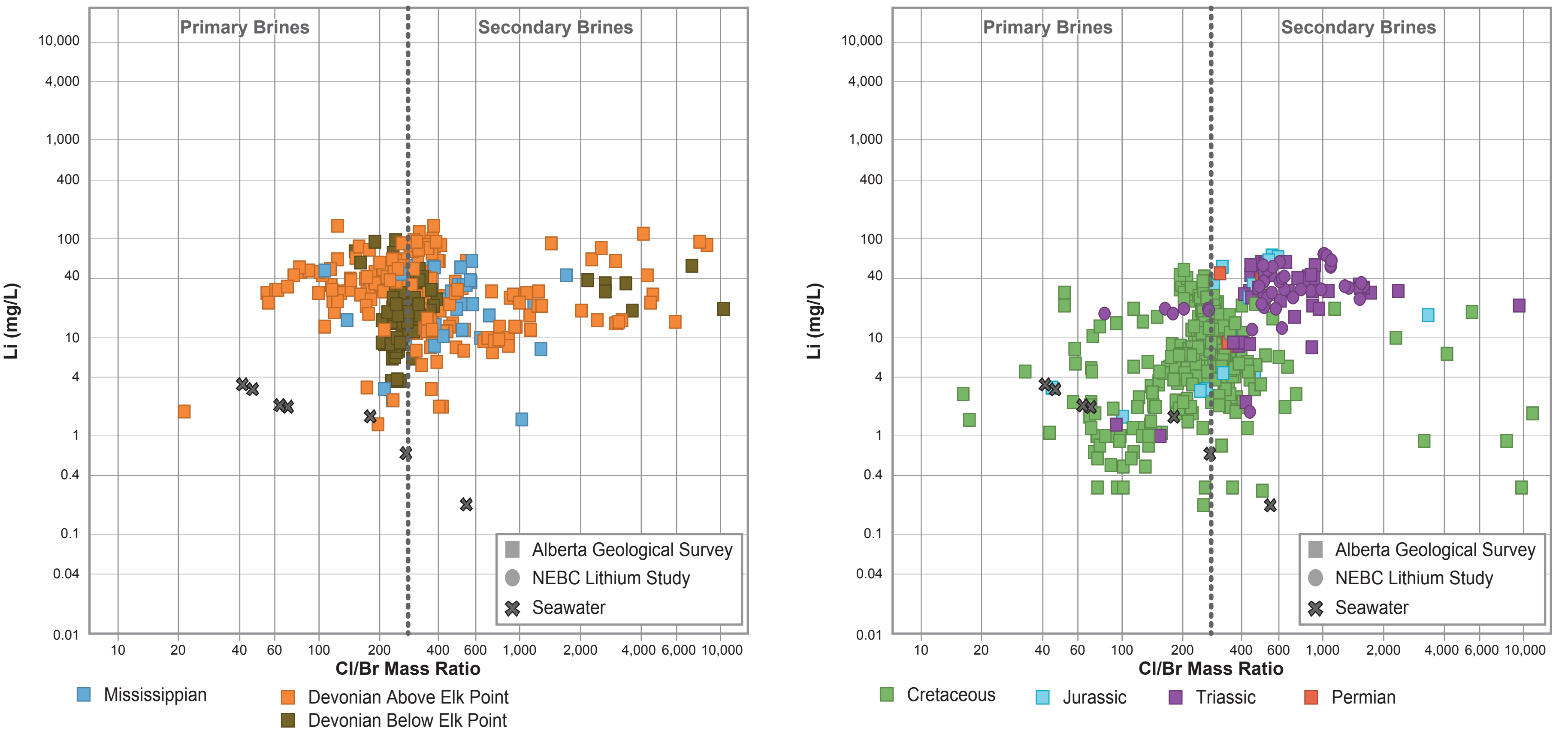

a. Li vs Cl/Br Mass Ratio (Mississippian and Devonian)

b. Li vs Cl/Br Mass Ratio (Post-Mississippian)

Source: AGS and this study

© Canadian Discovery Ltd. *Figure 2.13*

2.14 Lithium Concentration as a Function of Cl/Br Mass Ratio in Sedimentary Formation Waters

a. Li vs Cl/Br Mass Ratio

b. Li vs Cl/Br Mass Ratio

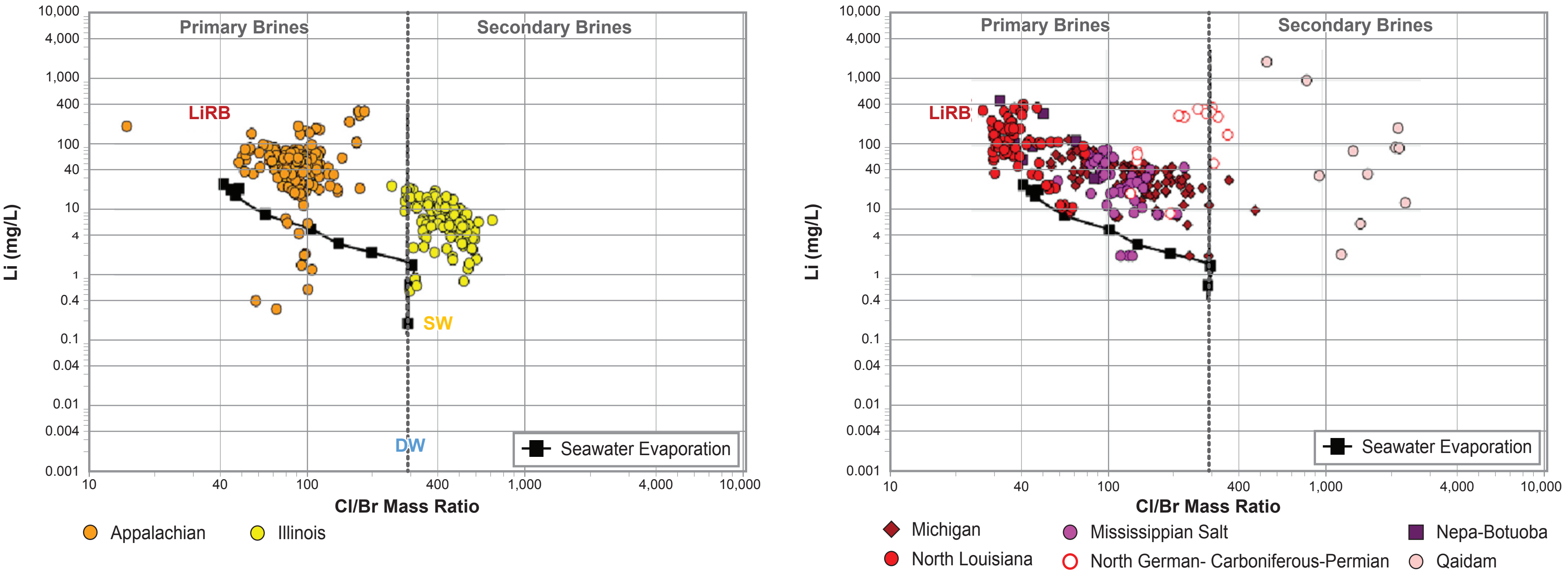

c. Li vs Cl/Br Mass Ratio

d. Li vs Cl/Br Mass Ratio

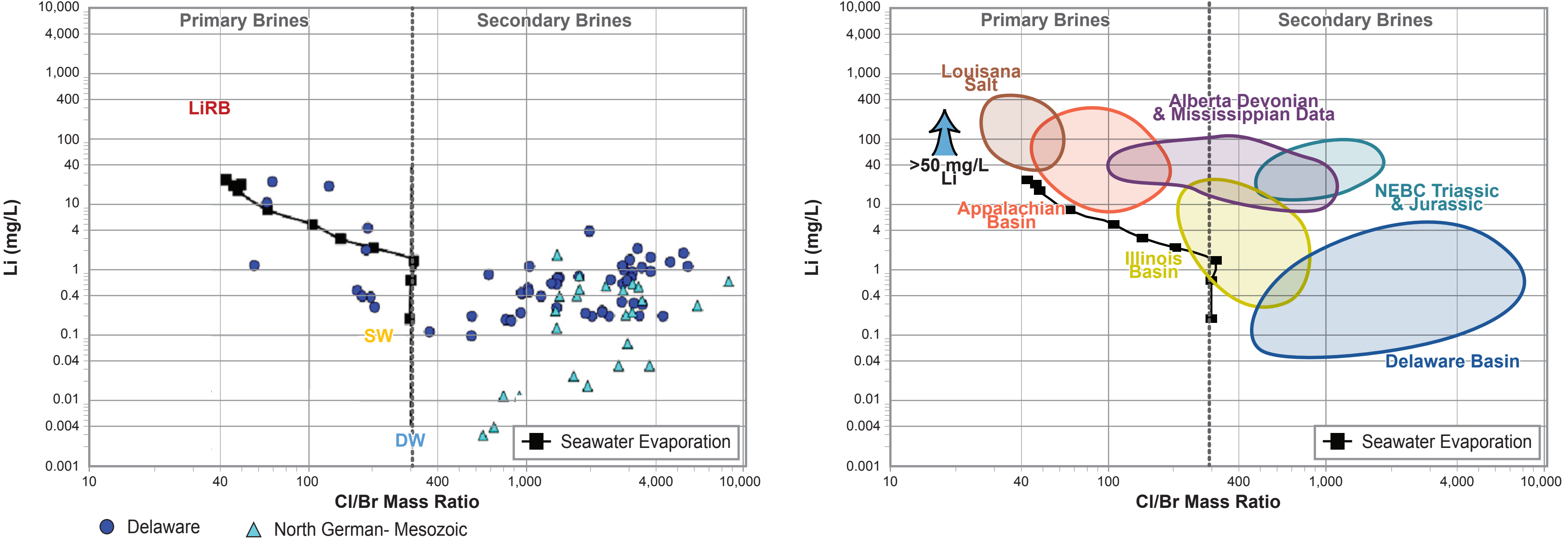

Source: Dugamin et al., 2023 and this study

© Canadian Discovery Ltd.

Figure 2.14

2.15 Rocks and Minerals Histogram: Lithium Concentrations

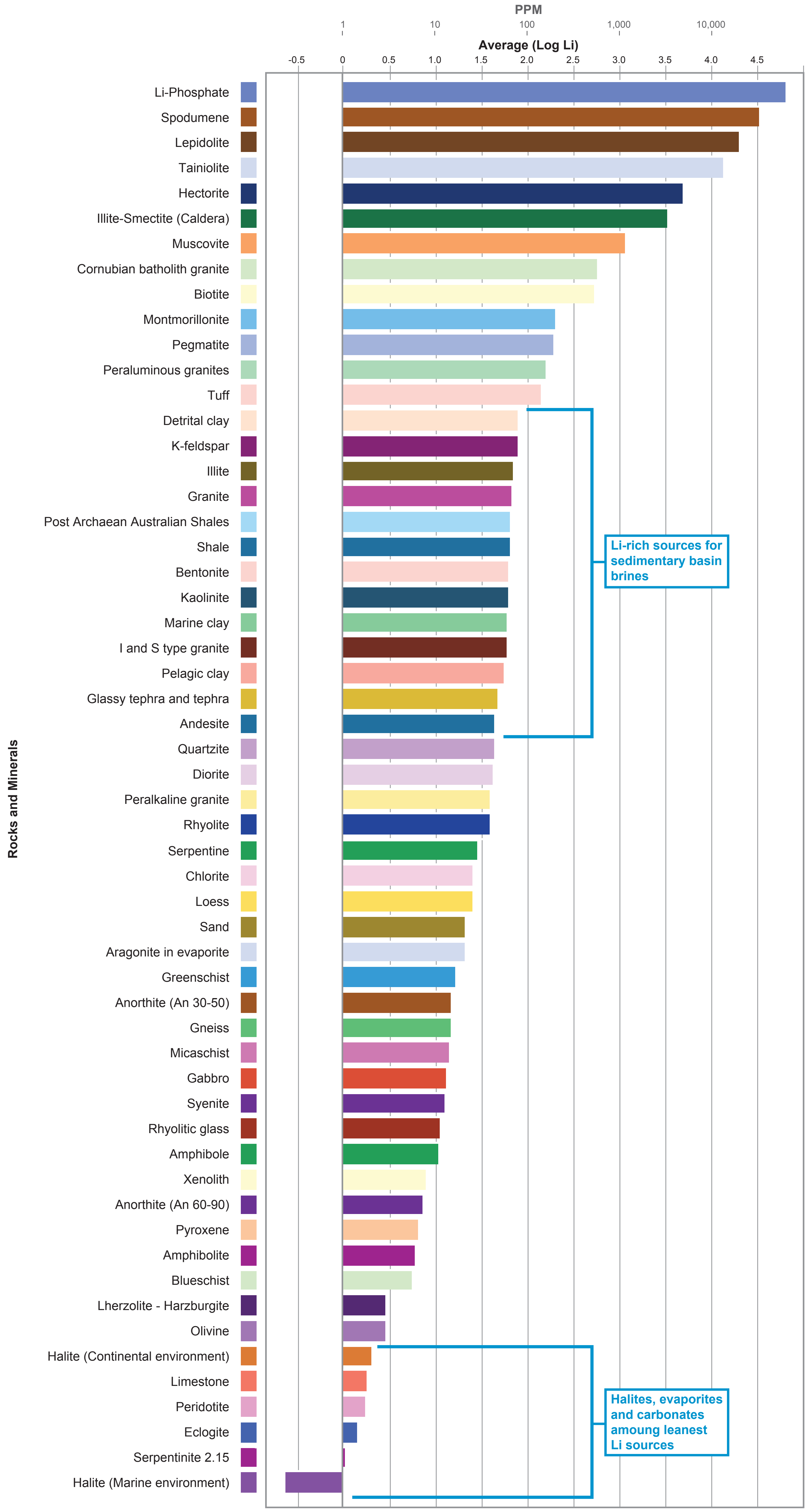

Li-rich sources for sedimentary basin brines

Halites, evaporites and carbonates amoung leanest Li sources

Source: Modified from Dugamin et al., 2023

Figure 2.15

Sources of Lithium

Later chapters of this report will discuss the potential enrichment of lithium in subsurface brines due to seawater evaporation and crystalline basement-derived radiogenic sources derived through circulating brines and hydrothermal fluid expulsion events. *Figure 2.15* depicts the average (of 25th and 75th percentile concentration values) of a variety of igneous intrusive, volcanic, metamorphic, and sedimentary rocks along with common clay minerals, silicates, and ore-bearing rocks. A detailed list of the data is provided in *Appendix D*. The lithium content of marine halite (<0.25 ppm), limestone (0.4 to 8 ppm) and aragonite in evaporites (20 ppm) are amongst the lowest of any rock type. These data suggest that despite the contribution of seawater evaporation (10 to 30X), the Devonian carbonate reservoir host rocks are unlikely candidates to enrich lithium through leaching by 500X or more relative to seawater. This leaves water-rock interactions with adjacent clay mineral-rich shales as the primary contributor where direct hydrothermal events have not occurred.

Lithium and Volcanically Sourced Clay Minerals

Searching for sources of lithium beyond evaporative brines naturally leads to volcanic ash as a potential, if not the most likely, source of lithium. Volcanic ash comprises fragments of rock and minerals set in a glassy matrix that forms upon quenching of magmatic eruptions. Volcanic glass is thermodynamically unstable and once deposited, it rapidly reacts with water to form clays, specifically smectite, which is also known as montmorillonite or bentonite. Lithium in the glass is liberated by the hydrolysis reaction and partitions between the aqueous phase and the solid phase where it is incorporated as an exchangeable cation in the interlayer site of smectite. The distribution of lithium between the aqueous and solid phases is governed by ion exchange equilibria amongst lithium, sodium, potassium, calcium, magnesium, and other exchangeable cations present in the rock (Dugamin et al., 2023; Starkey, H. C., 1982).

With burial, the smectite reacts with additional components in the rock to form more stable clay minerals. Smectite exists in a high-silica activity phase. With increasing burial, silica activity drops due to the formation of authigenic quartz, and smectite is irreversibly destroyed and replaced by illite, which is a more stable clay mineral (Abercrombie et al., 1994). Due to illite's comparatively lower interlayer charge, hence lower cation exchange capacity (CEC), it cannot accommodate all the interlayer cations held previously by smectite, and these ions are released to the aqueous phase or to participate in other mineralogical reactions. As a singly charged cation, lithium is stable in aqueous solution and does not participate in mineralogical reactions unless subjected to hydrothermal or deep burial processes.

Lithium and Temperature

The temperature interdependence of lithium in brines has been well established in the literature. This study uses the empirical relationship observed by Kharaka and Mariner (1989) *(figure 2.16)*, where the Na/Li relationship is often used as a geothermometer. The empirical relationship observed by Kharaka and Mariner (1989) suggests that sodium/lithium ratios increase by two orders of magnitude between 25°C and 200°C, temperatures through which clay mineral transformations are particularly active. Discussion and application of this methodology to the projects sample data are provided in the *Montney chapter 5* of this study.

2.16 | Na/Li Thermometer

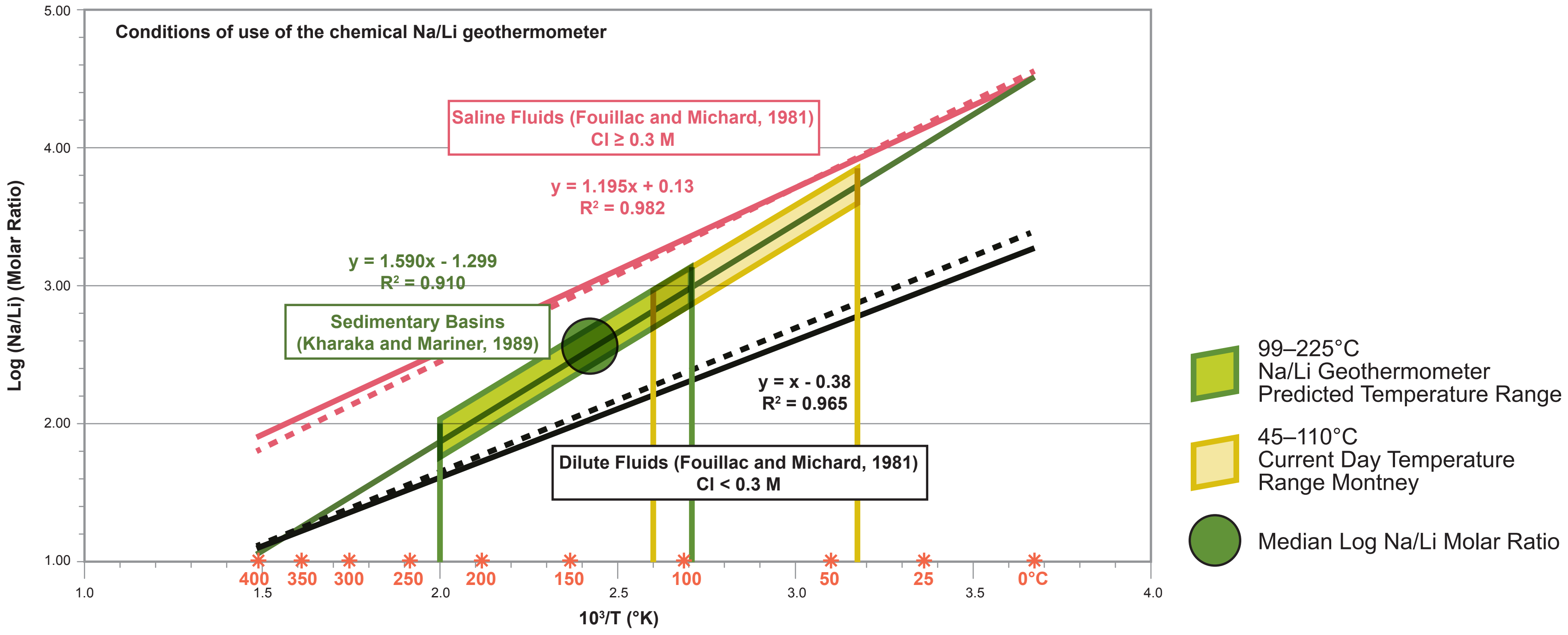

Empirical Na/Li geothermometer with measured Montney log Na/Li ratios. Data denoted observed lithium concentrations not in equilibrium or controlled by current day temperature.

Modified from Kharaka and Mariner, 1989

Figure 2.16

2.17 Subsurface Lithium-Enrichment Processes

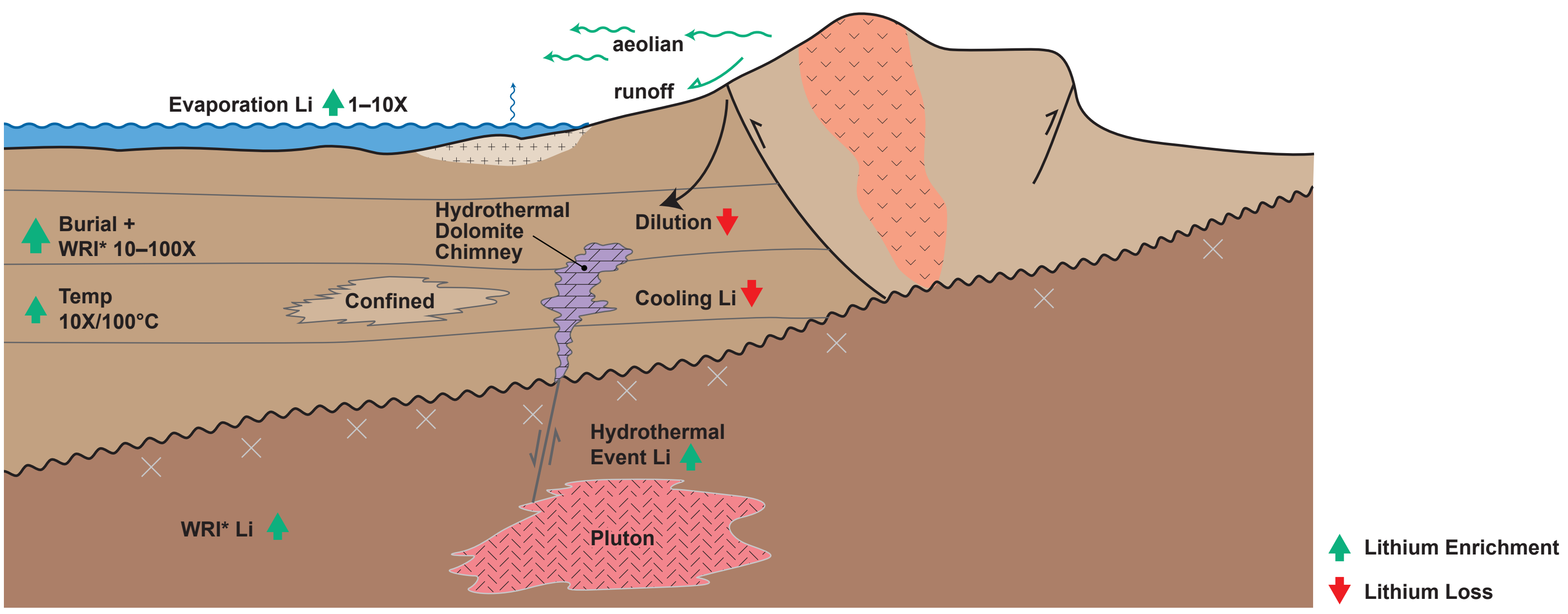

*Water-rock interaction

After Dugamin et. al., 2023

© *Canadian Discovery Ltd.*

Figure 2.17

The Lithium Concentration Model

There are multiple mechanisms that potentially lead to the enrichment of lithium in sedimentary basin brines, where lithium concentrations are found in excess of 1,000X that of seawater. In the WCSB, lithium-enrichment of over 500X relative to seawater is observed in parts of the Devonian. *Figure 2.17* shows a schematic of the various concentration and dilution processes, which have been quantified in the literature and through observations in this study. Processes such as circulation through, and subsequent leaching of, igneous basement rocks, hydrothermal events and enrichment through sedimentation or overland flow are more difficult to quantify. The scale of some of the enrichment processes as identified by Dugamin et al., (2023) are provided below:

- Seawater Evaporation
  - 1 to 10X, source = observed data at halite saturation
- Burial and Water-Rock Interaction
  - 10 to 100X, source = observed and Dugamin et al., 2023
- Temperature Gain (empirical)
  - 10X/100°C, source = observed and Kharaka and Mariner, 1989

Lithium loss can occur through brine dilution by mixing with seawater, halite-derived brines, and meteoric waters. Uplift or erosion and subsequent cooling can cause resorption of lithium in certain circumstances as well.

Lithium Compounds and Products

There are many compounds that contain lithium, some of which occur naturally and others that are manufactured in processing facilities. The most important lithium compounds are:

- Lithium oxide (Li_2O): Many mine operators will quote their grade figures in terms of lithium oxide content. This compound is formed by the reaction of lithium with oxygen in air and in turn, it reacts with water and steam to form lithium hydroxide.
- Lithium carbonate (Li_2CO_3): Lithium carbonate is the primary precursor to produce other lithium compounds and products. It is sold in various grades (purity and particle size) depending on the end use. It is produced from lithium chloride solutions through the addition of sodium carbonate, followed by water washing to remove the sodium chloride by-product.
- Lithium chloride (LiCl): It is the most common lithium compound found in brines. It can also be produced by reacting lithium carbonate with hydrochloric acid.
- Lithium bromide (LiBr): Lithium bromide can be produced by reacting lithium carbonate with hydrobromic acid. The compound is hygroscopic (tends to absorb moisture from the air) and thus, it is used as a desiccant.
- Lithium hydroxide (LiOH): Lithium hydroxide is produced by reacting lithium carbonate with calcium hydroxide.
- Lithium metal (Li): This metal is produced by the electrolysis of a mixture of lithium chloride and potassium chloride.

Table 2.3: Comparison of Lithium Extraction Technologies

	Mining	Evaporative Processing	DLE
Feedstock	Hard rock	Brine (high Li$^+$ concentration and low Mg^{2+}/Li$^+$ mass ratio)[2]	Brine
Product	Spodumene concentration (6-7% LiO$_2$)[1]	Lithium carbonate/lithium chloride	Lithium carbonate/lithium chloride
Production Time	Weeks to Months	Months to Years	Hours to Days
Lithium Recovery Rates	60-80% (processing)	40-60%	70-99%
Further Process Requirements	Yes	No, depending on end use	No, depending on end use
Costs	Medium to High	Low	Low to Medium
Land Requirements and Impacts	High	High	Low
Weather Dependence	Moderate	Strong	None
Water Consumption	High	High	Low
Energy Consumption	High	Low	Medium
Lithium Recovery Rates	6-7% LiO$_2$ in spodumene	~50%	70-99%
GHG Impact (Scope 1)	High	Low	Low

[1] Certain precipitants (e.g., aluminate method) have shown excellent Li$^+$ recovery from higher Mg^{2+}/Li$^+$ mass ratios using evaporative processing (Murphy and Haji, 2022).

[2] Most mining sites do not include the facilities to convert spodumene concentrate to a final lithium product.

Sources: Darcy, 2023. Goldman Sachs, 2023

© Canadian Discovery Ltd.

Table 2.3

Extraction and Processing

An overview of the methods for extracting and processing lithium from hard rock mining and various brines is provided below and summarized in *table 2.3*.

Hard Rock Mining and Processing

Hard rock deposits are mined using methods typically deployed for other metals such as surface (open-pit) or subsurface (underground) methods. The open-pit mining methods are used for deposits near the surface, usually less than 100 meters. In certain instances, both methods are employed simultaneously in order to access shallow and deeper parts of an ore body (e.g., Talison Lithium's Greenbushes Mine in Western Australia). After the ore has been mined, it goes through various physical and chemical processing stages.

The first stage is physical beneficiation, which starts with crushing the ore and separating the lithium minerals based on their physical, electrical, and magnetic properties to form a concentrate. The lithium concentration is increased further by froth flotation, dense media separation or a combination of both methods. The final concentrate will typically contain 6–7% Li$_2$O (~80% spodumene) (Warren, 2021). Most mines produce the spodumene concentrate as the final product, which is sold to lithium hydroxide or carbonate conversion plants, mostly located in Asia.

The conversion plant can also be located at the mine facility; recently more mine operators operators have been considering this addition given the higher profitability margins for lithium carbonate as opposed to the margins associated with spodumene concentrate (S&P Global, 2019). While several conversion methods have been developed such as carbonate or lime leaching, the most common method is acid leaching, which is comprised of the following steps:

- Roasting to convert α-spodumene (naturally occurring) to β-spodumene as the former has a monoclinic structure and is not chemically available to leaching
- Roasting of β-spodumene with sulphuric acid to form lithium sulphate followed by acid leaching
- Removal of impurities such as iron, aluminum and magnesium by dissolution water followed by filtration and ion exchange to produce a lithium sulphate solution with trace impurities
- Addition of sodium carbonate to the lithium sulphate solution to precipitate insoluble lithium carbonate
- Washing and drying the final product prior to shipment

The method for extracting lithium from spodumene is relatively fast (measured in days), is consistently productive and has high recovery rates. However, the process suffers from various challenges including high-energy demands for furnaces and machines for extraction and rock-crushing. Dust production and the use of concentrated chemicals, including acid, present environmental, and health and safety risks. In addition, the production costs of lithium carbonate from spodumene are approximately twice that of lithium from brine (Forbes, 2023).

Evaporative Brine Processing

The standard practice for lithium extraction from brines, such as continental deposits, relies on concentrating lithium through evaporation. Brines are first pumped to a series of ponds covering a large surface area. As water evaporates, compounds such as sodium chloride, potassium chloride, and calcium sulphate precipitate and are removed. The brine is kept in ponds until the lithium concentration reaches approximately 6,000 ppm, which is close to the saturation point of lithium chloride (Murphy and Haji, 2022). Impurities not removed through previous precipitation steps are separated by precipitation using chemical additives such as slaked lime ($Ca(OH)_2$). Other impurities are removed by various processes including solvent extraction, filtration, and ion exchange. The purified brine concentrate is treated with sodium carbonate to produce lithium carbonate that is subsequently filtered, water washed and dried to produce a pure lithium carbonate product. The specific processing steps can vary between deposits depending on their chemistry and can result in the production of various valuable by-products (e.g., potash, magnesium hydroxide, boric acid).

To date, evaporative processing is the most conventional and economical method of extracting lithium from brines, primarily because of its reliance on solar energy. The optimal conditions for evaporative brine processing include an arid climate with low rainfall and consistent, unidirectional wind. It also requires large areas of land for the immense series of ponds. While this lithium extraction process offers a lower carbon intensity relative to hard rock mining, it does have various environmental challenges. The chemicals for precipitation and impurity removal along with the associated waste streams have raised socio-environmental concerns (Murphy and Haji, 2022). There is also the risk of compounds leaching from ponds into the environment and contaminating the soil, air, and freshwater sources.

Drawbacks of this extraction method also include the fact that production schedules are measured in months to years and productivity is driven by environmental factors that are impossible to control. As such, this extraction method is uneconomical for low lithium concentration brines. For example, the Salar de Atacama has the world's highest lithium concentration (2,100 ppm) and very high evaporation rates and yet, the process ranges from 12 to 18 months depending on environmental conditions.

As a final consideration, the concentration of other ions in the brine can limit the applicability of evaporative processing. The concentrations of major ions (K^+, Na^+, Cl^-, SO_4^{2-}, Mg^{2+}, and Ca^{2+}) can be orders of magnitude higher than the concentration of Li^+. A key parameter of interest is the mass ratio of Mg^{2+}/Li^+. High amounts of Mg^{2+} slow the evaporation process and prevent lithium chloride formation. Additionally, higher amounts of precipitant are required leading to higher operating costs. There are, however, examples of the use of alternative precipitant extraction methods (e.g., aluminate method) that allows brines with high Mg^{2+}/Li^+ ratios to be concentrated to supersaturation through chemical reactions (Murphy and Haji, 2022). Nonetheless, evaporative processing is typically not considered economically viable for brines with a Mg^{2+}/Li^+ mass ratio of >10.

Direct Lithium Extraction from Brines

Given the challenges and limitations of lithium extraction of brines through evaporative processing, a variety of processes labelled as Direct Lithium Extraction (DLE) have been investigated and developed to increase the efficiency of lithium production from brines. Methods under development include solvent extraction, adsorption, ion exchange, membrane filtration, electrochemical processes, and various combinations of these technologies.

While some of these processes are relatively new to lithium extraction, they are already used in the production of other commodities at a commercial scale. DLE developments are focused on providing economically viable alternatives to evaporative processing, particularly for brines with relatively low Li^+ concentrations and high Mg^{2+}/Li^+ mass ratios. In addition, research and development are underway for the application of certain DLE technologies for lithium extraction of seawater. While seawater has a very low concentration of lithium (0.1–0.2 ppm), it is available to many nations and is estimated globally to contain 230 gigatonnes of Li^+ (Yang, 2018).

To date, the main challenges of DLE have been the technologies' selectivity of Li^+ versus other ions, separation efficiency, recovery rates, and lifetime. Various pilot projects using adsorption, ion exchange, or solvent extraction in different countries including Canada, France, U.S., Germany, and Argentina have proven the technical feasibility of DLE processes (IEA, 2023). However, the technology is still considered to be at a pre-commercial level when looking at its Technology Readiness Level (TRL).

The following sections provide an overview of the various DLE processes *(figure 2.18)* and are not an exhaustive list. Given the growth within the field of DLE, many recent technology reviews are available providing details of DLE processes (Murphy, 2022; and Liu, 2023). While DLE processes are advancing, it is important to note that oilfield and geothermal brines present unique challenges (e.g., organic content) to DLE processes that otherwise have been proven to be successful for other types of brines (Leece, 2023).

2.18 Direct Lithium Extraction Techniques

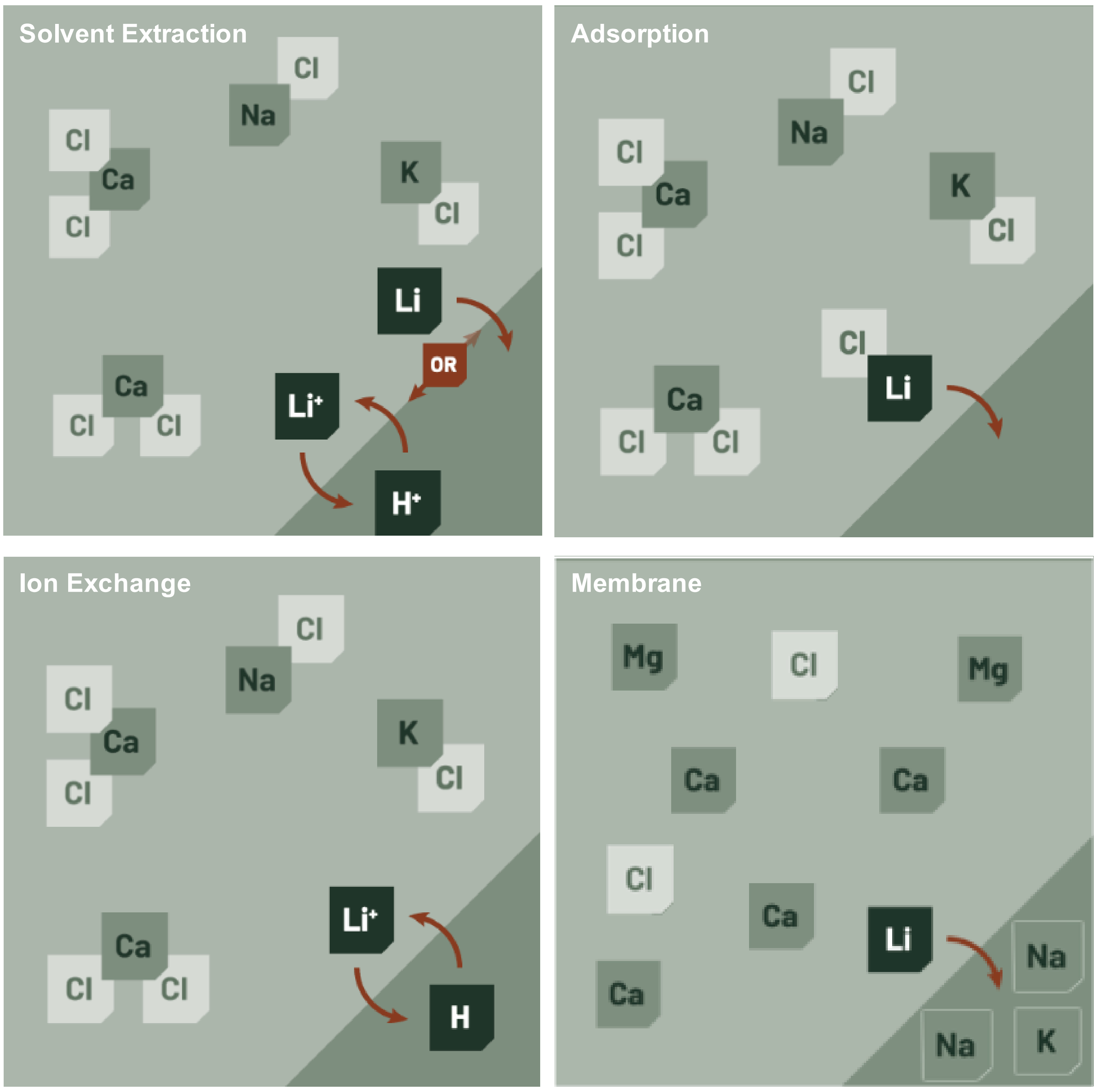

Modified from Prairie Lithium, 2023

© Canadian Discovery Ltd.

Figure 2.18

Solvent Extraction

Solvent extraction or liquid-liquid extraction (LLE) is a separation process that relies on the relative solubilities of a compound in two immiscible liquids: an organic phase and an aqueous phase. It is used widely in the metallurgical and chemical industries and its development for lithium extraction has grown rapidly.

The organic solution is first mixed with the aqueous brine solution whereby organic Li^+ complexes are formed along with complexes of other metals (Na^+, Mg^{2+}, Ca^{2+}). The lithium complexes and some impurity metals are transferred to the organic phase. The solvent extraction step is followed by a scrubbing stage to further remove impurities, and finally, the stripping stage (typically using acid) that produces high-purity lithium in solution. This extraction method can be used in conjunction with other methods to create a scrubbed and refined lithium hydroxide or lithium carbonate product.

Due to the variation in chemical concentrations of brines, the selection of a suitable solvent is a key element to consider. Groups have studied the use of various extractants including chelating, acidic and ionic liquid extractants (Murphy and Haji, 2022). One of the most commonly used systems is tributyl phosphate (TBP) combined with iron trichloride ($FeCl_3$) (Liu, 2023).

Solvent extraction is typically a stand-alone extraction process that does not require pre-concentrating Li^+ like other alternative processes. However, high concentrations of other metal impurities (e.g., Mg^{2+}) may require pre-treatment. Solvent extraction can also achieve high concentrations of lithium, limited by the theoretical solubility of lithium in the solvent. Some of the disadvantages of this technology include:

- Organic solvents have associated safety (including fire) and environmental risks
- Residual brine may require post-treatment to remove traces of solvent prior to disposal
- High volumes of acid are consumed and waste generated during the scrubbing and stripping stages
- The process fluids are corrosive and require particular attention to materials of construction and their inspection to mitigate the risks of loss of containment.

Adsorption

Adsorption is quickly becoming the most developed DLE technology with many projects employing it to some degree (Goldman Sachs, 2023). The process relies on the use of sorbents that are highly selective to the target compound. The materials are typically synthetic resin beads with tailored physical and chemical structures.

Adsorption's use in DLE relies on lithium chloride molecules from the brines permeating the atomic layers of the sorbent material. Once the sorbent material's interstitial space has been saturated with LiCl, it is then stripped, typically using warm-hot water. The loaded sorbent is then washed with a diluted lithium chloride stream to remove unwanted ions and then washed a second time to unload the lithium chloride.

This process does not require reagents apart from dilute salt solutions and the sorbent material can be reused. Some sorbents have been found to recover >90% of the lithium present. The latest materials being tested include lithium aluminum layered double hydroxide chloride (Al-LDH) sorbents.

Ion Exchange

Ion exchange is a well-known two-step process found throughout industrial applications as it separates ionic compounds from solution through a physicochemical process. Ions within a solid material are replaced with the targeted ions where both the targeted and displaced ions have the same electrical charge. The materials are designed to act as a sieve (thus called ionic sieves), such that only the target ion and its replacement are able to pass through and be exchanged.

In the case of DLE, the material porosity is such that only lithium and hydrogen ions are able to pass through. During the first step, lithium ions from the brine are adsorbed and are exchanged with H^+. The lithium-loaded ion sieves are then regenerated using acid allowing for the replacement of Li^+ with H^+ and the production of lithium. The ion exchange process is sensitive to pH, temperature, and stream composition. Similar to other DLE processes, ion exchange is expected to reach recoveries of 90% or greater.

One of the major challenges facing certain ion sieves is the loss of capacity, selectivity, and separation efficiency during the cycling between the adsorption/desorption process. Biofouling and the use of acid treatment for regeneration are two causes (Murphy and Haji, 2022). Organic compounds in the brine can have a significant impact on the process performance and certain pre-treatment processes have been proposed to remove organic compounds prior to ion exchange (Leece and Jiang, 2023).

Nevertheless, ion sieves demonstrate overall high Li^+ adsorption and selectivity. Additionally, ion sieves are not impacted by competing ions such as Na^+, K^+, Na^{2+} and $Mg^{2+}$and they demonstrate higher theoretical uptake capacity. This makes ion sieves well suited to lithium extraction from brines with Li^+ concentrations below 30 ppm and high Mg^{2+}/Li^+ mass ratios (Murphy and Haji, 2022).

Membranes

Membranes are commonly used in filtration systems throughout industry, particularly in water treatment applications. Their use for lithium extraction from brines is relatively recent. In the process, water is forced by a pressure differential through a semi-permeable membrane where larger molecules are prevented from passing through due to pore size and selective permeability. In the case of DLE, the membranes are designed to selectively allow smaller monovalent ions (e.g., Li^+) to pass through while retaining larger multivalent ions (e.g., Mg^{2+}).

The process has been demonstrated to work on high Mg^{2+}/Li^+ brines providing high rejection of Mg^{2+} and low rejection (loss) of Li^+ (Leece and Jiang, 2023). However, the presence of Na^+ and K^+ presents a challenge as these monovalent ions pass through the membrane and require additional treatment steps. Similar to ion sieves, organic content in the brine will cause fouling and degradation of the membranes and thus, must be removed in a pre-treatment step. Operating costs can be high as large volumes of brine are pumped at high pressure through the membrane systems.

Other DLE Methods

Ion-imprinted membranes have also been investigated for DLE applications. They are the combined product of membrane separation and ion-imprinting techniques where the latter is a technique that mimics the "lock and key" interaction between natural receptors and ligands[1]. Ion-imprinted membranes leverage the functionality of both technologies allowing for selectively separating and detecting target ions. The overall process is sensitive to pH, temperature, extraction time and the ratio of components in the membrane (including ligands and functional monomers) (Murphy and Haji, 2022).

Electrochemical lithium extraction techniques are another set of DLE processes. They use electricity to drive ion-separation often coupled with membrane separation. Electrochemical extraction processes are particularly attractive for high Mg^{2+}/Li^+ and low Li^+ concentration brines for a number of reasons including their environmental sustainability and attractive processing performance (good recovery capacity, scalability, cycling efficiency and selectivity) (Murphy and Haji, 2022). The drawbacks to electrochemical techniques are their relatively high energy consumption and material costs.

---

[1] An ion or molecule with a functional group that binds to the receptor.

2.19 Western Canada Brine-Hosted Lithium Crown Majority Rights Map

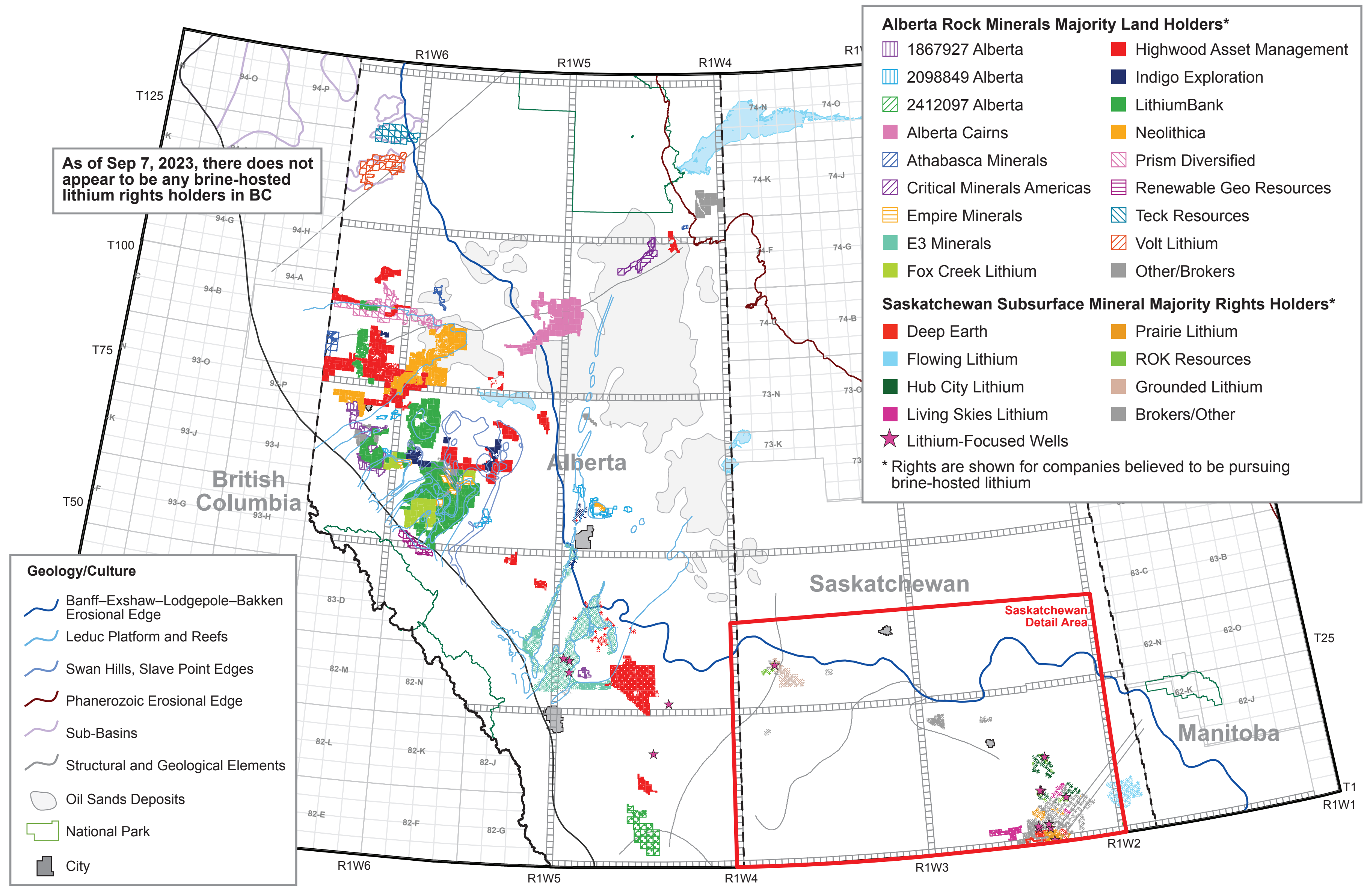

Data current to August 9, 2023.
Land data supplied by geoLOGIC. Reefs from the Geological Atlas of the Western Canada Sedimentary Basin, 1994

© Canadian Discovery Ltd. *Figure 2.19*

Lithium Tenure Framework

National

The 2022 Canadian Federal Budget proposed a new 30% critical mineral exploration flow-through tax credit for specified mineral exploration expenses incurred in Canada (Grieve et. al, 2023). This incentive includes minerals in solution such as lithium.

In Canada, National Instrument (NI) 43-101 is a mineral resource classification scheme used to disclose information about mineral exploration properties. Foreign and domestic companies listing on stock exchanges overseen by the Canadian Securities Administration (CSA) are required to abide by the NI 43-101 rules and guidelines for displaying information related to mineral properties (Lyons, 2023).

The following sections describe the current regulatory framework for oilfield and geothermal brine lithium resources in Western Canada.

British Columbia

In British Columbia (BC), if host formation brine is at or above 80°C when produced to surface, the rights to lithium are included in geothermal resources under the Geothermal Resources Act, specifically as part of "all substances dissolved in the steam, water or water vapour obtained from a well". If formation brine is lower than 80°C when produced to surface, geothermal tenure cannot be acquired (including any associated lithium in the brine). At the time of this report, there is no other mechanism in BC, other than through the Geothermal Resources Act, to acquire lithium tenure, either as a constituent of brine or through mining under the Mineral Tenure Act. A modification of these existing rights to allow development of brine-hosted minerals is currently under review (Donaldson, 2022).

Alberta

In Alberta, lithium resources, along with those of surficial deposits such as sand and gravel and any mineable substance (excluding oil sands and coal) are included under Metallic and Industrial Mineral (MIM) Rights and must be obtained separately from Petroleum and Natural Gas (P&NG) rights, even if they are hosted within an oil and/or gas producing geological zone. In December 2022, the Alberta Government modified this existing MIM tenure regulation to recognize both rock-hosted minerals and brine-hosted minerals (such as lithium). The new regulation provides specific tenure requirements for these two types of metallic and industrial minerals (AER, 2022). Beginning January 1, 2023, new tenure for lithium (and other brine-hosted minerals) will be granted via leases issued through a public offering, similar to how Alberta P&NG rights are presently obtained, and also more in line with the mineral tenure process in Saskatchewan (Podetz, 2023).

To summarize, oil and gas operators in areas of lithium-rich formation water have no legal ownership of lithium in those brines without also holding a MIM permit. This situation provides monopoly holders of lithium rights permits with a unique opportunity to partner with oil and gas tenure holders in Alberta, as exemplified by the collaboration between Imperial Oil and E3 Lithium's Clearwater project, which will produce lithium from the Leduc Field that was discovered in 1947 (Imperial Oil, 2023). *Figure 2.19* shows the distribution of MIM permits and leases within Alberta and Saskatchewan.

Saskatchewan

In Saskatchewan, rights to brine minerals are included under "Subsurface Mineral Rights", and are also separate from P&NG rights, but have been granted via a competitive bid process since December 2018. Rights are posted for bid three times a year in April, August, and December.

The extractive rights to subsurface minerals include "all natural mineral salts of boron, calcium, lithium, magnesium, potassium, sodium, bromine, chlorine, fluorine, iodine, nitrogen, phosphorus and sulfur, and their compounds, occurring more than sixty meters below the surface of the land"(Saskatchewan Energy and Resources, 2022). P&NG rights and subsurface minerals rights in the same area can belong to different companies for different purposes. As in Alberta, Saskatchewan oil and gas operators do not own the rights to the lithium within the brines they are producing.

Summary

The development of petro-lithium from the WCSB as a resource provides a means of leveraging existing oil and gas infrastructure, along with technical expertise, to provide a mineral that is crucial to technologies and energy solutions needed to reach climate goals. Collaborative relationships with oil and gas operators can provide an alternative to well and other infrastructure retirement in some end-of-life oil and gas fields, and a consequent reduction of liability for those operators. Saline formation brines that would otherwise be wastewater requiring disposal can be turned into a valuable resource.

References

- Abercrombie, H. J., Hutcheon, I. E., Bloch, J. D., de Caritat, P.; Silica activity and the smectite-illite reaction. Geology 1994. v. 22 (6): 539–542. doi: https://doi.org/10.1130/0091-7613(1994)022<0539:SAATSI>2.3.CO;2
- Alberta Energy Regulator (AER). 2022. Accessed September 2023. https://www.aer.ca/providing-information/by-topic/emerging-resources/mineral-resource-development
- Bishop, B. A., Robbins, L. J., 2023. Overview of potential lithium sources in the WCSB. Geoconvention 2023 abstract.
- Bowell, R., J., 2020. Classification and Characteristics of Natural Lithium Resources. Elements 2020, v. 16 (4), p. 259-264. doi:https://doi.org/10.2138/gselements.16.4.259
- Bradley, D.C., Stillings, L.L., Jaskula, B.W., Munk, LeeAnn, and McCauley, A.D., 2017, Lithium, chap. K of Schulz, K.J., DeYoung, J.H., Jr., Seal, R.R., II, and Bradley, D.C., eds., Critical mineral resources of the United States—Economic and environmental geology and prospects for future supply: U.S. Geological Survey Professional Paper 1802, p. K1–K21, https://doi.org/10.3133/pp1802K.
- British Geological Survey (BGS), 2016. Lithium. HYPERLINK "http://www.MineralsUK.com"www.MineralsUK.com. Grieve, S. A. J. R., Khan, A. A., Ward, P. B., Arrigo, N., Singh, S. G. K., 2023. Bennett Jones. https://www.bennettjones.com/Blogs-Section/Government-of-Canada-Trying-to-Focus-Policies-to-Make-Electric-Vehicles-Go
- Brown, T., Walters, A., Iodine, N., Gunn, G., Shaw, R. A., Rayner, D., British Geological Survey, Natural Environment Research Council. 2016. Lithium Profile.
- Bunker, Edward, Bolton, R., Crossley, R., Broadley, M., Thomas, A. 2022. Lithium Exploration Tools from Source to Sink. https://geoconvention.com/wp-content/uploads/abstracts/2022/73906-lithium-exploration-tools-from-source-to-sink.pdf
- Darcy Partners, 2023. An Introduction to Direct Lithium Extraction. https://darcypartners.com/research/an-introduction-to-direct-lithium-extraction-dle

- Donaldson, W.S. Canadian Discovery. 2022. 2022 Western Canada Year in Review: Critical Minerals Development, 2023. https://digest.canadiandiscovery.com/pdf?query=[{%22name%22:%22excludeComingSoon%22,%22value%22:%22true%22}]&id=8627&url=/private/CDD/articles/2023_02_Feb14_2021_StrategicMinerals.pdf
- Dugamin, E. J., Cathelineau, M., Boiron, M. C., Richard, A., Despinois, F. 2023. Chemical Geology, volume 635, Lithium enrichment processes in sedimentary formation waters. https://doi.org/10.1016/j.chemgeo.2023.121626.
- Eccles, D.R. and Jean, G.M. 2010. Lithium Groundwater and Formation-Water Geochemical Data. ERCB/AGS Digital Dataset 2010-0001 (tabular data, tab delimited format). https://static.ags.aer.ca/files/document/OFR/OFR_2011_10.pdf
- Eccles, D.R. and Berhane, H. 2011. Geological Introduction to Lithium-Rich Formation Water with Emphasis on the Fox Creek Area of West-Central Alberta (NTS 83F and 83K). ERCB/AGS Open File Report 2011-10.
- European Lithium, 2023. https://europeanlithium.com/lithium/
- Forbes, 2023. The Energy Transition Will Transform The Mining Industry. https://www.forbes.com/sites/woodmackenzie/2023/03/10/the-energy-transition-will-transform-the-mining-industry/?sh=17ffe9225c3f
- Fouillac, C., Michard, G., 1989. Solidum/lithium ratio in water applied to geothermometry of geothermal reservoirs, Geothermics, v. 10, issue 1, p. 55-70. https://doi.org/10.1016/0375-6505(81)90025-0
- Goldman Sachs. 2023. Direct Lithium Extraction: A Potential Game Changing Technology. Equity Research.
- Government of Canada, 2023. https://www.canada.ca/en/services/environment/weather/climatechange/climate-plan/net-zero-emissions-2050/canadian-net-zero-emissions-accountability-act.html
- Grieve, S. A. J. R., Khan, A. A., Ward, P. B., Arrigo, N., Singh, S. G. K., 2023. Bennett Jones. HYPERLINK "https://ww" https://www.bennettjones.com/Blogs-Section/Government-of-Canada-Trying-to-Focus-Policies-to-Make-Electric-Vehicles-Go
- Hitchon, B, Underschultz, J.R. and Bachu, S. 1993. Industrial mineral potential of Alberta formation waters. Alberta Research Council/Alberta Geological Survey Open File Report 1993-15.
- Huff, G.F. 2016. Evolution of Li-enriched oilfield brines in Devonian carbonates of the south-central Alberta Basin, Canada. Bulletin of Canadian Petroleum Geology, v. 64, pp. 438-448.
- IEA, 2023. ETP Clean Energy Technology Guide. https://www.iea.org/data-and-statistics/data-tools/etp-clean-energy-technology-guide. Accessed September 2023.
- Imperial Oil, 2023. https://www.imperialoil.ca/en-ca/sustainability/lithium
- Investing News Network. https://investingnews.com/daily/resource-investing/battery-metals-investing/lithium-investing/lithium-deposit-types-brine-pegmatite-and-sedimentary/
- Jensen, K. S. J., Kohlruss, D., 2023. Lithium Concentrations in the Duperow and Red River Formations: Results from Four Cores in Southeastern Saskatchewan. Saskatchewan Geological Survey.
- Kharaka, Y. K., Mariner, R. H., 1989. Chemical geothermometers and their application to formation waters from sedimentary basins.
- Leece, A.S., Jiang, C. 2023. A Preliminary Techno-economic Assessment of Lithium Extraction From Flowback and Produced Water from Unconventional Shale and Tight Hydrocarbon Operations in Western Canada. Geological Survey of Canada. Open File 8975.
- Liu, Y., Ma, B., Lu, Y., Wang, C., Chen, Y. 2023. A Review of Lithium Extraction from Natural Resources. International Journal of Minerals, Metallurgy and Materials. Vol 30., pp 209-221.
- Lopez, G., Weiss, J., Huff, R., 2018. Distribution and origin of lithium-enriched formation water in Alberta.
- Lyons, E. Tekhne Research Inc. 2018. NI 43-101 Technical Report on the Lithium Brines of the Clear Hills Property Alberta, Canada.
- Lyster, S., Hauck, T.E., Lopez, G. P., Playter, T. L., Reimert, C., Palombi, D. and Schultz, S. K., 2022. Lithium and Helium in Alberta: Data Compilation and Preliminary Observations, Alberta Energy Regulator and Alberta Geological Survey, Open File Report 2021-04.
- Mossop, G., Shelten, I., 1994. Atlas of the Western Canadian Sedimentary Basin.
- Murphy, O., Haji, M.N., 2022. A Review of Technologies for Direct Lithium Extraction from Low Li+ Concentration Aqueous Solutions. Frontiers in Chemical Engineering.
- Natural Resources Canada, 2023. https://natural-resources.canada.ca/our-natural-resources/minerals-mining/minerals-metals-facts/lithium-facts/24009

- Podetz, C. 2023. Q4 2022 Quarterly Crown Land Sale Analysis. Accessed September 2023. https://digest.canadiandiscovery.com/article/8612
- Prairie Lithium. https://www.prairielithium.ca/dle-direct-lithium-extraction
- Reuters, 2023. https://www.reuters.com/markets/commodities/lithium-price-slide-deepens-china-battery-giant-bets-cheaper-inputs-2023-02-28/
- Rostron, B., Maurer, Z., Hillier, C., Caplan, M., Kreis, L.K., 2022. Lithium in saline brines from the Duperow Aquifer in Southeastern Saskatchewan. https://www.youtube.com/watch?v=wTa_2DYnwcw
- Rumble, J. R., 2023. CRC The Handbook of Chemistry and Physics 104th edition.
- S&P Global, 2019. Lithium Section: Production Costs Outlook. https://pages.marketintelligence.spglobal.com/lithium-sector-production-costs-outlook-MS-demo-confirmation.html#:~:text=Lithium%20brine%20operations%27%20margins%20are,conversion%20facilities%20near%20their%20operations
- Saskatchewan Energy and Resources, 2022. Guidebook for Lithium from Formation Water (mineral brine) Exploration and Operations. https://www.saskatchewan.ca/business/agriculture-natural-resources-and-industry/mineral-exploration-and-mining/lithium
- Standard Lithium, 2023. https://cleantechnica.com/2021/06/07/interview-with-standard-lithium-ceo-robert-mintak/
- Starkey, H. C., 1982. The Role of Clays in Fixing Lithium, Geological Survey Bulletin 1278-F, Contribution to geochemical prospecting for minerals.
- Tadesse, B., Makuei, F., Albijanic, B., Dyer, L., 2019. The Benefication of Lithium Minerals from Hard Rock ores: A Review. Minerals Engineering, v. 131, pp. 170-184. United Nations, 2023.
- United Nations, 2023. https://unfccc.int/process-and-meetings/the-paris-agreement
- U.S. Geological Survey. Mineral commodity summaries 2023: U.S. Geological Survey, 112 p. https://pubs.usgs.gov/periodicals/mcs2023/mcs2023.pdf
- Warren, I. 2021. Techno-Economic Analysis of Lithium Extraction from Geothermal Brines. National Renewable Energy Laboratory.
- Yang, S., Zhang, F., Ding, H., He, P. Zhou, H. 2018. Lithium Metal Extraction from Seawater. Joule, vol. 2., pp. 1648-1651.

STUDY OVERVIEW

Introduction to the Study

The goals for the Northeastern British Columbia (NEBC) Lithium Formation Water Database are to:

1. Deliver a preliminary inventory dataset of lithium and other dissolved-metal brine data in NEBC via water sampling of wells producing from a variety of geological zones and over a wide geographical area.
2. Incorporate the data into a broader geological and hydrogeological framework and advance the understanding of geological controls and natural variability of lithium in formation waters.
3. Provide a preliminary and high-level assessment of aquifers considering factors such as producibility and economic viability of lithium extraction.

Chapter 2 focuses on an overview of why lithium is an important economic element; where and how it is extracted worldwide; how lithium may become enriched in brines; where it has been sampled in oilfield brines in the Western

3.1 Stratigraphic Chart

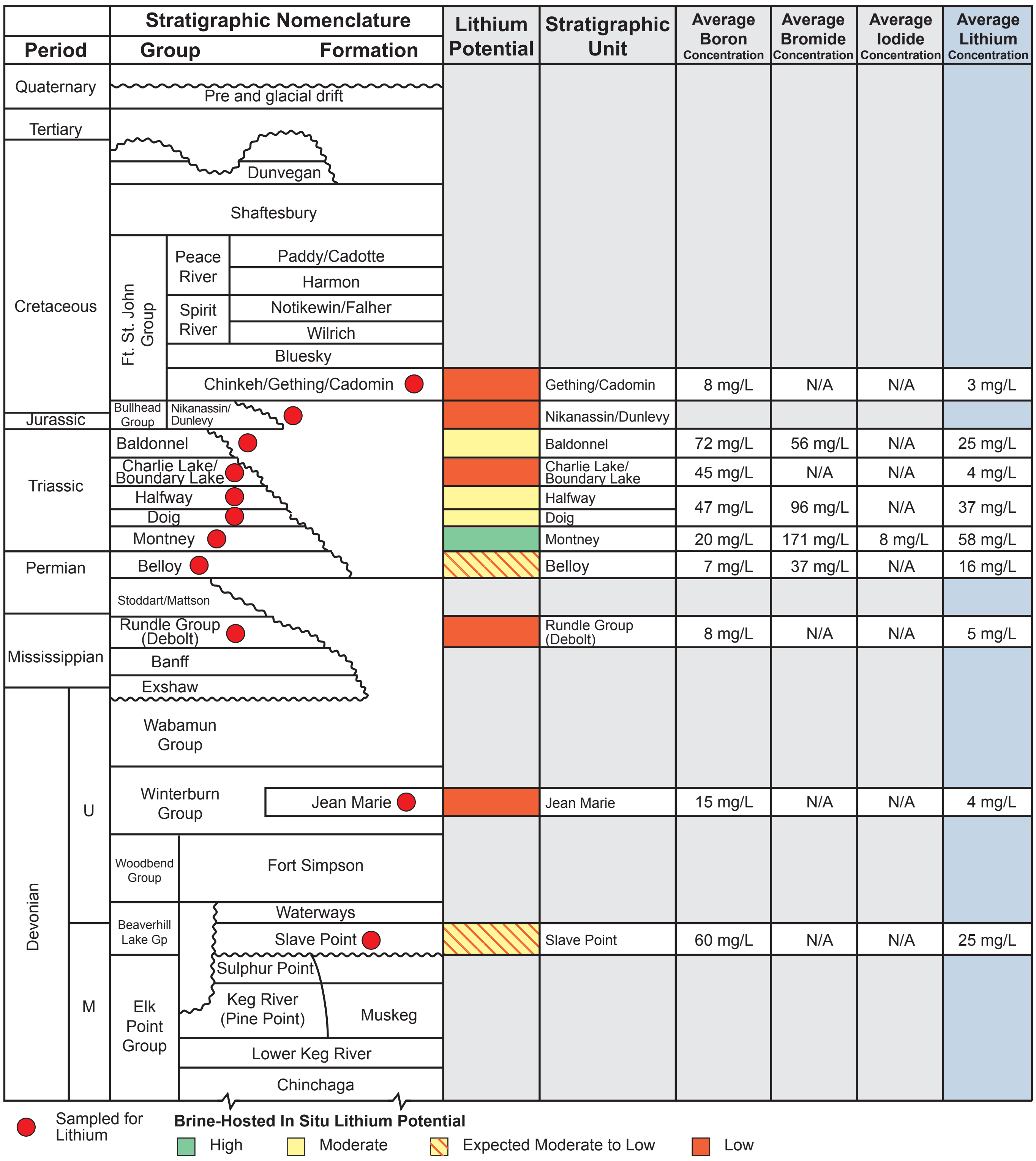

Lithium Potential	Stratigraphic Unit	Average Boron Concentration	Average Bromide Concentration	Average Iodide Concentration	Average Lithium Concentration
🟥	Gething/Cadomin	8 mg/L	N/A	N/A	3 mg/L
🟥	Nikanassin/Dunlevy				
🟨	Baldonnel	72 mg/L	56 mg/L	N/A	25 mg/L
🟥	Charlie Lake/Boundary Lake	45 mg/L	N/A	N/A	4 mg/L
🟨	Halfway	47 mg/L	96 mg/L	N/A	37 mg/L
🟨	Doig				
🟩	Montney	20 mg/L	171 mg/L	8 mg/L	58 mg/L
▨	Belloy	7 mg/L	37 mg/L	N/A	16 mg/L
🟥	Rundle Group (Debolt)	8 mg/L	N/A	N/A	5 mg/L
🟥	Jean Marie	15 mg/L	N/A	N/A	4 mg/L
▨	Slave Point	60 mg/L	N/A	N/A	25 mg/L

● Sampled for Lithium

Brine-Hosted In Situ Lithium Potential
🟩 High 🟨 Moderate ▨ Expected Moderate to Low 🟥 Low

Modified from Bachu (1995) and this study

Figure 3.1

Canada Sedimentary Basin (WCSB); and current technologies that extract lithium from brine. This chapter focuses on how this study addresses the above goals, as well as to provide some information regarding how components of the study were compiled, graphed, and mapped.

Chapter Organization

Chapter 4 focuses on Alberta, which leads Western Canada with respect to the availability of lithium data and investment in lithium brine extraction projects. Graphs and maps show the distribution of lithium data by geological unit, with a discussion of how lithium becomes enriched in brines. The lithium industry in Saskatchewan is also discussed; some of the highest lithium concentrations in the WCSB are found in that province and industry development is growing.

British Columbia becomes the focus starting in *Chapter 5*. Based on the number of samples and the lithium concentration in those samples, the BC chapters are divided into the Montney, Triassic aquifers, and other formations sampled. Each chapter has maps showing lithium data distribution, the distribution of total dissolved solids (TDS), which is used as a proxy for lithium concentration, reservoir quality and the brine-hosted in situ lithium potential (when calculated). There are also graph suites showing water chemistry and several other key factors.

The stratigraphic chart *(figure 3.1)* outlines the formations that exist in the subsurface of the study area. The red circles indicate formations that were sampled for this study, while the colour-coding in the Lithium Potential column indicates the interpreted potential of the formation to host economic concentrations of lithium within oilfield brines. Not all of the samples collected reached the current economic cutoff of 50 mg/L for lithium production. However, the correlation between TDS and lithium concentration suggests that there may be areas in several formations that could be prospective for economic lithium concentrations.

Formation Selection and Exclusion Criteria

Water sample data collected for this study were screened (see *Appendix C* for exact criteria), then were sorted into geological units and processed for statistics such as the maximum, minimum, median and average values. The Montney formation stood out, with several samples in the economic range (>50 mg/L) to warrant its own chapter. The sparsely sampled Halfway, Doig and Baldonnel formations were grouped into a Triassic aquifers chapter as some samples approach the economic limit, and the correlation between lithium concentrations and TDS, discussed in the *Montney chapter 5*, suggests that there could be lithium potential in areas not yet sampled. The rest of the sampled formations have low lithium potential based on the lithium concentration in the samples and the TDS correlation; these were grouped into their own chapter.

The data collected for this study were combined with Alberta Geological Survey (AGS) data, Geological Survey of Canada (GSC) data, and routine water chemistry data downloaded from geoLOGIC. All water samples in the various datasets were screened for pH imbalances and the presence of alcohols, mud filtrates, and corrosion inhibitors. For more detail, see the Appendices:

- *Appendix A* is the compiled lithium public datasets.
- *Appendix B* describes the sampling methods and analytical procedures followed for this study's data.
- *Appendix C* contains the water chemistry screening criteria.
- *Appendix D* is a table of whole rock lithium concentrations.
- *Appendix E* provides a list of lithium article references.
- *Appendix F* is a table of seawater ion concentrations for a number of ions.

Atlas Components

The formation chapters have a brief geological write-up and schematic to give general geological depositional information and stratigraphy of the formation(s). As this study is a high-level regional overview, the formation deposition and descriptions are generalized to encompass a broad area. Various maps indicate the distribution of lithium data, net reservoir mapping, and TDS mapping, and a summary map brings together the salient points. For the Montney, a high-level estimate of brine-hosted in situ lithium potential is included. Suites of graphs and crossplots provide insights on aspects of lithium-enrichment.

The *Montney chapter 5* has more detail as there are more sample data and lithium concentrations that exceed the current economic cutoff of 50 mg/L. As the Montney is not an aquifer, water production is addressed with a water production map and a suite of graphs showing water production through time in several areas. A lithium concentration map is presented that was interpreted using a number of inter-dependent variables. A high-level economic case study outlines the number of wells needed to produce economic amounts of lithium from a facility at three levels of water production.

Brine-Hosted In Situ Lithium Potential Calculation

High-level brine-hosted, in situ lithium potential volume calculations were done for the Montney using previously mapped pore volumes, water saturations, TDS concentrations, and applying a lithium concentration mapped for this study. The calculations were restricted to areas where the TDS exceeds 150 g/L, based on the correlation between lithium concentration and TDS developed in the Montney chapter.

ALBERTA AND SASKATCHEWAN OVERVIEW

Alberta and Saskatchewan Lithium Overview

The brine-hosted lithium industry is more advanced in both Alberta and Saskatchewan. Both provinces have numerous samples that exceed 75 mg/L *(figure 4.1)*. Several projects and pilots are underway in both provinces.

Table 4.1: Alberta Lithium Samples by Geologic Age

	Geologic Age	Lithium Samples (#)
🟩	Cretaceous	556
🟦	Jurassic	32
🟪	Triassic	72
🟥	Permian	8
🟪	Mississippian	63
🟫	Devonian	607
🟧	Cambrian	1
⬜	Undefined	721

Table 4.1

Alberta

Alberta leads Western Canada with respect to the availability of lithium analysis data from sedimentary basin brines and investment into lithium brine extraction projects. Elevated lithium concentrations in Alberta's oilfield brines were known as early as 1993 through the development of the Geofluids database by Rakhit Petroleum Consulting in conjunction with the Alberta Research Council. The industrial mineral potential in sedimentary formation brines was initially published by Hitchon et al., (1993) using 130,000 routine formation water analyses. Lithium was reported in 708 samples and exceeded 75 mg/L in 46 samples of Devonian-aged brines. In the 30 years since that publication, the lithium database in Alberta has expanded and several papers have advanced the understanding of lithium distribution and potential enrichment processes in the province (Eccles and Berhane, 2011; Huff, 2016; Huff, 2019; Lyster et al., 2022). To date, there are over 2,000 data points with lithium concentrations in Alberta. *Table 4.1* breaks down the database based on the geologic age of the sampled formation—over 50 unique formations are represented.

4.1 Western Canada Lithium Concentration Map

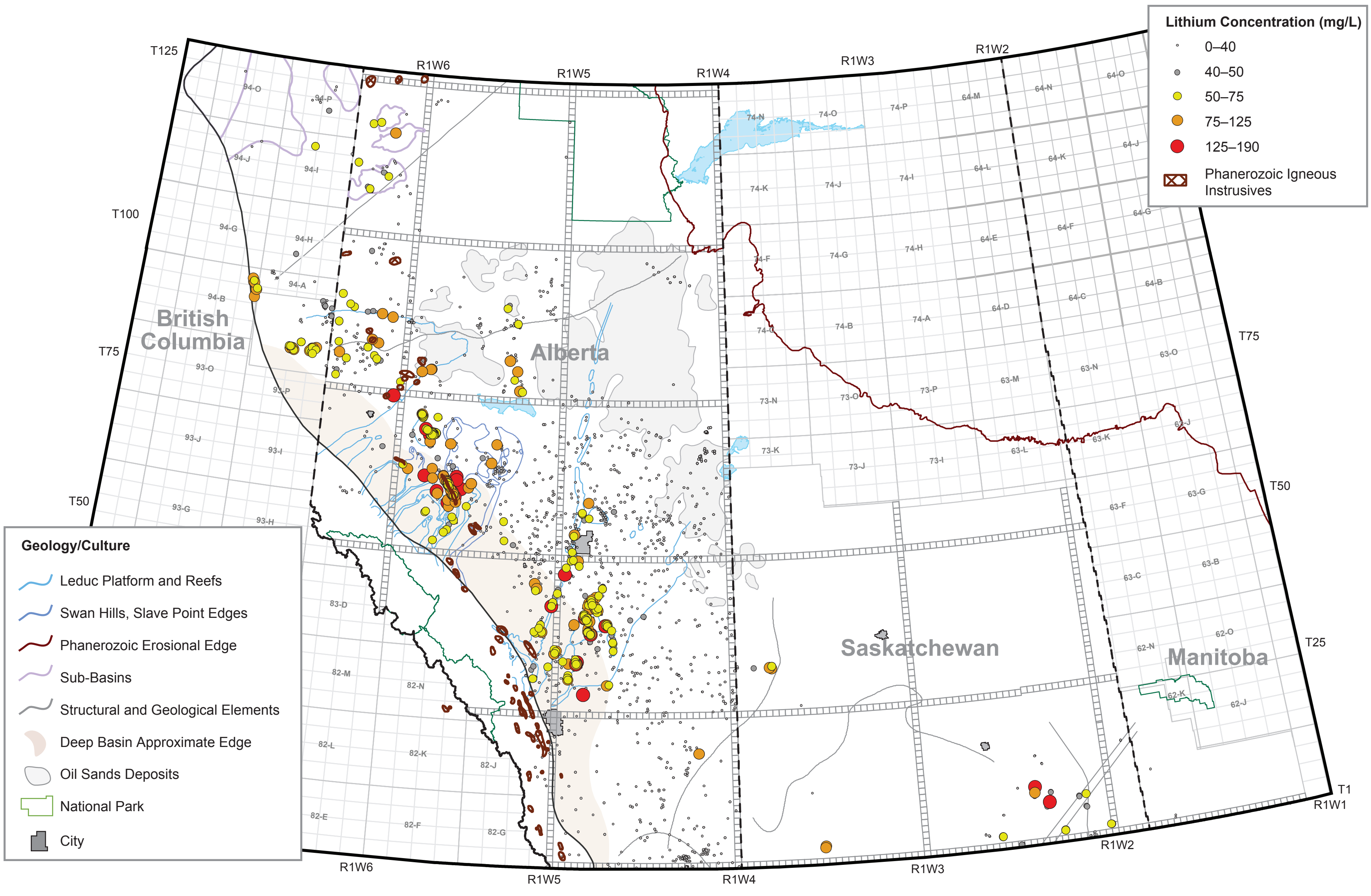

Lithium data from this study, AGS, SGS, GSC; Leduc reefs from WCSB Atlas, 1994

Figure 4.1

4.2 | Alberta Lithium Concentrations by Geological Age Map

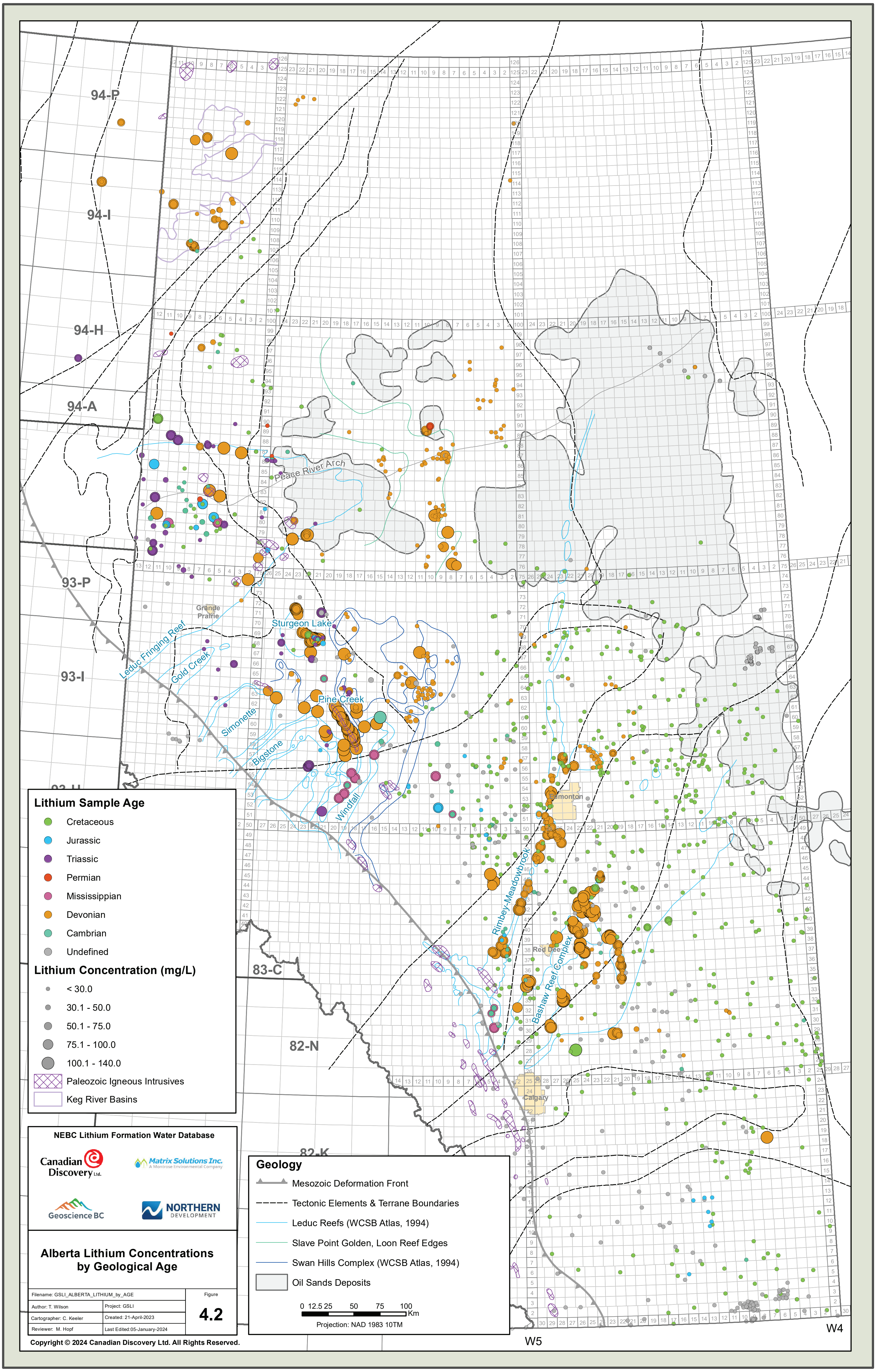

© Canadian Discovery Ltd. *Figure 4.2*

4.3 Alberta Lithium Metrics by Age

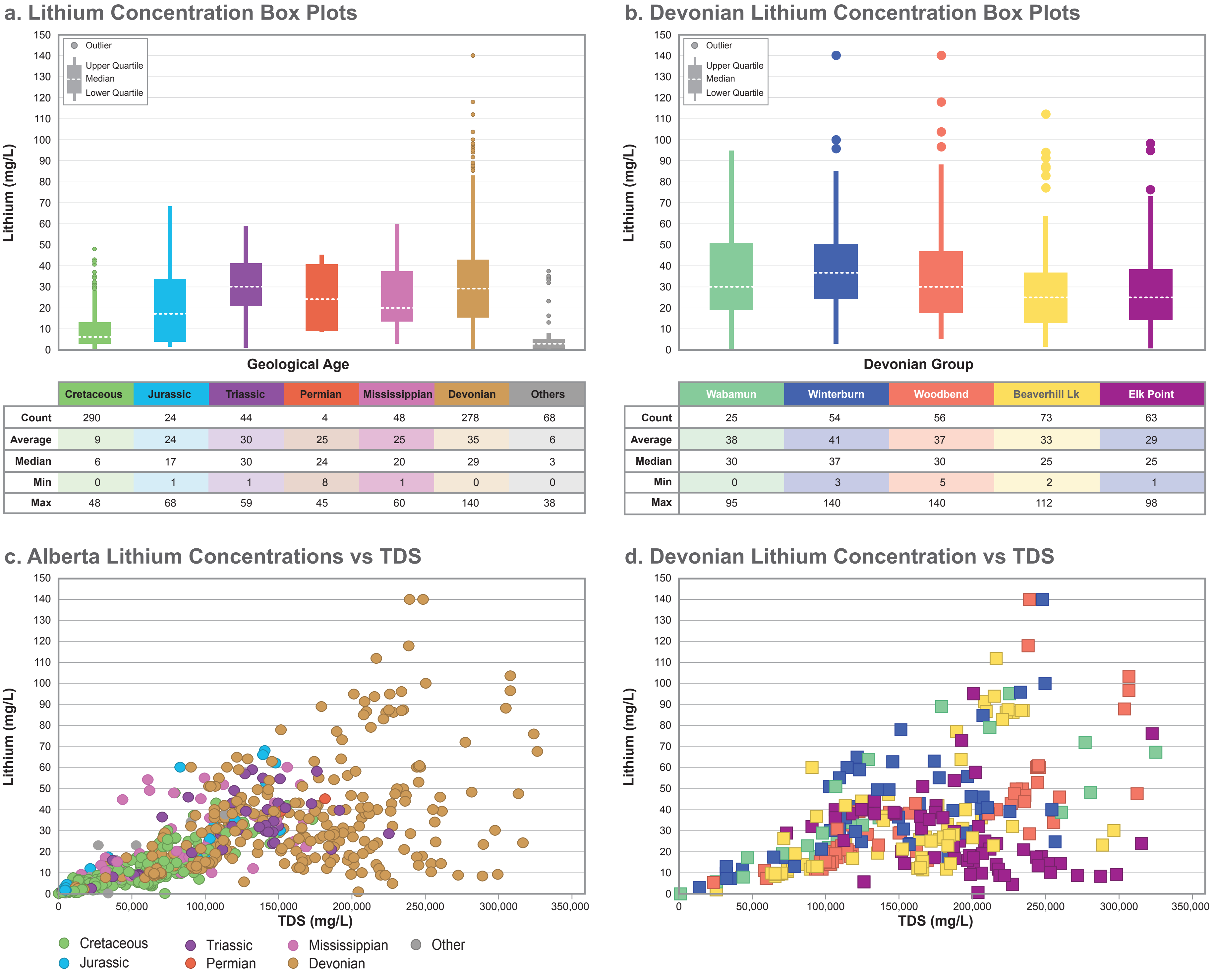

	Cretaceous	Jurassic	Triassic	Permian	Mississippian	Devonian	Others
Count	290	24	44	4	48	278	68
Average	9	24	30	25	25	35	6
Median	6	17	30	24	20	29	3
Min	0	1	1	8	1	0	0
Max	48	68	59	45	60	140	38

	Wabamun	Winterburn	Woodbend	Beaverhill Lk	Elk Point
Count	25	54	56	73	63
Average	38	41	37	33	29
Median	30	37	30	25	25
Min	0	3	5	2	1
Max	95	140	140	112	98

Data source AGS.

© Canadian Discovery Ltd.

Figure 4.3

Approximately 20% of the samples were analyzed for isotopes of hydrogen (δ^{2}H), oxygen (δ^{18}O), and strontium (^{87}Sr/^{86}Sr), with fewer samples analyzed for an additional suite of isotopic data (lithium, boron, sulphate, chloride) and dissolved inorganic carbon and dissolved organic carbon.

The Alberta lithium database has proved to be an excellent resource laying the groundwork for numerous exploration and appraisal projects in the province. This chapter analyzes the Alberta database, provides commentary on proposed lithium-enrichment mechanisms, and lays out the workflow used by prior authors and Canadian Discovery for analyzing lithium and water chemistry data.

Data Distribution and Analytics

The overall sample population has a representation bias from the most historically productive oil and gas reservoirs, namely the Devonian and Cretaceous. However, there are sufficient data to characterize the Cretaceous, Jurassic, Triassic, Permian, Mississippian and Devonian strata *(figure 4.2 and table 4.1)*.

After screening for ion imbalance and contamination (see *Appendix C* for screening procedures), the resulting dataset contains over 1,400 samples. Devonian samples have the highest individual lithium concentrations and the highest average lithium concentration at 140 mg/L and 35 mg/L respectively *(figure 4.3a)*. Triassic samples have the second highest average lithium concentration at 30 mg/L with a high of 59 mg/L. The sampled Triassic formation waters include the Montney, Halfway and Doig formations, with the Montney being the most lithium enriched. *Figure 4.3b* shows the range of data for the Devonian samples.

Other data of note are some moderately enriched Mississippian samples proximal to the Leduc Windfall trend in west-central Alberta and Jurassic samples in the Peace River Arch area *(figure 4.2)*. Lithium concentrations are less than 30 mg/L for most Cretaceous samples, and the average Cretaceous concentration is 9 mg/L. There is a rough correlation between lithium and total dissolved solids (TDS), with elevated lithium corresponding to brines exceeding 150,000 mg/L *(figures 4.3c and d)*. The relationship between lithium concentrations and TDS is described in detail in the following chapter. There are numerous ways to visualize and analyze ion and isotope chemistry data to understand the evolutionary pathways of formation waters and their relationship to lithium enrichment. For this section, the data are presented in a series of crossplots, some of which follow the workflows laid out by Eccles and Berhane (2011) and Huff (2016).

Below is an excerpt from Huff, (2016) that provides an overview of prior work conducted in Alberta and some of the proposed concentration mechanisms. Note that figures and references from Huff, (2016) are not included herein and the reader is referred to the original article for further details.

"There is a long and extensive history of study regarding the origins and characteristics of brines within the Alberta Basin of Canada (Fig. 1). White (1965) argued that brines of the Alberta Basin are connate in origin while Clayton et al. (1966) argued for complete flushing of the basin. Additional mechanisms advanced to explain the composition of Alberta Basin brines include membrane filtration coupled with halite precipitation (Billings et al., 1969), membrane filtration coupled with freshwater dilution (Hitchon et al., 1971) and diagenetic modification of seawater coupled with freshwater dilution (Hitchon and Friedman, 1969). In more recent work, Connolly et al. (1990a; b) proposed evaporation of seawater beyond halite saturation with subsequent dilution by meteoric water. Michael and Bachu (2002) proposed evapoconcentration of seawater combined with the effects of dolomitization, halite dissolution and dilution with meteoric water. Michael et al. (2003) proposed seawater evapoconcentration beyond gypsum but less than halite saturation combined with the effects of dolomitization, clay mineral and gypsum dewatering, sulphate reduction and halite dissolution. Gupta et al. (2012) proposed the presence of brine endmembers formed through evapoconcentration of seawater beyond halite saturation and through dissolution of halite coupled with mixing with seawater and meteoric water. The numerous and varied mechanisms proposed for the origin of Alberta Basin brines reflect the potentially complex history of these waters.

Enrichment of oilfield brines in Li has been documented in the Devonian of the Williston Basin in North Dakota, the Jurassic Smackover Formation of the US Gulf Coast, the Cretaceous of Texas and the southern coastal plain of Israel (Collins, 1976; Chan et al., 2002; Garrett, 2004). Li-enrichment of brines within Devonian carbonates of the Alberta Basin has been reported by Hitchon et al. (1993), Underschultz et al. (1994), Bachu et al. (1995) and Eccles and Berhane (2011). Hitchon et al. (1993) observed that Li concentrations increased with increasing brine salinity. Eccles and Berhane (2011) observed that Li concentrations in brines in the Swan Hills Formation correlated with radiogenically-enriched $^{87}Sr/^{86}Sr$ values and noted that these brines were associated with dolomitized carbonates. Furthermore, Eccles and Berhane (2011) argued that these Li-enriched brines had not been evapoconcentrated past halite saturation, lacked a meteoric water component and had become Li-enriched through mixing with fluids expelled from crystalline basement rocks."

Devonian Data Distribution and Analysis

This section focuses on the data distribution and observed trends for the Devonian Wabamun, Winterburn, Woodbend, Beaverhill Lake and Elk Point groups *(figures 4.4 and 4.5)*.

The chloride/bromide (Cl/Br) vs sodium/bromide (Na/Br) plot is an indicator of formation water chemistry evolution relative to seawater *(figure 4.5a)*. Data plotting below and to the left of seawater (Winterburn, Woodbend and Elk Point) are interpreted to represent evolution through evapoconcentration. Data that plot above and to the right of seawater are generally representative of halite dissolution; these are predominantly from the Beaverhill Lake Group and a limited subset from the Woodbend. It is likely that other controlling mechanisms impact these observations, which are discussed below using additional multi-variate analysis.

The potassium/bromide (K/Br) vs chloride/bromide (Cl/Br) plot is used to determine the extent of water-rock interaction with potassium feldspars, commonly found in volcanic rocks *(figure 4.5b)*. There appear to be two distinct clusters of data where K/Br ratio is depleted for the majority of Beaverhill Lake and the Elk Point samples and elevated for the Winterburn and Woodbend with the Wabamun samples straddling both trends. These data suggest that water-rock interaction with volcanically sourced feldspars may have been limited both temporally and areally in the Devonian. The location and potential contribution of volcanics in the Devonian has been discussed by Davies et al. (2006), who reported a widespread volcanic event at the Devonian-Mississippian boundary.

The magnesium/chloride (Mg/Cl) and calcium/chloride (Ca/Cl) crossplots are indicative of potential dolomitization through water-rock interactions or subsequent hydrothermal processes *(figures 4.5c and d)*. Magnesium concentration decreases with increased dolomitization—as magnesium replaces calcium in carbonate minerals with a corresponding enrichment of brines relative to seawater. Note that the majority of the Devonian data follow a similar pattern of magnesium- and calcium-enrichment with increasing chloride content, presumably as a function of seawater evaporation. A population of Beaverhill Lake samples appears depleted in both magnesium and calcium relative to other Devonian waters. Potassium (K) appears to have a strong correlation to lithium content across all the Devonian samples *(figure 4.5e)*. A subpopulation of Woodbend and Beaverhill Lake samples with potassium concentrations exceeding 3,000 mg/L mostly have lithium concentrations exceeding 50 mg/L.

Figure 4.5f shows that the relationship between lithium and sulphate (SO_4) appears to be inversely correlated with highest concentrations of sulphate being in the Elk Point and Beaverhill Lake samples, which also have the highest component of evaporite minerals. When lithium is observed as a function of strontium (Sr) *(figure 4.5g)*, there is a rough correlation of increasing lithium with strontium except in the Elk Point. Strontium 87 (^{87}Sr) is the by-product isotope of radioactive rubidium (^{87}Rb); elevated strontium ($^{87}Sr/^{86}Sr$) ratios are therefore indicative of potential interaction and enrichment from basement-derived radiogenic sources *(figure 4.6d)*. Elevated strontium ratios can also be associated with weathering of a continental source rock enriched in ^{87}Rb. However, the research published by Huff (2016, 2019) suggests that the Li/Br mass ratio and $^{87}Sr/^{86}Sr$ values could indicate hydrothermal fluids. Devonian seawater has an $^{87}Sr/^{86}Sr$ ratio of approximately 0.708; elevated $^{87}Sr/^{86}Sr$ ratios are observed within the Elk Point Group broadly, and in certain subsets of Beaverhill Lake and Woodbend data, with $^{87}Sr/^{86}Sr$ isotopic ratios >0.713. *Figures 4.6a–c* are provided for completeness.

4.4 | Alberta Devonian Lithium Sample Distribution Map

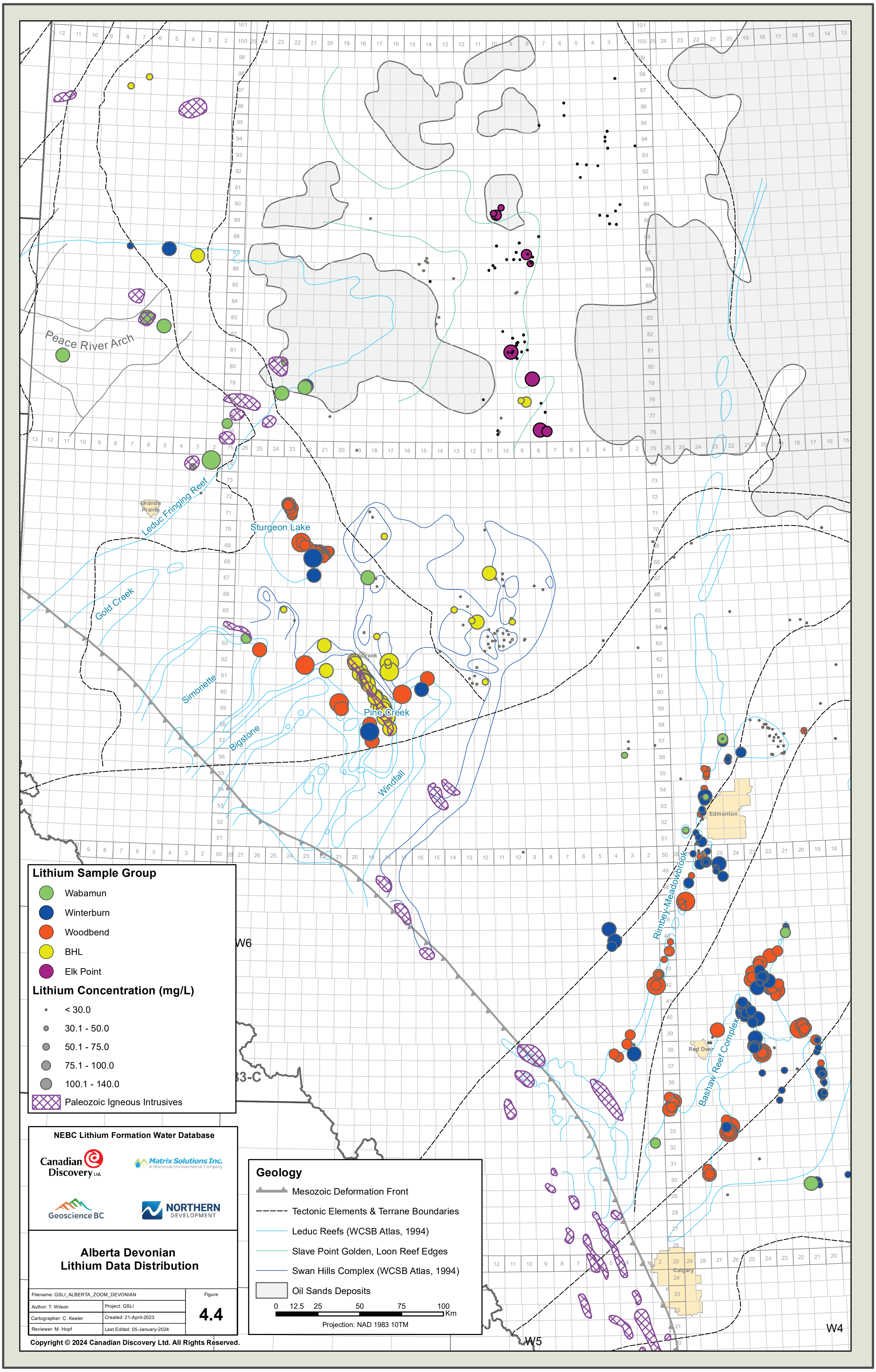

© Canadian Discovery Ltd. *Figure 4.4*

4.5 Devonian Water Chemistry Crossplots

a. Cl/Br vs Na/Br

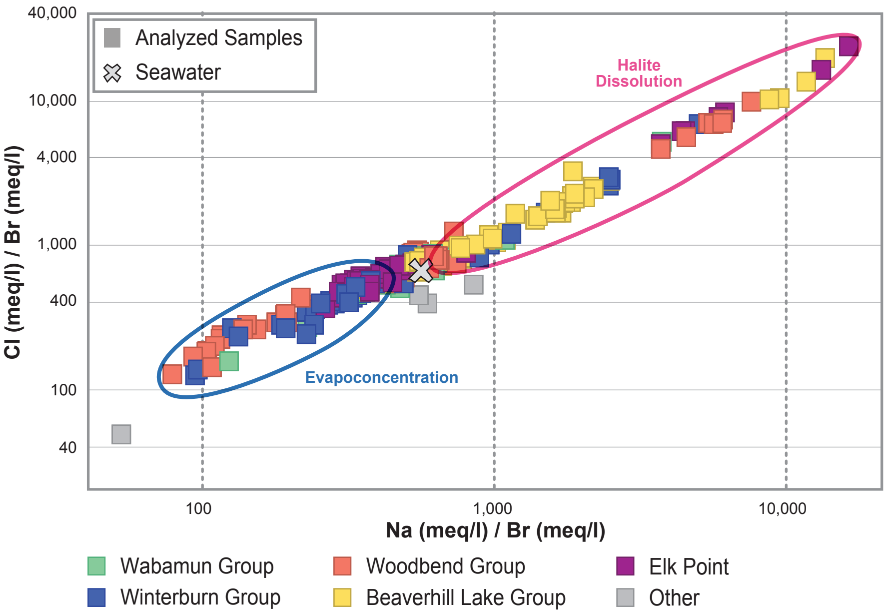

b. K/Br vs Cl/Br

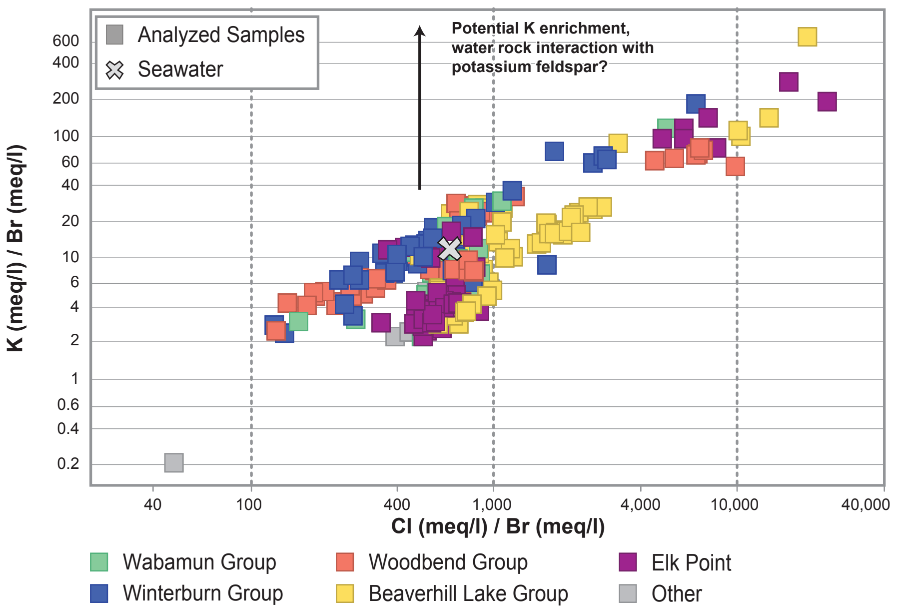

c. Mg vs Cl

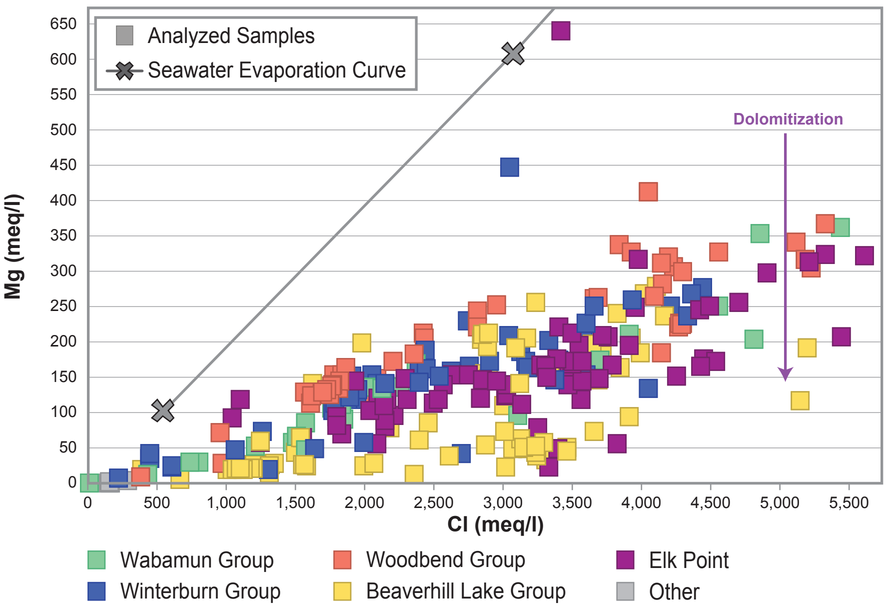

d. Ca vs Cl

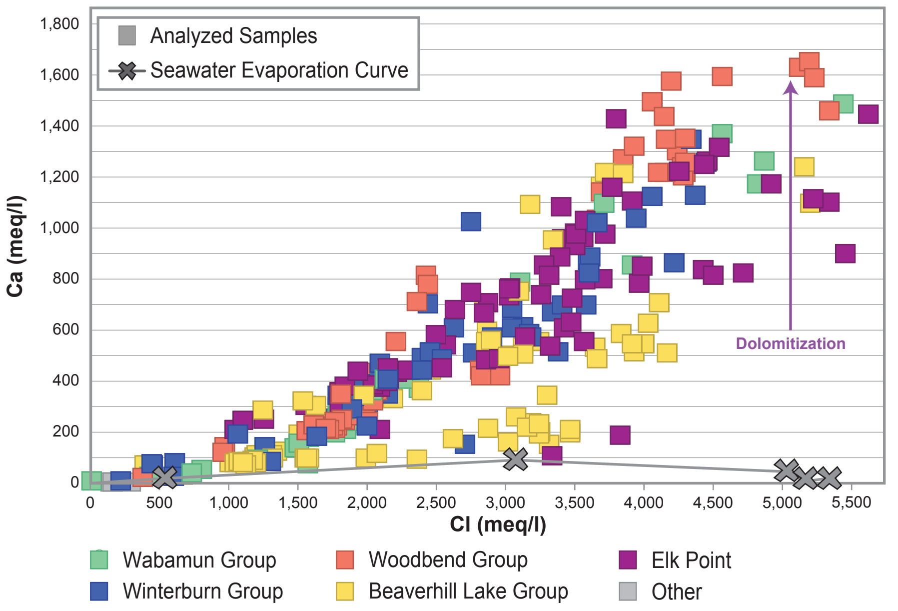

e. Li vs K

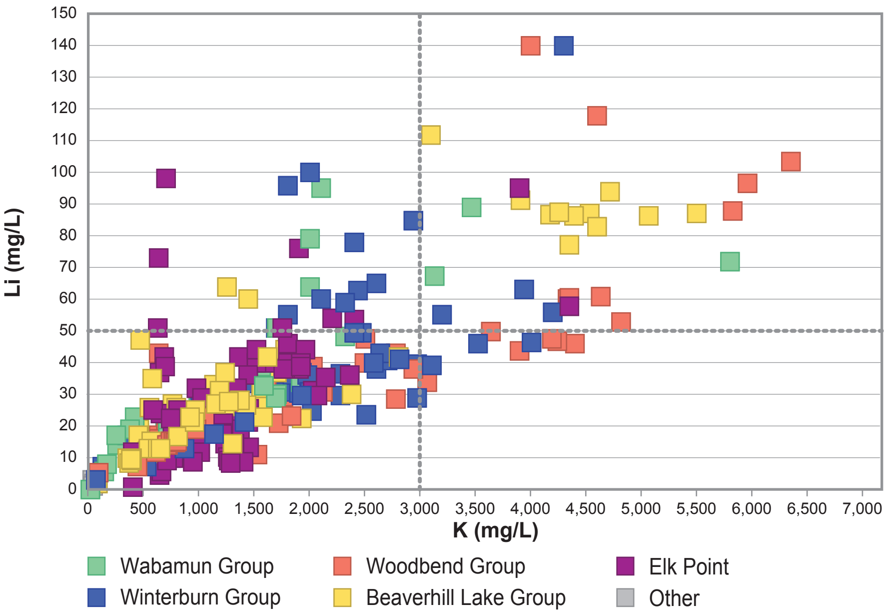

f. Li vs SO_4

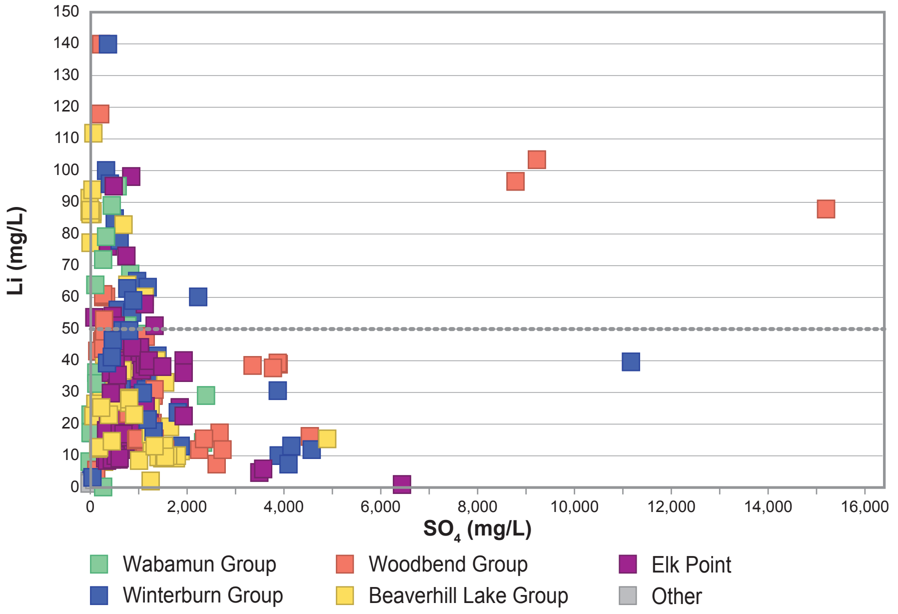

g. Li vs Sr

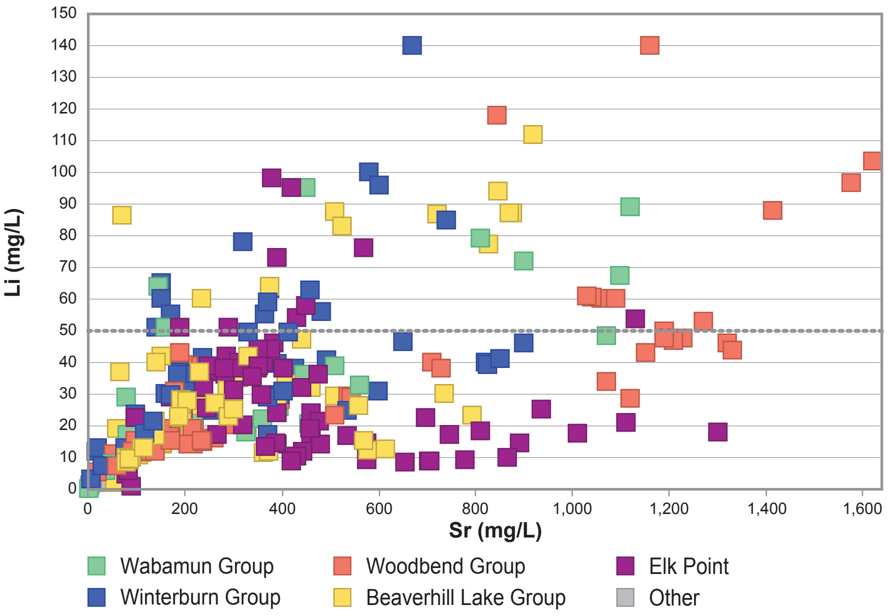

Data source AGS and figure annotations Eccles and Berhane, 2011

Figure 4.5

4.6 Devonian Isotope Crossplots

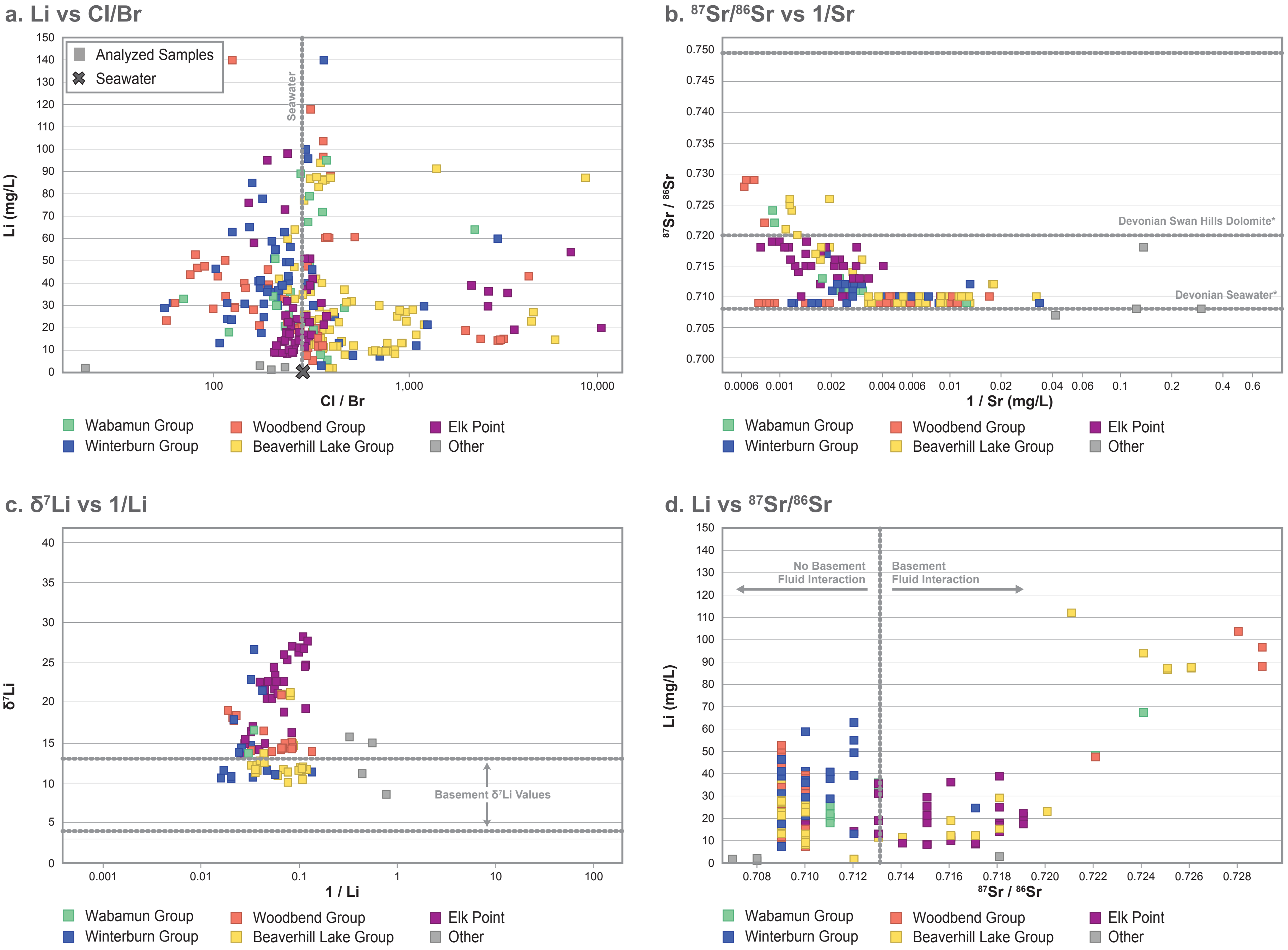

* Devonian concentrations taken from Eccles et al., 2011.
** Range from Eccles et al., 2011.

Lithium data sources Lyster et al., 2022. Data source AGS figure annotations from Eccles and Berhane, 2011.

© Canadian Discovery Ltd.

Figure 4.6

Wabamun Group

Brines sampled from the Wabamun Group have lithium concentrations ranging from 1 mg/L to 95 mg/L, averaging 38 mg/L with a median of 30 mg/L. The highest lithium concentrations are found on the Leduc fringing reefs of the Peace River Arch, while the next highest concentrations are found further southeast along the Simonette reef complex *(figure 4.4)*. The Cl/Br and Na/Br ratios span both above and below those of modern seawater values suggesting that the brines have evolved through a combination of evapoconcentration and halite dissolution (Huff, 2016) *(figure 4.5a)*. The relative magnesium-depletion and calcium-enrichment with respect to chloride concentration in certain samples indicate a limited degree of dolomitization *(figures 4.5c and d)*. In addition, low $^{87}Sr/^{86}Sr$ ratios (<0.713) suggest limited basement fluid interactions *(figure 4.6d)*.

Winterburn Group

Lithium concentrations in brines sampled from the Winterburn Group range from 3 mg/L to 140 mg/L, averaging 41 mg/L with a median value of 37 mg/L. The highest lithium concentrations are found on the Sturgeon Lake reef complex; the second highest concentrations are found on the northern edge of the Leduc fringing reef on the Peace River Arch *(figure 4.4)*. The Cl/Br and Na/Br ratios are lower than that of modern seawater, suggesting that the brine has evolved through evapoconcentration (Huff, 2016) *(figure 4.5a)*. The relative magnesium-depletion and calcium-enrichment with respect to chloride concentration indicates a degree of dolomitization *(figures 4.5c and d)*. The $^{87}Sr/^{86}Sr$ ratios are generally <0.713, indicating limited basement fluid interactions *(figure 4.6d)*. Huff (2016) noted that the δ^2H and $\delta^{18}O$ values are characteristic of evapoconcentration.

Woodbend Group

Lithium concentrations in brines sampled from the Woodbend Group are similar to the Winterburn and range from 5 mg/L to 140 mg/L, averaging 37 mg/L with a median value of 30 mg/L. The majority of the samples are aligned along reef margins including Bigstone, Sturgeon Lake, and the Rimbey-Meadowbrook and Bashaw reef complexes *(figure 4.4)*. Note that where porous Winterburn/Nisku aquifer is developed over Leduc reefs, it tends to be in hydraulic continuity with the Leduc; because of lithium's high solubility, sharing a common concentration signature is consistent. The Cl/Br and Na/Br ratios, magnesium-depletion and calcium-enrichment trends are similar to those observed in the Winterburn samples *(figures 4.5a–d)*. Huff, (2016) hypothesized that the Nisku (Winterburn) and Leduc (Woodbend) formations have experienced similar geological histories with respect to lithium-enrichment. The majority of the $^{87}Sr/^{86}Sr$ data indicates little basement influence *(figure 4.6d)*, except for three Leduc samples located near the Sturgeon Lake reef that appear to be relatively enriched in strontium and could indicate mixing with basement-derived radiogenic fluids, likely along deep-seated faults bounding the reef margins.

Beaverhill Lake Group

Lithium concentrations in Beaverhill Lake Group brines range from 2 mg/L to 112 mg/L, averaging 32 mg/L with a median value of 25 mg/L. The highest concentrations of lithium occur along the Swan Hills platform within the Windfall reef complex with values ranging from 86 mg/L to 112 mg/L *(figure 4.4)*. The Beaverhill Lake samples generally fall above modern seawater on the Cl/Br vs Na/Br plots, indicating they evolved through halite dissolution *(figure 4.5a)*. Lithium concentrations appear to increase when potassium exceeds 3,000 mg/L *(figure 4.5e)*, potentially indicating interaction with potassium feldspars. Elevated $^{87}Sr/^{86}Sr$ isotope ratios in Swan Hills samples could be a function of the potassium feldspar interaction, or it also may indicate mixing with basement-derived fluids, likely expelled during tectonic compression *(figures 4.6b and d)*.

Elk Point Group

The Lower and Middle Devonian Elk Point Group lithium concentrations range from 1 mg/L to 98 mg/L, averaging 29 mg/L with a median value of 25 mg/L, the lowest amongst Devonian samples. The Elk Point comprises clastics, red beds, salts, evaporites and carbonates that were deposited on a broad unconformity surface ranging from Precambrian basement to Silurian and Ordovician strata. Extensive dissolution of salts from within the Elk Point (halite, sylvite and epsomite) is one of the most likely sources of dissolved solids in formation waters that have mixed with overlying strata. The potential contribution of potassium (K) and magnesium (Mg) from salt dissolution is not well understood and could potentially overprint dolomitization and potassium feldspar dissolution signatures.

Elk Point $^{87}Sr/^{86}Sr$ isotope ratios *(figure 4.6d)* indicate moderate enrichment throughout, suggesting some interaction with basement-derived fluids. Because Elk Point samples have been retrieved from complex and highly varied lithologies, further work is required to determine the lithological relationship with observed lithium concentrations.

Fox Creek Area Lithium-Enrichment Processes

The Fox Creek area, which shows anomalous lithium-enrichment, has a unique set of features as outlined by Eccles and Berhane (2011):

- Thermal anomaly at the base of the stratigraphic section
- High Precambrian geothermal gradient
- Horizontal gravity anomaly
- Offsets the Peace River Arch, which was tectonically active in the past
- Offsets the Kimiwan isotopic anomaly
- On the northern edge of the Snowbird anomaly zone

Some of these features may have played a role in the liberation and subsequent mobilization of lithium-rich brines that eventually accumulated in Devonian reef complexes. This hypothesis partially explains the data trends observed in Beaverhill Lake samples and some of the Woodbend data at Fox Creek. Note that there is a Paleozoic igneous intrusive near the Windfall and Pine Creek reefs where some of the highest lithium values are observed *(figure 4.4)*. This intrusive may have provided an additional source of lithium-rich silicate fluid that migrated into the reef complexes.

4.7 Triassic Water Chemistry Crossplots

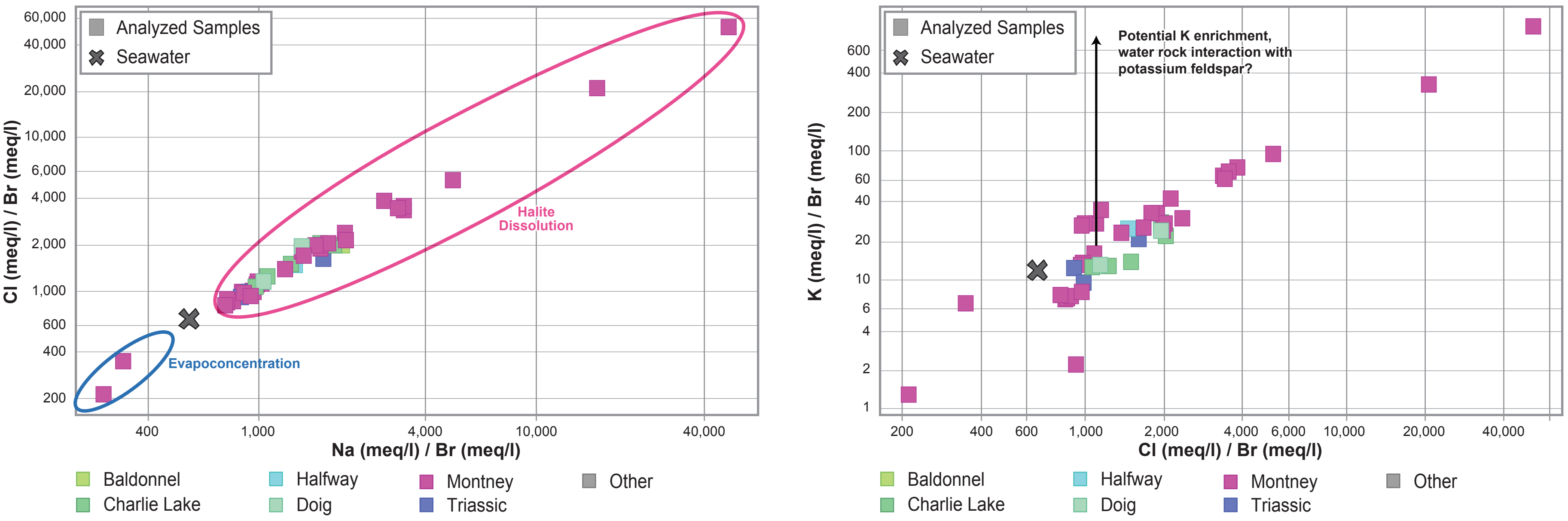

a. Cl/Br vs Na/Br

b. K/Br vs Cl/Br

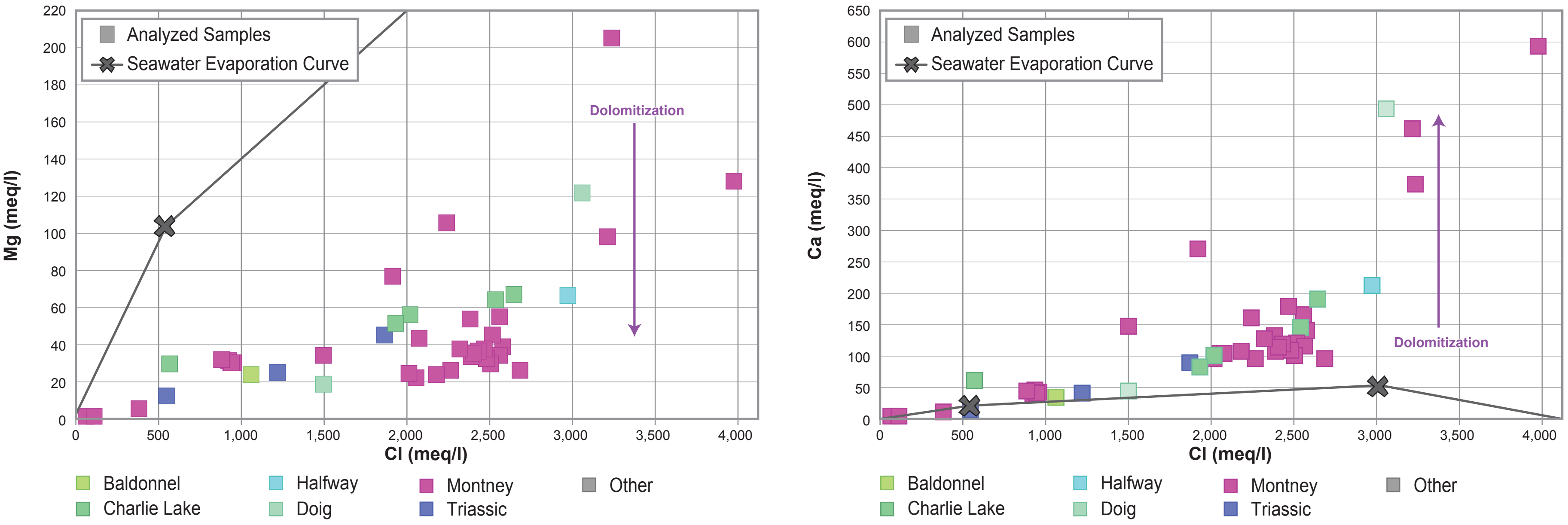

c. Mg vs Cl

d. Ca vs Cl

Data source AGS. Figure annotations from Eccles and Berhane, 2011.

Figure 4.7

Triassic Data Distribution

The Triassic, which includes the Montney, Halfway and Doig formations, hosts the second-highest average lithium concentrations in Alberta, with a range of 1 mg/L to 59 mg/L and average of 30 mg/L. The highest Triassic lithium concentrations are located predominantly along or on the Peace River Arch *(figure 4.2)*. The Cl/Br vs Na/Br plot *(figure 4.7a)* shows that most of the data plots above modern seawater, indicating salinity is predominantly gained through halite dissolution. Potassium is enriched relative to seawater in a majority of the Triassic samples *(figure 4.7b)*, indicating interaction with feldspathic minerals. Relative magnesium-depletion and calcium-enrichment with respect to chloride indicates dolomitization was an important diagenetic process *(figures 4.7c–d)*. The ^{86}Sr/^{87}Sr isotopic ratios are generally below 0.712, just slightly above seawater at 0.708, which does not suggest extensive interaction with basement-derived fluids *(figures 4.8b and d)*. To the contrary, δ^7Li isotopic values *(figure 4.8c)* fall within the range of basement-derived fluids as defined by Eccles and Berhane, (2011). Due to the limited availability of δ^7Li data at the time of writing, further research is required to characterize the lithium isotopes of both subsurface brines and basement-derived fluids.

4.8 Triassic Isotope Crossplots

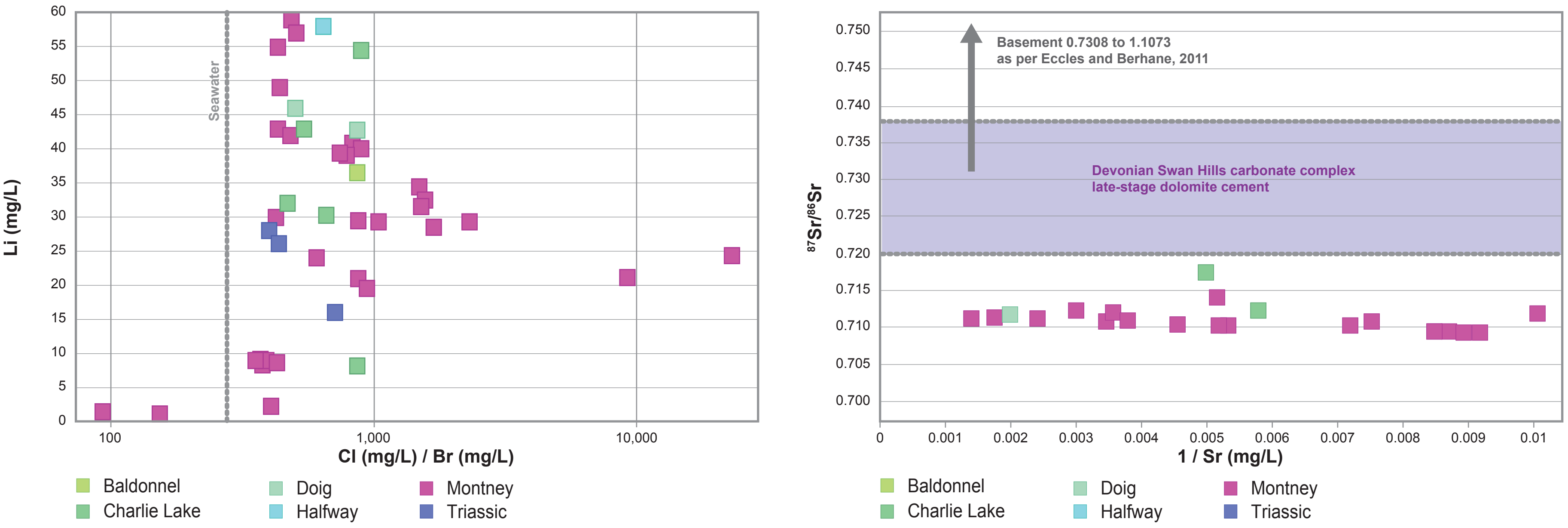

a. Li vs Cl/Br

b. $^{87}Sr/^{86}Sr$ vs 1/Sr

c. δ^7Li vs 1/Li

d. Li vs $^{87}Sr/^{86}Sr$

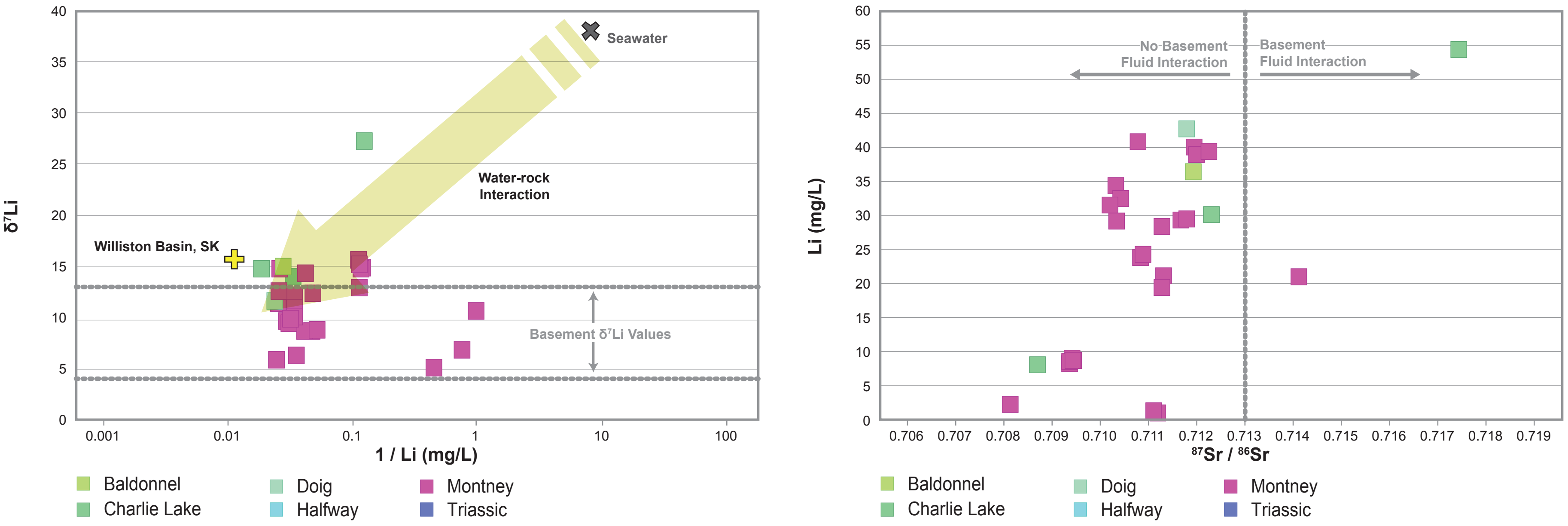

Data source AGS. Figure annotations from Eccles and Berhane, 2011.

Figure 4.8

4.9 Montney Seawater Evaporation Process and Normalized Chloride, Lithium and Bromide Concentrations

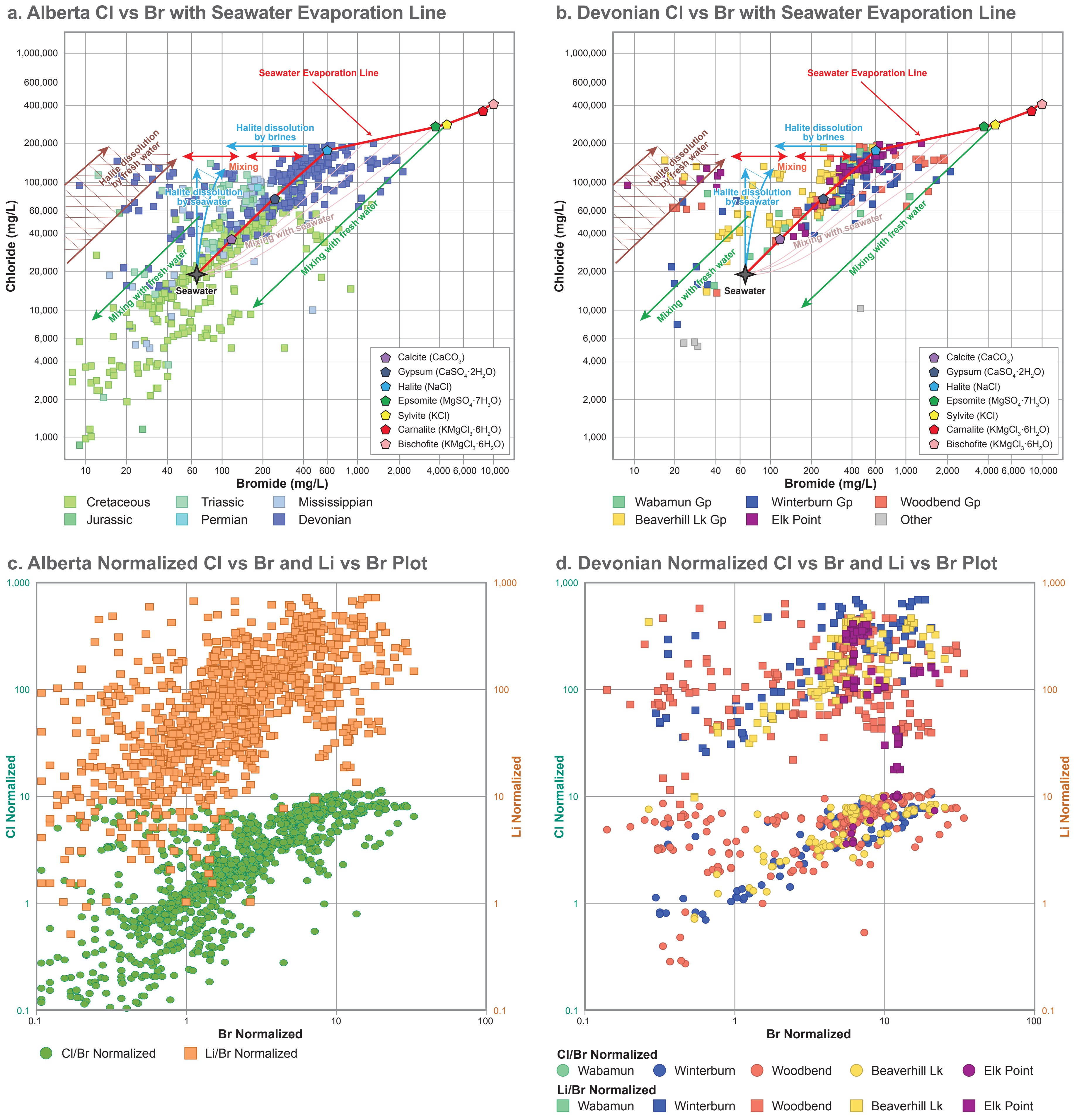

Source: Plot annotations from Shouakar-Stash, O., 2008. Lithium data from the AGS.

Figure 4.9

Brine Evolution and Potential Lithium-Enrichment Mechanisms

The evolution of brines in the Western Canada Sedimentary Basin (WCSB) and the related impact on lithium-enrichment is discussed in detail in *Chapters 2 and 5*, along with discussions of water-rock interaction and of clay minerals.

Data used in this study from Alberta are shown on the Cl vs Br graph in *figure 4.9a* along with their likely evolutionary trajectories using the seawater evaporation curve as a baseline. Chloride concentrations are observed to exceed halite saturation (~200,000 mg/L) in some samples from the Elk Point and Woodbend groups, indicating sylvite and epsomite saturation had been reached. Bromide, a conservative ion that which preferentially stays in solution during seawater evaporation, reaches a maximum concentration of 2,000 mg/L, which is below sylvite/epsomite saturations (~4,000 mg/L Br). These data suggest that Devonian formations have undergone extensive salt dissolution, brine migration and mixing with both seawater and fresh water over their geologic history *(figure 4.9b)*. Vertical brine migration is particularly evidenced by elevated bromide levels within certain Cretaceous samples at chloride concentrations above and below seawater. The location and areal extent of the various migration and mixing paths are likely controlled by vertical and lateral hydraulic continuity and the basin's tectonic and hydrogeological history.

4.10 Subsurface Lithium-Enrichment Processes

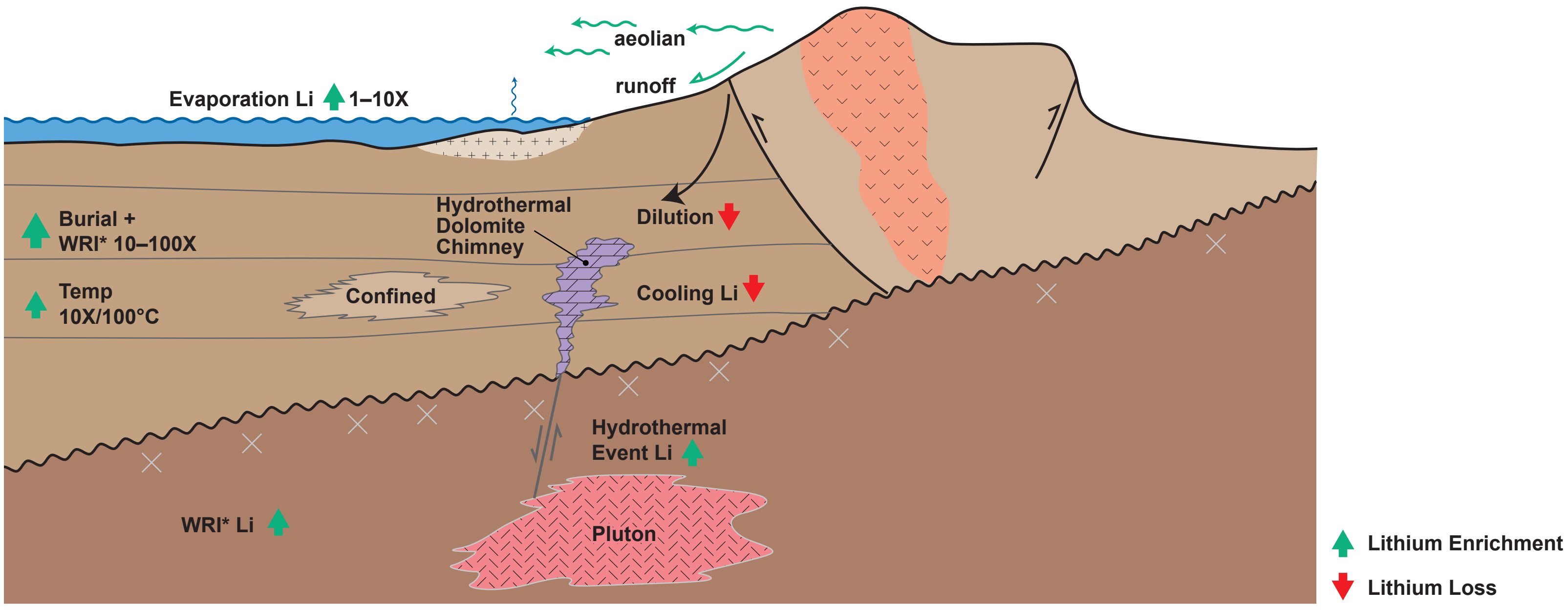

*Water-rock interaction

After Dugamin et. al., 2023

© Canadian Discovery Ltd. *Figure 4.10*

The main mixing and dilution processes occurring within the basin are:

- Vertical and lateral brine migration
- Evaporite, halite and K + Mg salt dissolution by brines seawater and fresh waters
- Mixing with seawater and/or fresh water

Lithium-Enrichment in WCSB Brines

In *figures 4.9c and d*, the concentrations of Cl and Li as a function of Br are plotted, normalized to their initial concentration in seawater. Chloride and bromide are enriched up to 15X and 30X respectively, whereas lithium is enriched well over 500X (to a maximum of 950X) relative to seawater. These data suggest that lithium concentration in seawater due to evapoconcentration is an insufficient process for yielding observed lithium concentrations.

There are multiple mechanisms that potentially lead to the enrichment of lithium in sedimentary basin brines, where lithium concentrations are found in excess of 1,000X that of seawater. In the WCSB, lithium-enrichment of over 500X relative to seawater is observed in parts of the Devonian. *Figure 4.10* is a schematic of the various concentration and dilution processes that have been quantified in the literature and through observations in this study. Processes such as water circulating through and leaching of igneous basement rocks, hydrothermal events and enrichment through sedimentation or overland flow are more difficult to quantify. The scale of some of the enrichment processes as identified by Dugamin et al., (2023) are:

- Seawater Evaporation
  - 1 to 10X, source = observed data at halite saturation
- Burial and Water-Rock Interaction
  - 10 to 100X, source = observed and Dugamin et al., 2023
- Temperature Gain (empirical)
  - 10X/100°C, source = observed and Kharaka and Mariner, 1989

Lithium loss can occur through brine dilution by mixing with seawater, halite-derived brines and meteoric waters. Uplift or erosion and subsequent cooling can cause resorption of lithium in certain circumstances as well.

4.11 Western Canada Brine-Hosted Lithium Crown Majority Rights Map

a. Western Canada Map

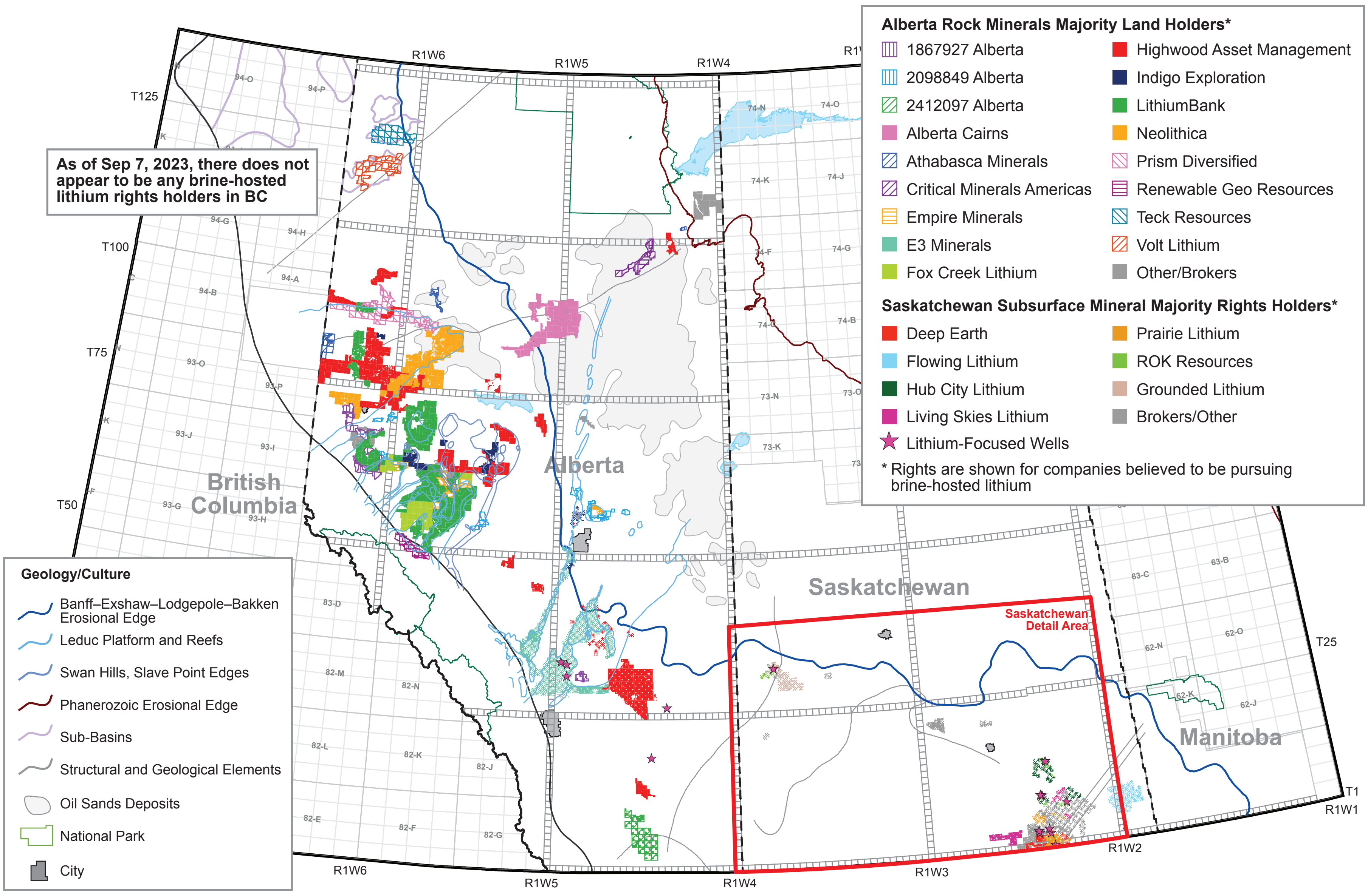

b. Saskatchewan Detail Map

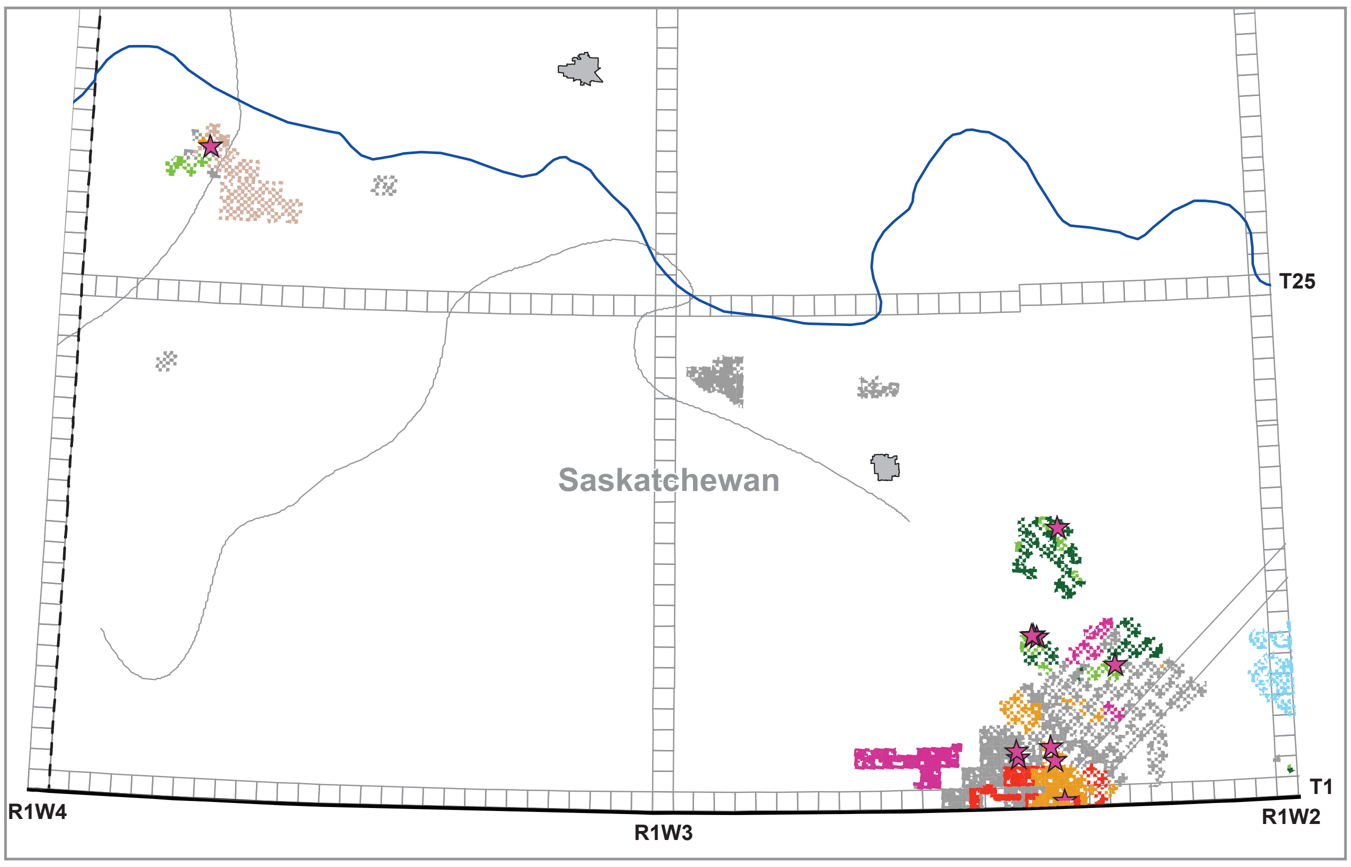

Saskatchewan Subsurface Mineral Majority Rights Holders*

🟥 Deep Earth	🟩 Hub City Lithium	🟧 Prairie Lithium	🟫 Grounded Lithium	★ Lithium-Focused Wells
🟦 Flowing Lithium	🟪 Living Skies Lithium	🟩 ROK Resources	⬛ Brokers/Other	

* Rights are shown for companies believed to be pursuing brine-hosted lithium

Data current to August 9, 2023.
Land data supplied by geoLOGIC. Reefs from the Geological Atlas of the Western Canada Sedimentary Basin, 1994

Figure 4.11

Alberta's Lithium Industry

Alberta is in the process of transitioning how lithium rights are permitted. Prior to 2023, lithium rights were acquired as metallic and industrial mineral (MIM) permits. Starting in 2023, tenure for lithium (and other brine-hosted minerals) will be granted via leases issued through a public offering, similar to how Alberta Petroleum and Natural Gas (P&NG) rights are presently obtained, and also more in line with the mineral tenure process in Saskatchewan (Podetz, 2023). The present state of tenure for brine-hosted minerals across the WCSB is shown in *figure 4.11a*.

LithiumBank

LithiumBank holds over 4 million acres of metallic and industrial mineral (MIM) permits across west-central Alberta. Within this larger area, the company is focused on two specific properties, namely Boardwalk and Park Place.

The Boardwalk Lithium Brine Project is located approximately 85 km east of Grande Prairie. The project comprises 40 contiguous Alberta MIM permits covering an area of 572,237 acres. The Sturgeon Lake oil and gas field, where the Boardwalk Project is situated, was discovered in 1952. LithiumBank used historical oil and gas drilling and seismic data to update National Instrument (NI) 43-101 Inferred Mineral Resource Estimate dated November 7, 2022. The Sturgeon Lake Leduc Formation Li-brine inferred resource estimate is 393,000 t Lithium Carbonate Equivalent (LCE) (indicated) at 71.6 mg/L and 5,808,000 t LCE (inferred) at 68.0 mg/L.

In September 2022, LithiumBank acquired 1,571,364 acres at its Park Place project where the Leduc reef complex (Woodbend Group) and the underlying Swan Hills carbonate complex (Beaverhill Lake Group) have hosted the highest grades of lithium-in-brine concentrations in Alberta *(figure 4.12)*. Lithium concentrations (from AGS samples that were collected by oil and gas operators) within the Park Place MIM permit area range from 76 mg/L to 130 mg/L; LithiumBank plans to verify these lithium concentrations with its upcoming work (LithiumBank, 2023).

4.12 LithiumBank Boardwalk and Park Place Projects Map

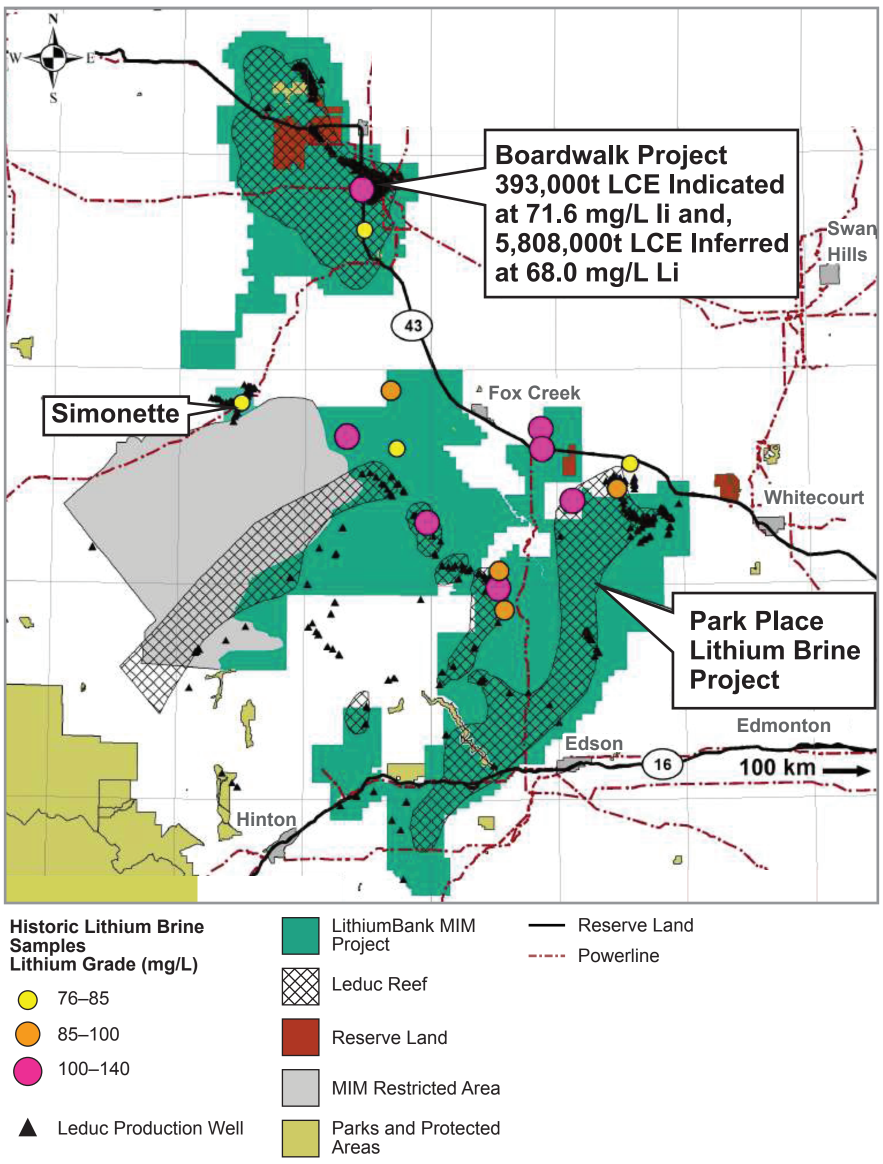

Modified from LithiumBank Corporate Presentation, January 2023

© Canadian Discovery Ltd. *Figure 4.12*

4.13 E3 Lithium Inaugural Drilling and Sampling Program

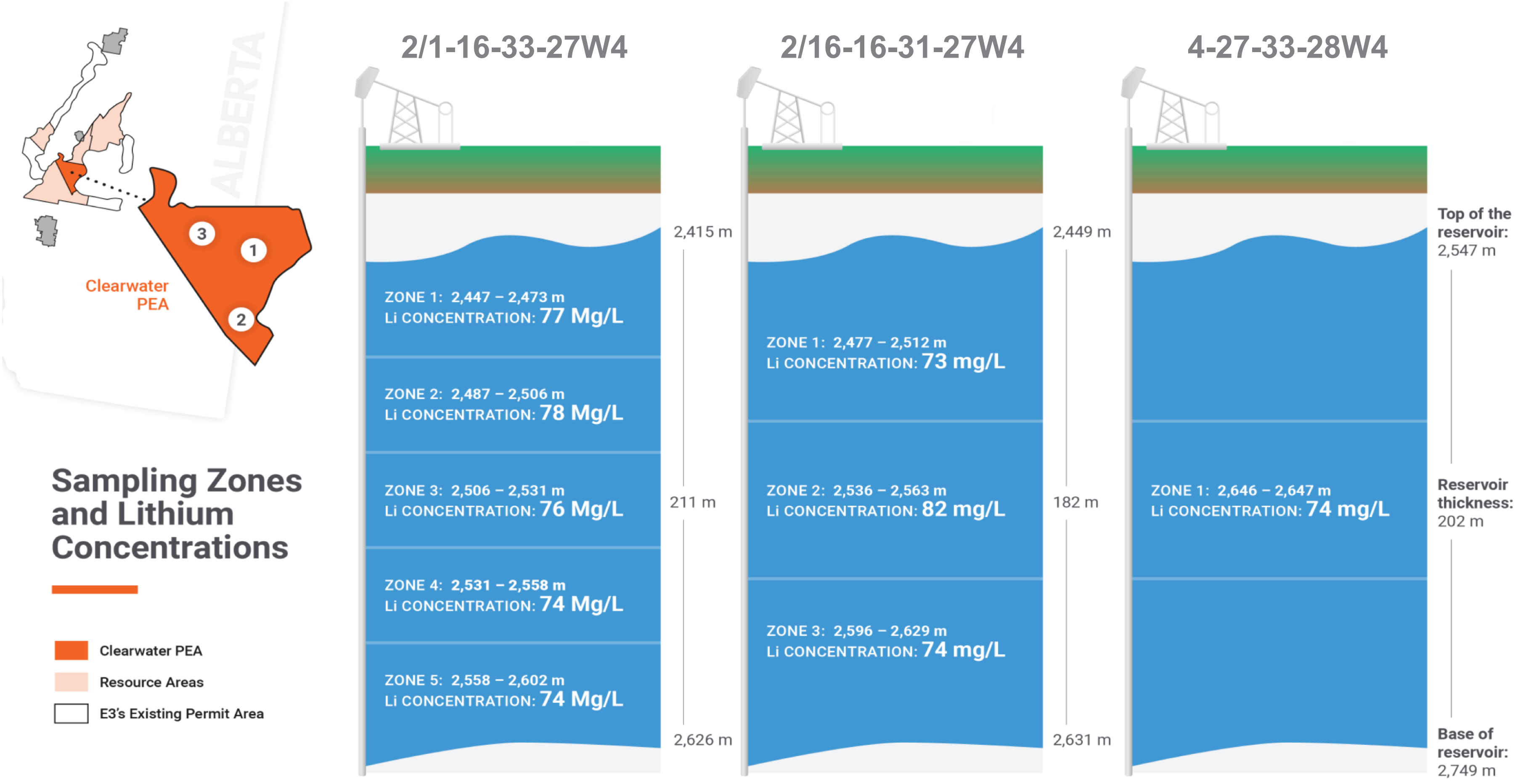

Modified from E3 Lithium, Corporate Presentation, April 2023

Figure 4.13

E3 Lithium

E3 is the largest permit holder in south-central Alberta, with 76 MIM permits totalling over 596,000 hectares (~1.5 million acres). These MIM permits overlie Devonian-age Leduc reef reservoirs that exhibit exceptional flow rates and deliverability because of favourable rock properties and pressure. E3 has three NI 43-101 Inferred Mineral Resources (North Rocky, Central Clearwater and Exshaw West) over its permit area in Alberta, totalling 16.0 million tonnes (Mt) of LCE. These resources cover only 34% of the total Leduc reservoir that E3 currently holds.

E3's planned development model involves using existing oil and gas sites and repurposing infrastructure for production and processing lithium brine. Its closed loop water processing system could result in virtually no waste or water use and no effluent discharges to the surface. The use of existing wells, rather than drilling new ones, should result in significant cost savings for the company. E3 currently has 14 operational collaborative relationships with area oil and gas producers.

In August 2023, E3 announced that the construction phase of its field pilot at Clearwater was completed and that commissioning work was in progress with operations to commence "in a matter of weeks." The Clearwater project will utilize E3's proprietary Direct Lithium Extraction (DLE) adsorbent. The goal of this field pilot is to demonstrate a near commercial-scale, modular design of the company's ion-exchange DLE process under real world operating conditions. The field pilot will be tied into an existing well (2/1-16-33-27W4) that produces brine directly from the Leduc aquifer *(figure 4.13)*. In November 2022, E3 had received a $27MM investment from the Government of Canada's Strategic Innovation Fund (SIF) to support all aspects of the company's resource and technology development, including drilling, piloting of E3's proprietary ion-exchange technology for lithium extraction, process development and engineering, including downstream lithium hydroxide conversion (E3 Lithium, 2023). This next stage of development follows from the company's DLE lab-pilot prototype that delivered successful results of up to 97% lithium recovery across multi-cycle testing. Also, in April 2023, E3 announced it had begun to evaluate the commercial-scale manufacturing of its proprietary adsorbent to be used in the field pilot. The combination of E3's adsorbent technology with a scaled-up ion-exchange system operating in real world conditions is an important step towards de-risking and demonstrating the DLE process and technology at a commercial scale (E3 Lithium, 2023).

In 2022, E3 drilled two wells and took possession of a third wellbore to better quantify reservoir parameters, lithium concentrations, flow rates and deliverability of the Leduc aquifer within the Clearwater project area. The first well (2/1-16-33-27W4) was drilled in July 2022 and the second (2/16-16-31-27W4) in August 2022. A third, existing well (4-27-33-28W4), which was drilled by Aspenleaf in October 2021, is now operated by E3. Results indicate that the properties of the aquifer, the chemistry of the brine and the grade of lithium sampled in all wells demonstrate consistency *(figure 4.13)*. This consistency allows the company to design and build a simpler commercial DLE facility, given that its design does not need to handle a large variation of fluid chemistry.

Highwood Asset Management

Highwood Asset Management is a Canadian-owned, public asset management entity overseeing current activities in the industrial metals and minerals (including lithium, iron, rare earth elements, vanadium, silica and alumina), oil production and oil midstream spaces. The asset management structure is positioned to potentially oversee other energy focused segments including clean tech energy transition subsectors and technologies in the future.

The company issued its first NI 43-101 Technical Report on lithium from brine on July 16, 2021. *Figure 4.11* shows the current distribution of its land. Subsequently, Highwood engaged APEX Geoscience to compile a NI 43-101 Resource Assessment specific to its Drumheller property in southeast Alberta. This resource assessment was released in February 2022 with encouraging results, as the combined total initial inferred lithium-brine resource at Drumheller within the Leduc and Nisku formations is estimated at 18.14 Mt LCE (Highwood, 2023).

Saskatchewan

In 2011, the Saskatchewan Geological Survey (SGS), along with the Ministry of Energy and Resources, initiated a wellhead brine sampling program, collecting data for major elements. This database currently contains 77 samples, exhibiting lithium concentrations ranging from 1 mg/L to 190 mg/L, and averaging 40 mg/L; six of these samples tested >75 mg/L *(figure 4.1)*. The highest lithium concentration of 190 mg/L from the Devonian Duperow Formation (Leduc-equivalent) is 50 mg/L higher than any brine sampled in Alberta. *Table 4.2* lists the data count by formation. Several samples have been tested for a number of other elements, including K, Na, Mg, Pb and Zn. The SGS is expected to publish an update to this database shortly, with an additional 37 lithium concentration values.

Data Distribution

Most data collected in Saskatchewan are from the Devonian Bakken, Torquay, Birdbear and Duperow formations within the Williston Basin *(figure 4.1)*. New data released by ROK Resources in February 2023 indicate that the Duperow has the highest lithium concentration, ranging from 36 mg/L to 259 mg/L with an average of 104 mg/L. These new values have increased the average in the Duperow by 18 mg/L and increased the maximum concentration by 69 mg/L (ROK, 2023). In the Mississippian Madison Group, the Ratcliffe, Midale and Frobisher formations were tested and have an average lithium concentration of 38 mg/L with a range of 1 mg/L to 56 mg/L. The Ordovician Red River Formation samples have an average lithium concentration of 32 mg/L and a range of 9 mg/L to 55 mg/L.

Duperow Lithium-Enrichment Mechanism

Rostron (2022) observed that the Duperow acquired salinity through evapoconcentration based on the Cl/Br and Na/Br ratios. This correlates well with the cyclical restricted marine carbonates and evaporitic geological setting at the time of deposition. Rostron (2022) further investigated the inconsistencies in the Duperow lithium data distribution and discovered that by mapping the 22 anhydrite layers, which are continuous across the area, the Duperow lithium concentrations are correlated to specific stratigraphic layers, and each layer has a unique geochemical signature.

Saskatchewan's Lithium Industry

Prairie Lithium

At year-end 2022, Prairie Lithium controlled over 362,000 acres of nearly contiguous mineral permits *(figure 4.11b)* in southeastern Saskatchewan, had drilled or acquired several wells to test lithium concentrations, and was working on the third iteration of its DLE pilot plant at its Emerald Park testing facility (Prairie Lithium, 2023). Finally, to cap 2022, Prairie Lithium announced that it had entered into a definitive pre-acquisition agreement with Arizona Lithium, a U.S. company focused on the sustainable development of the Big Sandy Lithium Project in Arizona. The transaction closed in late March 2023 (Arizona Lithium, 2023).

The company's land base includes 40 townships acquired in an acreage rights swap with Deep Earth Energy Production (DEEP), which is developing a geothermal project at Torquay. In this agreement, Prairie Lithium acquired subsurface mineral permits from the top of the Madison Group down to the top of the Red River Formation from DEEP's subsurface mineral tenure. In exchange, DEEP acquired the subsurface mineral permits from the top of the Red River down to the Precambrian from Prairie Lithium's subsurface mineral tenure. DEEP retained all lithium potential from the top of the Red River to the Precambrian (DEEP, 2023).

Prairie Lithium drilled Canada's first lithium brine well near Torquay in September 2021, targeting the Duperow. The reservoir was approximately 110m thick with a cumulative net pay thickness of roughly 53m. The targeted aquifer is a series of multiple, highly productive zones enriched in lithium. Early results indicate that the well tested some of the highest known lithium brine concentrations in Canada (Business Wire, 2023).

In September 2022, Prairie Lithium acquired three wells from Crescent Point that were scheduled to be abandoned due to their limited oil production. Although no longer useful for oil production, these wells provide Prairie Lithium with access to the production and disposal zones required for its lithium operations. Prairie Lithium plans to deepen one of these wells by 180m, and then case and perforate it within the zones of interest. Testing is planned to evaluate the productivity of the well across the zones of interest (Business Wire, 2022a).

Table 4.2: Saskatchewan Lithium Samples by Geologic Unit

Geologic Unit	Lithium Samples (#)
Madison Group (Ratcliffe Beds, Midale Fm, Frobisher Fm)	10
Bakken Formation	1
Torquay Formation	5
Birdbear Formation	21
Duperow Formation	8
Winnipegosis Formation	13
Red River Formation	19

Table 4.2

In October 2022, Prairie Lithium converted two Crown mineral exploration permits with a combined area of 6,795 acres into 21-year mineral leases. These are the first Crown mineral leases issued for lithium by the province. This is important because leases are required before companies are allowed to produce a resource at commercial scale production rates (Business Wire, 2022b).

In November 2022, the company announced the commissioning of the third iteration of its DLE pilot plant at its Emerald Park testing facility. This DLE pilot is designed to process deep subsurface brines sourced from Prairie Lithium's fall 2022 drilling program when 600 m^3 of lithium-rich brine was reserved for ongoing DLE technology testing (Business Wire, 2022c).

Grounded Lithium

Grounded Lithium increased its land base by a factor of four during 2022, exiting the year with a land position of just over 300 sections *(figure 4.11b)*. The company also successfully drilled the second-ever dedicated lithium test well in Saskatchewan (Grounded Lithium, 2023). Well 2/4-15-32-23W3 was spudded in July 2022 to test the Duperow. Initial well testing indicated lithium concentrations ranging from 74 mg/L to 81 mg/L (Newswire, 2023).

Hub City Lithium

Hub City Lithium holds 37 mineral permits totalling 212,633 acres (86,050 ha) of subsurface Crown mineral dispositions in southern Saskatchewan *(figure 4.11b)*. The company is a subsidiary of EMP Metals, which holds a 75% interest; ROK Resources holds the balance. EMP is a Canadian-based exploration company focused on the acquisition and exploration of mineral projects with significant development potential.

Hub City spudded its first lithium well (2-22-7-9W2) at Viewfield, Saskatchewan in November 2022, targeting the Duperow (IQ FIN, 2023). Partner ROK reported lithium concentrations up to 259 mg/L with high flow rates (ROK Resources, 2023).

Flowing Lithium

Flowing Lithium is the latest entrant to lithium development in Saskatchewan. Incorporated in October 2022, the company picked up four blocks of subsurface mineral rights in southeast Saskatchewan at the November 21, 2022 Crown mineral rights sale *(figure 4.11b)* (Pipeline Online, 2022).

Conclusion

The lithium brine extraction industry is growing in Canada. Companies are racing to bring economic commercial projects to fruition and to create a local source of lithium to help power Canada's green energy future. Alberta is leading the way with over 2,000 samples tested and more becoming public each year. This wealth of publicly available data has allowed several advancements in the understanding of lithium brine enrichment processes. Saskatchewan is following suit, gathering more samples and laying out a regulatory framework to entice companies and investments into the province. In Alberta, companies are focusing their efforts on the Woodbend Group, specifically the Leduc reefs, as the main target for lithium brine extraction. The Sturgeon Lake reef has, to date, the highest lithium readings found in Alberta.

Further sampling is required along the Sturgeon Lake, Simonette, Bigstone, Fir, Pine Creek and Gold Creek reefs. The proximity to the high lithium concentrations on the Sturgeon Lake reef, as well as the general observation of high lithium concentrations along reef margins, leads to the conclusion that these could be areas of high lithium potential.

References

- Arizona Lithium, 2023. AZL completes acquisition of Prairie Lithium. https://www.arizonalithium.com
- Bachu, S. 1995. Synthesis and model of formation-water flow, Alberta Basin, Canada. American Association of Petroleum Geologists Bulletin, v. 79, p. 1159–1178.
- Billings, G.K., Hitchon, B. and Shaw, D.R. 1969. Geochemistry and origin of formation waters in the Western Canada Sedimentary Basin: 2. Alkali metals. Chemical Geology, v. 4, p. 211–223.
- Business Wire. 2022a. Prairie Lithium Acquires Oil Wells Slated for Abandonment to Advance their Lithium Resource Research. Accessed February 2023. https://www.businesswire.com/news/home/20220920005109/en/
- Business Wire. 2022b. Prairie Lithium Converts Mineral Exploration permits into 21-Year Mineral leases, Demonstrating the Government of Saskatchewan's Commitment to Advancing Lithium Development. Accessed February 2023. https://www.businesswire.com/news/home/20221019005155/en/
- Business Wire. 2022c. Prairie Lithium Commissions New Direct Lithium Extraction (DLE) Pilot Plant to Further De-Risk Commercial Deployment. Accessed February 2023. https://www.businesswire.com/news/home/20221129005235/en/
- Clayton, R.N., Friedman, I., Graf, D.L., Mavenda, T.K., Meents, W.F. and Shimp, N.F. 1966. The origin of saline formation waters. I. Isotopic composition. Journal of Geophysical Research, v. 71, p. 3869–3882.
- Collins, A.G. 1976. Lithium abundance in oilfield waters. In: Lithium resources and requirements by the year 2000. J.D. Vine (ed.). U.S. Geological Survey Professional Paper 1005, p. 116–123.

- Connolly, C.A., Walter, L.M., Baadsgaard, H. and Longstaffe, F.J. 1990a. Origin and evolution of formation waters, Alberta Basin, Western Canada sedimentary basin: I. Chemistry. Applied Geochemistry, v. 5, p. 375–395.
- Davies, G.R. and Smith, L.S., 2006 Structurally controlled hydrothermal dolomite reservoir facies: An overview. AAPG Bulletin, V. 90, No. 11, pp 1641-1690.
- Deep Earth Energy Production (DEEP), 2023. https://deepcorp.ca/deep-and-prairie-lithium-sign-mineral-permit-agreement-advance-lithium-extraction-potential
- Dugamin, E. J., Cathelineau, M., Boiron, M. C., Richard, A., Despinois, F. 2023. Lithium enrichment processes in sedimentary formation waters. Chemical Geology 635 (2023) 121626.
- Eccles, D.R. and Berhane, H. 2011. Geological Introduction to Lithium-Rich Formation Water with Emphasis on the Fox Creek Area of West-Central Alberta (NTS 83F and 83K). ERCB/AGS Open File Report 2011-10.
- E3 Lithium, 2023. https://www.e3lithium.ca
- Garrett, D.E. 2004. Handbook of lithium and natural calcium chloride, Elsevier Academic Press, Oxford, United Kingdom, 488 p.
- Grounded Lithium Corp, 2023. https://fmm760.a2cdn1.secureserver.net/wp-content/uploads/2023/03/GLC-Corp-Presentation-External-MARCH-2023_2.pdf
- Gupta, I., Wilson, A.M. and Rostron, B.J. 2012. Cl/Br compositions as indicators of the origin of brines: Hydrogeologic simulations of the Alberta Basin, Canada. Geological Society of America Bulletin, v. 124, p. 200–212.
- Highwood Asset Management, 2023. https://highwoodmgmt.com/media/documents/HAM_February_28_2022_-_Lithium_43-101_Resource_Assessment.pdf
- Hitchon, B. and Friedman, I. 1969. Geochemistry and origin of formation waters in the Western Canada sedimentary basin-I. Stable isotopes of hydrogen and oxygen. Geochimica et Cosmochimica Acta, v. 33, p. 1321–1349.
- Hitchon, B., Billings, G., K., Klovan, J. E., 1971. Geochemistry and origin of formation waters in the Western Canada sedimentary basin-III. Factors controlling chemical composition. Geochimica et Cosmochimica Acta, v.35, p. 567-598.
- Hitchon, B, Underschultz, J.R. and Bachu, S. 1993. Industrial mineral potential of Alberta formation waters. Alberta Research Council/Alberta Geological Survey Open File Report 1993-15.
- Huff, G.F. 2016. Evolution of Li-enriched oilfield brines in Devonian carbonates of the south-central Alberta Basin, Canada. Bulletin of Canadian Petroleum Geology, v. 64, pp. 438-448.
- Huff, G.F. 2019. Origin and Li-Enrichment of Selected Oilfield Brines in the Alberta Basin, Canada. AER/AGS Open File Report 2019-01.
- IQ FIN, 2023. https://www.newswire.ca/news-releases/emp-metals-spuds-first-lithium-well-in-viewfield-saskatchewan-811670606.html
- Kharaka, Y. K., Mariner, R. H., 1989. Chemical geothermometers and their application to formation waters from sedimentary basins.
- Lithium Bank, 2023. https://www.lithiumbank.ca/project/exploration/park-place
- Lyster, S., Hauck, T.E., Lopez, G.P., Playter, T.L., Reimert, C., Palombi, D. and Schultz, S.K., 2022. Lithium and Helium in Alberta: Data Compilation and Preliminary Observations. AER/AGS Open File Report 2021-04.
- Machel, H.G. and Bachu, S. 2003. New insights into the origin and migration of brines in deep Devonian aquifers, Alberta, Canada. Journal of Geochemical Exploration, v. 80, p. 193–219.
- Michael, K. and Bachu, S. 2002. Origin, chemistry and flow of formation waters in the Mississippian-Jurassic sedimentary succession in the west-central part of the Alberta Basin, Canada. Marine and Petroleum Geology, v. 19, p. 289–306.
- News Wire, 2023. https://www.newswire.ca/news-releases/grounded-lithium-reports-2022-year-end-financial-and-operating-results-809465949.html
- Pipeline Online. 2022. Lithium in SK, Part 3: Crown land sale reveals sixth entrant in Saskatchewan lithium exploration race. Accessed February 2023. https://pipelineonline.ca/lithium-in-sk-part-3-crown-land-sale-reveals-sixth-entrant-in-saskatchewan-lithium-exploration-race/#/?playlistId=0&videoId=0
- Podetz, C. 2023. Q4 2022 Quarterly Crown Land Sale Analysis. Accessed February 2023. https://digest.canadiandiscovery.com/article/8612
- Prairie Lithium, 2023. https://www.prairielithium.ca/dle-direct-lithium-extraction
- ROK Resources, 2023. ROK Resources Inc. Announces Record Lithium Concentrations. https://www.accesswire.com/739942/ROK-Resources-Inc-Announces-Record-Lithium-Concentrations

- Rostron, B., Maurer, Z., Hillier, C., Caplan, M., Kreis, L.K., 2022. Lithium in saline brines from the Duperow Aquifer in Southeastern Saskatchewan. https://www.youtube.com/watch?v=wTa_2DYnwcw
- Shouakar-Stash, O., 2008. Evolution of Stable Chlorine and Bromine Isotopes in Sedimentary Formation Fluids, Department of Earth Sciences, University of Waterloo.
- Underschultz, J.R., Yuan, L.P., Bachu, S. Cotterill, D.K. and Hitchon, B. 1994. Industrial mineral resources in Alberta formation waters. Alberta Geological Survey Open File Report 1994-13, 71 p. http:// www.ags.gov.ab.ca/publications/abstracts/OFR_1994_13.html.
- White, D.E. 1965. Saline waters of sedimentary rocks. In: Fluids in Subsurface Environments. A. Young and J.E. Galley (eds.). American Association of Petroleum Geologists Memoir 4, p. 342–366.

MONTNEY

Montney Overview

This chapter provides an overview of the Montney Formation's (Montney) geologic setting, historical development, data distribution, ion concentration relative to time on production, mixing trends and proxy analytics, potential lithium sources, water production, and recoverable lithium economics.

Fifty-one Montney brine samples were collected and analyzed for lithium (Li) and trace element data in the study area *(figures 5.1 and 5.2)*. The concentration of lithium in these samples ranges from 12 to 100 mg/L (milligram per litre), with a median value of 63 mg/L and an average of 58 mg/L *(table 5.1)*. The skewness of the data population likely results from lower lithium concentrations in samples obtained from the Swan area. In addition, the concentrations of boron, bromide, and iodide average 20 mg/L, 171 mg/L, and 8 mg/L, respectively. *Table 5.1* provides average, median, minimum, and maximum values of all analyzed major ions and trace elements in the program, including total dissolved solids (TDS).

5.1 Stratigraphic Chart

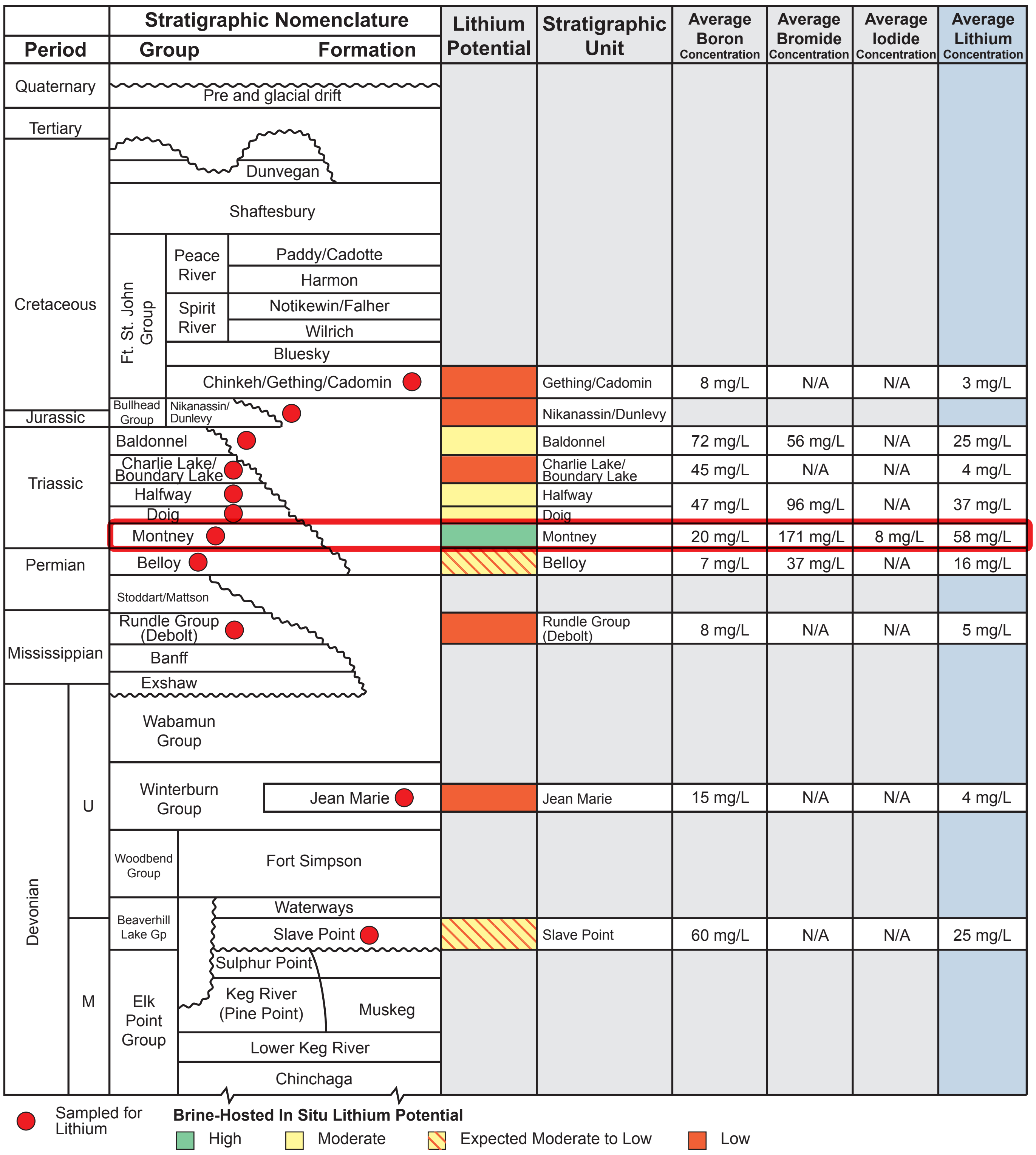

Lithium Potential	Stratigraphic Unit	Average Boron Concentration	Average Bromide Concentration	Average Iodide Concentration	Average Lithium Concentration
🟥	Gething/Cadomin	8 mg/L	N/A	N/A	3 mg/L
🟥	Nikanassin/Dunlevy				
🟨	Baldonnel	72 mg/L	56 mg/L	N/A	25 mg/L
🟥	Charlie Lake/ Boundary Lake	45 mg/L	N/A	N/A	4 mg/L
🟨	Halfway Doig	47 mg/L	96 mg/L	N/A	37 mg/L
🟩	Montney	20 mg/L	171 mg/L	8 mg/L	58 mg/L
▨	Belloy	7 mg/L	37 mg/L	N/A	16 mg/L
🟥	Rundle Group (Debolt)	8 mg/L	N/A	N/A	5 mg/L
🟥	Jean Marie	15 mg/L	N/A	N/A	4 mg/L
▨	Slave Point	60 mg/L	N/A	N/A	25 mg/L

● Sampled for Lithium

Brine-Hosted In Situ Lithium Potential

🟩 High 🟨 Moderate ▨ Expected Moderate to Low 🟥 Low

Modified from Bachu (1995) and this study

Figure 5.1

5.2 | Montney Lithium Sample Distribution Map

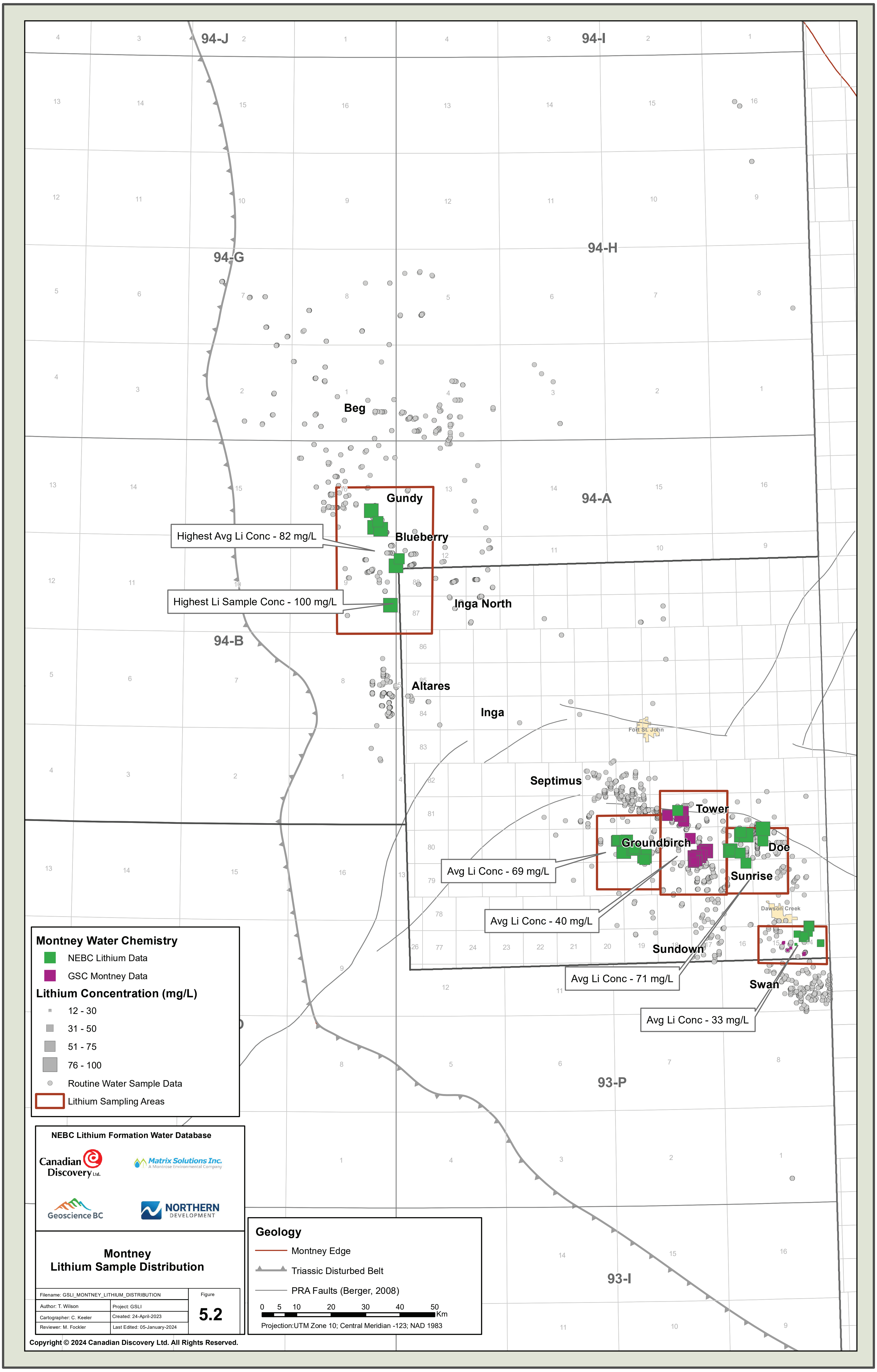

© Canadian Discovery Ltd.

Figure 5.2

Table 5.1: Statistics by Age for Analyzed Major Ions and Trace Elements

Major Ions and Trace Elements (Dissolved) (mg/L)	Montney				Triassic Aquifers				Triassic - Others			
	Average	Median	Min	Max	Average	Median	Min	Max	Average	Median	Min	Max
Potassium	2,227	2,205	125	3,910	1,074	1,026	230	1,960	804	910	521	980
Sodium	59,122	66,870	3,780	91,200	42,845	53,450	8,851	65,600	31,500	36,800	18,500	39,200
Calcium	15,508	16,430	841	23,320	2,182	2,420	33	5,800	2,127	2,267	1,520	2,595
Magnesium	1,550	1,495	182	2,850	511	534	15	1,100	413	409	400	430
Chloride	132,821	140,750	6,870	199,200	73,370	90,600	9,140	124,000	50,423	61,640	27,200	62,430
Aluminum	7	5	0.03	20	9	2	2	20	1	1	0.02	2
Antimony	3	1	0.01	10	2	0.50	0.50	5	0.17	0	0	0.50
Arsenic	6	2	0.01	30	5	1	1	10	1	1	1	1
Barium	245	10	0.05	1260	0.30	0.27	0.10	0.82	0.11	0.11	0.11	0.11
Beryllium	1	1	0	5	0.23	0.05	0.05	0.50	0.02	0	0	0.05
Boron	20	17	0.50	177	53	43	34	200	173	173	173	173
Bromide	171	169	17	306	82	65	27	152				
Cadmium	8	0.05	0	40	0.23	0.05	0.05	0.50	0.02	0	0	0.05
Chromium	0.40	0.50	0.01	1	0.24	0.05	0.05	0.50	0.02	0.01	0.01	0.05
Cobalt	0.59	1	0.01	1	0.46	0.10	0.10	1	0.04	0	0	0.10
Copper	0.56	1	0.01	1	0.46	0.10	0.10	1	0.04	0	0	0.10
Iodide	8	8	0	18								
Lead	8	2	0.01	20	9	2	2	20	1	1	0	2
Lithium	58	65	2	100	33	34	17	44	20	20	20	20
Molybdenum	0.66	1	0	1	0.46	0.10	0.10	1	0.03	0	0	0.10
Nickel	0.88	0.20	0.01	2	0.92	0.20	0.20	2	0.07	0	0	0.20
TDS (Calculated)	**211,607**	**228,119**	**14,128**	**309,457**	**122,516**	**151,861**	**21,774**	**196,029**	**88,070**	**105,374**	**51,412**	**107,425**

Major Ions and Trace Elements (Dissolved) (mg/L)	Cretaceous				Permian				Devonian-Mississippian			
	Average	Median	Min	Max	Average	Median	Min	Max	Average	Median	Min	Max
Potassium	104	102	67	175	598	467	162	1,490	379	119	31	1,105
Sodium	8,566	10,500	3,700	13,900	21,166	16,900	5,330	50,800	13,558	9,377	6,150	35,250
Calcium	523	173	29	1,280	1,580	1,330	436	3,810	2,185	1,658	129	8,390
Magnesium	114	74	24	230	301	253	88	708	308	209	159	867
Chloride	12,442	17,860	2,760	20,800	39,820	30,900	10,700	103,000	23,648	14,440	12,000	64,000
Aluminum	2	2	2	2	2	2	2	2	2	2	0.10	2
Antimony	0.50	0.50	0.50	0.50	0.50	0.50	0.50	0.50	0.36	0.50	0	0.50
Arsenic	1	1	1	1	1	1	1	1	0.87	1	0.01	1.49
Barium	49	5	1	119	6	6	0.07	11	590	392	1.07	1890
Beryllium	0.05	0.05	0.05	0.05	0.05	0.05	0.05	0.05	0.04	0.05	0	0.05
Boron	8	8	4	11	6	6	6	6	25	8	5	61
Bromide	65	65	65	65	37	35	0	73				
Cadmium	0.05	0.05	0.05	0.05	0.05	0.05	0.05	0.05	0.04	0.05	0	0.05
Chromium	0.05	0.05	0.05	0.05	0.05	0.05	0.05	0.05	0.05	0.05	0.01	0.09
Cobalt	0.10	0.10	0.10	0.10	0.10	0.10	0.10	0.10	0.07	0.10	0	0.10
Copper	0.10	0.10	0.10	0.10	0.10	0.10	0.10	0.10	0.11	0.10	0.01	0.33
Iodide												
Lead	2	2	2	2	2	2	2	2	1	2	0	2
Lithium	3	3	2	4	16	16	16	16	16	5	4	30
Molybdenum	0.10	0.10	0.10	0.10	0.10	0.10	0.10	0.10	0.08	0.10	0	0.10
Nickel	0.20	0.20	0.20	0.20	0.20	0.20	0.20	0.20	0.15	0.20	0.01	0.20
TDS (Calculated)	**23,641**	**31,190**	**9,297**	**36,773**	**63,658**	**50,181**	**16,865**	**159,975**	**41,117**	**27,098**	**20,344**	**107,775**

Table 5.1

Geologic Setting

The Lower Triassic Montney Formation covers a 130,000 km^2 area in total (65,300 km^2 in BC) and ranges from 0 to over 400m thick. It is 200 to 300m thick through the main productive unconventional gas fairway (gas from low porosity reservoirs such as shales that require hydraulic fracturing to produce hydrocarbons) and extends from the Prophet River south of Fort Nelson in NEBC to Edson in west-central Alberta. The Montney is a mixed siliciclastic-carbonate wedge deposited in shallow marine and shelf environments. It comprises various sedimentary facies, ranging from distal shoreface siltstones with turbidite complexes, to proximal shoreface-associated fine-grained sandstones and coquinas primarily up-dip in Alberta *(figures 5.3 and 5.4)*. Situated between the North American Craton to the east and an island arc system to the west, depositional contributions are likely sourced from multiple environments (Wust et al., 2018). The Montney has a complex structural history that includes the reactivation of older tectonic elements such as the Peace River Arch (PRA) and the Hay River Fault zone (Zonneveld and Moslow, 2018; Davies et al., 2018), as well as significant burial during the Laramide Orogeny and subsequent uplift during the Tertiary (Ness, 2001). Burial history plots for the Montney *(figure 5.5)* indicate maximum burial in excess of 8,000m at Tumbler Ridge, BC corresponding to maximum burial temperatures in excess of 250°C.

Variable reservoir quality, multiple source rocks and multiple phases of hydrocarbon migration, plus a complex structural and geothermal history have all contributed to a complex hydrodynamic, fluid phase and fluid saturation system in the Montney. The offshore distal siltstone and turbidite facies represent the bulk of the unconventional Montney where gas and gas liquids are the continuous fluid phase. These areas, particularly where overpressured, have low water saturation or are undersaturated. Towards the northeast, the Montney thins due to erosion and transitions to storm-dominated shoreface and shoreface facies. These areas have conventional water saturation and hydrocarbon trapping characteristics and come into hydraulic communication with the underlying Permian and

5.3 Montney Regional Facies Map

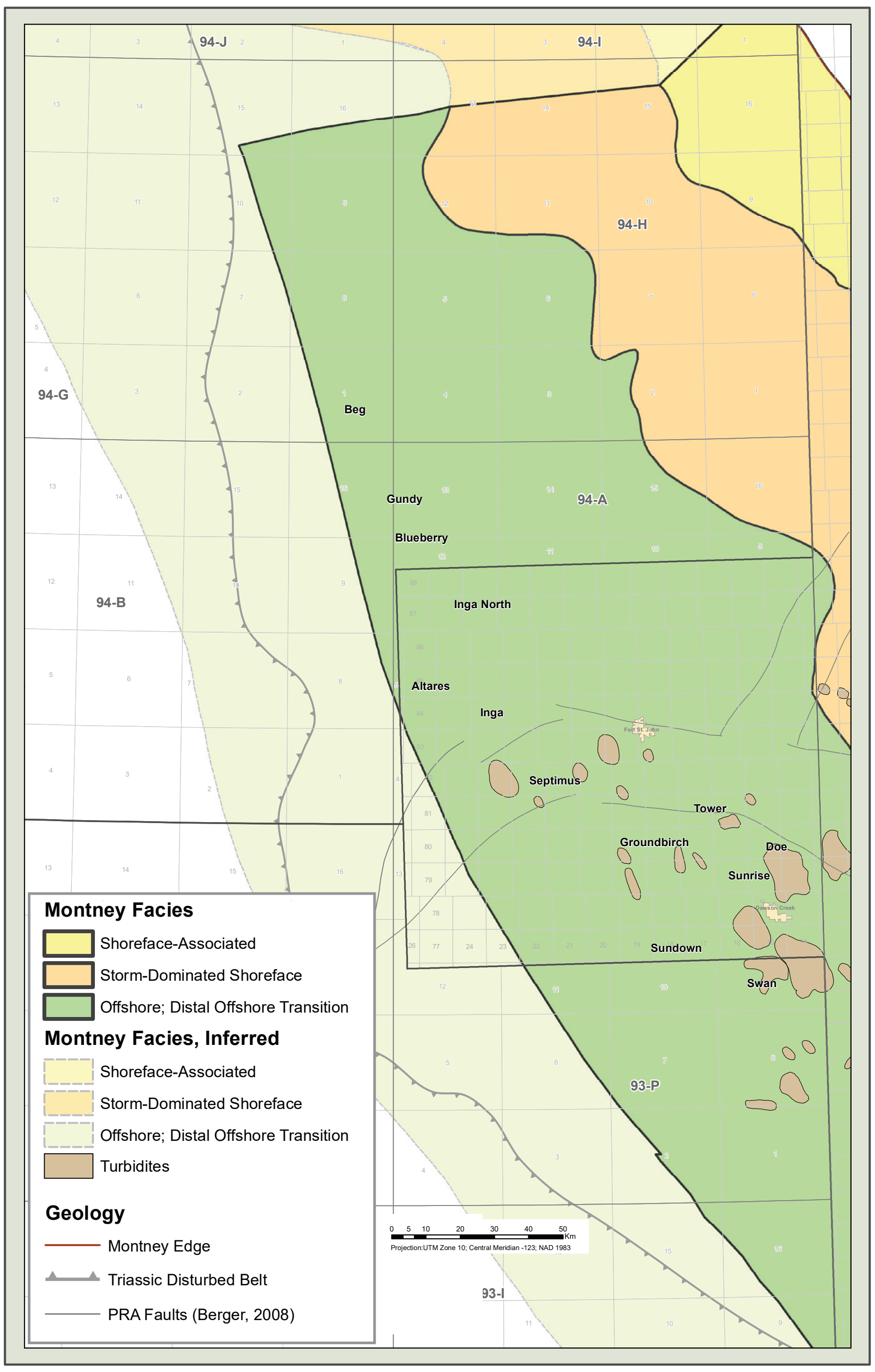

© Canadian Discovery Ltd. *Figure 5.3*

5.4 Montney Simplified Schematic Cross-Section

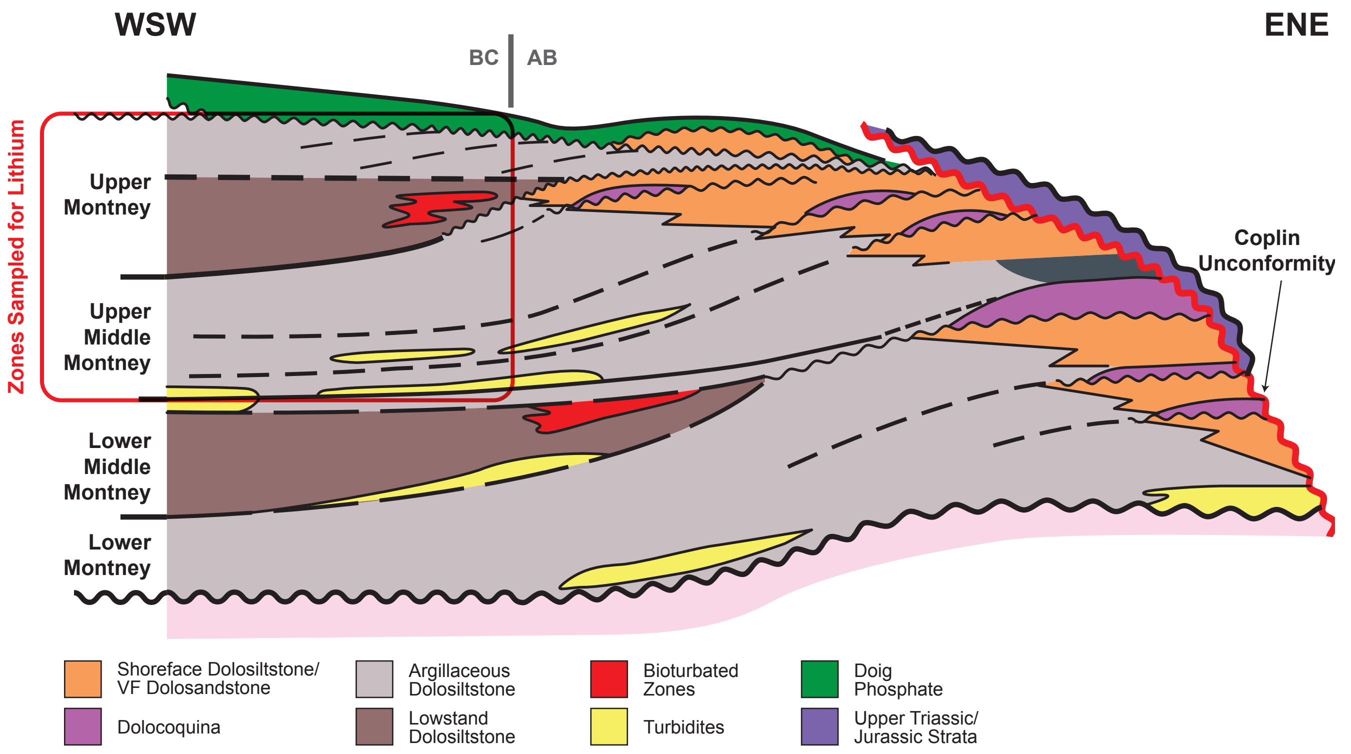

Modified from Davies et al., 2018

© Canadian Discovery Ltd. *Figure 5.4*

5.5 Montney Burial History

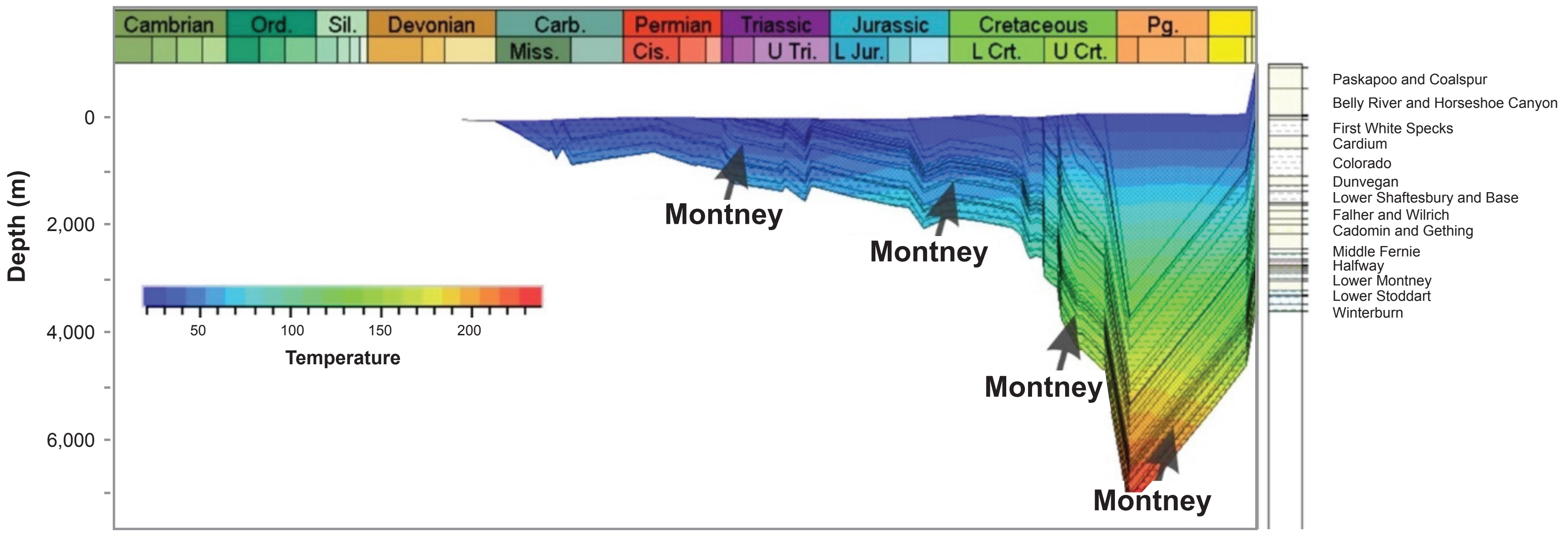

One-dimensional burial history of the basin at a location in BC, highlighting the Montney Formation and showing as overlays.

Source: Chalmers et al., 2022.

Figure 5.5

Mississippian aquifers. Within the conventional system to the northeast, hydrocarbon pools such as Ring Border occur within discrete stratigraphic and structural traps.

All the Montney brine samples obtained in the field program for this study are from the Upper and Upper Middle zones *(figure 5.4)* where most of the current Montney producing horizontal wells have been targeted by the industry.

Historical Montney Development

The Montney has been the target of conventional oil and gas exploration in the Western Canada Sedimentary Basin (WCSB) since the 1960s; however, development of the gas-saturated low porosity, low permeability distal siltstone and turbidite facies started around 2005. Advances in horizontal drilling and multi-stage hydraulic fracturing made it possible to economically develop this extensive unconventional resource. The total resource or gas-in-place (GIP) for the Montney across both BC and Alberta is 23,998 billion m^3 or 847 Tcf of unconventional petroleum product with an ultimate marketable resource of 4,726 billion m^3 or 167 Tcf (BCER, 2022). The Montney gas play in Western Canada is considered one of the world's most significant resource plays (Financial Post, 2016).

Hydraulic fracturing involves injecting large volumes of hydraulic fracturing fluid, comprising water, proppants (usually sand) and minor additives, at high pressure into the formation. The induced fracture network stimulates the reservoir sufficiently to enhance hydrocarbon flow, which allows previously inaccessible or uneconomic hydrocarbon resources to be produced. The induced fractures increase the amount of rock surface area accessible to the injected fluids and naturally occurring formation water. During fracture completion and production, pressure is released and a portion of hydraulic fracturing fluid flows back to the surface along with formation fluids. This mixture of flowback and produced formation water typically has higher concentrations of dissolved metals than the injected fluids (Leece and Jiang, 2023). Understanding the concentrations of the dissolved trace metals and major ions in the produced water, and their volumes, is critical for determining potentially economic extraction schemes.

5.6 Montney Lithium Concentrations by Area

a. Lithium Concentration by Area

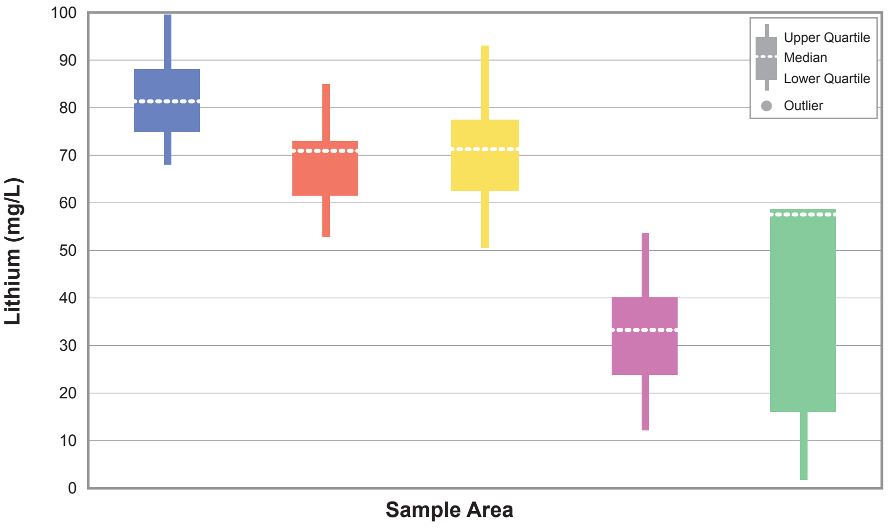

	Blueberry/Gundy	Groundbirch	Parkland/Doe	Swan	Tower/Septimus
Count	14	20	20	15	6
Average	82	69	71	33	40
Median	82	71	71	33	59
Min	68	53	51	12	2
Max	100	85	93	54	59

b. Lithium Concentration vs TDS

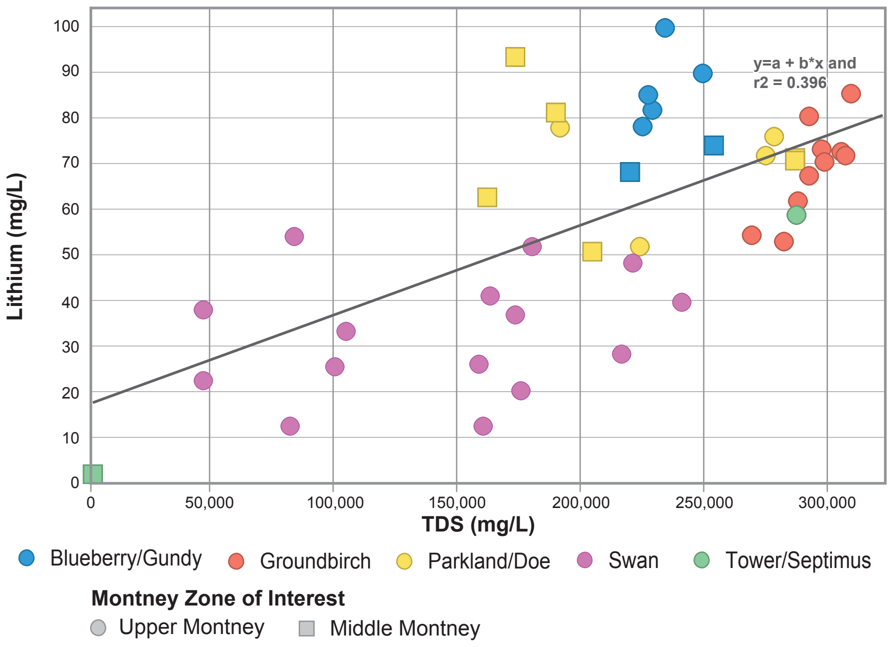

Lithium data sources from the current study

© Canadian Discovery Ltd.

Figure 5.6

Data Distribution

Participants in the sampling program in this study provided access to samples from the Upper and Middle Montney zones in five areas where the Montney is currently being developed, specifically Blueberry/Gundy, Groundbirch, Tower/Septimus, Parkland/Doe, and Swan *(figure 5.6)*. Fifty-one individual samples were collected and analyzed; these data are listed in *Appendix A*. In addition, the Geologic Survey of Canada (GSC) collected and analyzed samples from 74 wells, 64 of which are in NEBC (Kingston et al., 2023). The locations of the GSC samples and those from this study are shown in *figure 5.2*. Analytical data from these GSC samples are incorporated into the discussion on water chemistry trends and mapping later in this chapter.

Lithium concentrations for the samples range from 12 to 100 mg/L. Although DLE technologies are able to extract lithium from brines with very low concentrations of lithium, concentrations greater than 50 mg/L are typically considered to be of economic interest (Standard Lithium, 2021; LithiumBank, 2023). *Figure 5.6a* displays the range of concentrations from samples obtained in the five main areas from this study. Blueberry/Gundy has the highest average lithium concentration at 82 mg/L (median is 82 mg/L) and the highest single sample (100 mg/L), while Swan has the lowest average concentration at 33 mg/L (median is also 33 mg/L). The R2 fit for these data is 0.396 as compared to the entire WCSB dataset of 0.83 on a log-log data plot *(figure 5.6b)*. It is observed that data from Swan downgrade the correlation, however, all other data appear to have lithium concentrations greater than 50 mg/L where the TDS exceeds 150,000 mg/L *(figure 5.6b)*. The lithium concentrations within produced fluids from the Montney appear significantly higher than other sampled geological zones in NEBC; however, other viable aquifers identified by Canadian Discovery (CDL, 2022) have a paucity of data and remain inadequately characterized.

In the following sections, various aspects of the program and the derived data that may impact sampling bias/validity and interdependent ionic relationships that have been used to interpolate lithium distribution between sampled areas are analyzed. These include:

- Time on-production
- Screening protocols
- Mixing trends

Dissolved Ion Concentrations, Time On-Production, and Quality Control

Aqueous chemistry time series plots record the chemical evolution of flowback and produced water over the production period of a well, generally evolving from lower TDS and lithium concentrations that mimic "frac water" composition to a representative formation-like brine (Kingston et al., 2023). When plotting TDS values vs time on-production for wells with multiple samples, a late-time area on each curve where the TDS values plateau is apparent *(figures 5.7a-e)*. A general correlation between lithium and TDS is observed; as the concentration of TDS increases, the concentration of lithium and other dissolved ions such as chloride also increases. Data from the Alberta Montney *(figure 5.7f)* (Kingston et al., 2023) indicate a strong correlation between TDS and chloride with lithium, where 90% of a stabilized value is reached after about 100 days of cumulative on-production. Due to this time lag to reach stabilization, sample timing can create a bias in sample analysis results in both TDS and lithium reported concentrations.

While each area in this study is unique with respect to reaching the stabilized plateau, most of the areas appear to plateau around 100 days on-production. Therefore, dissolved ion concentrations after this time period tend to be more representative of formation water concentration. Samples taken earlier may have lower TDS and lithium concentrations and therefore may be less representative. In addition to the normal quality-control (QC) process for routine water chemistry data, TDS vs time on-production plots have been used as another screening tool.

Detailed information regarding sample collection protocols and chain of custody for this dataset can be found in *Appendix B*. Due to the nature of Montney flowback and produced water evolution, care was taken, where possible, to only sample wells that had been on-production for longer than 100 days; however, a small subset were on-production for a shorter period of time.

5.7 Montney TDS with Time Curves

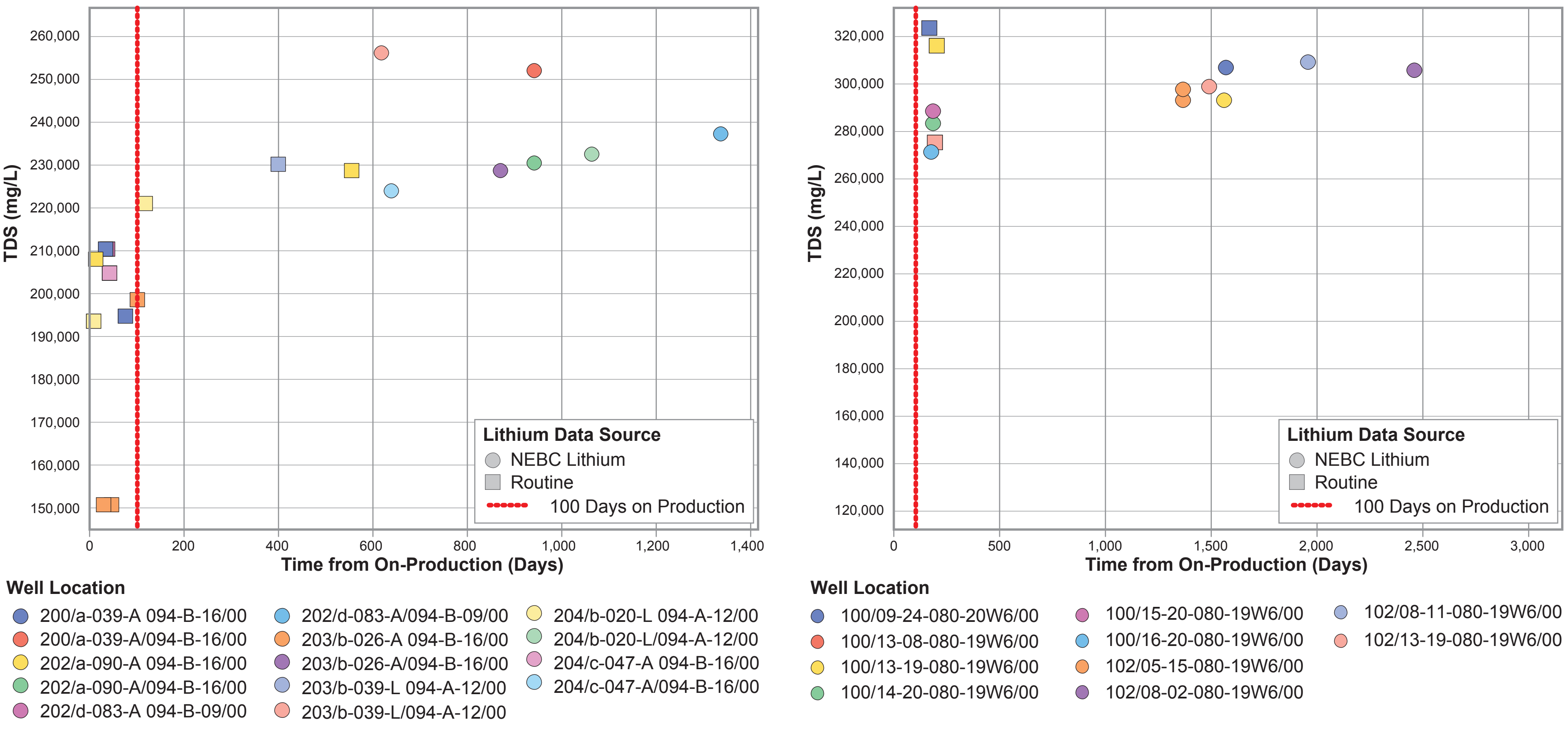
a. Blueberry/Gundy

b. Groundbirch

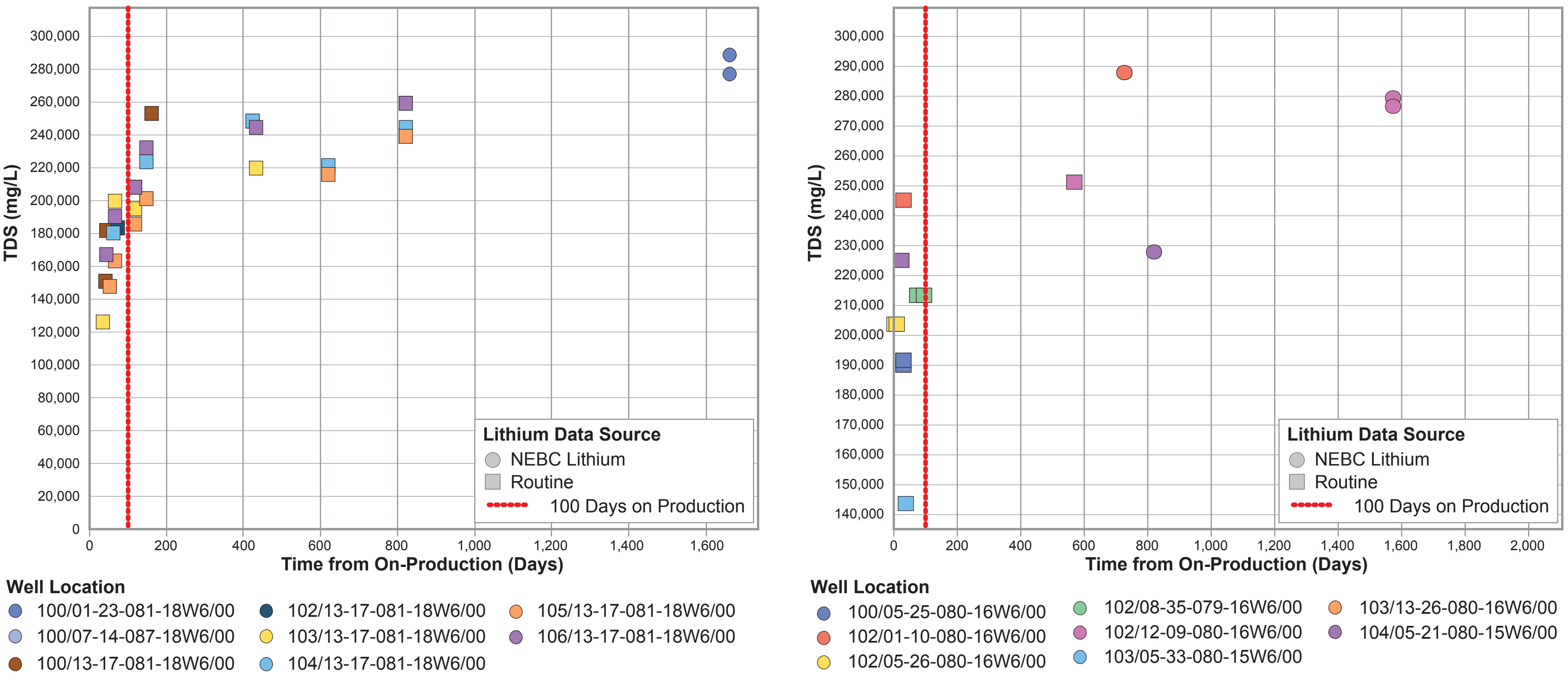
c. Tower/Septimus

d. Parkland/Doe

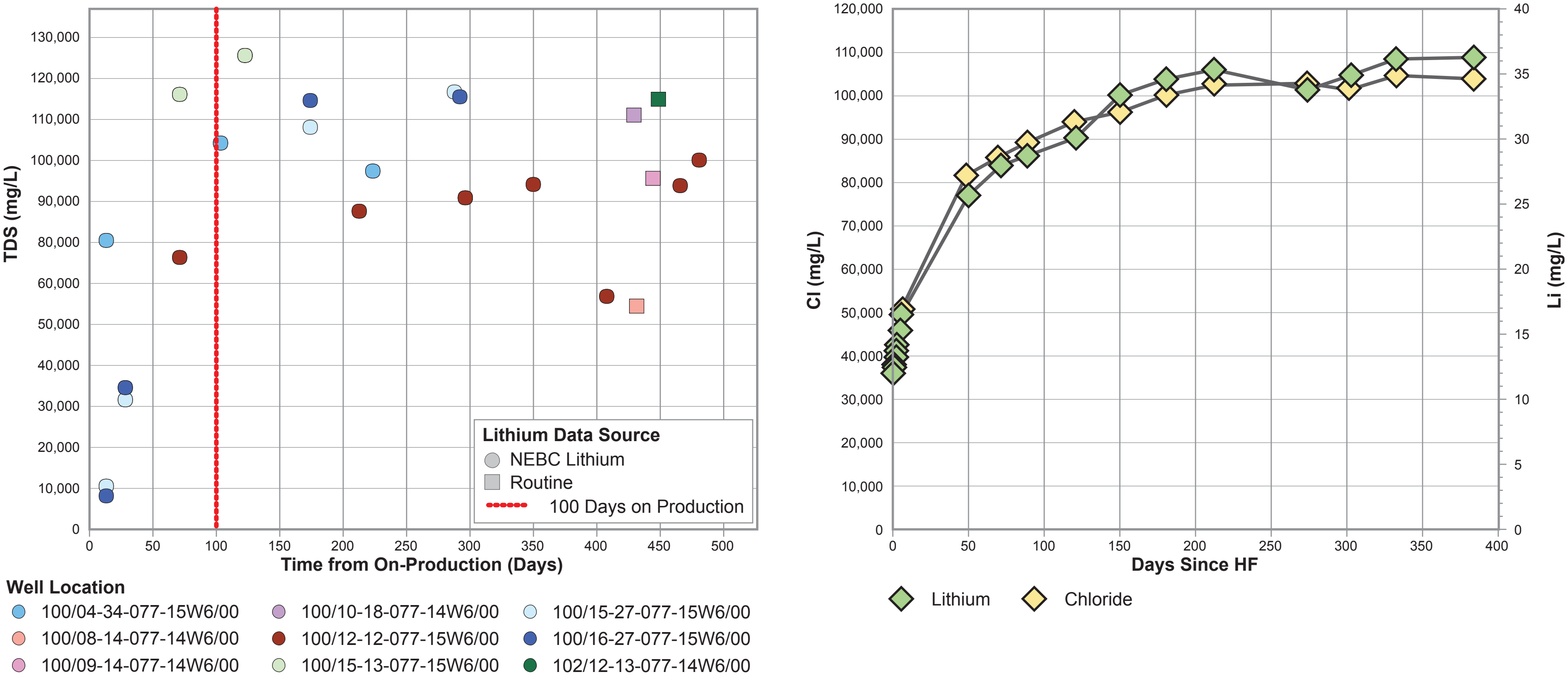
e. Swan

f. Li and Cl vs Days Since Hydraulic Fracturing (HF)

Data from geoLOGIC and current study. 5.7f Li and Cl data from Kingston et al., 2023

Figure 5.7

TDS, Mixing Trends and Proxy Analysis

Due to the limited extent of the sampling program, several other datasets were included in this analysis. Routine water analyses from geoLOGIC for Montney tested or producing wells were examined and statistically analyzed for indicative/proxy chemical signatures to those observed in areas of higher lithium concentrations. Focus was placed on wells with late-time water sampling (>100 days on-production), and then the data went through the routine water chemistry screening process outlined in *Appendix C*. The regional distribution of "maximum" formation water salinity for the screened samples is shown on the Montney TDS map *(figure 5.8)*. In general, TDS within NEBC increases from 25,000 parts per million (ppm) in the northeast near the erosional edge at Ring-Border to >250,000 ppm southwest of Groundbirch.

Two additional datasets with lithium concentrations have been included in the water chemistry characterization and proxy analyses:

1. Geologic Survey of Canada (GSC) Open File 8974 (Kingston et al., 2023), which reported 64 samples in NEBC
2. Alberta Geological Survey (AGS) lithium database from Alberta, introduced in *Chapter 4*

These datasets were combined for the multi-variate analyses and are provided in *Appendix A*. *Figures 5.9 and 5.10* show the correlation and dependency relationships of major ions typically measured in routine water analysis as compared to lithium data from this study. The relationship between TDS and lithium has been discussed in earlier sections and can be found in *figures 5.6 and 5.8*. The purpose of this analysis is to determine the genetic evolution of Montney formation waters and which ions provide proxy indicators for lithium concentration.

Chloride and bromide are considered to be conservative ions during water-rock interactions because both ions have a constant ratio to salinity and tend to stay in solution. They have been used for multi-variate analytics for normalization purposes. The Cl/Br vs Na/Br plot *(figure 5.9a)* provides a reference for formation water chemistry evolution relative to modern seawater. If data plot below and to the left of modern seawater, it is generally interpreted to represent salinity acquired through evapoconcentration. If data plot above and to the right, it is generally interpreted that salinity is acquired through halite dissolution. Most of the Montney data have Cl/Br and Na/Br ratios higher than seawater, indicating halite dissolution. *Figure 5.9b* is a plot of Cl vs Br relative to the seawater evaporation and mixing curves as defined by Shouakar-Stash (2008). With respect to chloride levels, most samples only reach gypsum saturation, with some at halite saturation, but all samples appear to be depleted in bromide, which suggests mixing.

Figures 5.9c and 5.9d are plots of Mg vs Cl and Ca vs Cl as indicators of potential dolomitization due to the interaction with the brines. The magnesium concentration decreases with increased dolomitization, as it replaces calcium in carbonate minerals causing relative enrichment of calcium in brines relative to seawater.

The majority of samples from this study with higher lithium values fall into a narrow range of magnesium concentrations from approximately 100 to 180 milliequivalent per litre (meq/l) *(figure 5.9c)*. This tends to correlate to calcium levels between 400 – 1,200 meq/l and chloride concentrations >3,000 meq/l *(figure 5.9d)*. When the data that fall within these Mg-Ca-Cl concentration ranges are displayed on a map including routine water analyses *(figure 5.11)*, several areas stand out. Altares, as well as the southern portion of Beg, Inga North, Sundown and the southern part of Swan/Pouce Coupe are areas with Mg-Ca-Cl concentrations within the ranges mentioned above (i.e., a proxy for potential higher lithium concentration). Observed magnesium and calcium ranges in areas of elevated lithium should be investigated to determine the role of hydrothermal dolomitization.

The K/Br vs Cl/Br plot is commonly used to indicate water-rock interaction with volcanically derived potassium feldspars (K-feldspars) *(figure 5.9e)* (Wust et al., 2018). The K/Br ratio is slightly elevated relative to the Cl/Br ratio, particularly for the NEBC samples, which suggests water-rock interactions involving silicate alteration as a source of lithium (Eccles and Berhane, 2011). Silicates such as K-feldspars are reported to have lithium concentrations ranging from 5 to 1,200 ppm by Dugamin et al., 2023.

The multi-variate analyses of the relationships between lithium concentrations and potassium (K), sulphate (SO_4), calcium (Ca), magnesium (Mg), bromide (Br), strontium (Sr), and chloride (Cl) are shown in *figure 5.10*. The correlation between lithium and potassium *(figures 5.10a and b)* shows generally greater variability in the NEBC sample dataset (broader geographic area) vs the GSC and AGS data (localized sampling). The lithium versus potassium relationship for the BC and Alberta data *(figure 5.10b)* provides an R2 fit of 0.857. *Table 5.2* shows that K-feldspars weight % in whole rock samples at Altares (Vaisblat et al., 2017) was ~6.9%; Dugamin (2023) reported a lithium concentration range in K-feldspars from 5 to 1,200 ppm. These data, along with late stage activation of feldspar dissolution/precipitation (>90°C) appear to support the theory of water-rock interaction with volcanically derived K-feldspars. Potassium concentration over the Montney area is shown in *figure 5.12*. Further research is required to quantify the sources and distribution of K-feldspars and their relationship to lithium enrichment.

Table 5.2: Montney Whole Rock Geochemistry for Altares 16-17-083-25W6

a. Concentration Ranges of Lithium in Minerals and Minerals in Whole Rock

Li Concentration in Mineral (Dugamin et al., 2023)	K-feldspar (ppm)	Plagioclase (ppm)	Muscovite (ppm)	Biotite (ppm)	Kaolinite (ppm)	Chlorite (ppm)	Illite/MLIS (ppm)	Balance of Rock (ppm)
Lowest quartile (Q1)	5	100	480	200	10	15	35	0
Highest quartile (Q3)	1,100	1,000	2,300	1,200	340	40	120	0
Average	552.5	550	1390	700	175	27.5	77.5	0

Concentration of Mineral in Whole Rock (Vaisblat et al., 2017)	K-feldspar (wt%)	Plagioclase (wt%)	Muscovite (wt%)	Biotite (wt%)	Kaolinite (wt%)	Chlorite (wt%)	Illite/MLIS (wt%)	Balance of Rock (wt%)
Minimum	0.96	2.96	1.09	0.08	0.32	0.12	4.69	89.78
Maximum	11.5	12.87	7.42	1.09	1.83	1.95	29.23	34.11
Average	6.89	8.8	4.3	0.39	0.68	0.79	15.06	63.09

b. Estimated Lithium Concentration in Whole Rock (ppm)

Concentration of Mineral in Whole Rock	Li Concentration in Mineral (ppm)			
	Q1	Average	Q3	Egobabawaye, 2016
Minimum	10.1	41.5	73.0	11.0
Average	36.0	162	288	16.8
Maximum	61.9	271	481	26.9

Sources: 5.4a Li Concentration in Mineral, Dugamin et al., 2023; Concentration of Mineral in Whole Rock, Vaisblat et al., 2017. 5.4b Egobabawaye, 2016

Table 5.2

5.8 | Montney Total Dissolved Solids Map

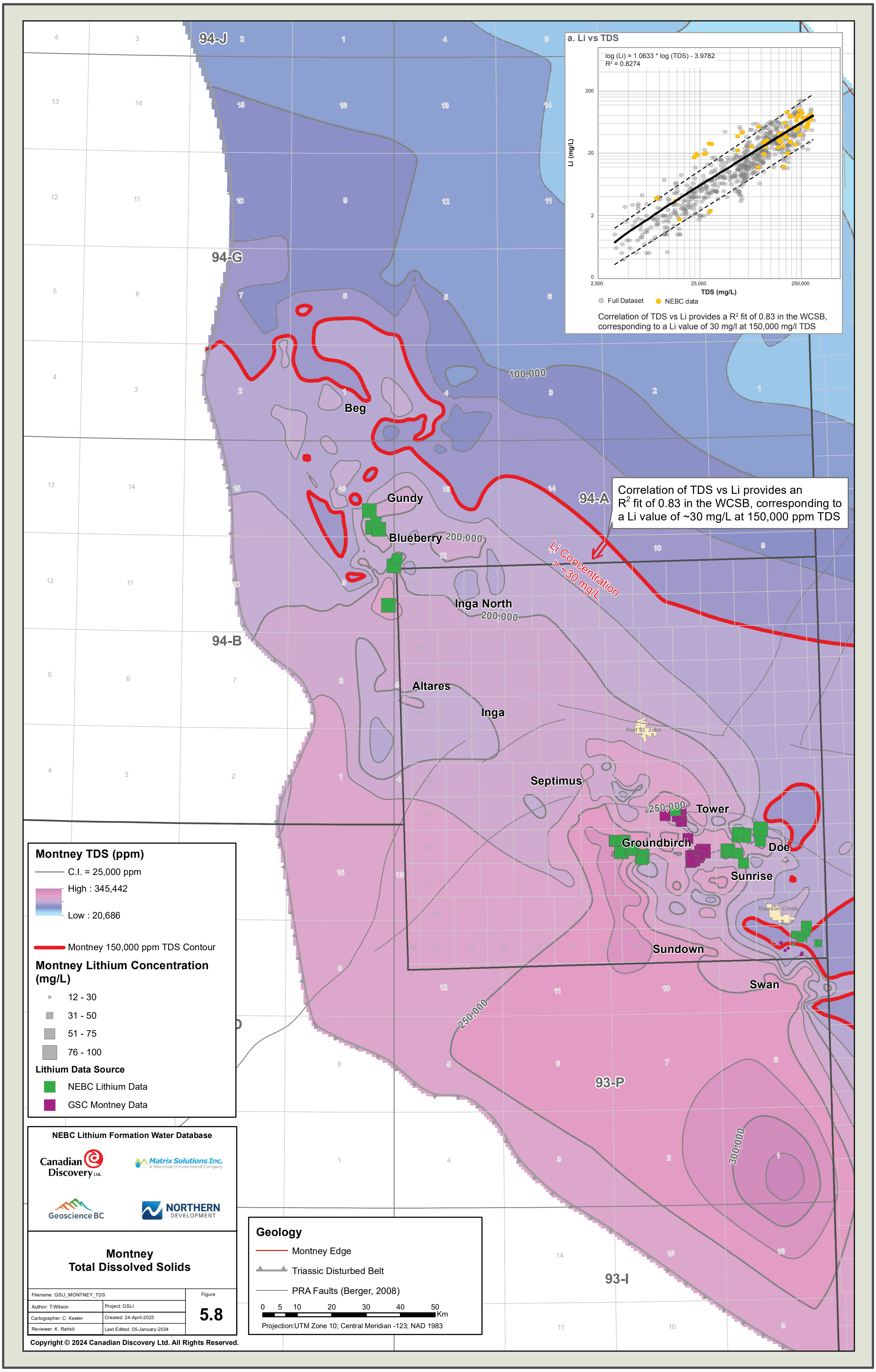

Correlation of TDS vs Li provides a R² fit of 0.83 in the WCSB, corresponding to a Li value of 30 mg/l at 150,000 mg/l TDS

Correlation of TDS vs Li provides an R² fit of 0.83 in the WCSB, corresponding to a Li value of ~30 mg/L at 150,000 ppm TDS

Montney
Total Dissolved Solids

Filename: GSLI_MONTNEY_TDS
Author: T.Wilson
Project: GSLI
Cartographer: C. Keeler
Created: 24-April-2023
Reviewer: K. Rahkit
Last Edited: 05-January-2024
Figure 5.8

© Canadian Discovery Ltd. *Figure 5.8*

5.9 Montney Water Chemistry Crossplots

a. Cl/Br vs Na/Br

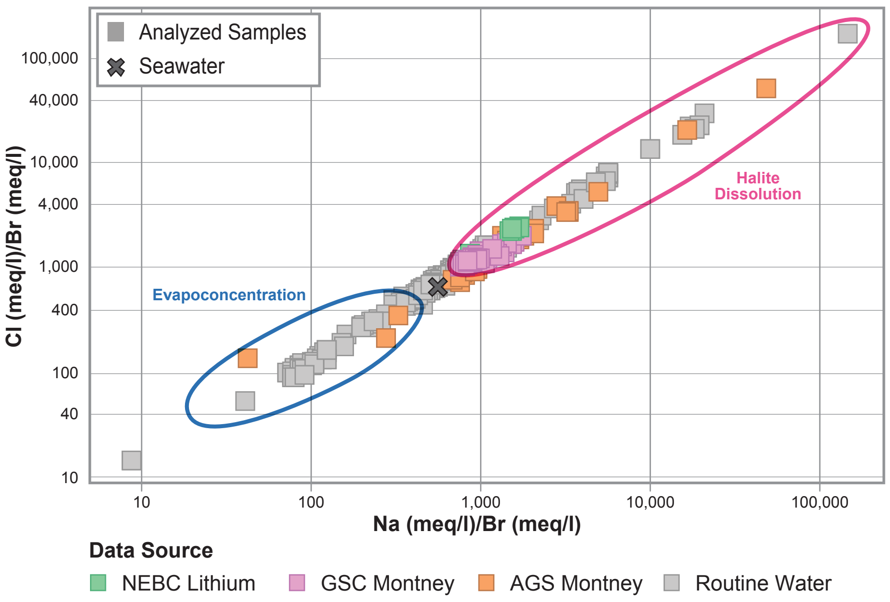

b. Montney Cl vs Br with Seawater Evaporation Line

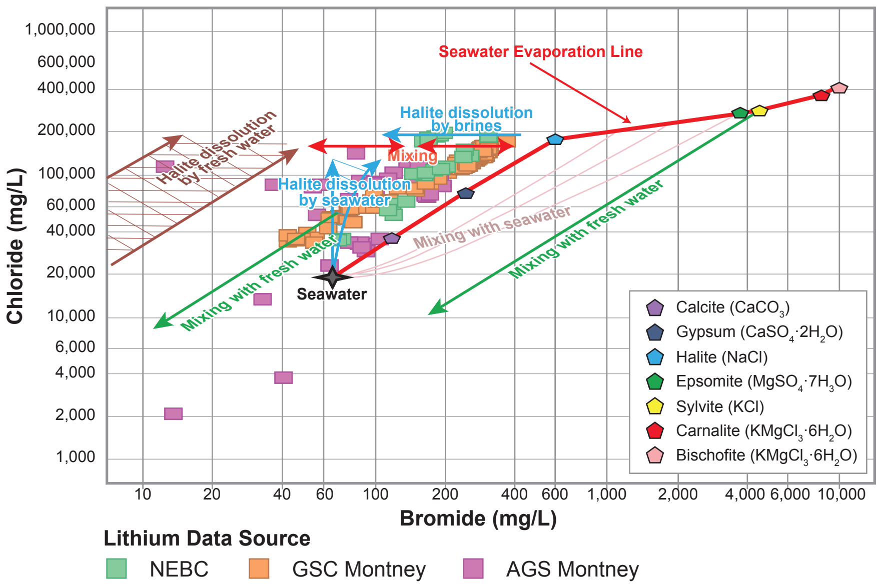

c. Mg vs Cl

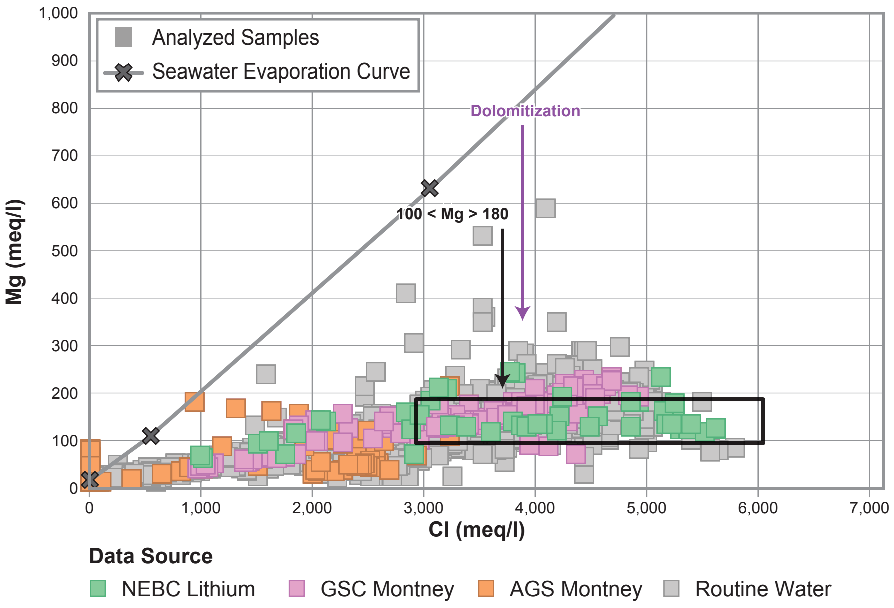

d. Ca vs Cl

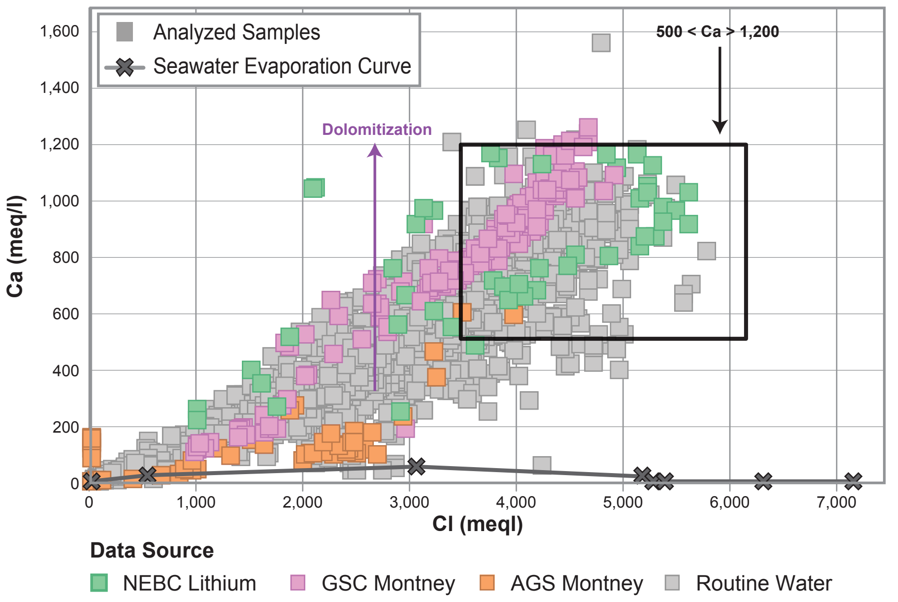

e. K/Br vs Cl/Br

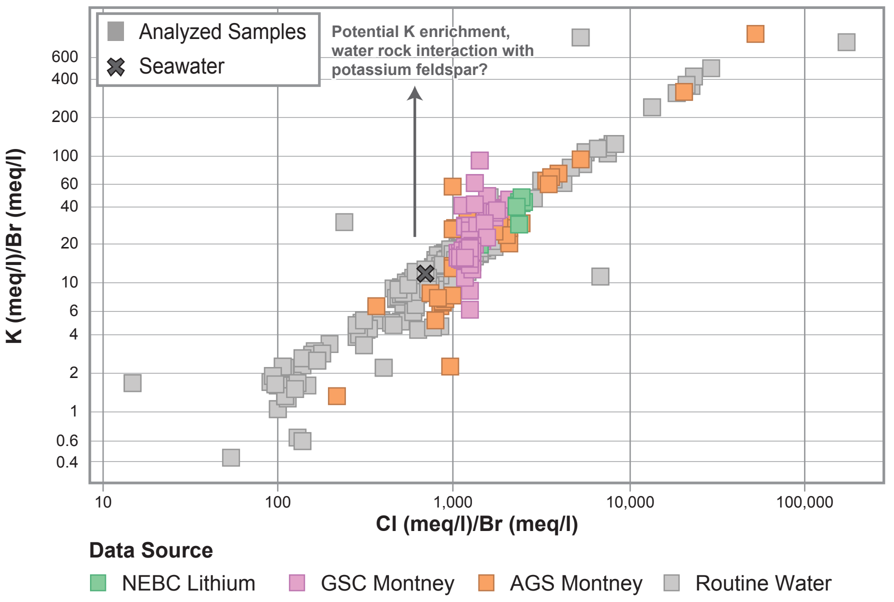

Lithium data from the AGS, GSC, geoLOGIC and the current study. Figure 5.9b data from Shouakar-Stash, 2008

Figure 5.9

5.10 Montney Water Chemistry Lithium Crossplots

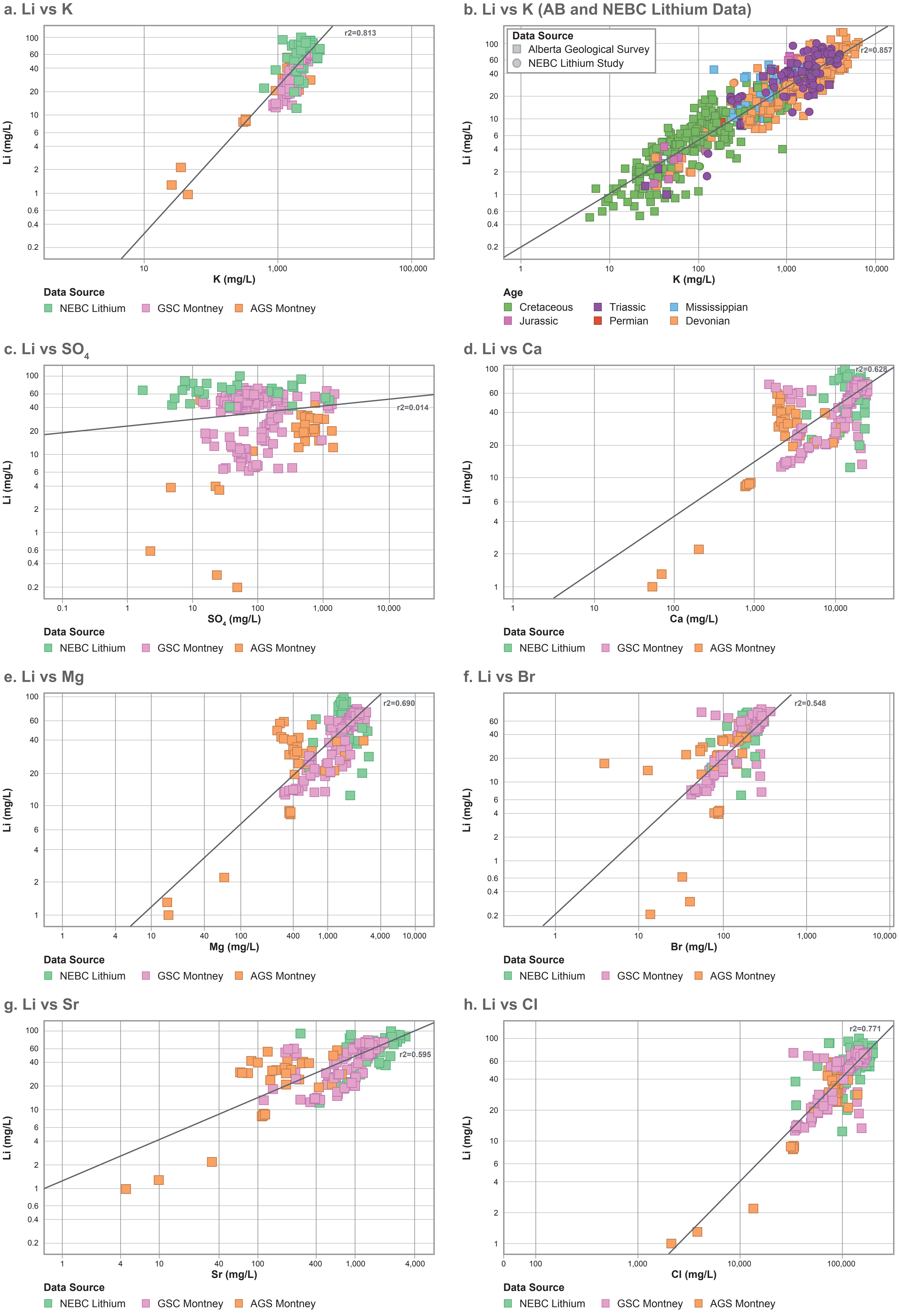

Lithium data from the AGS, GSC, geoLOGIC and the current study.

Figure 5.10

5.11 | Montney Mg- and Ca-Enriched Areas Map

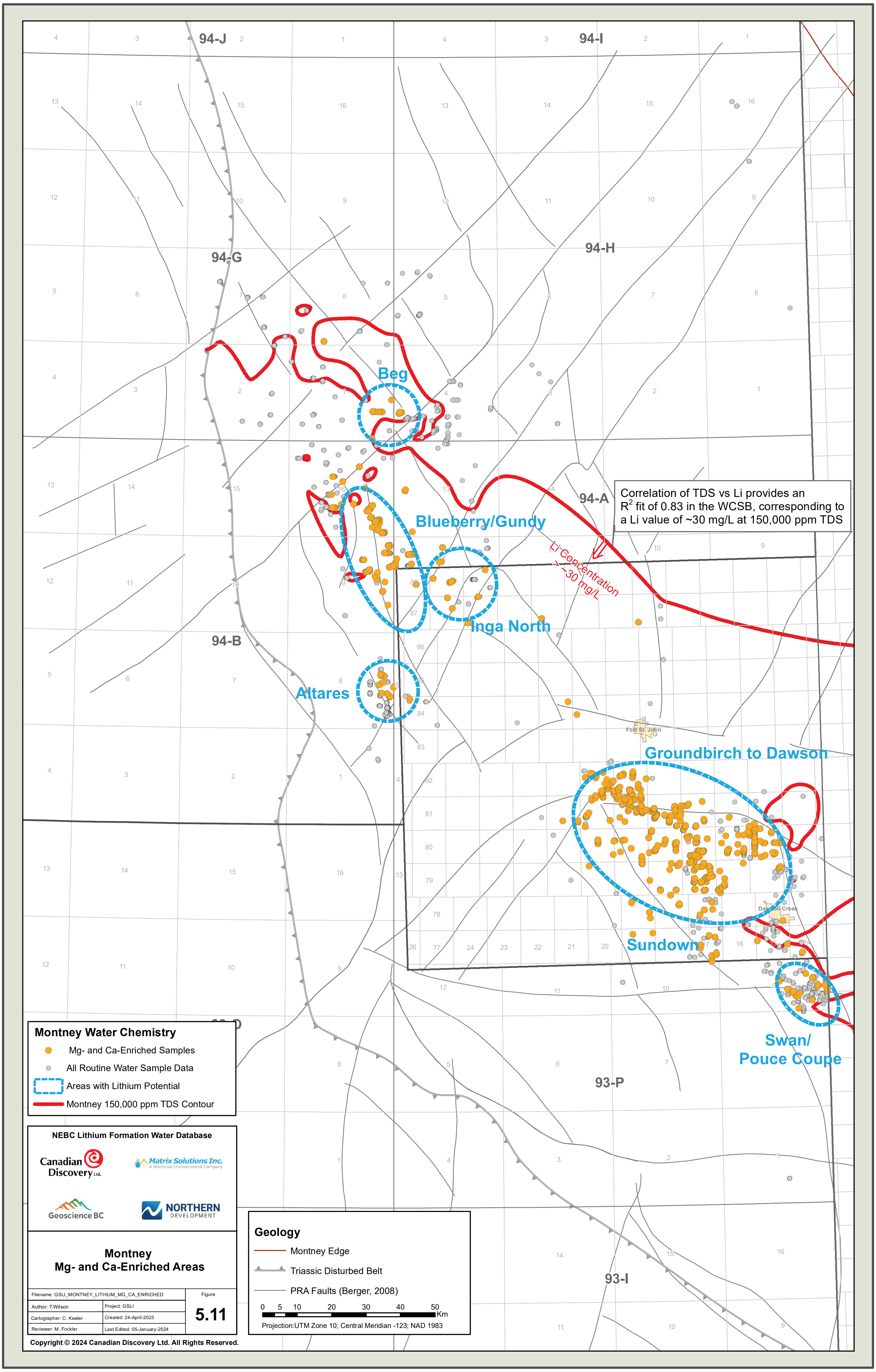

Correlation of TDS vs Li provides an R^2 fit of 0.83 in the WCSB, corresponding to a Li value of ~30 mg/L at 150,000 ppm TDS

© Canadian Discovery Ltd. *Figure 5.11*

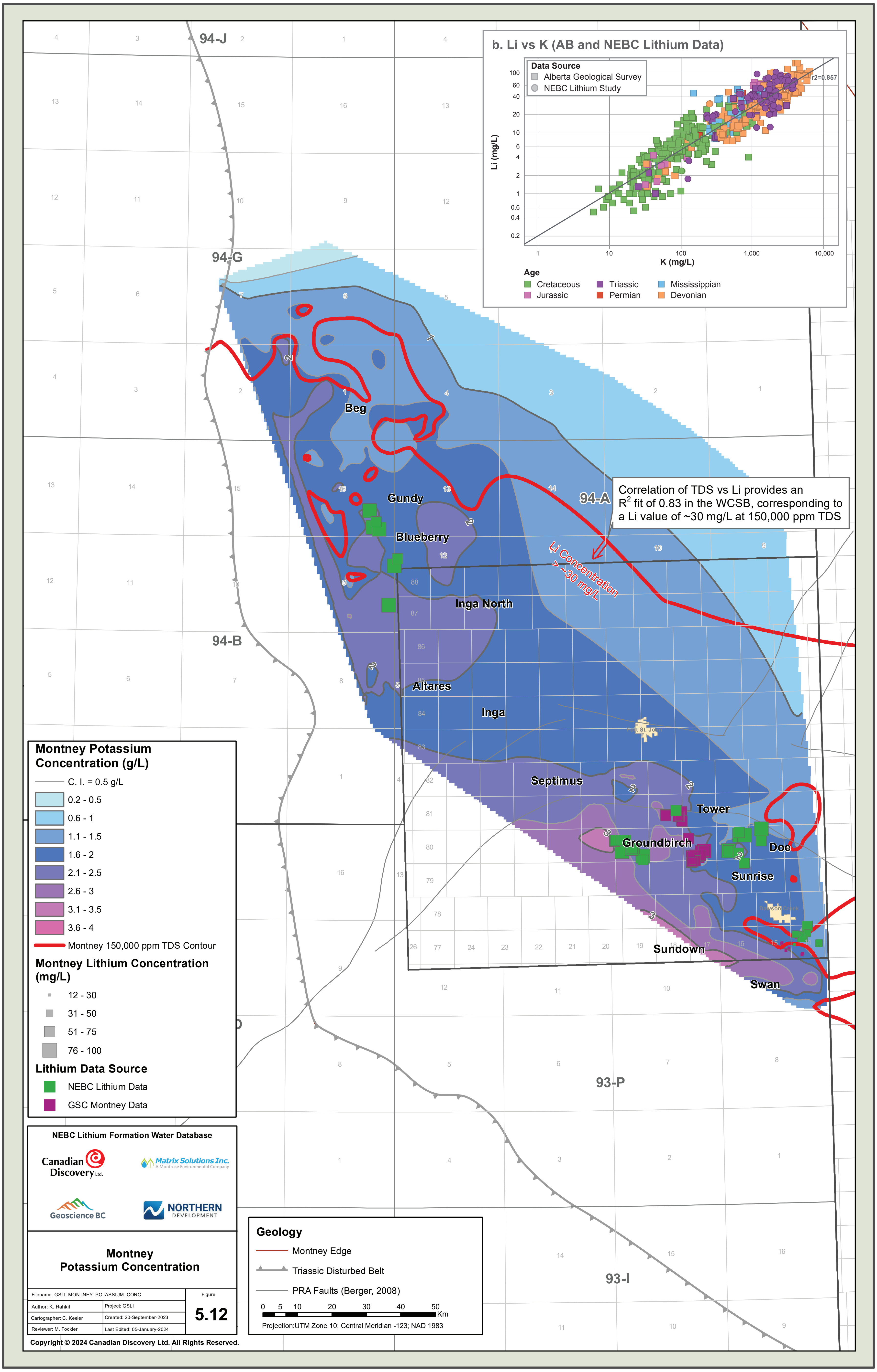

Correlation of TDS vs Li provides an R^2 fit of 0.83 in the WCSB, corresponding to a Li value of ~30 mg/L at 150,000 ppm TDS

© Canadian Discovery Ltd.

Figure 5.12

5.13 Montney Temperature and Geothermal Gradient Maps

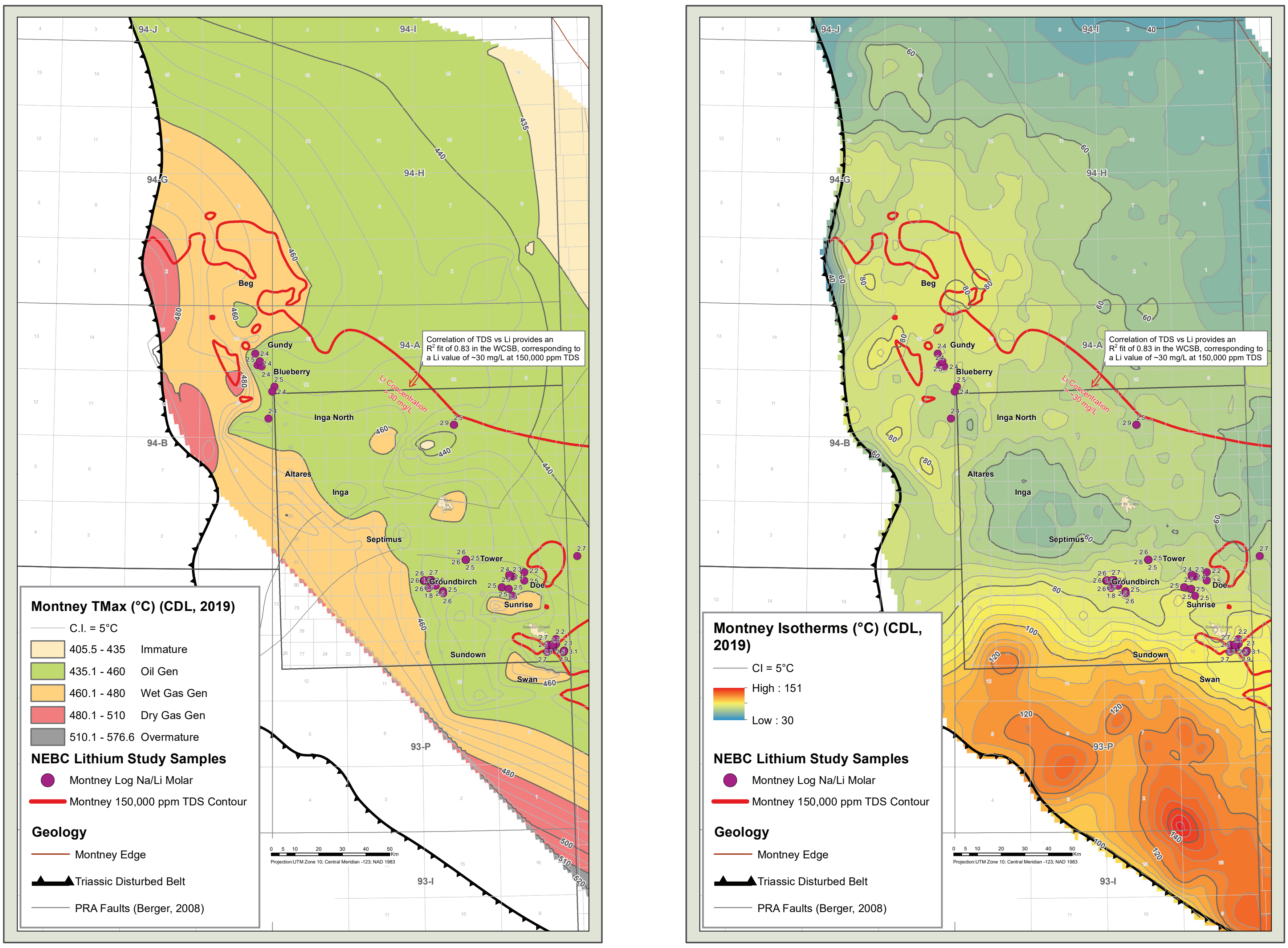

a. Montney Tmax

b. Montney Present Day Temperature

Correlation of TDS vs Li provides an R^2 fit of 0.83 in the WCSB, corresponding to a Li value of ~30 mg/L at 150,000 ppm TDS

c. Permian and Younger Geothermal Gradient

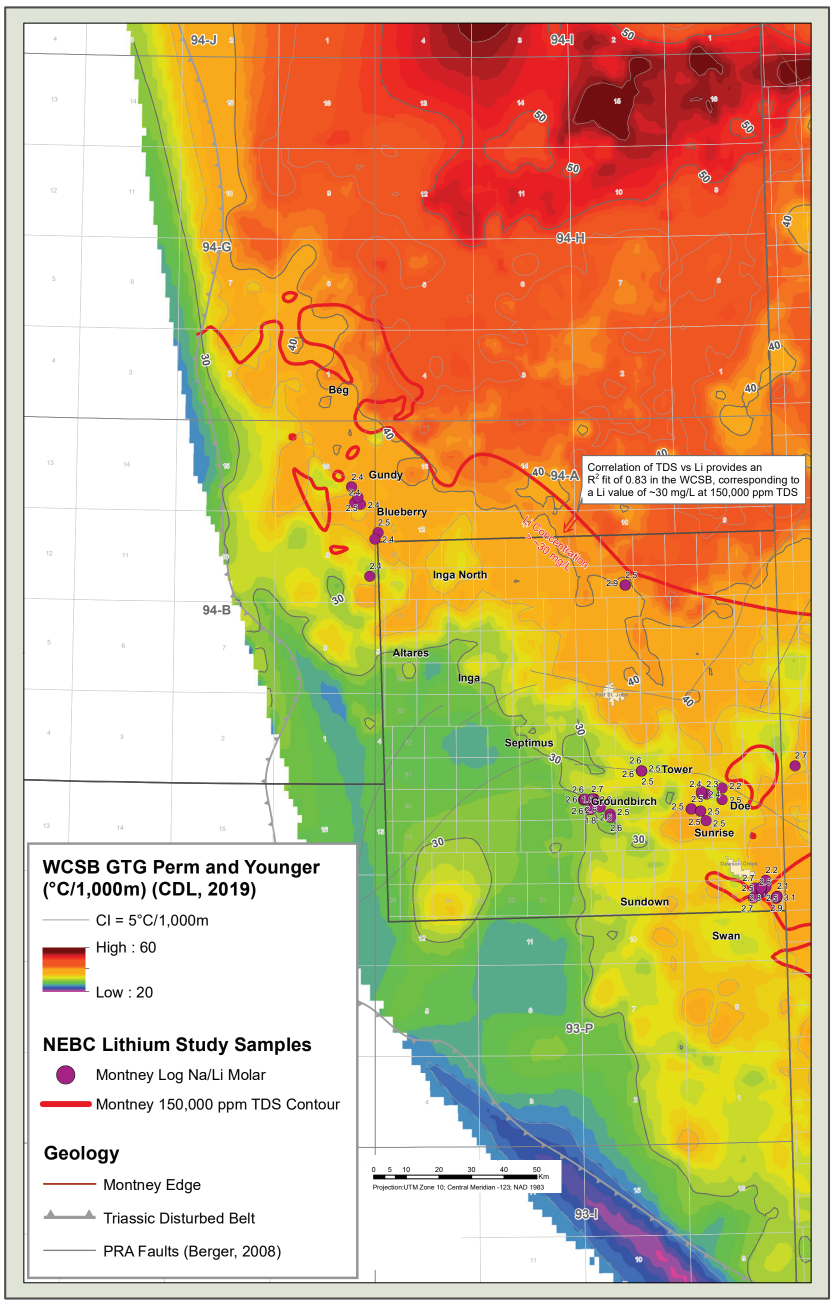

Correlation of TDS vs Li provides an R^2 fit of 0.83 in the WCSB, corresponding to a Li value of ~30 mg/L at 150,000 ppm TDS

Figure 5.13

5.14 Na/Li Thermometer

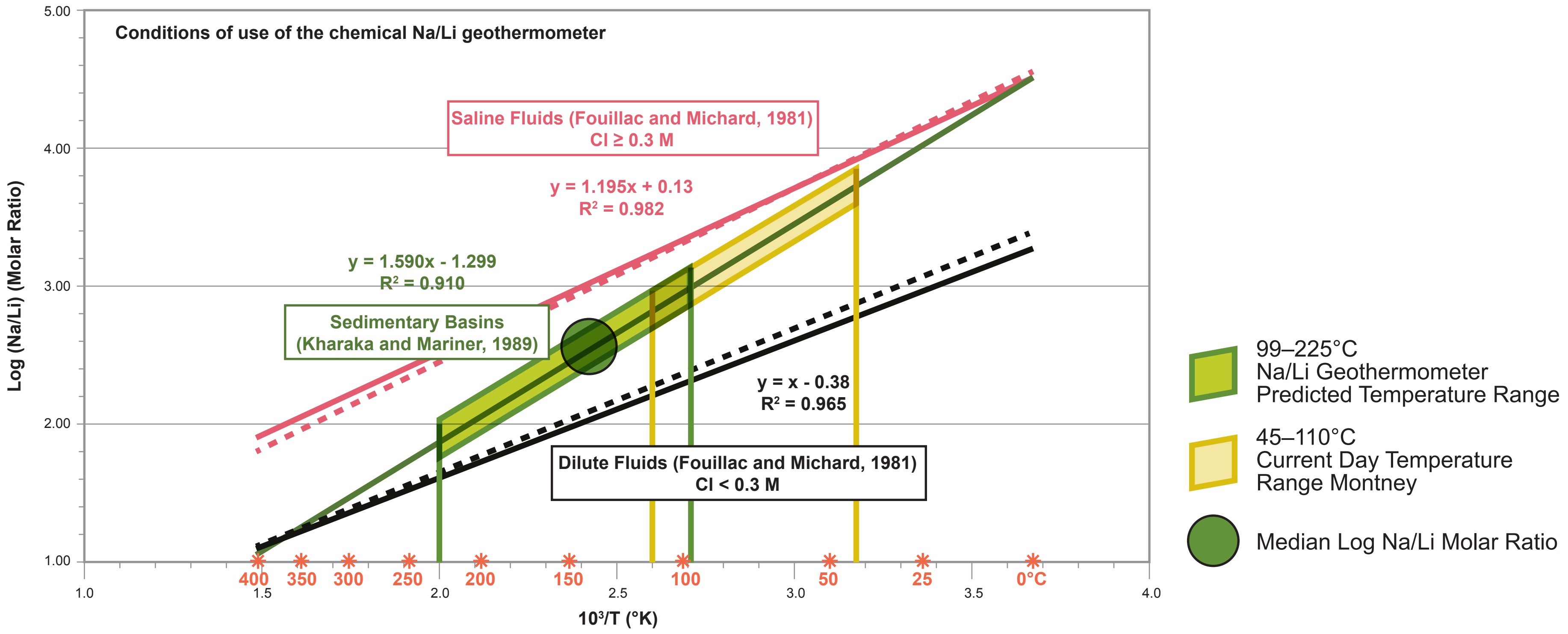

Empirical Na/Li geothermometer with measured Montney log Na/Li ratios. Data denoted observed lithium concentrations not in equilibrium or controlled by current day temperature.

Modified from Sanjuan, B. and Millot, R., 2009

Figure 5.14

The Na/Li Geothermometer

In the Montney, the Na/Li relationship, discussed in detail in *Chapter 2*, is investigated to determine the impact of burial temperatures on observed lithium concentrations.

Chalmers et al. (2022) provide one-dimensional burial history curves with calculated maximum temperatures reaching 250°C *(figure 5.5)*. Determining maximum burial temperatures for the BC Montney in two dimensions was beyond the scope of this study. As such, Na/Li ratios are compared as a function of Tmax (from Rock-Eval pyrolysis data), current day temperature, and geothermal gradient *(figures 5.13 a–c)*. On *figure 5.14*, the observed Na/Li ratios from the NEBC, GSC, and AGS datasets are plotted on the Kharaka and Mariner geothermometer graph. The Montney Na/Li ratios are indicative of temperatures that conform more closely to maximum burial temperatures (99°C to 225°C) than current day temperatures (45°C to 110°C). The plot suggests that the observed lithium concentrations in the Montney are higher than expected relative to current day temperatures. Due to the variability in maximum burial and uplift throughout the WCSB, further investigation is warranted to see if similar relationships exist in the Devonian of Alberta and Saskatchewan where elevated lithium concentrations are observed.

Montney Lithium Distribution

Based on the various investigative approaches discussed in prior sections, it is apparent that multiple factors impact the concentration and distribution of lithium in formation waters. A hand-contoured Montney lithium concentration map is provided in *figure 5.15*. In interpolating the lithium concentration between sample points, many observations that have been discussed previously were considered; including proxies from routine water analysis such as TDS and potassium concentration, the Na/Li geothermometer and regional variations in geothermal gradients. The interpolations extend the potential Montney fairway of enriched lithium (>50 mg/L), which roughly correlates to TDS >200,000 ppm, potassium >1.5 g/L, current day temperature >70°C and areas of high geothermal gradients >40°C/km (specifically observed for the northwestern Montney). Future sampling programs and data should aid in further refining relationships in order to develop improved exploration models. It is important to note that the enriched lithium fairway does not require all of these parameters to overlap concomitantly and does not incorporate other factors this study has not considered.

Montney Brine-Hosted In Situ Lithium Potential

A regional high-level brine-hosted in situ lithium potential estimate was calculated for the Montney based on many assumptions. The estimate is intended to provide guidance on where future sampling and more in-depth work could take place, and not as a rigorous number. The estimate is based on volumetrics only and does not take into account many factors that are necessary for a rigorous mineral resource assessment such as permeability (strictly hydraulic conductivity), transmissivity, storativity (a function of fluid and aquifer compressibility) and dispersivity as these parameters are beyond the scope of this study. Furthermore, Montney operators tend to develop a "bench" at a time; that is, they do not hydraulically fracture the entire 300m of the section but concentrate on a single zone where hydraulic fracturing may access a few tens of metres thickness of the formation.

The brine-hosted in situ lithium potential for the Montney was calculated on a volumetric basis for the entire water saturated percentage (Sw) of the pore volume where TDS of the formation water exceeds 150,000 ppm, an area of approximately 32,000 km^2. The in situ lithium potential calculation is based on CDL's proprietary net reservoir, porosity and water saturation mapping. A map of the net reservoir is provided in *figure 5.16* for reference. Lithium mass was calculated on a 2.8 km^2 (approximately 1 mile x 1 mile; approximately 1 section) grid within the saturated pore space, summed for the entire mapped area and converted to tonnes of Lithium Carbonate Equivalent (LCE).

- Water-saturated pore volume = area of a section (m^2) x net reservoir height (m) x porosity fraction x water saturation fraction
- Brine-hosted in situ lithium potential = water-saturated pore volume x lithium concentration x LCE conversion
- (1 tonne Li = 5.3 tonnes LCE) (Brown, 2016)

Figure 5.17 is a map showing the Montney in situ lithium potential based on the above calculations throughout the extent of the Montney where the TDS exceeds 150,000 ppm. The calculated in situ lithium potential for the Montney is estimated to be 9.8 million tonnes LCE. The net reservoir thickness can have a large effect on the in situ lithium potential calculation. However, when water saturation is very low such as at Groundbirch, the saturated pore volume is greatly reduced, and therefore, the in situ lithium potential is also reduced. There is a fairway of in-situ lithium potential that is >1,000 tonnes LCE/section (in green) running from Swan and Sundown through Tower/Septimus to Town and Blueberry/Gundy that corresponds to a trend of thick net reservoir and also relatively high lithium concentration *(figure 5.15)*.

The volumetric calculation is one method to estimate brine-hosted in situ lithium potential. This method may underestimate the Montney in situ lithium potential as it does not take water-rock interactions with completions fluids into consideration and may be considered as a minimum value. Brine-saturated pore volume accounts for only 13% of the total pore volume of the Montney as summarized in *table 5.3*. If there are water-rock interactions within a zone after completion fluids are pumped in, using the water saturation of the desiccated Montney may result in an underestimation of in-situ lithium potential. In areas of very low water saturations (Groundbirch), water production is low, and it is expected that the recovery of pumped frac fluid will be relatively low due to imbibition. Water production is covered in a later section in this chapter, but refer to *table 5.4d* to see the low rates of water production at Groundbirch.

5.15 | Montney Estimated Lithium Concentration Map

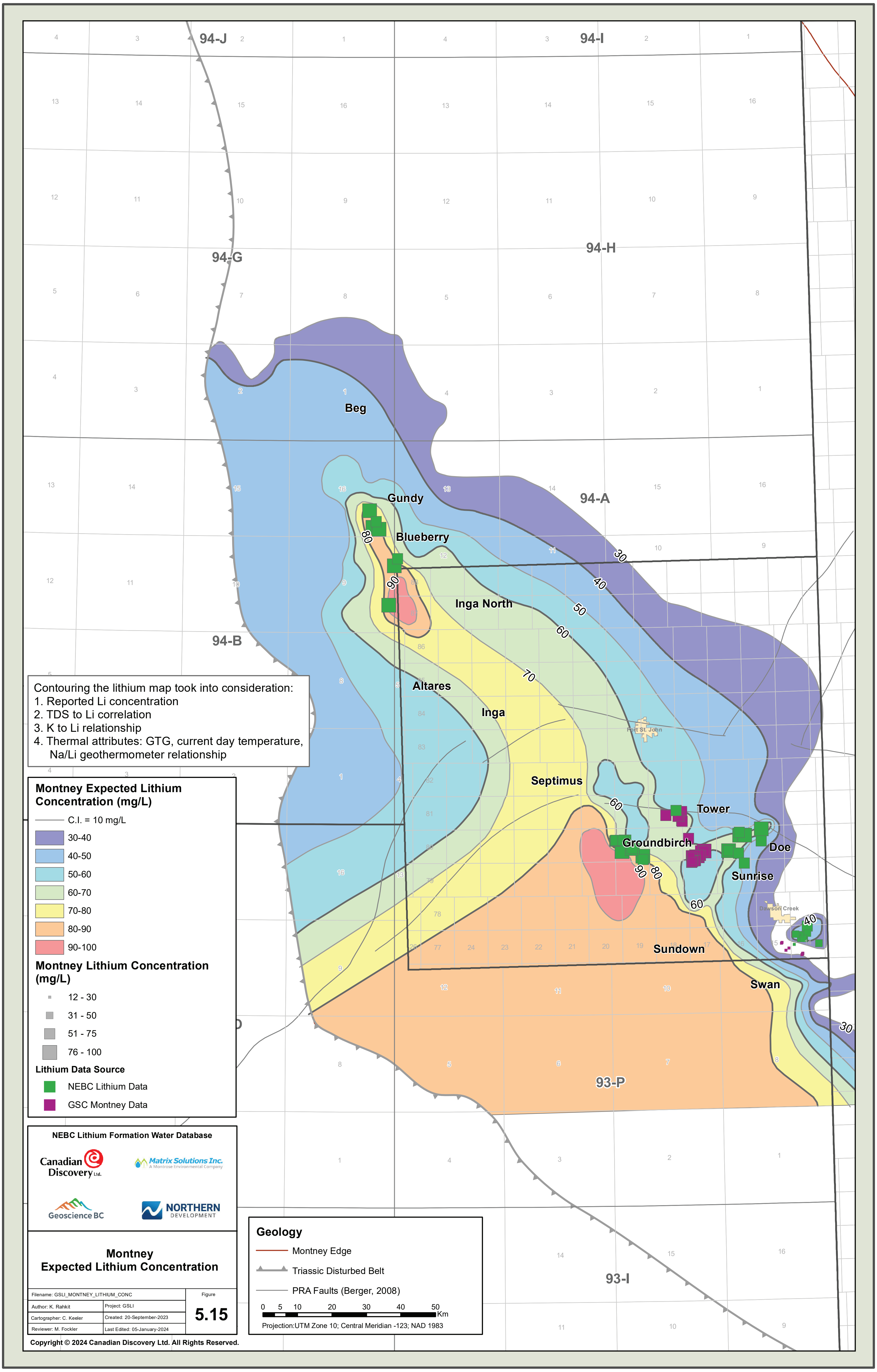

Contouring the lithium map took into consideration:
1. Reported Li concentration
2. TDS to Li correlation
3. K to Li relationship
4. Thermal attributes: GTG, current day temperature, Na/Li geothermometer relationship

© Canadian Discovery Ltd.

Figure 5.15

5.16 | Montney Net Reservoir Map

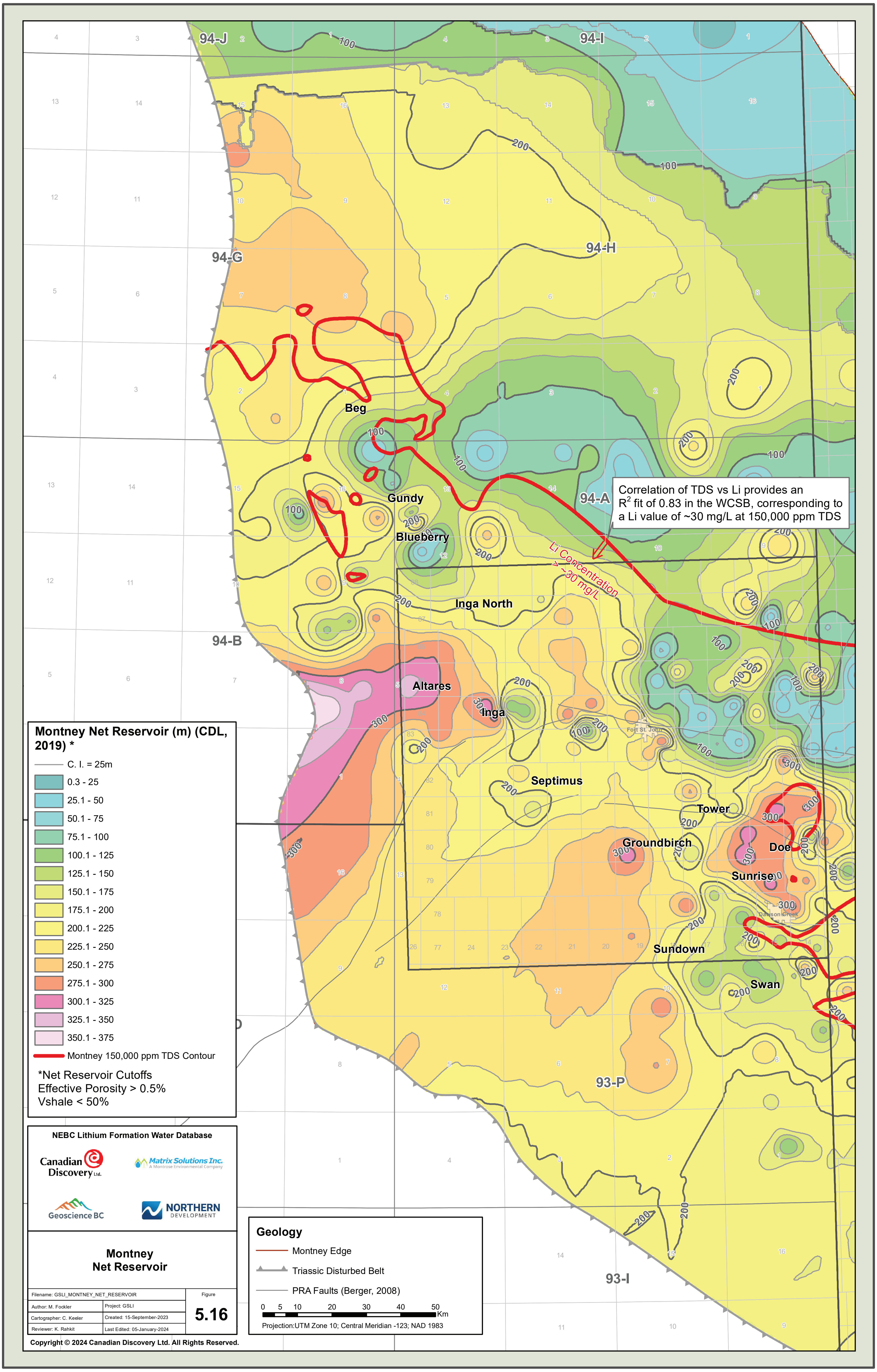

Correlation of TDS vs Li provides an R^2 fit of 0.83 in the WCSB, corresponding to a Li value of ~30 mg/L at 150,000 ppm TDS

© Canadian Discovery Ltd. *Figure 5.16*

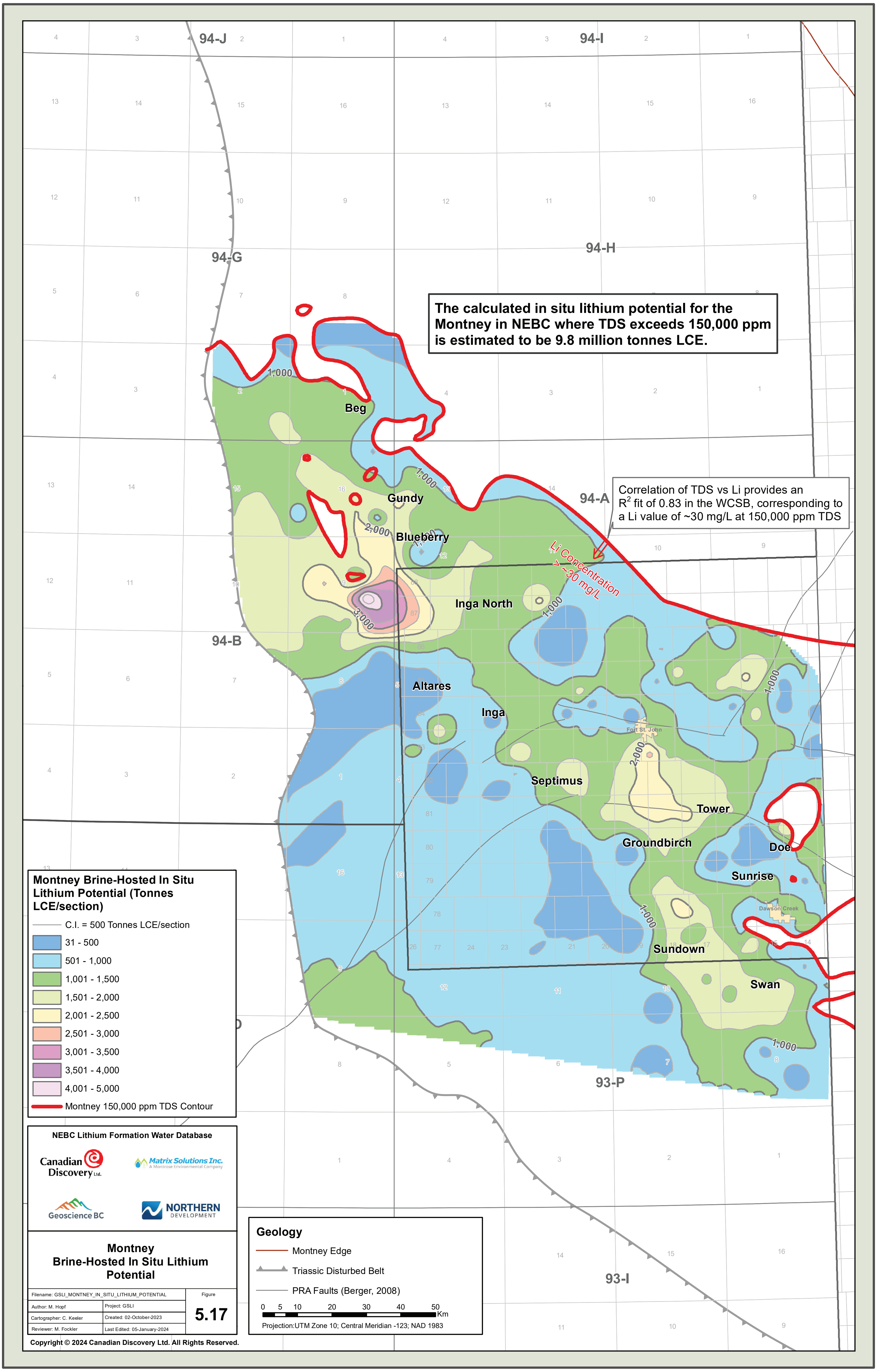

The calculated in situ lithium potential for the Montney in NEBC where TDS exceeds 150,000 ppm is estimated to be 9.8 million tonnes LCE.

Correlation of TDS vs Li provides an R^2 fit of 0.83 in the WCSB, corresponding to a Li value of ~30 mg/L at 150,000 ppm TDS

Montney
Brine-Hosted In Situ Lithium
Potential

Filename: GSLI_MONTNEY_IN_SITU_LITHIUM_POTENTIAL		Figure 5.17
Author: M. Hopf	Project: GSLI	
Cartographer: C. Keeler	Created: 02-October-2023	
Reviewer: M. Fockler	Last Edited: 05-January-2024	

© Canadian Discovery Ltd.

Figure 5.17

5.18 Subsurface Lithium-Enrichment Processes

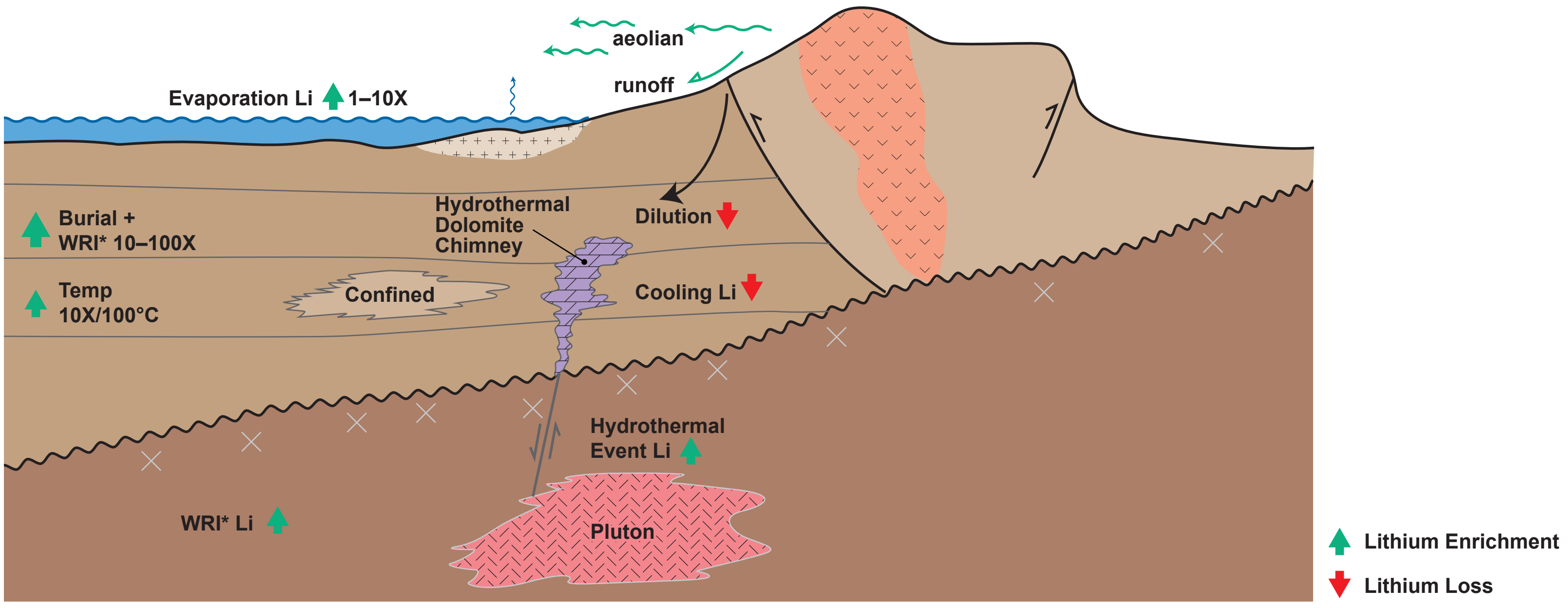

*Water-rock interaction

After Dugamin et. al., 2023

Figure 5.18

Potential Lithium Sources for the Montney

The concentration and dilution mechanisms for lithium in brines were developed and discussed in *Chapter 2*. Lithium-enrichment processes in the Montney may be attributed to a combination of several enrichment methods, including evapoconcentration, hydrothermal fluid migration through fault systems, temperature and high geothermal gradients, and water-rock interactions within the formation itself *(figure 5.18)*.

Evapoconcentration

Montney data used in this study from BC are shown on the Cl vs Br graph in *figure 5.19a* along with their likely evolutionary trajectories. Chloride concentrations are observed to reach almost 200,000 mg/L, while bromide concentrations reach 400 mg/L. The complete evapoconcentration process causes the precipitation of, in order, calcite, gypsum, halite, epsomite, sylvite, carnalite, and bischofite, and is well depicted by the relationship of chloride to bromide. Montney brines never exceed the halite precipitation level, which is consistent with the offshore environment of deposition. In *figure 5.19b*, the Montney concentrations of Br as a function of Cl and Li are plotted normalized to their initial concentration in seawater, along with their likely evolutionary trajectories. Chloride and bromide are enriched up to 10X and 70X respectively, whereas lithium is enriched up to 350X relative to seawater. These data suggest that seawater evaporation alone is insufficient as a lithium concentration mechanism in the Montney. See the section on Lithium-Enrichment in WCSB Brines in *Chapter 2* for a more robust discussion.

Hydrothermal Dolomitization

The Mg- and Ca-Enriched Areas map *(figure 5.11)* shows the wells with Mg-Ca-Cl concentration ranges associated with higher lithium values, along with regional faults. There may be a rough correlation with proximity to northwest-southeast trending faults and the Mg-Ca-Cl ranges within which lithium is enriched. Hydrothermal dolomites (HTD) have been extensively discussed by Davies et al. (2006) see *figure 5.18*. Although HTD may play a role in lithium-enrichment, the distribution and concentration of lithium are too broadly developed within the Montney and the Alberta Devonian for it to be the sole mechanism.

An elevated ^{87}Sr/^{86}Sr ratio is indicative of hydrothermal basement fluid interaction, while a lower ^{87}Sr/^{86}Sr ratio is consistent with the isotopic composition of Devonian seawater (Lyster et al., 2022) as discussed in *Chapter 4*. Strontium isotope data could help in the understanding of hydrothermal fluid interactions and the chemical evolution of brines including inputs of weathered sediments from radiogenic crustal sources but was outside the scope of this project.

Current and Maximum Burial Temperature and Geothermal Gradients

The relationship of lithium to maximum burial temperatures, current day temperatures and geothermal gradients has been discussed in *Chapter 2*. Lithium concentrations can increase by a factor of 10 per 100°C. However, given the 50-fold observed increases in lithium relative to evaporated seawater at halite saturation (2.0 mg/L in evaporated seawater from 0.2 mg/L in seawater), this mechanism alone is insufficient.

Water-Rock Interaction and Ion-Exchange During Illitization

In *Chapter 2*, lithium-enrichment processes were discussed in detail including the contribution of volcanically derived clay minerals. Volcanically derived ashes and glass are thermodynamically unstable and react rapidly with water to form clay minerals such as smectite, also known as montmorillonite and bentonite. The distribution of lithium between the aqueous and solid phases is governed by ion exchange equilibria amongst lithium, sodium, potassium, calcium, magnesium, and other exchangeable cations present in the rock. Wahlberg et al. (1965) reported the propensity for strontium to partition more effectively in sodium-rich solutions versus calcium-rich solutions, illustrating the complexities of the ion exchange process.

5.19 Montney Seawater Evaporation Process and Normalized Chloride, Lithium and Bromine Concentrations

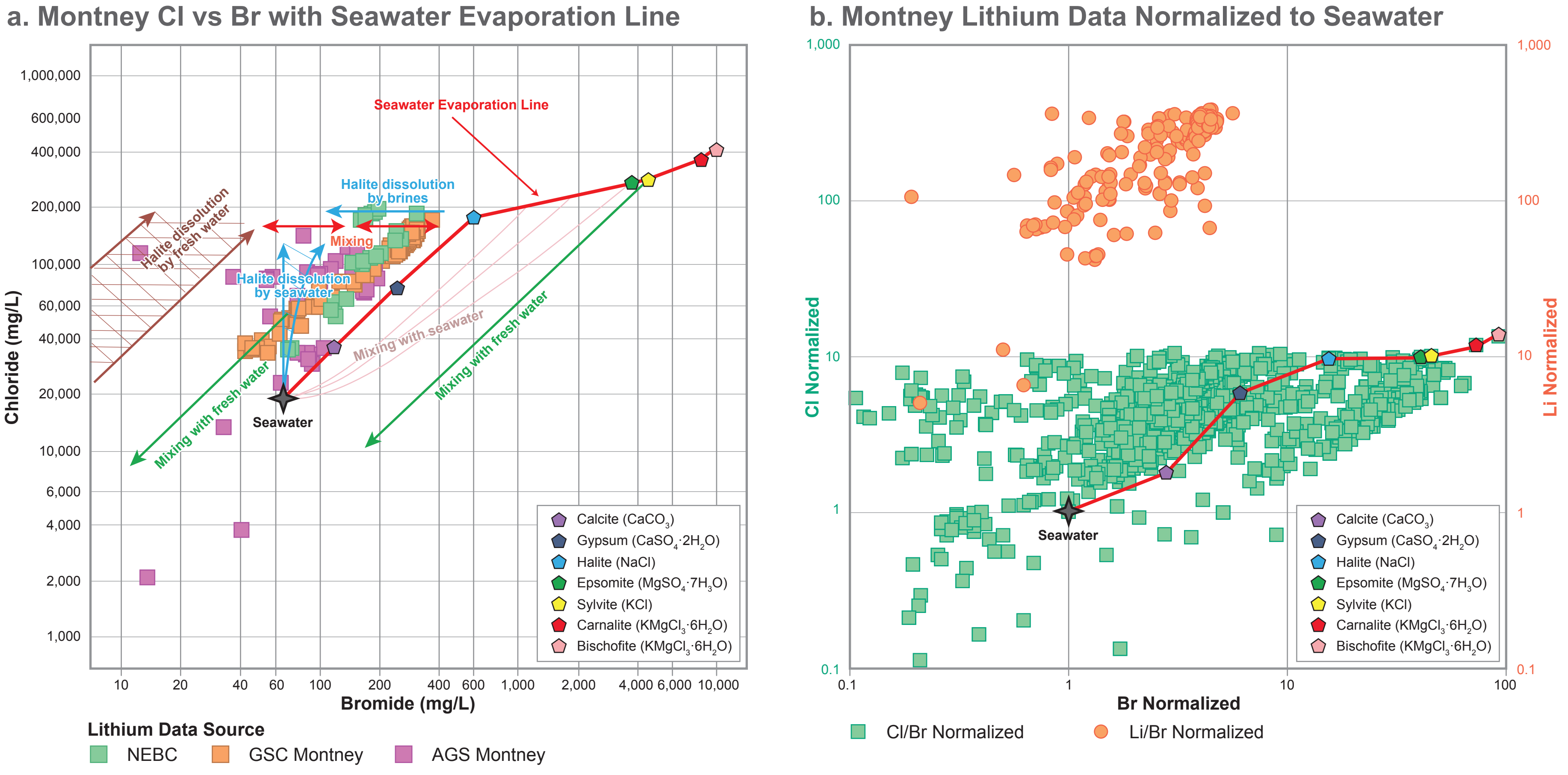

Lithium data from the AGS, GSC, geoLOGIC and the current study. Seawater Evaporation Lines from Shouakar-Stash, 2008.

Figure 5.19

With burial, the smectite reacts with additional components in the rock to form more stable clay minerals. The paragenetic sequence for the Montney *(figure 5.20)* shows the activation of several processes during late burial >90°C, including feldspar precipitation and dissolution, smectite illitization, quartz cementation and fibrous illite formation. With increasing burial, silica activity drops due to the formation of authigenic quartz, and smectite is irreversibly converted to illite, which is a more stable clay mineral (Abercrombie et al., 1994). Due to illite's comparatively lower interlayer charge, hence lower cation exchange capacity (CEC), it cannot accommodate all the interlayer cations held previously by smectite, and these ions are released to the aqueous phase or to participate in other mineralogical reactions. As a singly charged cation, lithium is stable in aqueous solution and does not participate in mineralogical reactions unless subjected to hydrothermal or deep burial processes.

Wust et al. (2018) provides a view of the early and middle Triassic paleogeography *(figure 5.21)* indicating a potential volcanic source of clay and silicate minerals derived from the Yukon-Tanana island arc complex immediately to the west of the Triassic seaway. The volcanic arc was determined to emit rhyolitic ash and ignimbrite (welded tuff) phenocrysts with high lithium concentrations (Ellis et al., 2018; Coffey et al., 2021). This ash would have blown in (an aeolian process) from the west and settled to the Montney seabed.

5.20 Montney Paragenetic Sequence

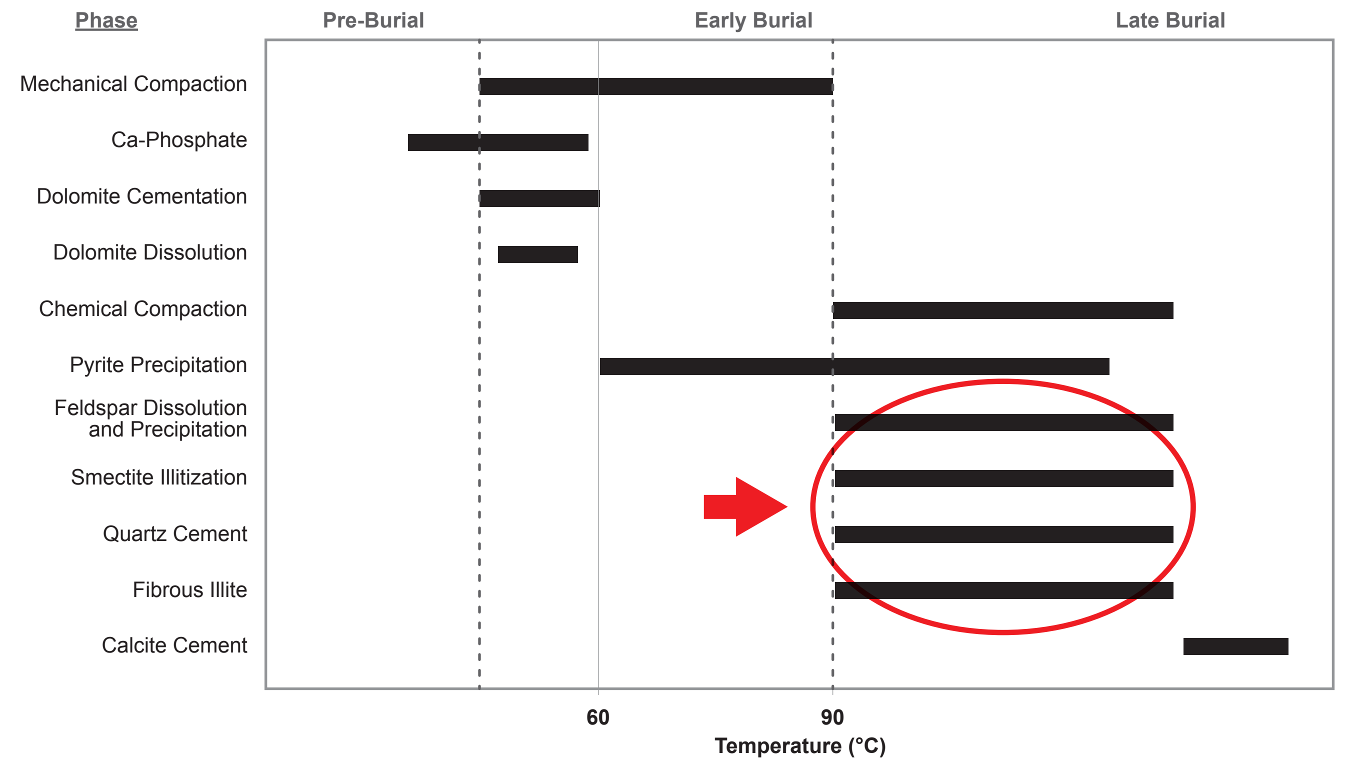

The paragenetic sequence for the Montney Formation in the deep basin, northeastern British Columbia.

Modified from Vaisblat, 2019.

Figure 5.20

5.21 Early-Middle Triassic Paleogeography

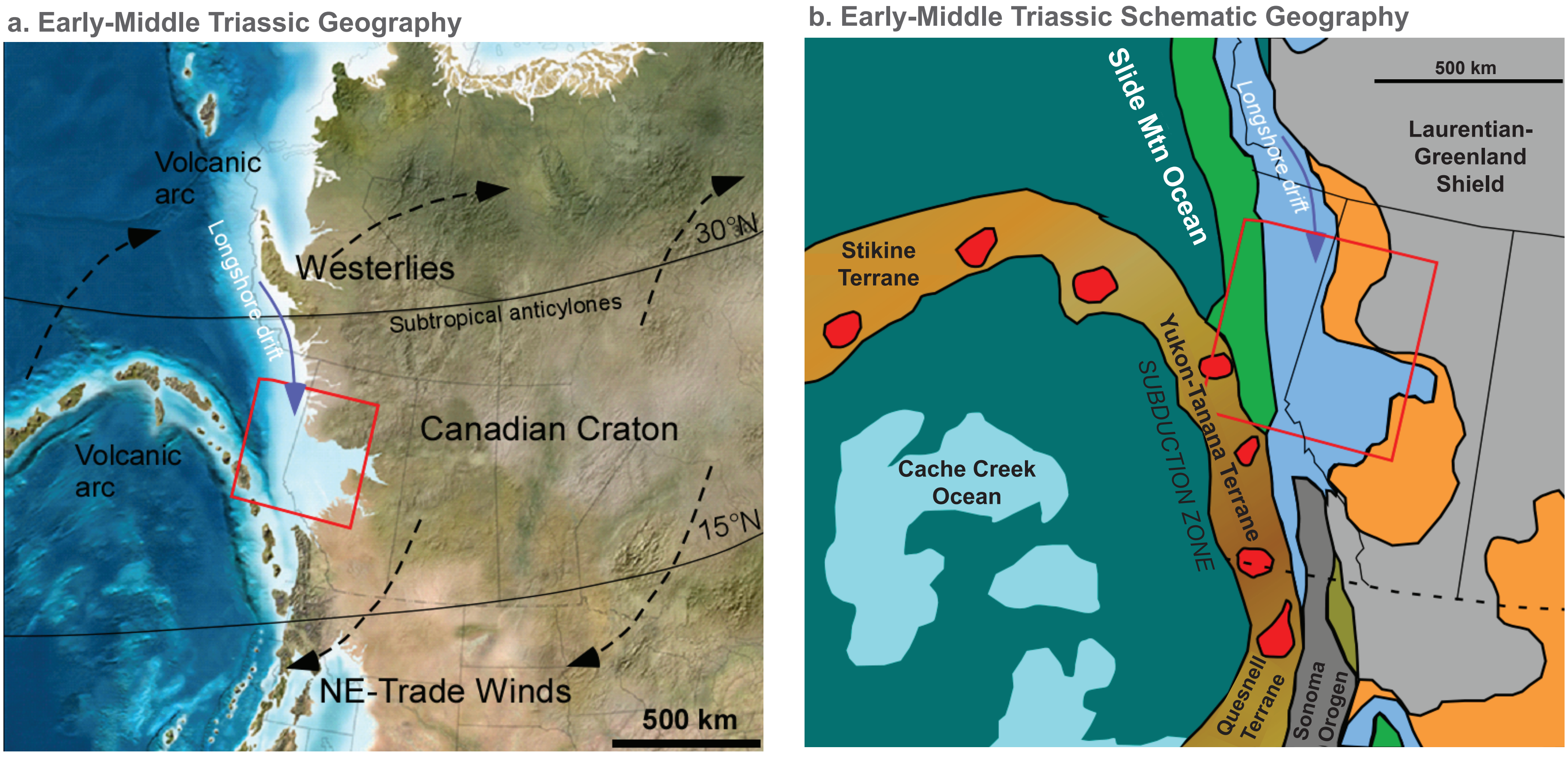

From Wust et al., 2018

© Canadian Discovery Ltd.

Figure 5.21

Table 5.3: Montney In Situ Lithium Potential

Montney Total Tonnes LCE	Montney Median Lithium Concentration (mg/L)	Montney Total Pore Volume (m^3)	Montney Brine-Saturated Pore Volume (m^3)
9.8 million	50.3	293 billion	38.6 billion

© Canadian Discovery Ltd.

Table 5.2

Integration of whole rock geochemistry along with formation fluid chemistry is an area that has received little attention in the literature. This is a promising area of investigation as it directly ties rock mineralogy to fluid chemistry and thermodynamics to better understand the role of water-rock interaction to the lithium resources. The section herein is based on a very limited dataset and relatively broad assumptions that likely result in a broad range of outcomes but do offer an interesting avenue for further research.

Whole rock geochemical analyses for trace metals were conducted by Egbobawaye (2016) for five Montney cores in the Swan and Dawson area and are provided in *table 5.4*. The samples are primarily from the Upper Montney, which has a relatively low illite fraction. The measured whole rock values for lithium concentrations in illite average 17 ppm, with a minimum and maximum range of 11 ppm and 27 ppm respectively. *Table 5.2a* summarizes whole rock geochemistry data from the Altares 16-17-083-25W6 well, where 62 samples were analyzed (Vaisblat et al., 2017). The range of lithium concentrations for each mineral is also provided in *table 5.2a* (Dugamin et al., 2023). The lithium concentration in the whole rock was then calculated for the various concentrations of lithium in minerals, and minerals in the whole rock *(table 5.2b)*. The results show a significant range starting from the minimum concentration of lithium in minerals and minerals in whole rock to the case of maximum concentration of lithium in minerals and minerals in whole rock. The lithium concentrations in whole rock obtained by Egbobawaye (2016) are also provided as a comparison in *table 5.2b*. The average lithium concentration for the entire Montney ranges from 36 to 288 ppm. These calculated whole rock values are substantially higher than those reported by Egbobawaye (2016). The results could be a function of the wide minimum to maximum range of lithium in minerals reported by Dugamin (2023), where the average was used due to a lack of statistical data and both vertical and lateral variations in the mineral content of the Montney.

K-feldspar, plagioclase and muscovite are substantial contributors of lithium as they have relatively high concentrations of lithium and also represent a significant weight percent of the whole rock. In contrast, illite represents a relatively high percentage of the whole rock but has a low concentration of lithium in the mineral itself. However, given the very high reported lithium values in smectite clays (the precursor to illite), substantial potential exists for liberated lithium to remain in solution during the conversion process. *Figure 5.22*, a graph of illite (and mixed layer-illite-smectite (MLIS)) vs depth from the Altares 16-17 core that covered most of the Montney, shows that illite increases with depth from 10% to 25% by weight. It is unknown what the stable equilibrium concentration of lithium in whole rock would be at formation temperature, pressure and fluid compositions given a certain rock composition. These data and analysis indicate that self-sourcing lithium through water-rock interaction of the host brine and host rock could be a very important contributing factor to lithium concentrations.

Table 5.4: Whole Rock Geochemical Analyses for Five Montney Cores

		Major Elements								Trace Elements							
		Mg	**Al**	**P**	**K**	**Ca**	**Ti**	**Fe**	**Mn**	**Li**	**Be**	**B**	**Co**	**Cu**	**Zn**	**V**	**Cr**
		2	0.2	5	6	31	0.09	3.7	0.03	0.3	0.05	0.03	0.03	0.08	0.1	0.05	2
Well Location	**Depth (m)**	ppm	ppm	ppm	ppm	ppm	ppm	ppm	ppm	ppm	ppm	ppm	ppm	ppm	ppm	ppm	ppm
b-39-H-93-p-9	2042 m	**42,120**	31,116	809	24,111	**90,976**	2795	16,707	297	26.9	51.9	39.1	18.3	43.1	1.2	51.4	<DL
d-39-F-93-p-9	2668.8 m	18,820	33,638	1246	24,251	71,508	3021	14,427	266	15	85.7	64.2	13.7	22.7	1.3	46.4	<DL
d-39-F-93-p-9	2685.4 m	13,338	40,861	2249	30,359	49,140	3668	20,717	253	17.3	77.7	42.5	23.5	89.6	1.4	62.8	<DL
d-39-F-93-p-9	2685.4 m	13,475	41,234	2289	30,453	48,968	3676	20,575	246	17.5	77.9	39	25	111	2	63	<DL
2-19-79-14W6	2048 m	19,780	45,633	1955	36,036	45,915	3877	19,687	253	21	288	26.7	24.1	33.8	1.8	69.3	<DL
2-19-79-14W6	2069.5 m	20,116	36,583	914	29,177	47,584	3397	16,679	332	17.9	530	28.7	19.1	221	1.5	61.2	<DL
2-19-79-14W6	2085 m	11,512	40,016	1493	32,310	36,429	3856	18,929	287	14.4	56.6	39.4	21.2	29.6	1.9	66.1	<DL
7-13-79-15W6	2055.22 m	**48,152**	24,438	1582	20,397	**98,597**	2080	22,999	364	21.8	271	27	30.5	24.6	1.1	70.1	<DL
7-13-79-15W6	2061.3 m	36,224	28,526	688	22,992	79,426	2704	14,057	355	12.7	55.2	40.5	15.2	28.3	1	52.4	<DL
7-13-79-15W6	2084.5 m	26,671	35,233	1717	27,941	61,980	3182	20,491	385	15.7	68.2	27.7	18.6	96.3	1.7	58.9	<DL
7-13-79-15W6	2101.78 m	14,456	39,659	2139	33,885	37,952	3576	26,134	324	12.4	78.5	58.7	29.3	270	2	65.7	<DL
9-29-79-14W6	1973 m	13,408	41,779	938	30,649	50,042	3938	16,527	296	15.6	504	45.1	19.2	82.3	1.6	68.2	<DL
9-29-79-14W6	1973 m	13,545	42,786	1003	31,695	51,007	3832	16,575	295	15.4	494	65.5	16.8	86.1	1.7	66.7	<DL
9-29-79-14W6	1999 m	11,761	36,736	2465	30,541	53,523	3347	15,951	331	11	46.9	28.1	18.1	68.7	1.1	49.9	<DL
GSP-2		**4993**	**61,382**	**1309**	**45,681**	**16,528**	**3521**	**27,936**	**288**		**46.4**	**9.41**	**38**	**121**	**1.3**	**19.8**	**<DL**
Certified value		**5800**	**78,800**	**1300**	**44,800**	**15,000**	**4000**	**34,300**	**320**	**36**	**52**	**7.3**	**43**	**120**	**1.5**	**20**	**-**
% recovery		**86.1**	**77.9**	**100.7**	**102**	**110.2**	**88**	**81.4**	**90**	**88.6**	**89.3**	**128.8**	**88.3**	**100.7**	**87.1**	**99.2**	**-**

🟨	Most Dolomitized Intervals in the Montney Formation Based on Analyzed Samples
⬛	Magnesium/Calcite

Source: Egbobawaye, 2016

© Canadian Discovery Ltd. *Table 5.3*

5.22 Illite/MLIS vs Depth Altares 16-17-083-25W6

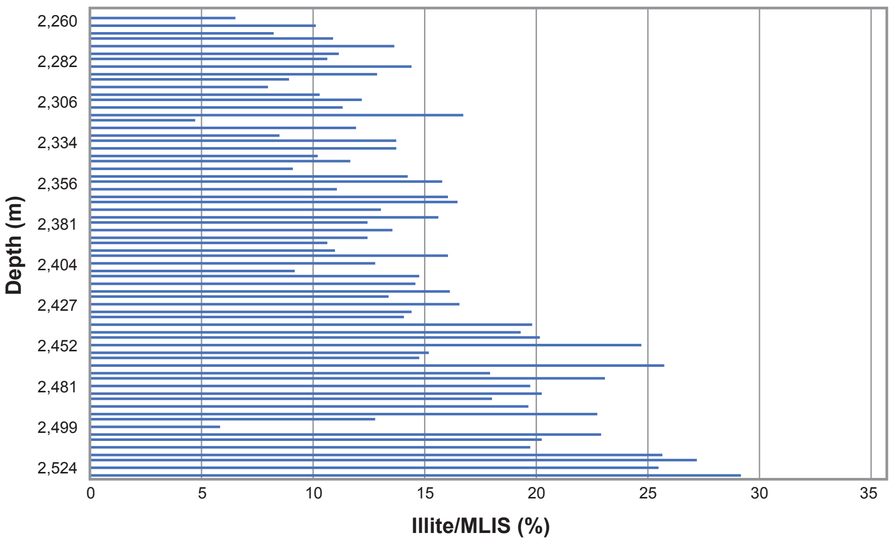

Data from Vaisblat et al., 2019

© Canadian Discovery Ltd. *Figure 5.22*

Refining the analytical technique(s) discussed above holds promise for enhancing exploration efforts and constraining in situ lithium resources. This would include obtaining a broader suite of samples including from areas that have low TDS and have undergone limited thermal alteration.

Water-Rock Interactions with Completion Fluids

Hydraulic fracture fluid has been shown to spontaneously imbibe into tight reservoirs and shales. This allows for mixing of fracturing fluids with highly saline connate water. Often this fluid is trapped within the small pores, but ions are able to diffuse back to the invaded frac fluids and fractures.

Formation water chemistry data show that the Montney reached gypsum and halite saturation. Liseroudi et al. (2018) suggests that the BC Montney underwent early anhydrite precipitation directly from coeval seawater. Whereas, in Alberta, late-stage anhydrite formation associated with elevated H_2S is derived from Devonian-sourced evaporite brines. Wood et al. (2021) observed dynamic fluid movement (during SEM analysis of Montney siltstone cores) created during the formation of expulsion structures as preserved core underwent depressurization. Wood et al. noted that "Dynamic brine behaviour is evident from strings of halite crystals overlying pores between minerals. The halite crystals precipitated from hypersaline brine that migrated from the interior to the surface of the sample. This behaviour indicates well-connected brines exist in Montney siltstone pores." Wood et al. (2021) analyzed two wells at 04-23-72-09W6M in Alberta and C16-06-81-17W6M in BC. TDS mapping for this study indicates values at the C16-06 well are in the 200,000 ppm range. Owen (2017) cites that increasing concentrations in flowback waters indicate mixing between fracture fluids and formation waters and that "mixing explains the Na and K concentrations, while mixing with ion exchange is influencing Ca, Mg, and Sr concentrations. Sulphate concentrations are influenced by pyrite oxidation and sulfate reduction. The rate of increase of the major ions varies between wells, although it is often, but not always, similar between wells completed at the same site." The process of imbibition is discussed by Ghanbari (2013) while Zolfaghari (2016) discussed simultaneous imbibition and ion diffusion.

From these combined observations it is surmised that:

- Montney formation waters reached early gypsum/anhydrite saturation and in certain areas are at or near halite saturation (although the timing of reaching halite saturation is uncertain, the authors suggest this may be caused in part by H_2O stripping during gas migration, effectively reducing water saturation causing in situ concentration of the remaining pore water).
- Induced fractures may have the ability to communicate with an interconnected pore water system, even though water saturations in the Montney are reported to be very low.
- Additional data are required to determine if there are lower limits to water saturation where the brine ceases to behave dynamically, and whether this leads to reduced formation water production and/or ion exchange with injected water.
- Real time dynamic brine behaviour and halite precipitation/dissolution are potentially resultant from pressure drawdown within the stimulated reservoir volume during production. However, the following questions remain:
    - How did Montney formation waters reach halite saturation given its offshore marine depositional environment?
    - Since lithium content in halite is extremely low and would, at best, elevate to 2 mg/L as seawater evaporates to halite precipitation, what is the source of the excess lithium?

5.23 Montney Water Production Case Study

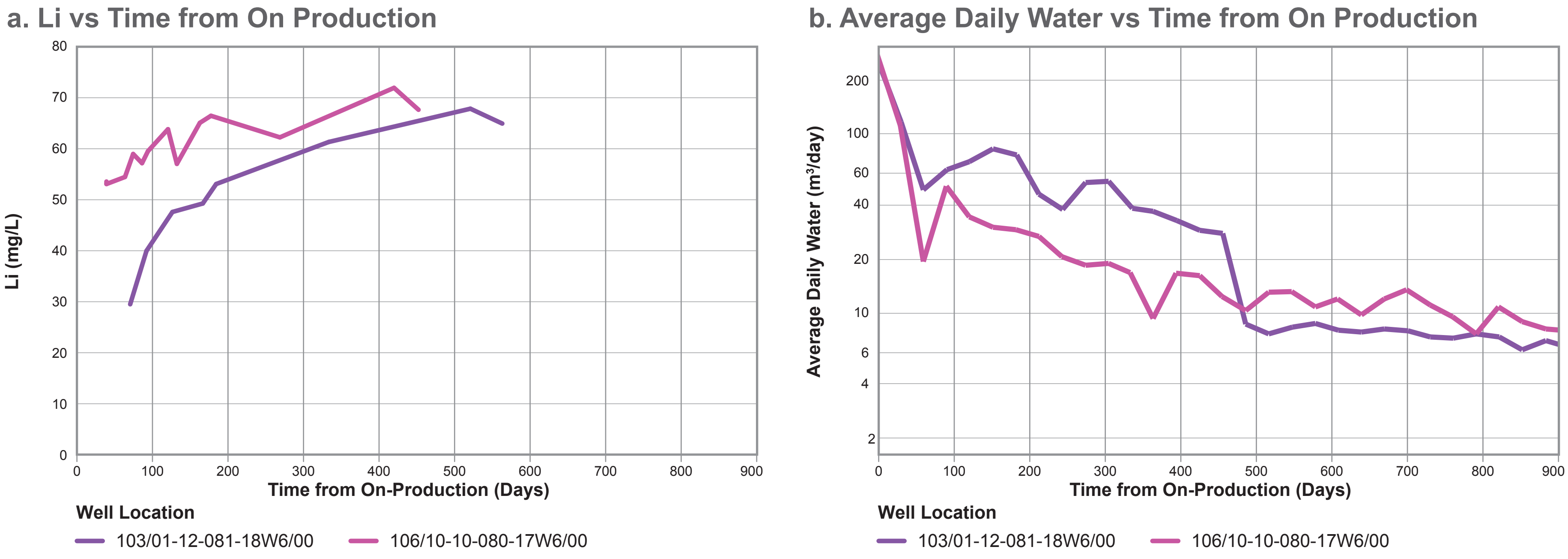

Source: Figure 5.23a data from Kingston et al., 2023; Figure 5.23b data from geoLOGIC

Figure 5.23

Water Production and Economics

The GSC recently completed two studies in tandem, namely, Kingston et al. (2023) and Leece and Jiang (2023), to establish an economic case for co-produced lithium. In Kingston et al. (2023), water chemistry data were presented from two datasets, the first being a collection from numerous wells in the Montney and Duvernay formations while the second provides time series samples from a limited number of wells in the Montney and Duvernay. Jensen and Rostron (2018) conducted repeat sampling over a six-year time frame from two wells completed in the Winnipegosis Formation in southeast Saskatchewan with relatively consistent lithium and other trace ion concentrations at a stratigraphic level with repeatable results but also variations within vertically segregated beds. These studies demonstrate the importance of obtaining spatial and temporally varied sample data in order to verify the distribution of lithium concentration.

To illustrate the importance of temporal variations in lithium concentration, the time series data for two Dawson Creek wells over the first 18 months of production are shown in *figure 5.23a*. Within approximately 200 calendar days, the average lithium concentration of the two wells averaged around 60 mg/L and the production could be considered economically viable for lithium extraction based on the cutoff of 50 mg/L (refer to earlier discussion on economic cutoff employed by DLE lithium project developers). While the average lithium concentration may be considered stable and economically viable by this time frame, it is important to consider water production and the production decline over time *(figure 5.23b)*. By this 200-day time frame, the daily water production rate averaged around 50 m^3/day. Lithium concentrations exceeding 50 mg/L were reached in both wells before 200 days, and water production steadily decreased over time. This study determined that both wells produced back the volume of frac fluid pumped after about nine months (~270 days) of production.

Leece and Jiang (2023) provided a review of DLE technologies and their application to lithium extraction from flowback and produced waters (FPW) along with an economic evaluation of various scenario projects in the Duvernay and Montney regions. The study modelled a hypothetical lithium extraction facility processing 1,300 m^3/day based on the chemical and physical properties of the sampled FPW. The capacity of 1,300 m^3/day of water was selected based on a specific processing facility operating in the Fox Creek Duvernay area and its volumes of water for disposal injection. The modelling suggests that lithium extraction from FPW at these rates (1,300 m^3/d) and concentrations (>45 mg/L) is economically viable, assuming extraction technology advances sufficiently (from pilot and demonstration scale to proven commercial scale) and the current relatively high market pricing of lithium continues into the foreseeable future.

Having observed areas in NEBC that exhibit lithium concentrations meeting the economic threshold of >50 mg/L (Standard Lithium, 2021), the average cumulative water production over time and monthly water production rates were examined by area in this study to determine which areas produce sufficient volumes of fluid to support a lithium extraction project. A first-year monthly average water production rate map *(figure 5.24)* highlights areas with high and low water production rates. To make the map, the first-year accumulation of water was divided by 12 (months) to derive an average monthly rate for all Montney producing wells. Water is often allocated back to wells from group separators and may not be entirely representative on a well-by-well basis, but in general, the map provides an indication of the water production distribution geographically.

Table 5.5: Montney Lithium Deliverability Scenarios

Scenario	Monthly Water Production Per Well (m^3/mo)	Average Lithium Concentration (mg/L)	Facility Monthly Lithium Production (T of Li/mo)[1,2]	Yearly Lithium Production (T LCE/yr)[3,4]
High Water Production	300	56	1.51	86.5
Average Water Production	150	56	0.76	43.3
Low Water Production	90	56	0.45	26.0

[1] DLE recovery efficiency assumed to be 90%
[2] As a base case, 100 wells are assumed to feed a single facility
[3] Facility utilization rate assumed to be 90%
[4] One tonne of Li = 5.3 tonnes of Li_2CO_3 or Lithium Carbonate Equivalent (LCE)

© Canadian Discovery Ltd. Table 5.5

Figure 5.25 shows the monthly average water production in the five areas sampled in the study, as well as Altares and Beg, which are two areas where additional lithium sampling is recommended. A vertical line has been added at the 100-day mark, suggesting that, as the economic lithium threshold is reached in these areas, the majority of wells will still be producing several hundred m^3/day of water. The horizontal line, at 90 m^3/month, reflects a potential shift below economically favourable fluid production rates. While most areas maintain high rates for up to three years, Altares, which is yet to be sampled for lithium, may be able to maintain high water production rates for up to five years.

Figure 5.26 shows the cumulative monthly water production by well from these areas. The blue line indicates average cumulative production over three years. Tower/Septimus appears to have the highest average cumulative water production of the areas examined.

Table 5.5 provides an indication of potential lithium production based on various water production rates from wells. Assuming 100 wells feed into a single processing facility and supply water with an average lithium concentration of 56 mg/L, which is the average of Montney samples from this study, the yearly lithium production varies between approximately 86 to 26 tonnes of LCE per year when looking at high and low water production rates. As a comparison, the base case scenario modeled by Leece and Jiang assumed water production of 1,300 m^3/day (39,000 m^3/month) feeding a DLE facility versus 30,000 m^3/month (based on 100 wells) in the high water production case shown in *table 5.5*. Leece and Jiang's work indicated that at a capacity of 1,300 m^3/day, a facility could be economically viable. However, smaller scale facilities would be penalized with higher capital and operating costs per tonne of lithium production and thus, economic returns would deteriorate. Given that DLE technologies have not reached a commercial level and that the cost estimate data is highly preliminary, further development work is required before an economic capacity threshold can be estimated (Alberta Innovates, 2022; and Murphy and Haji, 2022).

5.24 | Montney Water Production First Year Monthly Average Rate Map

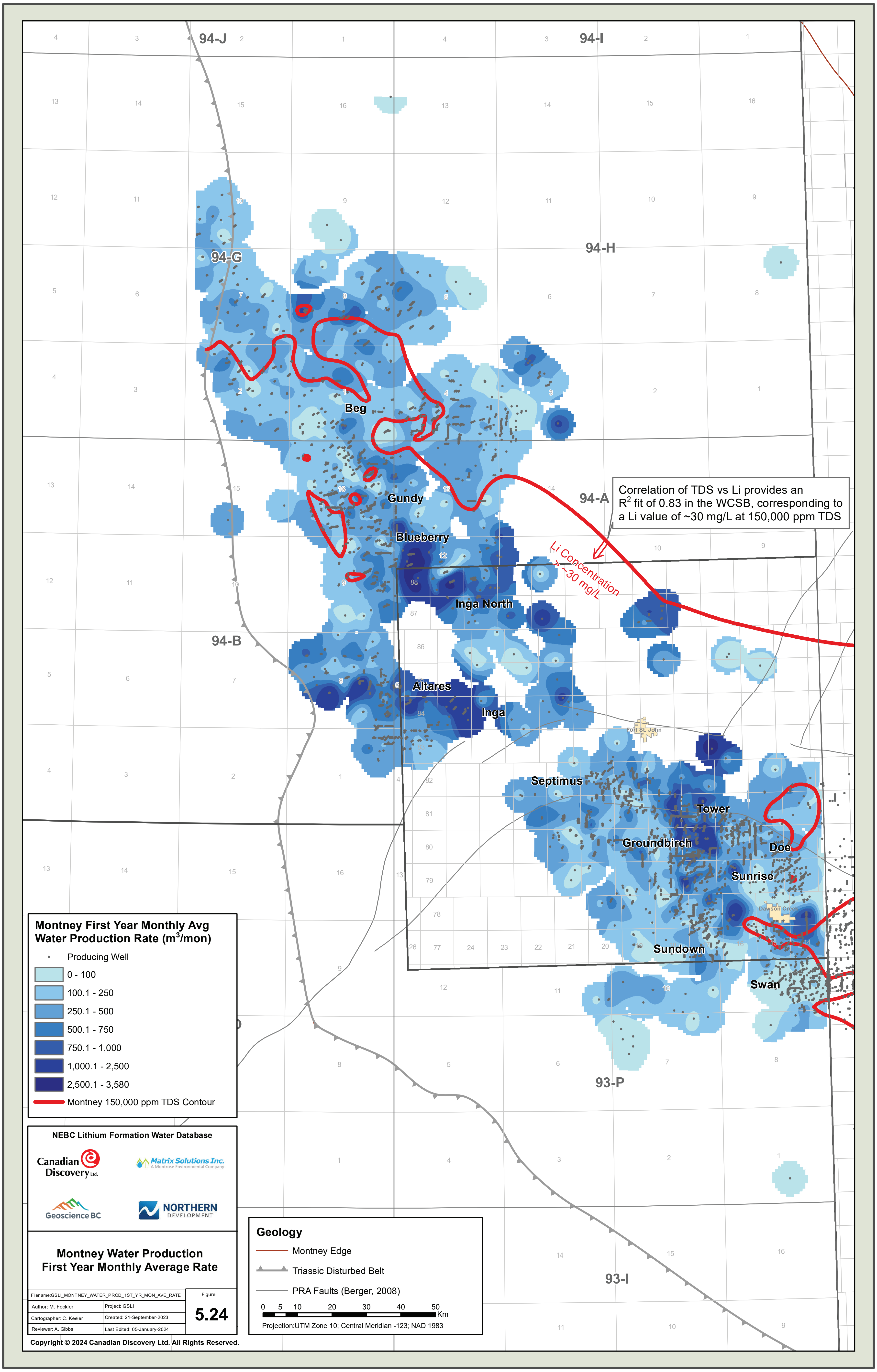

Correlation of TDS vs Li provides an R^2 fit of 0.83 in the WCSB, corresponding to a Li value of ~30 mg/L at 150,000 ppm TDS

Montney Water Production
First Year Monthly Average Rate

Filename:GSLI_MONTNEY_WATER_PROD_1ST_YR_MON_AVE_RATE
Author: M. Fockler
Project: GSLI
Cartographer: C. Keeler
Created: 21-September-2023
Reviewer: A. Gibbs
Last Edited: 05-January-2024
Figure 5.24

© Canadian Discovery Ltd. *Figure 5.24*

5.25 Montney Average Monthly Water Production Trends by Area

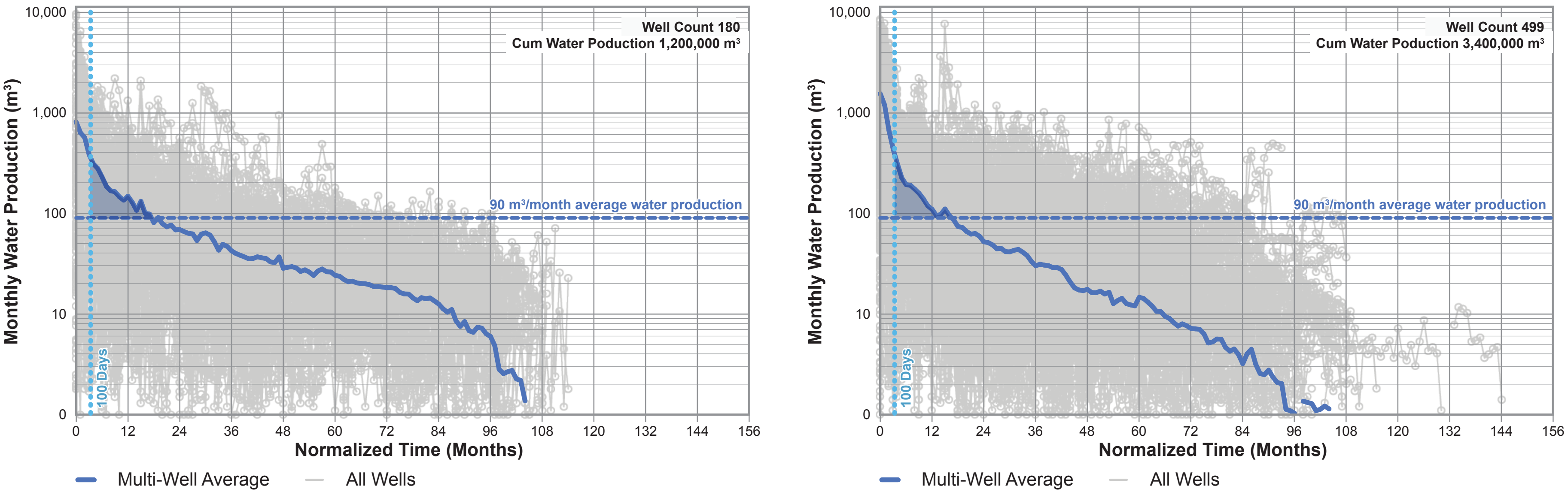
a. Beg

b. Blueberry/Gundy

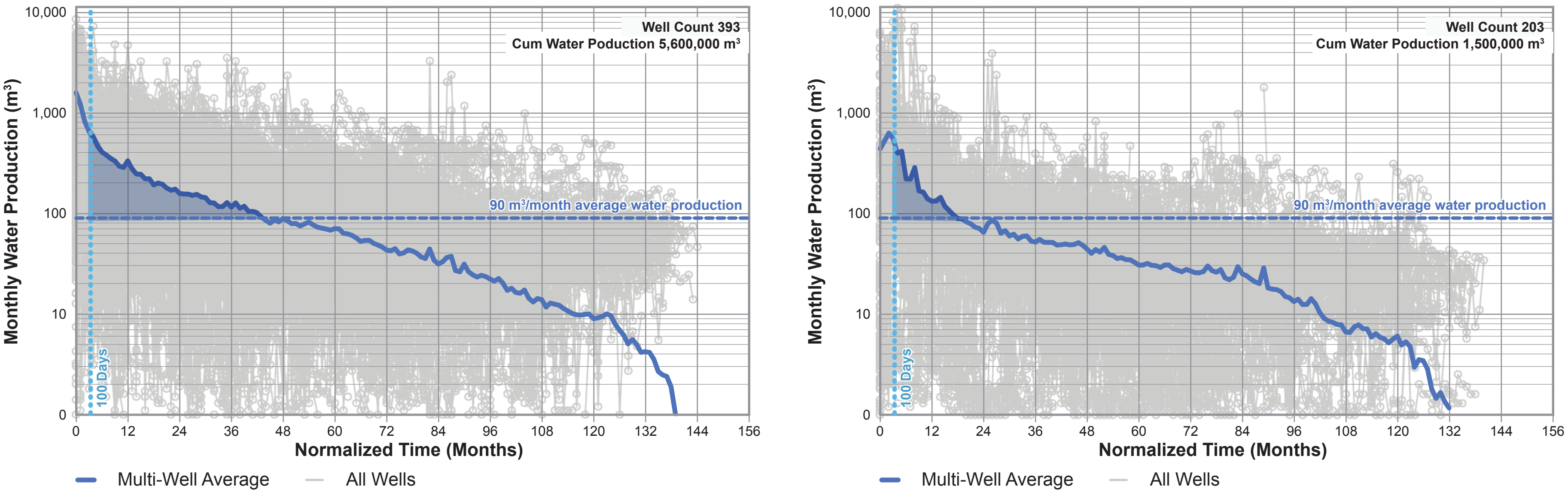
c. Altares

d. Groundbirch

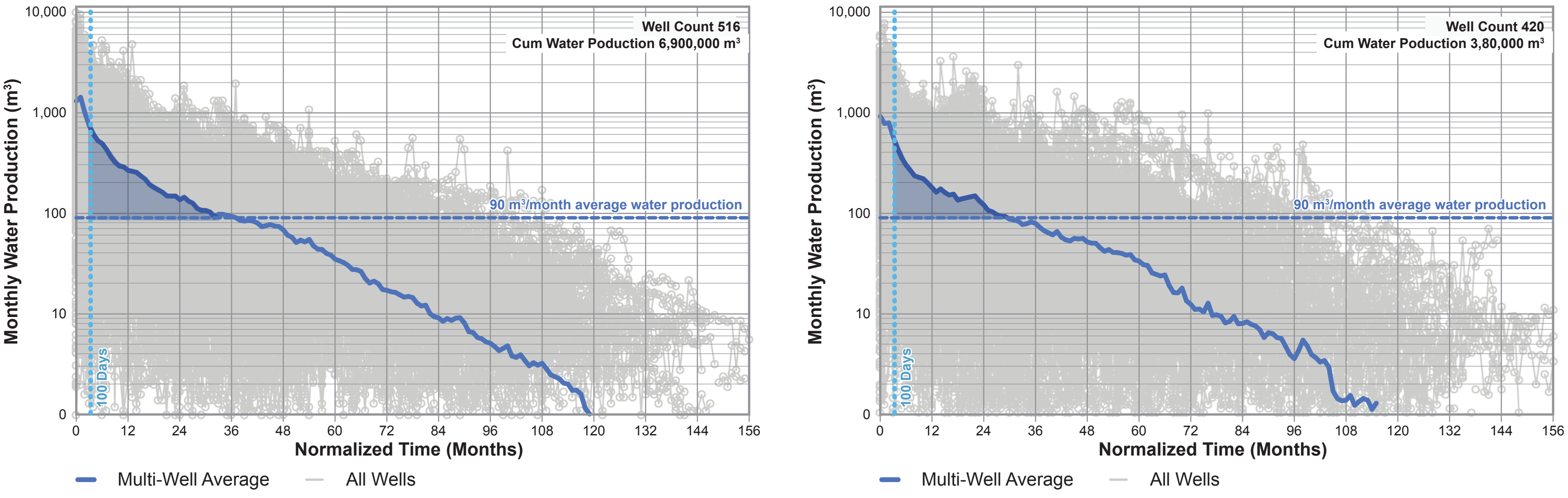
e. Tower/Septimus

f. Parkland/Doe

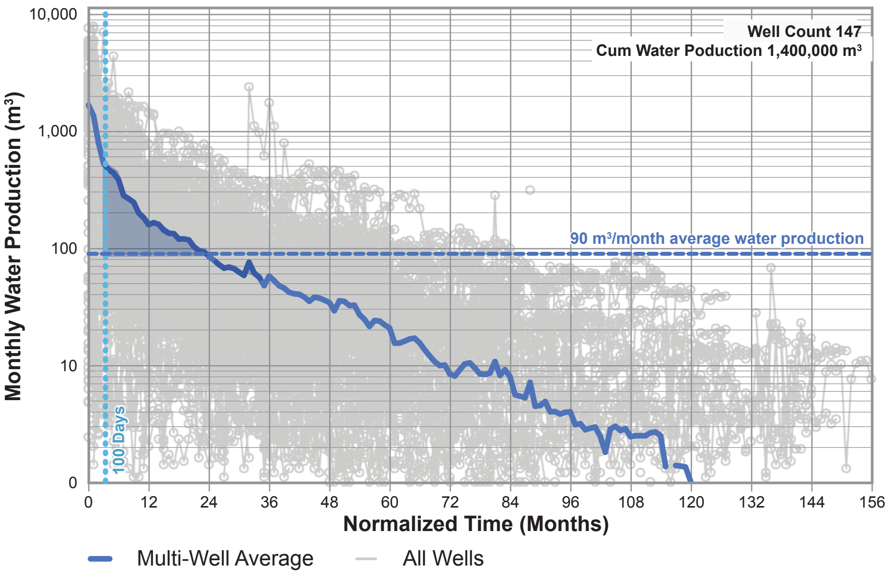
g. Swan

Water data from geoLOGIC

Figure 5.25

5.26 Montney Cumulative Water Production Trends by Area

a. Beg

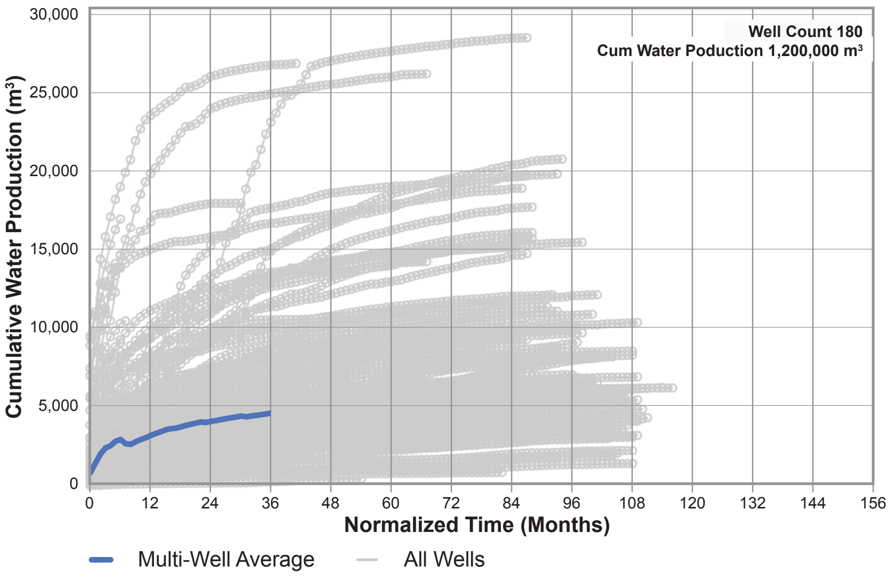

b. Blueberry/Gundy

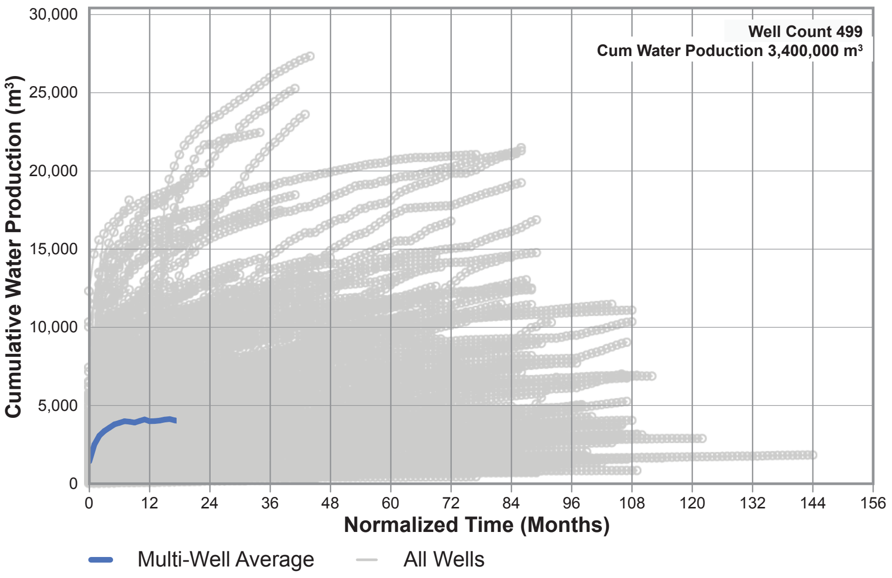

c. Altares

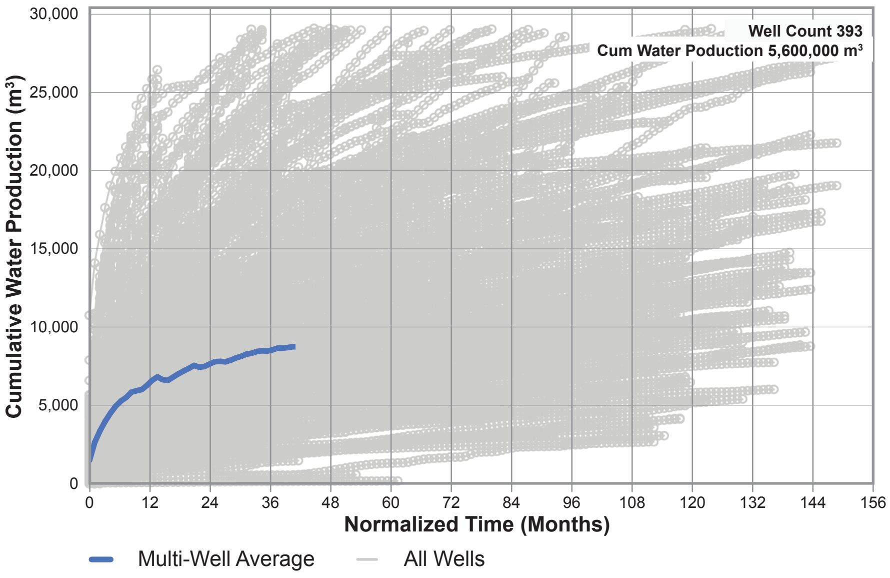

d. Groundbirch

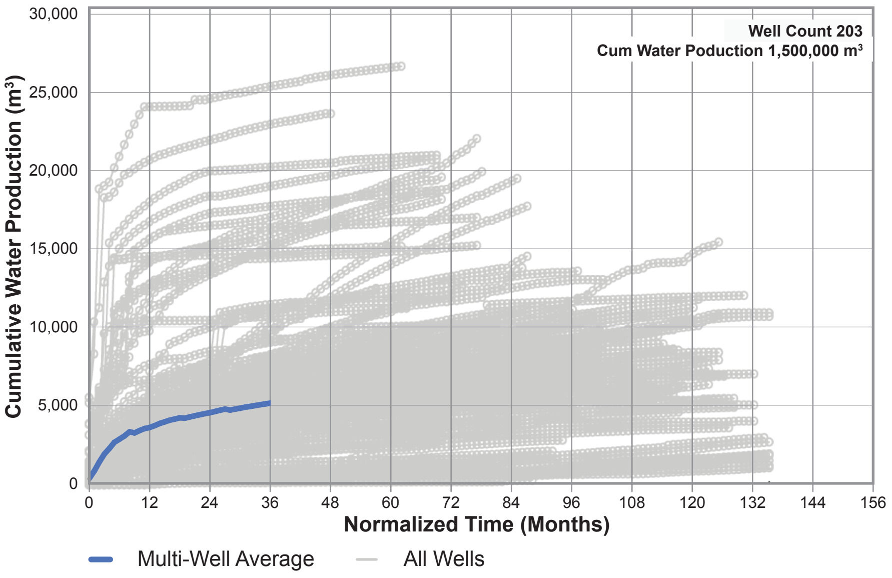

e. Tower/Septimus

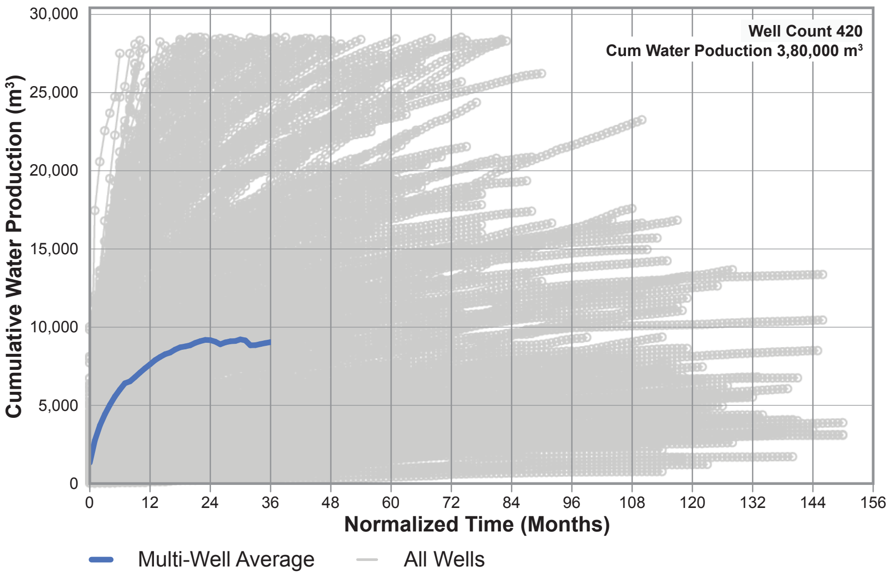

f. Parkland/Doe

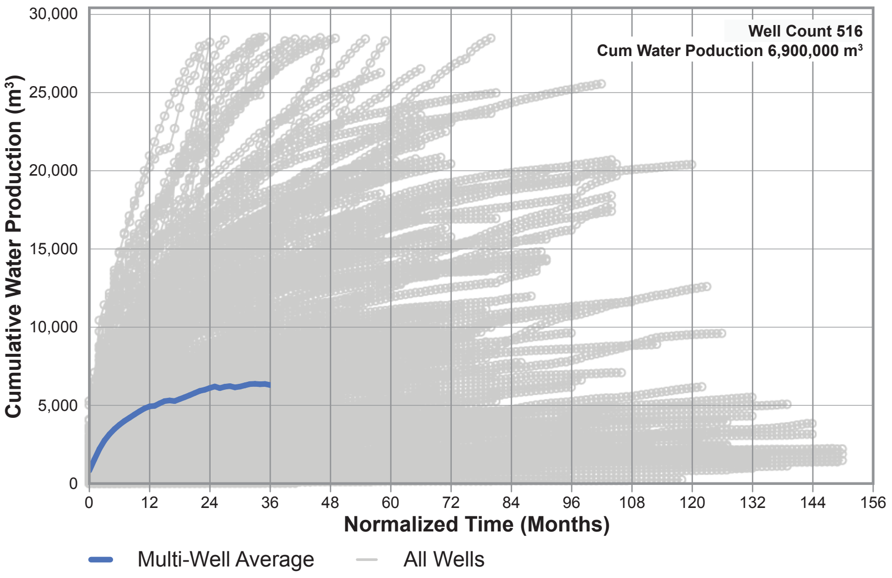

g. Swan

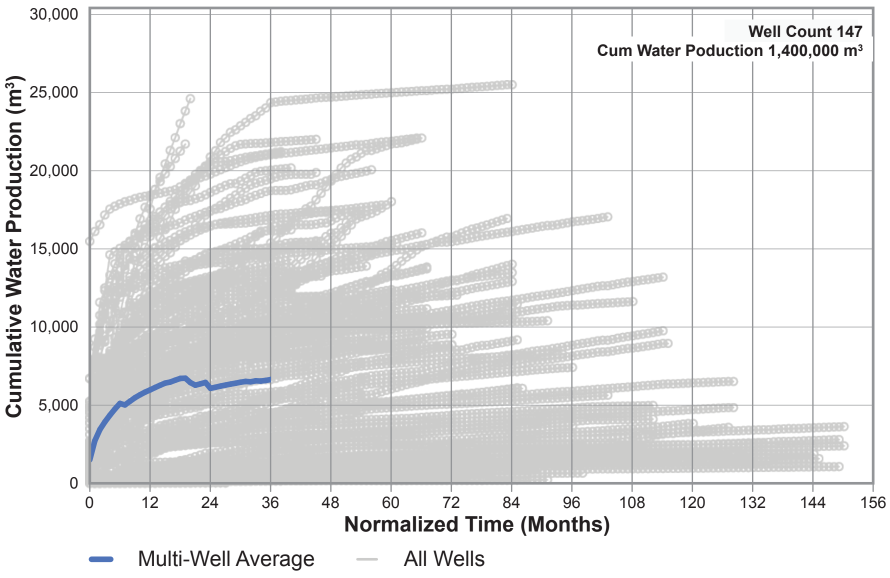

Water data from geoLOGIC

Figure 5.26

Future Sampling and Analysis Recommendations

The findings from this study and recommendations for future sampling/work in the NEBC Montney are summarized in *figure 5.27*.

The data collected for this study, along with the publicly available data from the GSC and AGS, suggest that there is significant economic potential within the Montney in NEBC. Further Montney sampling and testing is recommended across its expanse to increase the size and scope of the public database, which will help lithium-brine exploration efforts within NEBC. Areas to concentrate sampling efforts include regions with interpreted high lithium concentration *(figure 5.15)* and high water production *(figure 5.24)*, such as Blueberry, Inga North, Inga and Altares. Additional data would help to refine areas of lithium enrichment, improve the understanding of the main enrichment mechanisms, and enhance the exploration model for future lithium extraction projects.

In the current study, samples have been taken from the Upper and Middle Montney zones. Sampling the Lower Montney is recommended to provide insight on the economic potential of brine-hosted lithium over the entire Montney succession; the potential for stacked lithium pay could improve economics. Furthermore, the Lower Montney overall has a higher illite content than the Upper and Middle zones, which could translate into higher lithium concentrations. The hydrocarbon development of the Lower Montney is currently not as advanced as the Upper and Middle Montney zones, but as development occurs, it could be attractive for Montney lithium extraction.

Magnesium, calcium, and potassium were determined to be key proxy ions for lithium enrichment. Potassium concentrations in excess of 1,000 mg/L may be associated with enriched lithium values. Magnesium and calcium values between 100-180 meq/l and 400–1.200 meq/l, respectively, are associated with lithium concentrations of 50 mg/L or above. Future sampling should be undertaken in areas with such concentrations of magnesium, calcium, and potassium to further test this relationship, and to continue to delineate areas of lithium enrichment. Altares is a prime area where this should be undertaken *(figure 5.11)*. Further sampling should be considered at Beg as well, due to the enriched magnesium and calcium values. Another proxy ion to consider is strontium as values above 1,000 mg/L are associated with potentially economic values of lithium.

It is imperative to consider water production within the Montney in NEBC where the majority of wells target unconventional siltstones that are not aquifer-supported. Detailed analysis of water production over time is required to delineate areas that are more likely to have sufficient long-term water production capable of producing lithium in economic quantities. Turbidite zones may be more economic from this perspective as they tend to have better reservoir parameters due to their more conventional nature. It is recommended that operators collect and analyze water samples on a monthly basis for the first two years of production. It is imperative that lithium metal analysis be incorporated in routine water analysis

5.27 | Montney Lithium Summary Map

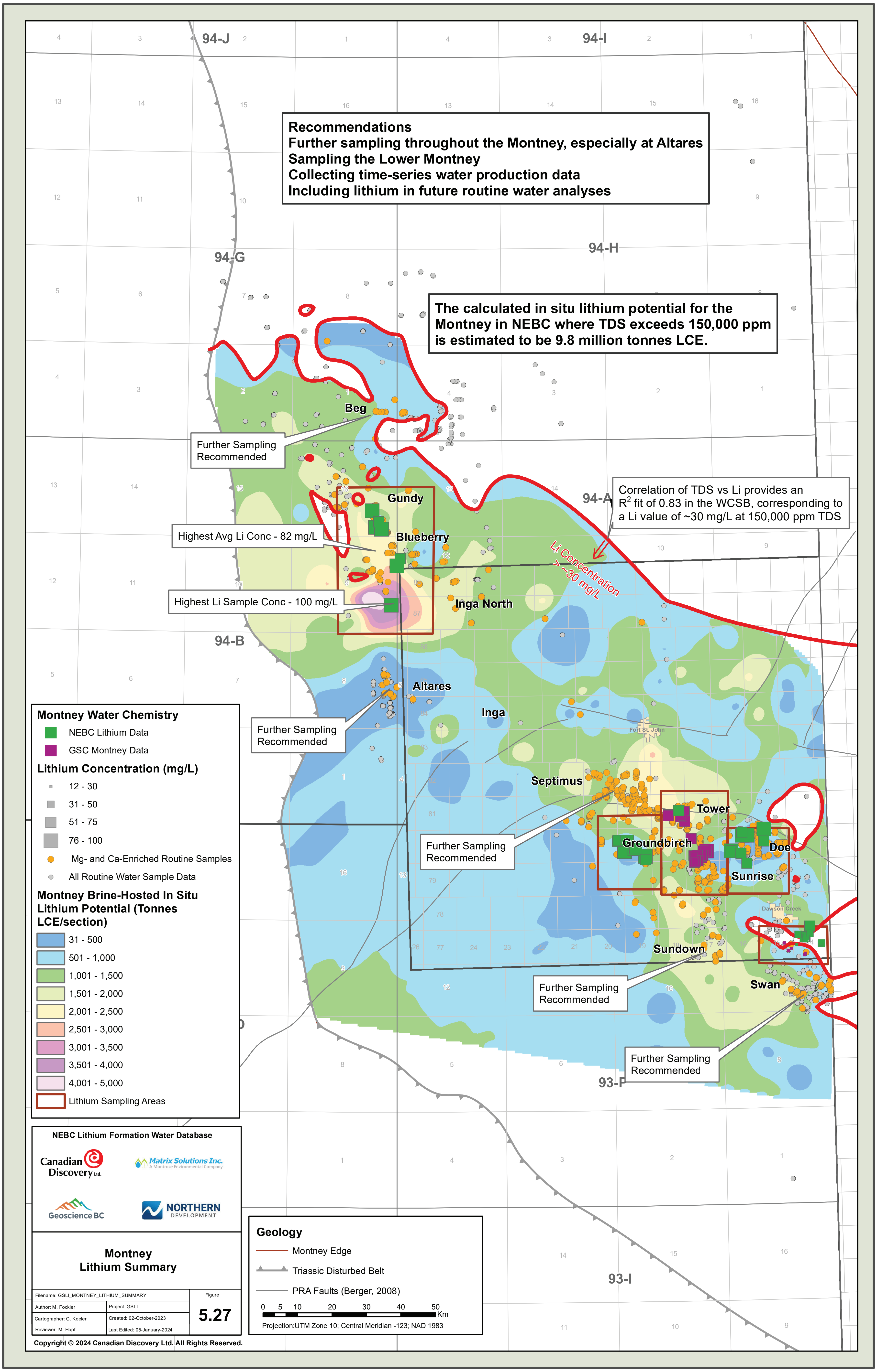

© Canadian Discovery Ltd.

Figure 5.27

References

- Abercrombie, H. J., Hutcheon, I. E., Bloch, J. D., de Caritat, P., 1994. Silica activity and the smectite-illite reaction. Geology 1994, Volume 22, No. 6, pages 539-542.
- Alberta Innovates, 2022. Alberta's First Direct Lithium Extraction Pilot. https://albertainnovates.ca/wp-content/uploads/2022/06/Albertas-First-Direct-Lithium-Extraction-Pilot-E3Metals-Project-Summary.pdf
- British Columbia Energy Regulators (BCER), 2022. British Columbia's 2021 Oil and Gad Reserves and Production Report. https://www.bc-er.ca/files/reports/Technical-Reports/2021-Oil-and-Gas-Reserves-and-Production-Report.pdf
- Brown, Teresa, 2016. British Geological Survey, Page 39, Mineral Profile: Lithium. https://nora.nerc.ac.uk/id/eprint/534440/1/lithium_profile.pdf
- Canadian Discovery Ltd. (CDL) and Geoscience BC, 2022. Northeast BC Geological Carbon Capture and Storage Atlas. https://www.geosciencebc.com/projects/2022-001/
- Chalmers, G. R. L., Silva, P. L., Bustin, A. A., Sanlorenzo, A., Bustin, R. M., 2022. Geology and Geochemistry of the Hydrocarbon Compositional Changes in the Triassic Montney Formation, Western Canada, Energies 2022, 15, 8877.
- Coffey D. M., Munk L. A., Ibarra D. E., Butler K. L., Boutt D. F., Jenckes J., 2021. Lithium storage and release from lacustrine sediments: Implications for lithium enrichment and sustainability in continental brines, Geochemistry, Geophysics, Geosystems, 22, e2021GC009916.
- Davies, R. G., and Smith, Langhorne, B., Jr. 2006. Structurally controlled hydrothermal dolomite reservoir facies: An overview, AAPG Bulletin, Volume 90, No. 11, pages 1614-1690.
- Davies, R. G., Watson, N., Moslow, T. F., MacEachern, J. A., 2018. Regional subdivisions, sequences, correlations and facies relationships of the Lower Triassic Montney Formation, west-central Alberta to northeaster British Columbia, Canada- with emphasis on role of paleostructure, Bulletin of Canadian Petroleum Geology, Volume 66, No. 1, pages 23-92.
- Dugamin, E. J., Cathelineau, M., Boiron, M. C., Richard, A., Despinois, F. 2023. Lithium enrichment processes in sedimentary formation waters.
- Eccles, D.R. and Berhane, H. 2011. Geological Introduction to Lithium-Rich Formation Water with Emphasis on the Fox Creek Area of West-Central Alberta (NTS 83F and 83K). ERCB/AGS Open File Report 2011-10.
- Egbobawaye, E., I., 2016. Whole-Rock Geochemistry and Mineralogy of Triassic Montney Formation, Northeastern British Columbia, Western Canada Sedimentary Basin, International Journal of Geosciences, Volume 7, pages 91-114.
- Ellis B. S., Szymanowski D., Magna T., Neukampf J., Dohmen R., Bachmann O., Ulmer P., Guillong M. 2018. Post-eruptive mobility of lithium in volcanic rocks, Nature Communications 9, Article Number: 3228 (2018).
- Financial Post, 2016. One of North America's Top Plays: Why the Montney is Canada's Answer to U.S. Shale. https://financialpost.com/news/one-of-north-americas-top-plays-why-the-montney-is-canadas-answer-to-u-s-shale.
- Ghanbari, E., Abbasi, M.A., Dehghanpour, H. and Bearinger, D. 2013. Flowback volumetric and chemical analysis for evaluating load recovery and its impact on early-time production, SPE 167165-MS, Prepared for presentation at the SPE Unconventional Resources. Conference – Canada, November 5-7, 2013, Calgary, Alberta, Canada, doi:10.2118/167165-ms.
- Kharaka, Y. K., Mariner, R. H., 1989. Chemical geothermometers and their application to formation waters from sedimentary basins.
- Kingston, A., Jiang, C., Wang, X. and Hobbs, T. 2023. Chemical compositions of flowback and produced water from the Duvernay shale and Montney tight reservoir developments in Western Canada: potential for lithium resources from wastewater, Geological Survey of Canada, Open File 8974.
- Jensen, G. K. S., Rostron, B. J., 2018. Investigating the Mineral Potential of Brines In Saskatchewan: New Results from the Brine Sampling Project for 2018: Summary of Investigations 2018, v. 1, Saskatchewan Geological Survey, Saskatchewan Ministry of Energy and Resources, Miscellaneous Report 2018-4.1, Paper A-5, 8p.
- Leece A. S., Jiang, C. 2023. A preliminary techno-economic assessment of lithium extraction from flowback and produced water from unconventional shale and tight hydrocarbon operations in Western Canada, Geological Survey of Canada, Open File 8975.
- Liseroudi, M., Ardakani, O. H., Sanei, H., Pedersen, P. K., Wood, K. M., 2018. Diagenetic Controls on the Occurrence of Anhydrite Cement in the Siltstone Dominated Montney Formation, Western Canadian Sedimentary Basin

- LithiumBank, 2023. LithiumBank Reports US$2.7 Billion Pre Tax NPV From Preliminary Economic Assessment on a 31,350 TPA LHM Operation at Boardwalk Lithium Brine Project, Alberta, Canada. https://www.lithiumbank.ca/news/2023/ithiumankeports27illionreaxromrelimin20230525071202#:~:text=The%20Li%2Dbrine%20resources%20were,resource%20has%20units%20of%20grams.
- Lyster, S., Hauck, T.E., Lopez, G. P., Playter, T. L., Reimert, C., Palombi, D. and Schultz, S. K., 2022. Lithium and Helium in Alberta: Data Compilation and Preliminary Observations, Alberta Energy Regulator and Alberta Geological Survey, Open File Report 2021-04.
- Murphy, O., Haji, M.N., 2022. A Review of Technologies for Direct Lithium Extraction from Low Li+ Concentration Aqueous Solutions. Frontiers in Chemical Engineering.
- Ness, S. M., 2001. The Application of Basin Analysis to the Triassic Succession, Alberta Basin: an Investigation of Burial and Thermal History and Evolution of Hydrocarbons in Triassic Rocks. The Faculty of Graduate Studies (Department of Geology and Geophysics) The University of Calgary.
- Owen, J. N., 2017. An Investigation into the controls and Variability of the Flowback Water Inorganic Geochemistry of the Montney Formation, northeast British Columbia and northwestern Alberta, Canada. The Faculty of Graduate and Postdoctoral Studies (Geological Sciences) The University of British Columbia.
- Sanjuan B., Millot R. (2009) - Bibliographical review about Na/Li geothermometry and lithium isotopes applied to worldwide geothermal waters. Report BRGM/RP-57346-FR, 58 p., 1 tabl., 9 figs., 1 appendix.
- Shouakar-Stash, O., 2008. Evolution of Stable Chlorine and Bromine Isotopes in Sedimentary Formation Fluids, Department of Earth Sciences, University of Waterloo.
- Standard Lithium, 2021. Standard Lithium Announces Positive Preliminary Economic Assessment and Update of Inferred Mineral Resource at South-West Arkansas Lithium Project. https://www.standardlithium.com/investors/news-events/press-releases/detail/99/standard-lithium-announces-positive-preliminary-economic
- Vaisblat, N., Harris, N.B., DeBhur, C., Euzen, T., Gasparrini, M., Crombez, V., Rohais, S., Krause, F. and Ayranci, K. (2017): Diagenetic model for the deep Montney Formation, northeastern British Columbia; in Geoscience BC Summary of Activities 2016, Geoscience BC, Report 2017-1, p. 37–48.
- Wahlberg, J. S., Baker, J. H., Vernon, R. W., Dewar, R. S., 1965. Ion Exchange on Mineral Materials: Exchange Adsorption of Strontium on Clay Minerals. Geological Survey Bulletin 1140-C.
- Wood, J. M., Curtis, M. E., Ardakani, O. H., Sanei, H., 2021. Movement of native fluids during scanning electron microscopy imaging of petroliferous siltstone: Evidence from the Montney Formation, western Canada. Fuel, volume 290.
- Wust, R. A. J., Tu, S., Nassichuk, B., Bozart, T., Tucker, J., Cui, A., 2018. Chemostratigraphy, petrography, and SEM investigations of the Lower Triassic Montney Formation in Alberta: Implications for a new and revised diagenetic and depositional model. Bulletin of Canadian Petroleum Geology, V. 66, No 2, Pg. 436-471.
- Zolfaghari, A., Dehghanpour, H., Noel, M. and Bearinger, D. 2016. Laboratory and field analysis of flowback water from gas shales: Journal of Unconventional Oil and Gas Resources, v. 14, p. 113-127, doi: 10.1016/j.juogr.2016.03.004.
- Zonneveld, J. P. and Moslow, T. F., 2018. Palaeogeographic setting, lithostratigraphy, and sedimentary framework of the Lower Triassic Montney Formation of western Alberta and northeastern British Columbia, Bulletin of Canadian Petroleum Geology, Volume 66, No. 1, pages 93-127.

Triassic Aquifers: Halfway-Doig and Baldonnel Overview

Lithium data were collected for 17 Halfway, 5 Doig and 7 Baldonnel samples (including duplicates) with concentrations ranging from 17 to 44 mg/L *(figure 6.1 and table 6.1)*. The samples were collected from the Birch, Fireweed, Peejay, Boundary Lake, Boundary Lake North and Mica fields *(figure 6.2)*. *Table 6.1* provides average, median, minimum and maximum values of all analyzed major ions and trace elements in the program, including total dissolved solids (TDS). For the Triassic aquifers, boron and bromide concentrations average 53 mg/L and 82 mg/L respectively, and there are no analyses for iodide *(table 6.1)*.

Looking at hydrodynamics, the Halfway, Doig and Baldonnel are all conventional aquifers in NEBC where the water produced is formation water from the aquifer. The Montney is different hydrodynamically; it is a very fine-grained unconventional reservoir that must be hydraulically fractured to produce hydrocarbons, and also to co-produce lithium from the frac and formation water.

This chapter provides an overview of the Halfway-Doig and Baldonnel geologic settings, historical oil and gas development, data distribution, proxy analytics, and potential lithium sources.

6.1 Stratigraphic Chart

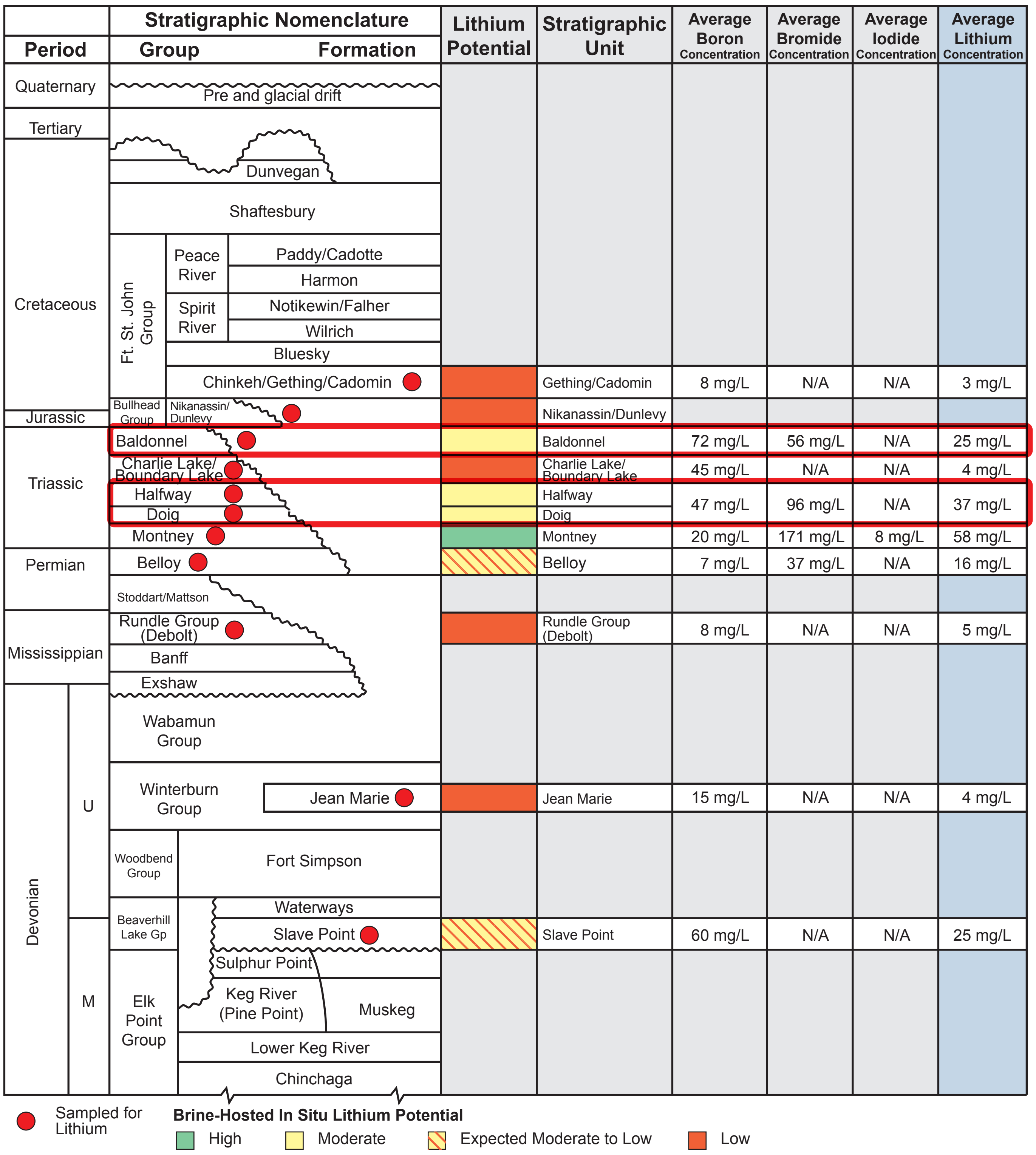

Modified from Bachu (1995) and this study

Figure 6.1

6.2 | Triassic Aquifers Lithium Sample Distribution Map

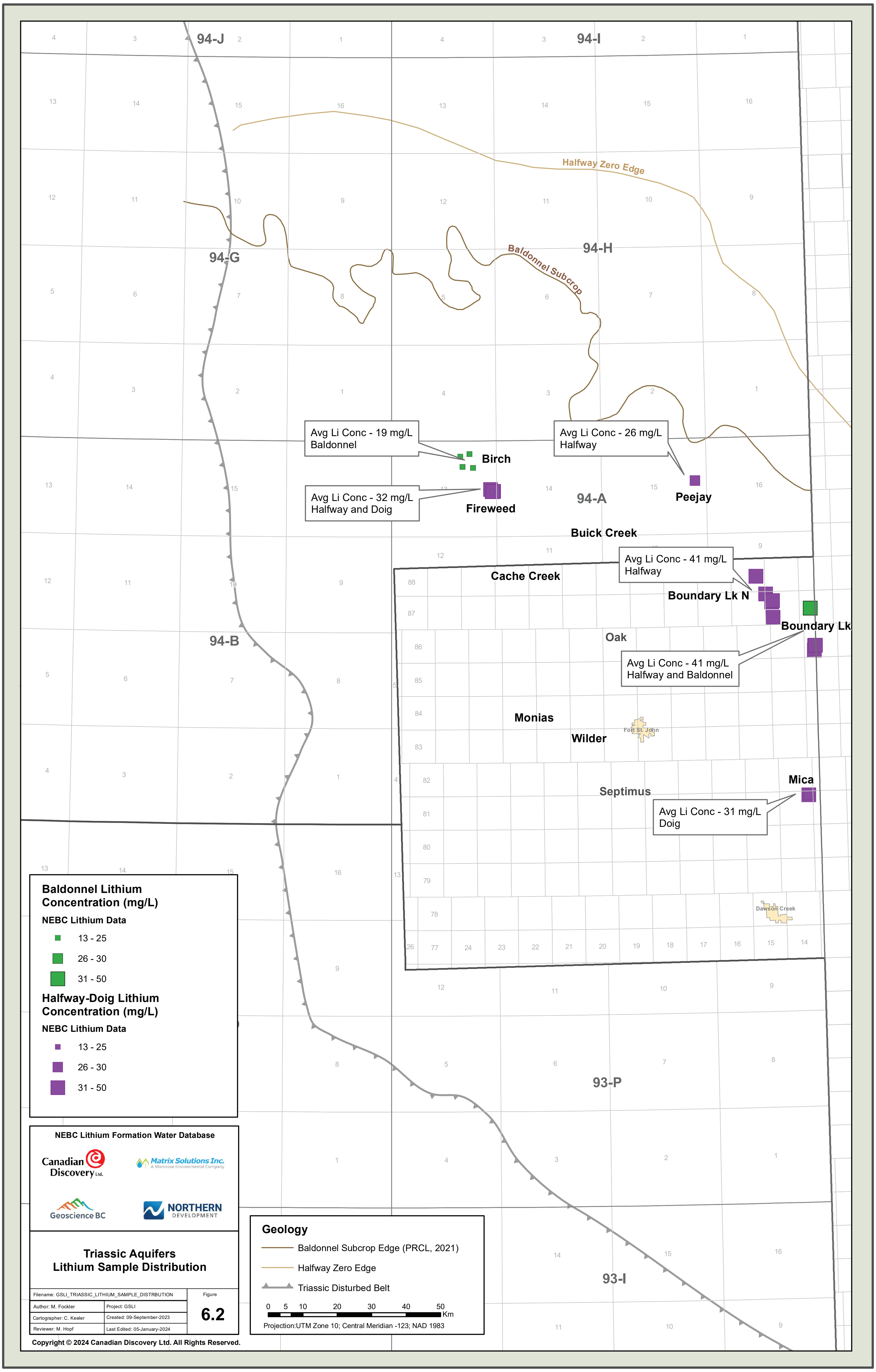

© Canadian Discovery Ltd.

Figure 6.2

Table 6.1: Statistics by Age for Analyzed Major Ions and Trace Elements

Major Ions and Trace Elements (Dissolved) (mg/L)	Montney				Triassic Aquifers				Triassic - Others			
	Average	Median	Min	Max	Average	Median	Min	Max	Average	Median	Min	Max
Potassium	2,227	2,205	125	3,910	1,074	1,026	230	1,960	804	910	521	980
Sodium	59,122	66,870	3,780	91,200	42,845	53,450	8,851	65,600	31,500	36,800	18,500	39,200
Calcium	15,508	16,430	841	23,320	2,182	2,420	33	5,800	2,127	2,267	1,520	2,595
Magnesium	1,550	1,495	182	2,850	511	534	15	1,100	413	409	400	430
Chloride	132,821	140,750	6,870	199,200	73,370	90,600	9,140	124,000	50,423	61,640	27,200	62,430
Aluminum	7	5	0.03	20	9	2	2	20	1	1	0.02	2
Antimony	3	1	0.01	10	2	0.50	0.50	5	0.17	0	0	0.50
Arsenic	6	2	0.01	30	5	1	1	10	1	1	1	1
Barium	245	10	0.05	1260	0.30	0.27	0.10	0.82	0.11	0.11	0.11	0.11
Beryllium	1	1	0	5	0.23	0.05	0.05	0.50	0.02	0	0	0.05
Boron	20	17	0.50	177	53	43	34	200	173	173	173	173
Bromide	171	169	17	306	82	65	27	152				
Cadmium	8	0.05	0	40	0.23	0.05	0.05	0.50	0.02	0	0	0.05
Chromium	0.40	0.50	0.01	1	0.24	0.05	0.05	0.50	0.02	0.01	0.01	0.05
Cobalt	0.59	1	0.01	1	0.46	0.10	0.10	1	0.04	0	0	0.10
Copper	0.56	1	0.01	1	0.46	0.10	0.10	1	0.04	0	0	0.10
Iodide	8	8	0	18								
Lead	8	2	0.01	20	9	2	2	20	1	1	0	2
Lithium	58	65	2	100	33	34	17	44	20	20	20	20
Molybdenum	0.66	1	0	1	0.46	0.10	0.10	1	0.03	0	0	0.10
Nickel	0.88	0.20	0.01	2	0.92	0.20	0.20	2	0.07	0	0	0.20
TDS (Calculated)	**211,607**	**228,119**	**14,128**	**309,457**	**122,516**	**151,861**	**21,774**	**196,029**	**88,070**	**105,374**	**51,412**	**107,425**

Major Ions and Trace Elements (Dissolved) (mg/L)	Cretaceous				Permian				Devonian-Mississippian			
	Average	Median	Min	Max	Average	Median	Min	Max	Average	Median	Min	Max
Potassium	104	102	67	175	598	467	162	1,490	379	119	31	1,105
Sodium	8,566	10,500	3,700	13,900	21,166	16,900	5,330	50,800	13,558	9,377	6,150	35,250
Calcium	523	173	29	1,280	1,580	1,330	436	3,810	2,185	1,658	129	8,390
Magnesium	114	74	24	230	301	253	88	708	308	209	159	867
Chloride	12,442	17,860	2,760	20,800	39,820	30,900	10,700	103,000	23,648	14,440	12,000	64,000
Aluminum	2	2	2	2	2	2	2	2	2	2	0.10	2
Antimony	0.50	0.50	0.50	0.50	0.50	0.50	0.50	0.50	0.36	0.50	0	0.50
Arsenic	1	1	1	1	1	1	1	1	0.87	1	0.01	1.49
Barium	49	5	1	119	6	6	0.07	11	590	392	1.07	1890
Beryllium	0.05	0.05	0.05	0.05	0.05	0.05	0.05	0.05	0.04	0.05	0	0.05
Boron	8	8	4	11	6	6	6	6	25	8	5	61
Bromide	65	65	65	65	37	35	0	73				
Cadmium	0.05	0.05	0.05	0.05	0.05	0.05	0.05	0.05	0.04	0.05	0	0.05
Chromium	0.05	0.05	0.05	0.05	0.05	0.05	0.05	0.05	0.05	0.05	0.01	0.09
Cobalt	0.10	0.10	0.10	0.10	0.10	0.10	0.10	0.10	0.07	0.10	0	0.10
Copper	0.10	0.10	0.10	0.10	0.10	0.10	0.10	0.10	0.11	0.10	0.01	0.33
Iodide												
Lead	2	2	2	2	2	2	2	2	1	2	0	2
Lithium	3	3	2	4	16	16	16	16	16	5	4	30
Molybdenum	0.10	0.10	0.10	0.10	0.10	0.10	0.10	0.10	0.08	0.10	0	0.10
Nickel	0.20	0.20	0.20	0.20	0.20	0.20	0.20	0.20	0.15	0.20	0.01	0.20
TDS (Calculated)	**23,641**	**31,190**	**9,297**	**36,773**	**63,658**	**50,181**	**16,865**	**159,975**	**41,117**	**27,098**	**20,344**	**107,775**

Table 6.1

6.3 Halfway-Doig Schematic Cross-Section

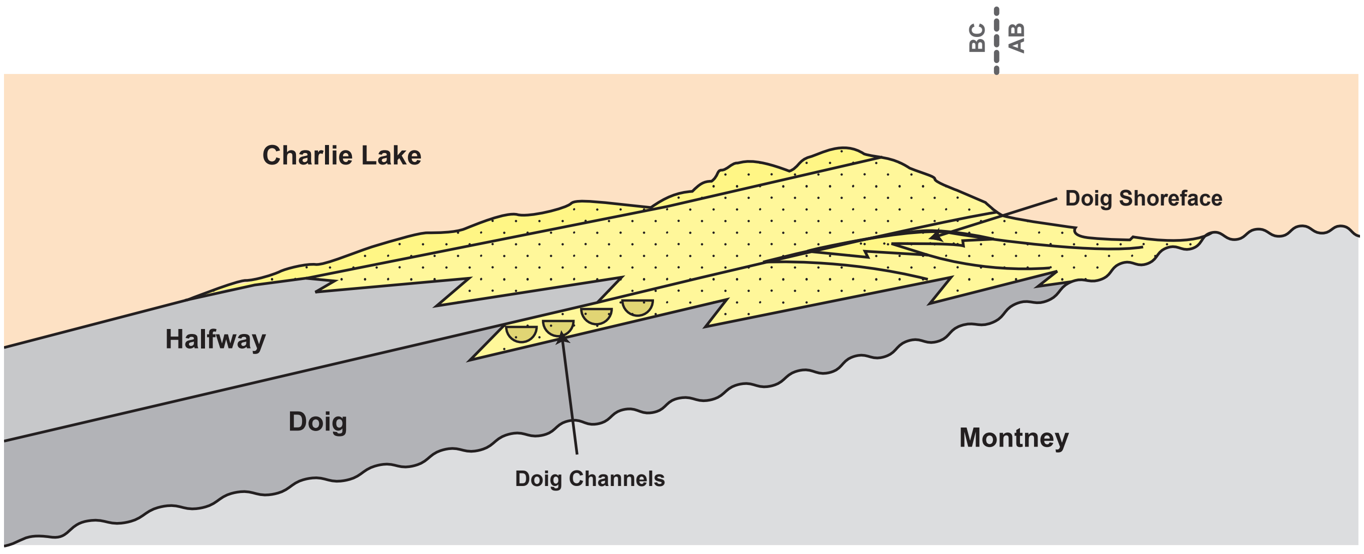

Source: Strategy 2K5 Study, Canadian Discovery Ltd.

Figure 6.3

Geologic Setting

The Triassic Doig and Halfway formations *(figure 6.1)* were deposited within a prograding clastic coastal system along the western margin of the North American craton. Deposition occurred in proximal to distal marine environments. They are preserved across the southern and Peace River areas within the study area, thinning to a northeasterly subcrop edge. The Doig comprises offshore to lower shoreface shales, siltstones and sandstones, with thick, cleaner, more proximal sandstones in isolated bodies and linear trends *(figure 6.3)*. Doig sandstones are well-sorted, very fine- to fine-grained sublithic to quartz arenites, with interbedded bioclastic (coquinoid) packstones and grainstones. A complex diagenetic history has produced highly variable reservoir quality.

The overlying Halfway mainly comprises shallow marine sandstones and coquinas deposited in barrier island, shoreface and tidal inlet channel environments. Halfway sandstones are primarily quartz arenites and sublitharenites, with local bioclastic (shell debris) sandstones and coquinas. Grain sizes generally range from very fine to fine, as most clastic sediment was derived through aeolian (wind) transport from the craton. The best (and volumetrically dominant) reservoir facies in many pools in the updip Halfway are tidal channel fills. To the south and west, reservoir quality generally deteriorates, although secondary dissolution of lithic and bioclastic grains can create significant reservoir sweet spots (BC EMPR, 2006). The boundary between the Doig and Halfway can be challenging to demarcate on logs where Doig sand bodies are present. For this study, these formations will be treated together. Note that during Halfway-Doig deposition, there was an active island arc system located along the western margin of the North American continent (Wust et al., 2018, Ellis et al., 2018) *(figure 6.4)*, which could have provided volcanically derived potassium feldspars with elevated lithium concentrations.

6.4 Early-Middle Triassic Paleogeography

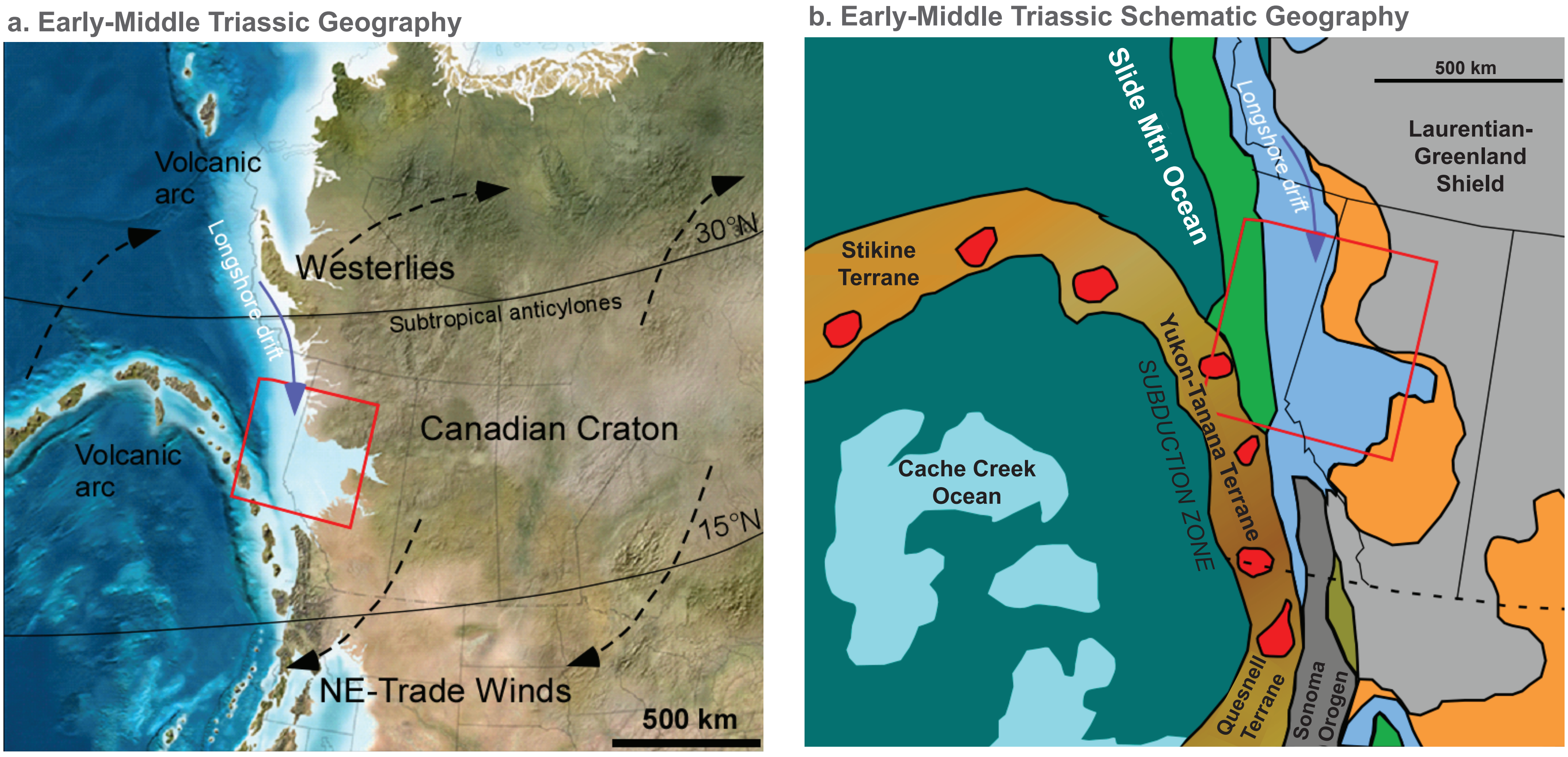
a. Early-Middle Triassic Geography

b. Early-Middle Triassic Schematic Geography

From Wust et al., 2018

Figure 6.4

6.5 Baldonnel Schematic Cross-Section

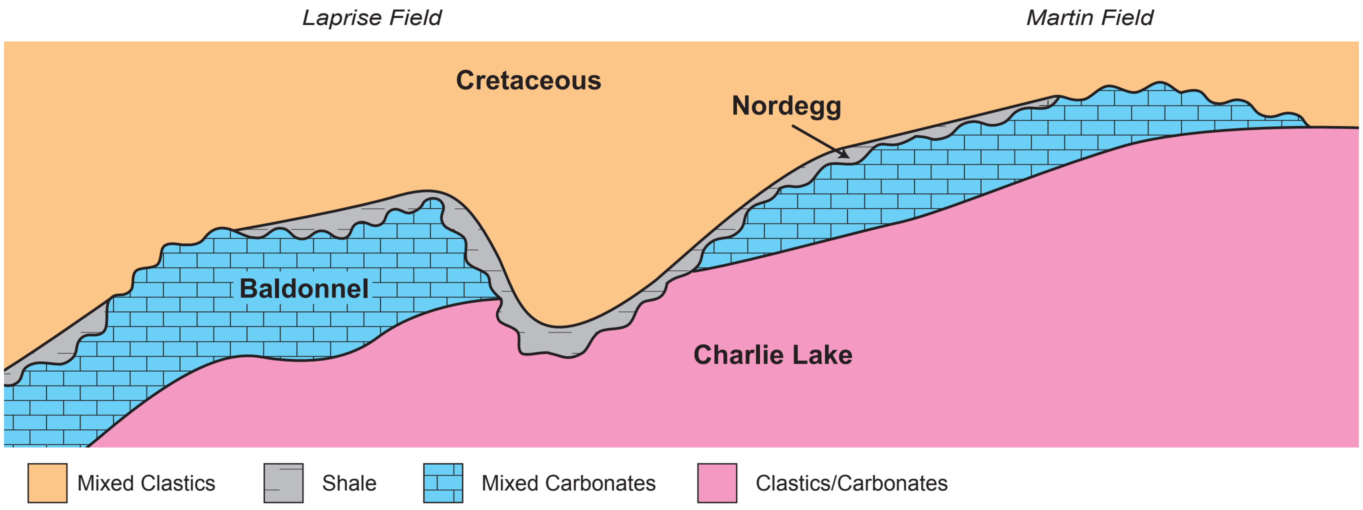

Modified from Bird et al., 1994

© Canadian Discovery Ltd.

Figure 6.5

As shown in *figures 6.1 and 6.3*, the Charlie Lake Formation is located above the Halfway-Doig formations (and below the Baldonnel Formation). It was deposited in widespread, low-relief environment in an arid climate, and therefore, reservoir units tend to be thin and discontinuous, which is not conducive to massive water production. The Charlie Lake samples had lithium concentrations well under 50 mg/L, it is discussed in *Chapter 7*.

Baldonnel strata are widespread shallow marine to shelfal carbonates, deposited during a regional late Triassic transgression that drowned Charlie Lake arid coastline environments (Davies, 1997). As described in NEBC Play Atlas (2006), reservoir rocks are primarily dolomitized skeletal calcarenites, with considerable variation in reservoir quality arising from the interplay of depositional facies, diagenesis and structural overprint *(figure 6.5)*. The Baldonnel can be mapped continuously from the southern part of the study area to a northern subcrop edge (see grids 94G and 94H in *figure 6.2*). The Baldonnel lies, more or less, conformably on the Charlie Lake, and is unconformably overlain by Jurassic Nordegg and/or Fernie marine shales.

Historical Halfway-Doig and Baldonnel Oil and Gas Development

The Triassic Halfway, Doig and Baldonnel formations have been targeted for oil and gas development since the late 1940s and early 1950s. The zones were developed in a conventional manner with vertical wells up until the late 2000s when production from hydraulically fractured horizontal wells became common. Targeting these zones has slowed down considerably in NEBC since about 2018 as the Montney has become the primary target.

6.6 Triassic Aquifers Lithium Concentrations by Area

a. Lithium Concentration by Formation

b. Lithium Concentration by Area

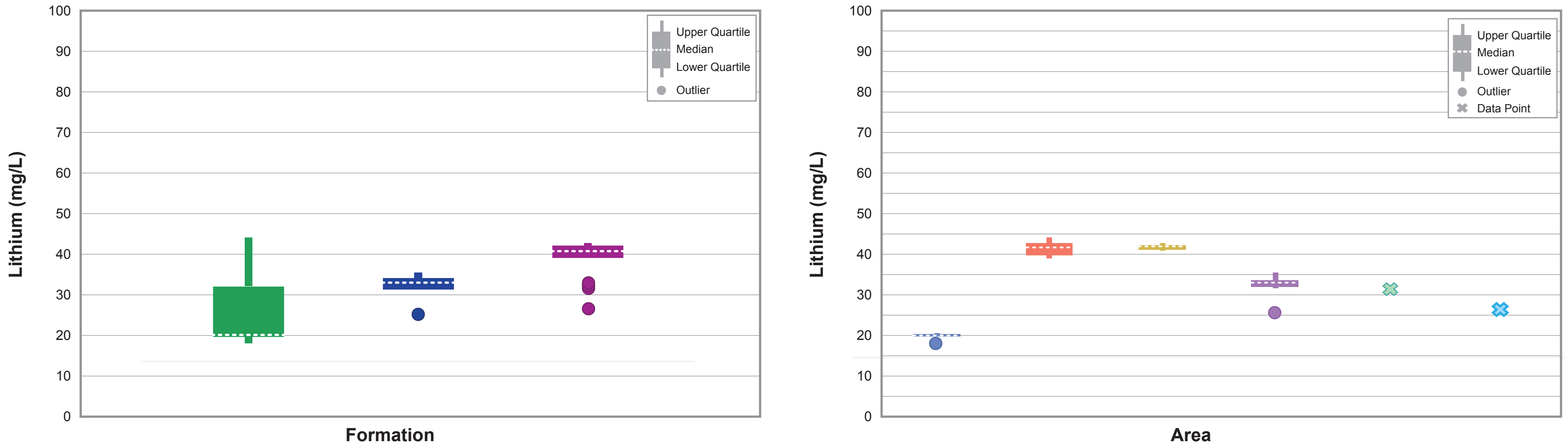

	Baldonnel	Doig	Halfway
Count	7	5	17
Average	26	32	38
Median	20	33	41
Min	18	25	26
Max	44	35	42

	Birch	Boundary Lake	Boundary Lake North	Fireweed	Mica	Peejay
Count	5	8	7	7	1	1
Average	19	41	41	32	31	26
Median	20	41	42	33	-	-
Min	18	39	41	25	31	26
Max	20	44	42	35	31	26

c. Lithium Concentration vs TDS

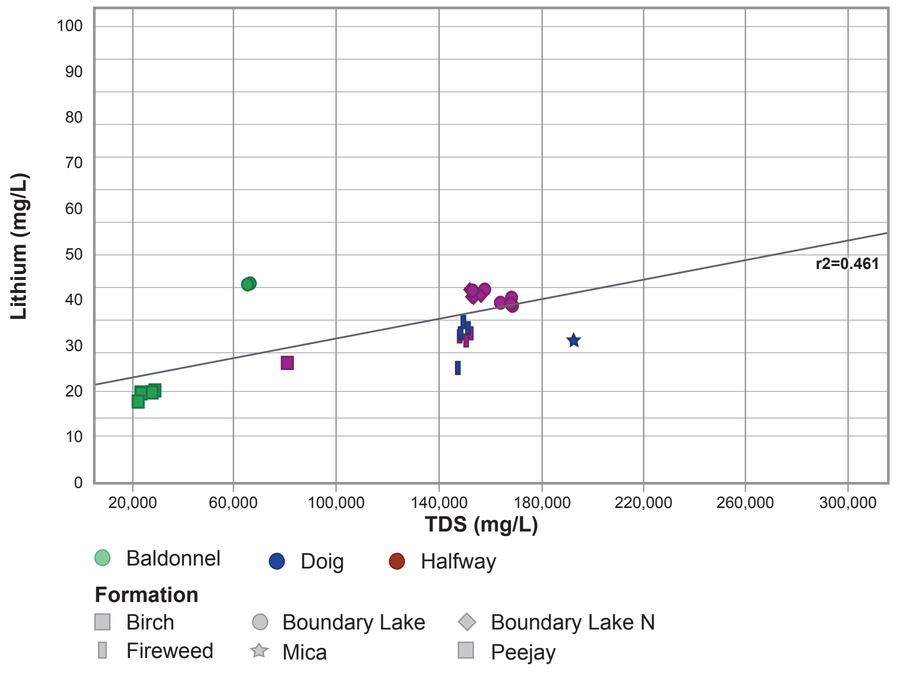

Lithium data sources from the current study

© Canadian Discovery Ltd.

Figure 6.6

Lithium Data Distribution

Participants to the sampling program in this study provided access to samples from the Baldonnel, Halfway and Doig formations in six areas where these formations are currently being developed by horizontal and vertical wells *(figure 6.2)*. In total, 29 individual samples were collected and analyzed (including duplicates; see *Appendix A* for samples used in the analyses).

Lithium concentrations from the samples collected from the Triassic aquifers range from 18 to 44 mg/L; the Halfway has the highest average concentration at 38 mg/L with a median of 41 mg/L; the Baldonnel has the single highest lithium concentration at 44 mg/L and the largest spread in data *(figure 6.6a)*. Currently, lithium concentrations above 50 mg/L are generally considered to be economically viable for production (Standard Lithium, 2021; LithiumBank, 2023). *Figure 6.6b* displays the range of sampled concentrations in the six main areas; Boundary Lake has the highest average lithium concentration at 41 mg/L and the highest single sample (44 mg/L), Birch has the lowest average concentration at 19 mg/L. In general, areas with high lithium concentrations tend to have high total dissolved solids (TDS) *(figure 6.6c)*.

The Halfway-Doig produced fluids appear to have lithium concentrations just below 50 mg/L, potentially making them attractive prospects for future lithium development assuming extraction technologies improve in the foreseeable future.

Quality Control and Time On-Production

When collecting water samples from hydrocarbon wells, there are common contaminants that are present due to drilling, testing and completions practices. As such, various screening methods are used to distinguish between true formation water and erroneous samples containing mud filtrates or completions fluids. Water chemistry screening was run on all data and detailed criteria can be found in *Appendix C*.

The timing of sample collection is less of a concern in the Halfway-Doig and Baldonnel formations versus the Montney where wells must flow for some time (determined to be around 100 days in *Montney Chapter 5*) to clear frac fluid contamination from the system. Because porosity and permeability are much higher in these aquifers compared to the Montney, water production rates are higher, the formations clean up more quickly, and true formation water chemistry is achieved faster.

Also note that Halfway-Doig and Baldonnel samples were collected later in the productive life of the wells than the Montney samples, decreasing the chance of any completion fluid contamination.

Water Chemistry and Potential Lithium Sources in Triassic Aquifers

The Triassic aquifer and Montney datasets (from this study, the Geologic Survey of Canada (GSC) Open File 8974 (Kingston et al. 2023), and various sources from the Alberta Geological Society (AGS)) were combined in *figures 6.7 and 6.8* to investigate if there are any ionic relationships from the Triassic aquifers that can be correlated to the Montney, which is considered to have economic concentrations of lithium, and also to investigate if the sources of lithium within the Triassic aquifers are similar to the Montney.

To understand the source of the lithium in the Triassic aquifers, several ions were plotted and compared to investigate potential sources of lithium within the formations and determine whether select ions tested in routine water analysis can be used to signify higher lithium concentration in brines. Chloride (Cl) and bromide (Br) are used to normalize data, as they tend to be conservative ions that remain in solution once dissolved and are not easily removed from the system by water-rock interactions. The Triassic aquifer dataset is compared to the Montney datasets looking for similarity in trends.

The Cl/Br vs Na/Br plot *(figure 6.7a)* is used to determine formation brine chemistry relative to modern seawater and to interpret the concentration mechanism of the ions in solution (Eccles and Berhane, 2011). If data plot below and to the left of modern seawater, it is generally interpreted to represent salinity acquired through evapoconcentration. If data plot above and to the right, it is generally interpreted to represent salinity acquired through halite dissolution. Most of the Halfway-Doig, and Montney plot above seawater, indicating that salinity is partially derived from halite dissolution. This enrichment could have come from water-rock interactions within the overlying Charlie Lake formation. The Baldonnel data plot below and to the left of seawater, indicating that salinity is derived from evapoconcentration.

The complete seawater evapoconcentration process causes the precipitation of, in order, calcite, gypsum, halite, epsomite, sylvite, carnalite and bischofite, and is well depicted by the relationship of chloride to bromide, as discussed in the *Overview chapter*. Halfway-Doig brines never exceed the gypsum precipitation level, which is consistent with the offshore environment of deposition *(figure 6.7b)*. Most of the Baldonnel samples plot below modern seawater.

The K/Br vs Cl/Br plot is commonly used to indicate water-rock interaction with volcanically derived potassium feldspars. The Halfway-Doig samples have an elevated Cl/Br ratio vs the Baldonnel samples, but are roughly in line with most of the Montney samples *(figure 6.7e)*. For the Halfway, this suggests water-rock interactions involving silicate alteration as a source of lithium (Eccles and Berhane, 2011). Like the Montney, the volcanically derived potassium feldspars could have been sourced by the island arc system off the west coast that was emitting rhyolitic ash and ignimbrite (welded tuff) phenocrysts with elevated lithium concentrations (Ellis et al., 2018).

The Baldonnel shows some similar trends to that of the Alberta Montney, but with lower overall TDS concentrations. The K/Br and Cl/Br ratios are too low to indicate silicate alterations due to water-rock interactions *(figure 6.7a)*. Cl/Br and Na/Br ratios indicate slight evapoconcentration as compared to sea water *(figure 6.7b)* (Eccles and Berhane, 2011). Further sampling is required for the Baldonnel before any theories can be made about the source of lithium as it would be inappropriate to base an entire sourcing model on two samples from one location.

Mg vs Cl and Ca vs Cl crossplots *(figures 6.7c and d)* are used to investigate potential dolomitization of the rocks as they interact with the brines. The magnesium concentration decreases with increased dolomitization, as magnesium replaces calcium in carbonate minerals and the brine is enriched in calcium, resulting in low magnesium and high calcium brine relative to seawater. The majority of the samples from all formations fall well below the seawater concentration on the Mg vs Cl plot indicating potential dolomitization *(figure 6.7c)*; this tends to correlate to calcium levels above sea level *(figure 6.7d)*. Halfway-Doig samples are on trend with the NEBC Montney data while the Baldonnel data do not seem to correlate and have especially low concentrations of magnesium and calcite. The Mg-Ca-Cl ranges used in the Montney chapter to delineate areas of higher lithium potential do not correspond to the Triassic aquifers.

Relationships between lithium concentrations and potassium (K), sulphate (SO_4), calcium (Ca), magnesium (Mg), bromide (Br), strontium (Sr), and chloride (Cl) were also examined *(figures 6.8 a–g)*. Note that the correlation lines on the graphs apply only to the Triassic aquifer data and not the Montney data. There is a strong correlation between lithium and strontium and a moderate correlation between lithium and calcium and lithium and magnesium.

TDS as a Proxy for Lithium Concentration

Because there is a limited number of samples in these formations, and the geographical extent of those samples is limited, the total dissolved solids (TDS) to lithium concentration correlation developed in the Montney chapter can be used to high-grade or low-grade formations. The correlation established that a TDS value of 150,000 mg/L (150 g/L) suggests a lithium concentration of about 30 mg/L. The 150 g/L contour from regional TDS mapping is used to approximate where lithium concentrations could come into the realm of economic viability. Note that while higher lithium concentrations are often associated with higher TDS concentrations, high TDS concentrations do not necessarily imply high lithium concentrations.

In the *Montney chapter* it was shown that the chemical evolution of flowback and produced water over the production period of a well, generally evolves from lower TDS and lithium that mimic "frac water" composition to a representative

6.7 Triassic Aquifers Water Chemistry Crossplots

a. Cl/Br vs Na/Br

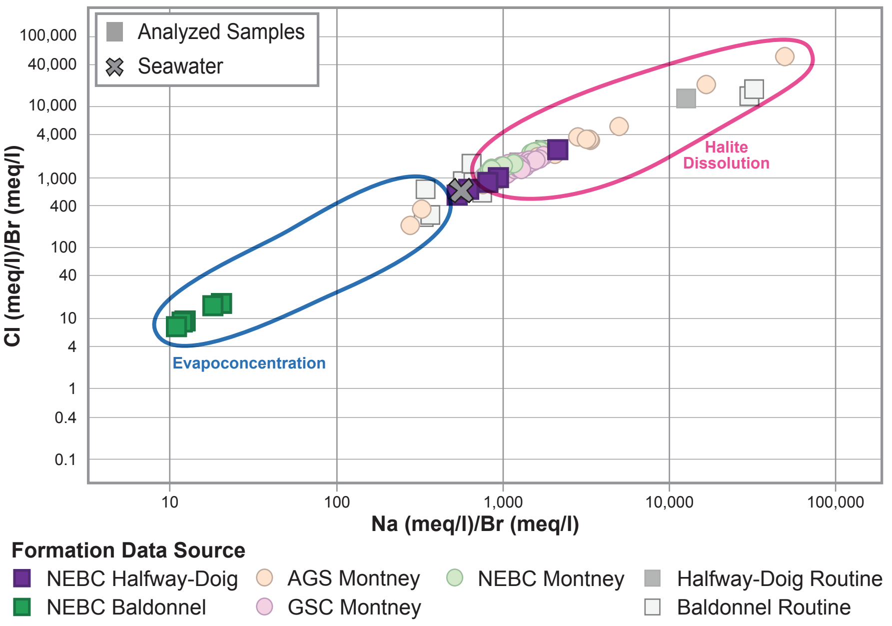

b. Halfway-Doig/Baldonnel Cl vs Br Seawater Evaporation Line

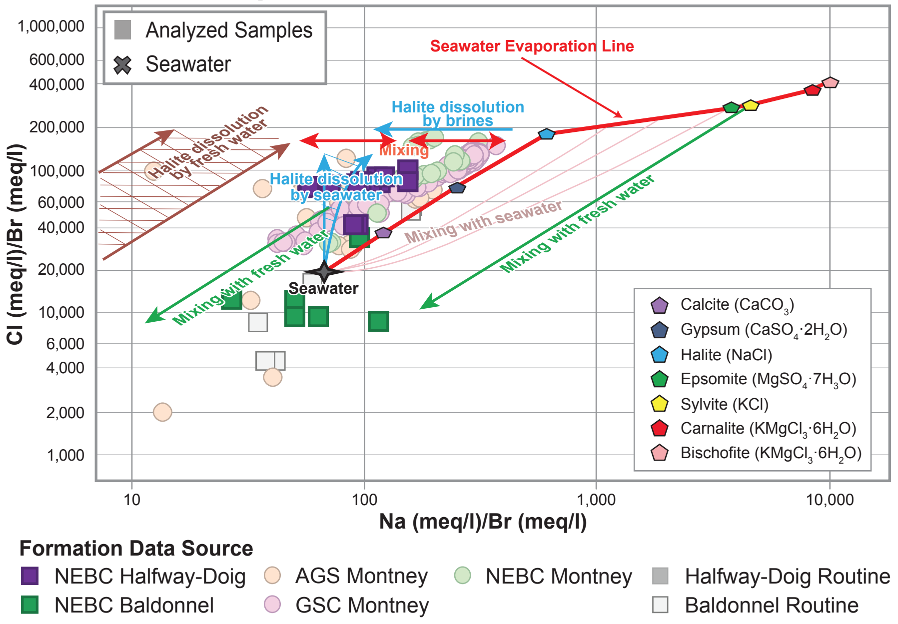

c. Mg vs Cl

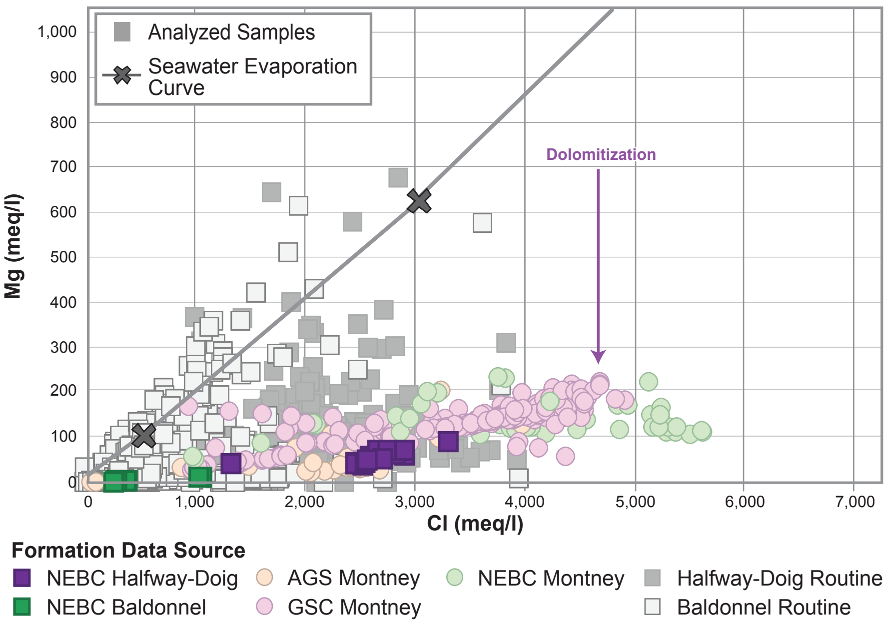

d. Ca vs Cl

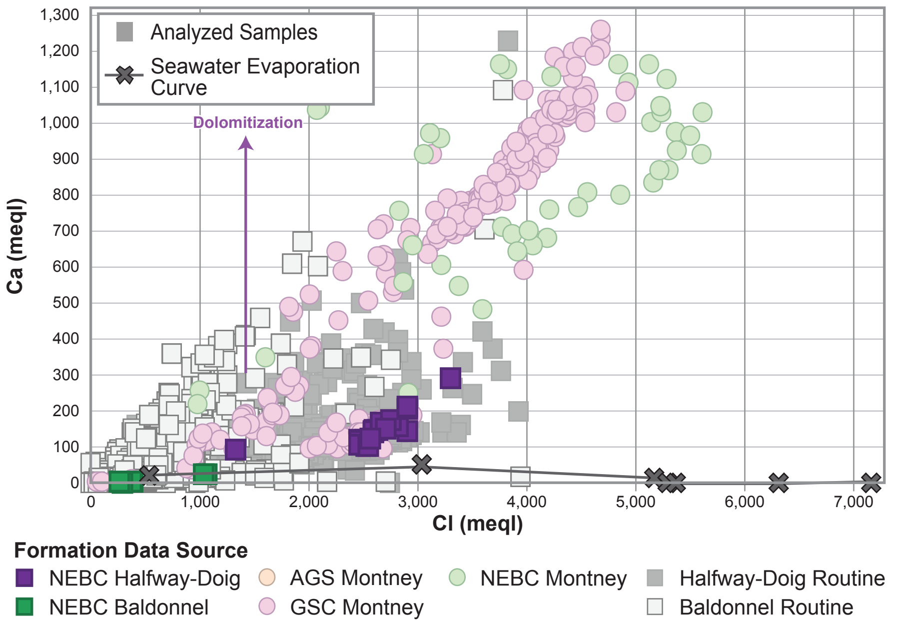

e. K/Br vs Cl/Br

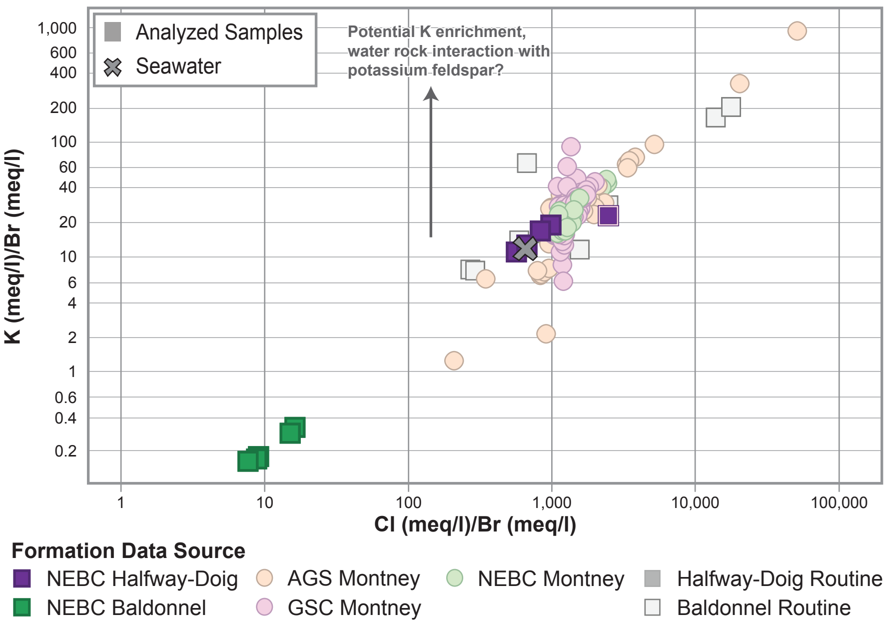

Lithium data from the current study

Figure 6.7

6.8 Triassic Aquifers Water Chemistry Lithium Crossplots

a. Li vs K

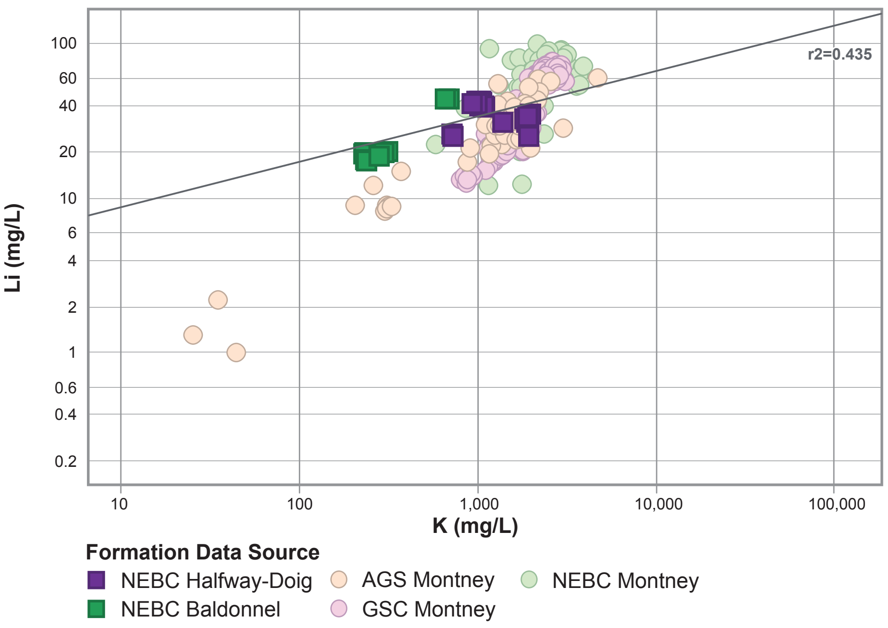

b. Li vs SO$_4$

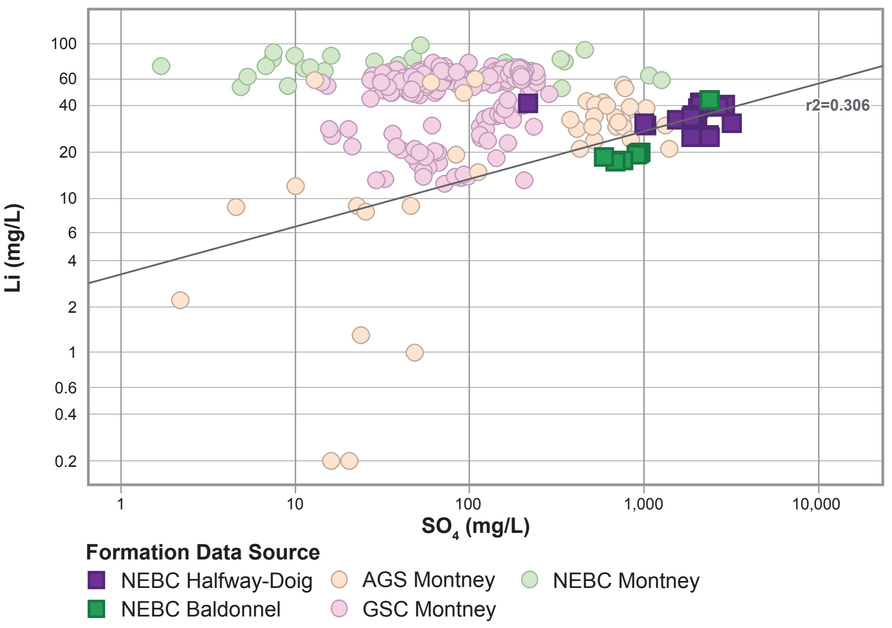

c. Li vs Ca

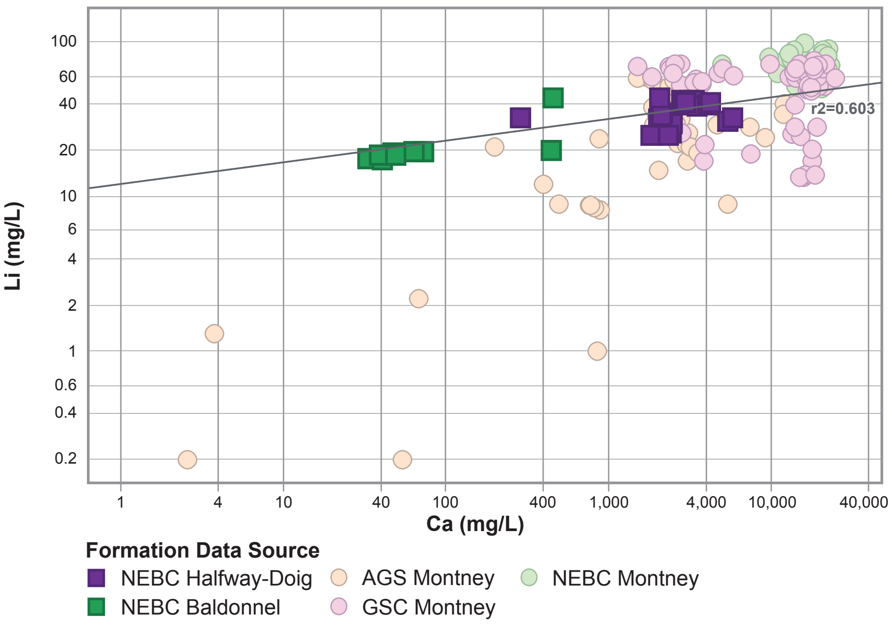

d. Li vs Mg

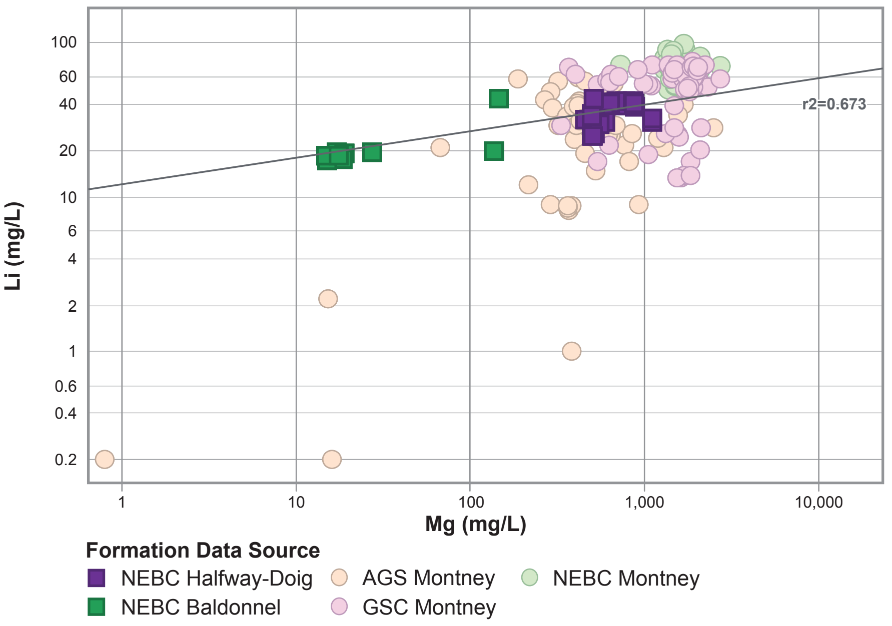

e. Li vs Br

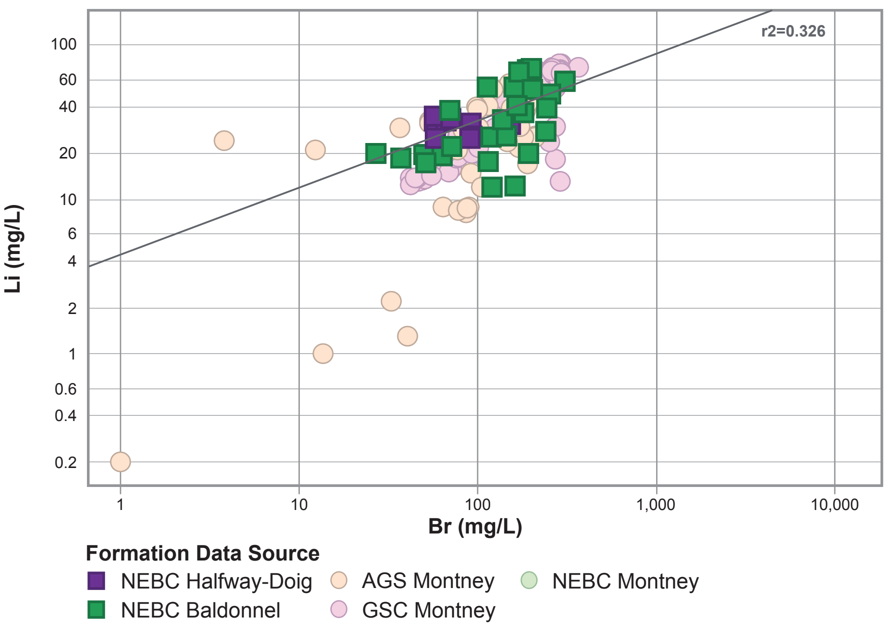

f. Li vs Sr

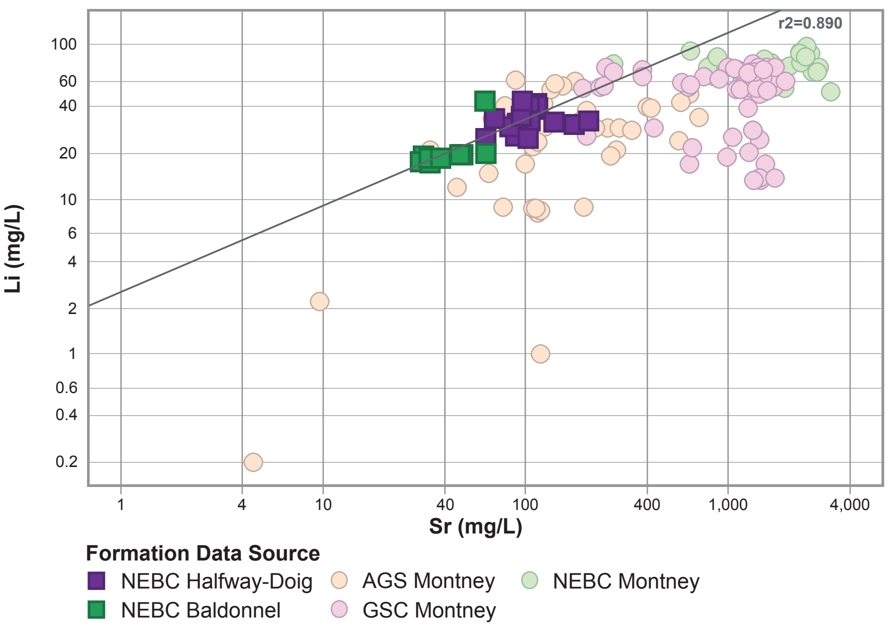

g. Li vs Cl

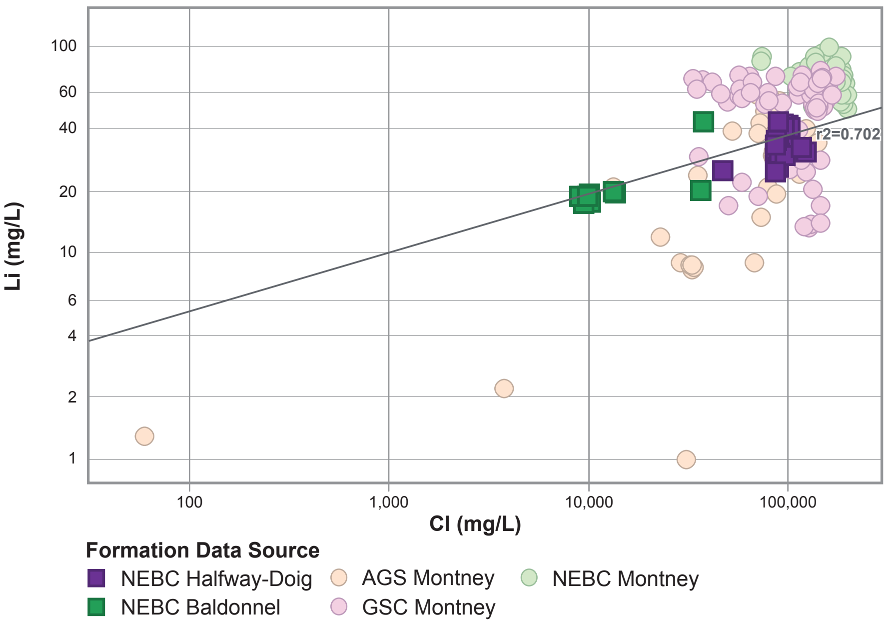

Lithium data from the current study

Figure 6.8

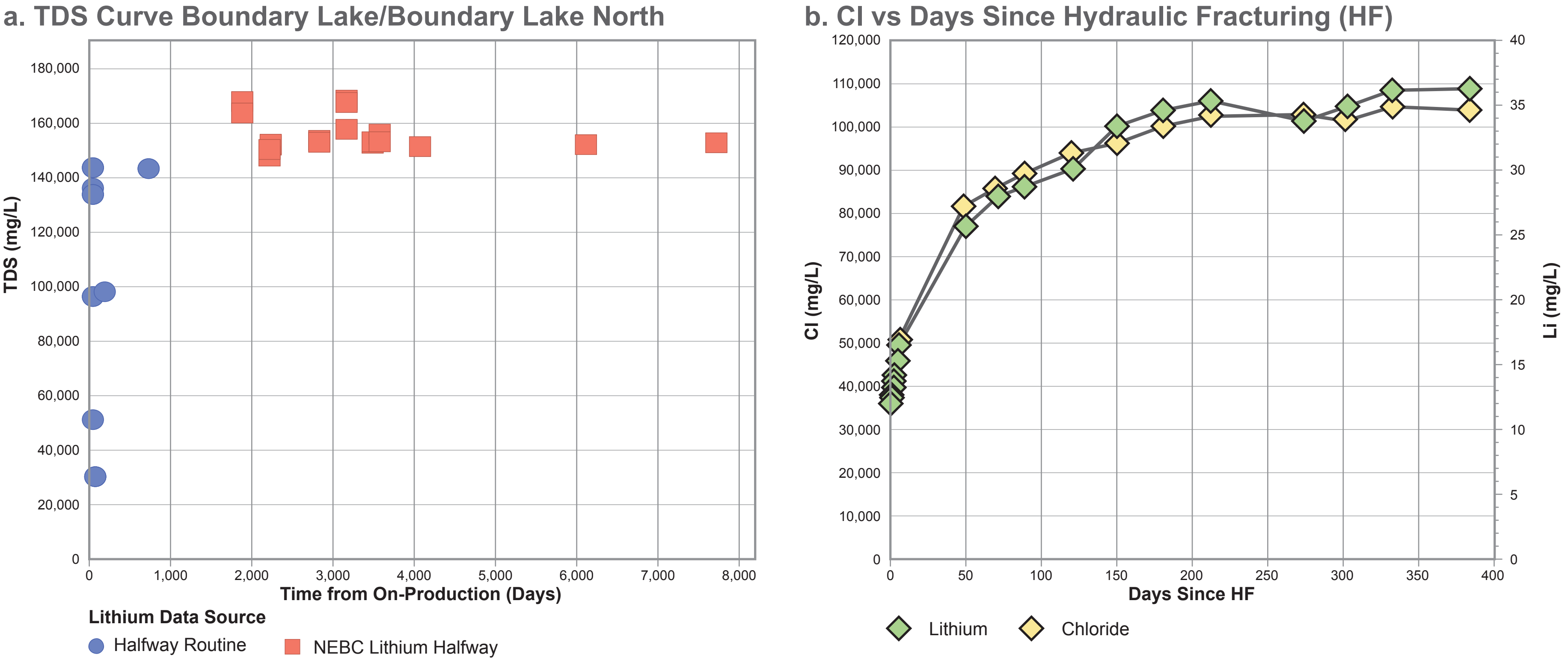

6.9 Triassic Aquifers TDS Curves

a. TDS Curve Boundary Lake/Boundary Lake North

b. Cl vs Days Since Hydraulic Fracturing (HF)

a. Data from geoLOGIC. b. Source Kingston et al., 2023

© Canadian Discovery Ltd.

Figure 6.9

formation-like brine (Kingston et al., 2023). *Figures 5.7a–e* in *Chapter 5 Montney* show that when plotting TDS values vs time on-production for wells with multiple samples, a late-time area on each curve where the TDS values plateau late-time area is apparent on each curve. A similar trend is seen in the Triassic aquifers; plotting TDS values vs time on-production for wells where there are multiple samples (Boundary Lake and Boundary Lake North), a late-time area on each curve where the TDS values plateau is apparent *(figure 6.9a)*. Data from the Alberta Montney *(figure 6.9b)* (Kingston et al., 2023) indicate a strong correlation between TDS and chloride with lithium, where 90% of a stabilized value is reached after about 100 days on-production. Due to this lag, sample timing can create a bias in both reported TDS and lithium concentrations.

Aquifer Reservoir Quality and TDS

Looking at hydrodynamics, the Halfway, Doig and Baldonnel are all conventional aquifers in NEBC where the water produced is formation water from the aquifer. The Montney is different hydrodynamically; it is a very fine-grained unconventional reservoir that must be hydraulically fractured to produce hydrocarbons, and also to co-produce lithium from the frac and formation water.

Halfway

Halfway aquifers are relatively continuous throughout the Peace River block and to the north. However, several areas can be differentiated by variations in reservoir quality. The Halfway net reservoir map that was made for the NEBC Geological Carbon Capture and Storage Atlas Net (CDL, 2022) shows that net reservoir, which is rock with porosity >6%, ranges up to 24m *(figure 6.10)*. *Figure 6.11* is a map of Halfway TDS from Rakhit Petroleum's 1995 Hydrogeological Atlas of the Western Canada Sedimentary Basin. Three areas (Fireweed/Cache Creek, Buick Creek, Monias/Septimus) stand out on the Halfway Net Reservoir map with TDS close to or exceeding 150 g/L, net reservoir exceeding 10m, and with Halfway production. A sample from this study at Fireweed that lies just outside the 150 g/L TDS contour has a lithium concentration of 32 mg/L, which correlates well to the 150 g/L TDS value. A fourth area at Oak has TDS exceeding 150 g/L and Halfway production, though the reservoir is thinner, in the 5 to 10 m range.

Baldonnel

Baldonnel TDS contours (PRCL, 2021) were overlain on the extent of the Baldonnel aquifers mapped for the NEBC Geological Carbon Capture and Storage Atlas to determine areas of high TDS, and by correlation, potentially high lithium concentrations *(figure 6.12)*. Baldonnel formation water hosts much lower TDS values than the Halfway or Montney; the maximum TDS values of 85 g/L are in the Boundary Lake area. While this is consistent with the location of the highest Baldonnel lithium concentrations sampled for this study (44 mg/L), the overall low TDS values suggest that the Baldonnel is unlikely to host economic concentrations of lithium.

Pore Space Challenges within Aquifers

At the time of this report there is no mechanism in BC, other than through the Geothermal Resources Act to acquire lithium tenure, either as a constituent of brine or through mining under the Mineral Tenure Act. A modification of these existing rights to allow development of brine-hosted minerals is currently under review (Donaldson, 2022).

The current regulations state that if host formation brine is at or above 80°C when produced to surface, the rights to lithium are included in geothermal resources under the Geothermal Resources Act, specifically in the Act as "all substances dissolved in the steam, water or water vapour obtained from a well". If formation brine is lower than 80°C when produced to surface, geothermal tenure cannot be acquired including any associated lithium in the brine.

Producing water from aquifers comes with a unique set of challenges compared to the Montney where the produced water is essentially a waste product that must be disposed or recycled. In aquifers, producing water in large enough

6.10 | Halfway-Doig Aquifer Net Reservoir Map

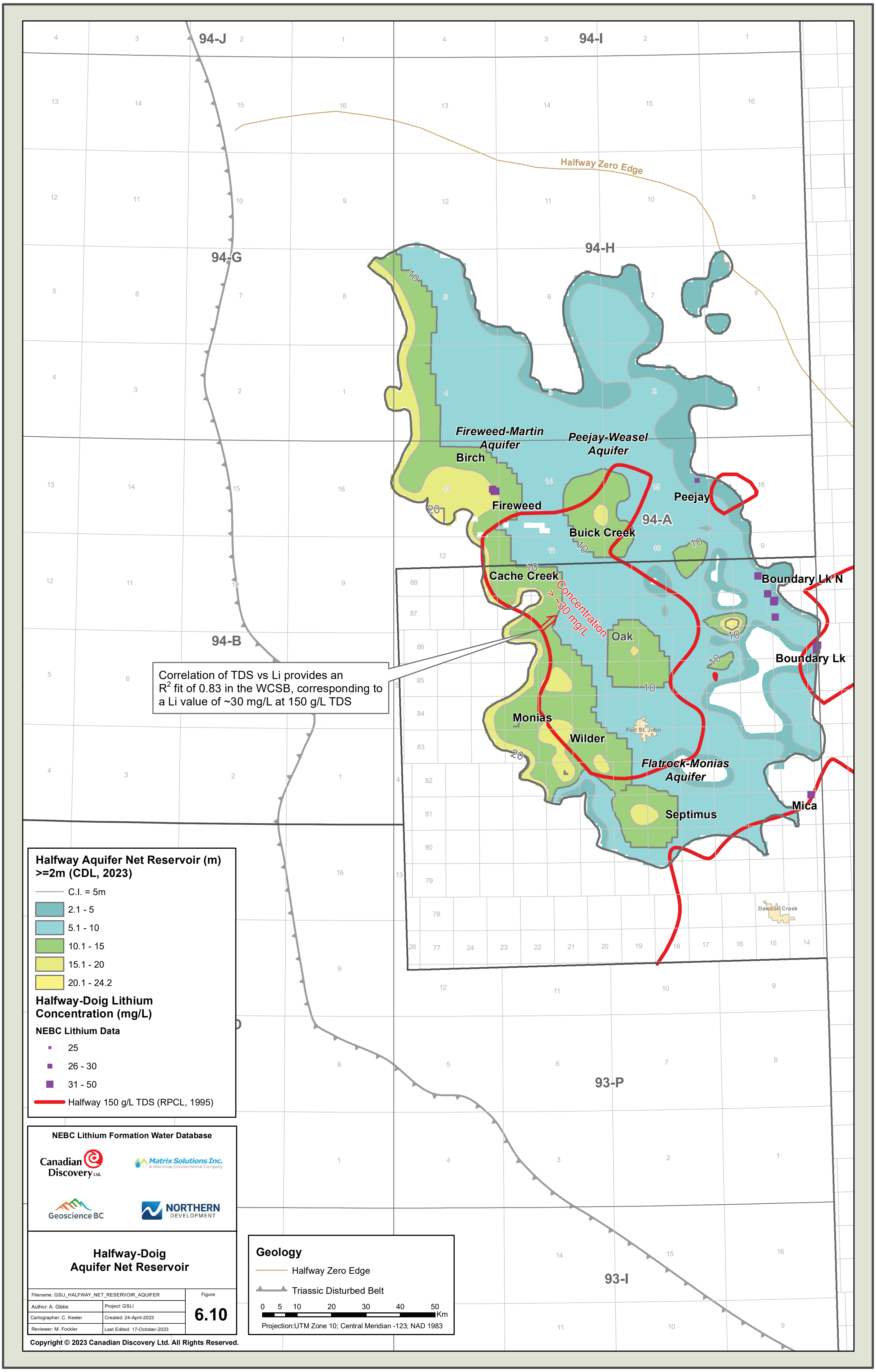

Correlation of TDS vs Li provides an R^2 fit of 0.83 in the WCSB, corresponding to a Li value of ~30 mg/L at 150 g/L TDS

© Canadian Discovery Ltd.

Figure 6.10

6.11 | Halfway-Doig Aquifer TDS Map

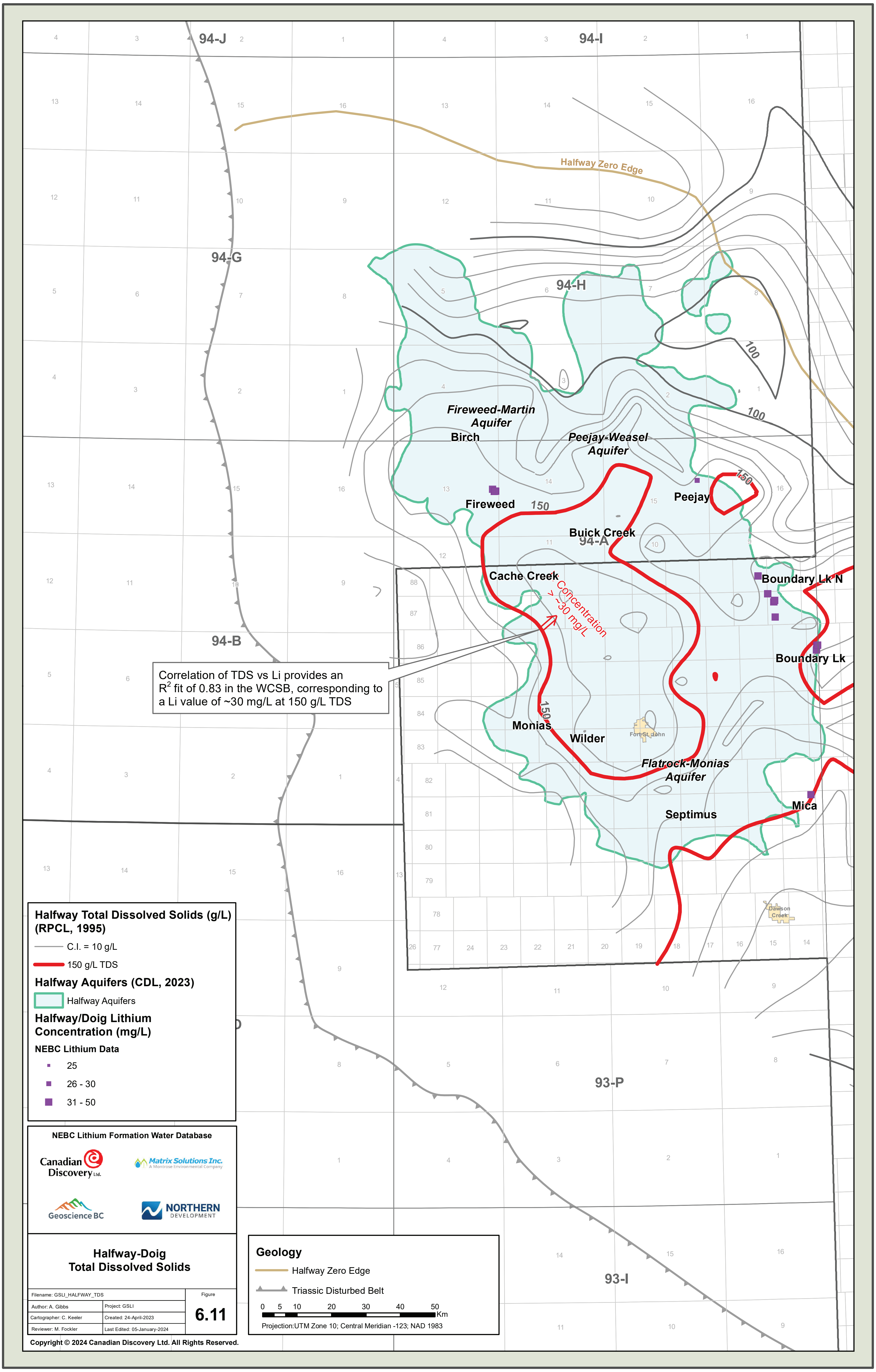

Correlation of TDS vs Li provides an R^2 fit of 0.83 in the WCSB, corresponding to a Li value of ~30 mg/L at 150 g/L TDS

© Canadian Discovery Ltd.

Figure 6.11

6.12 | Baldonnel TDS Map

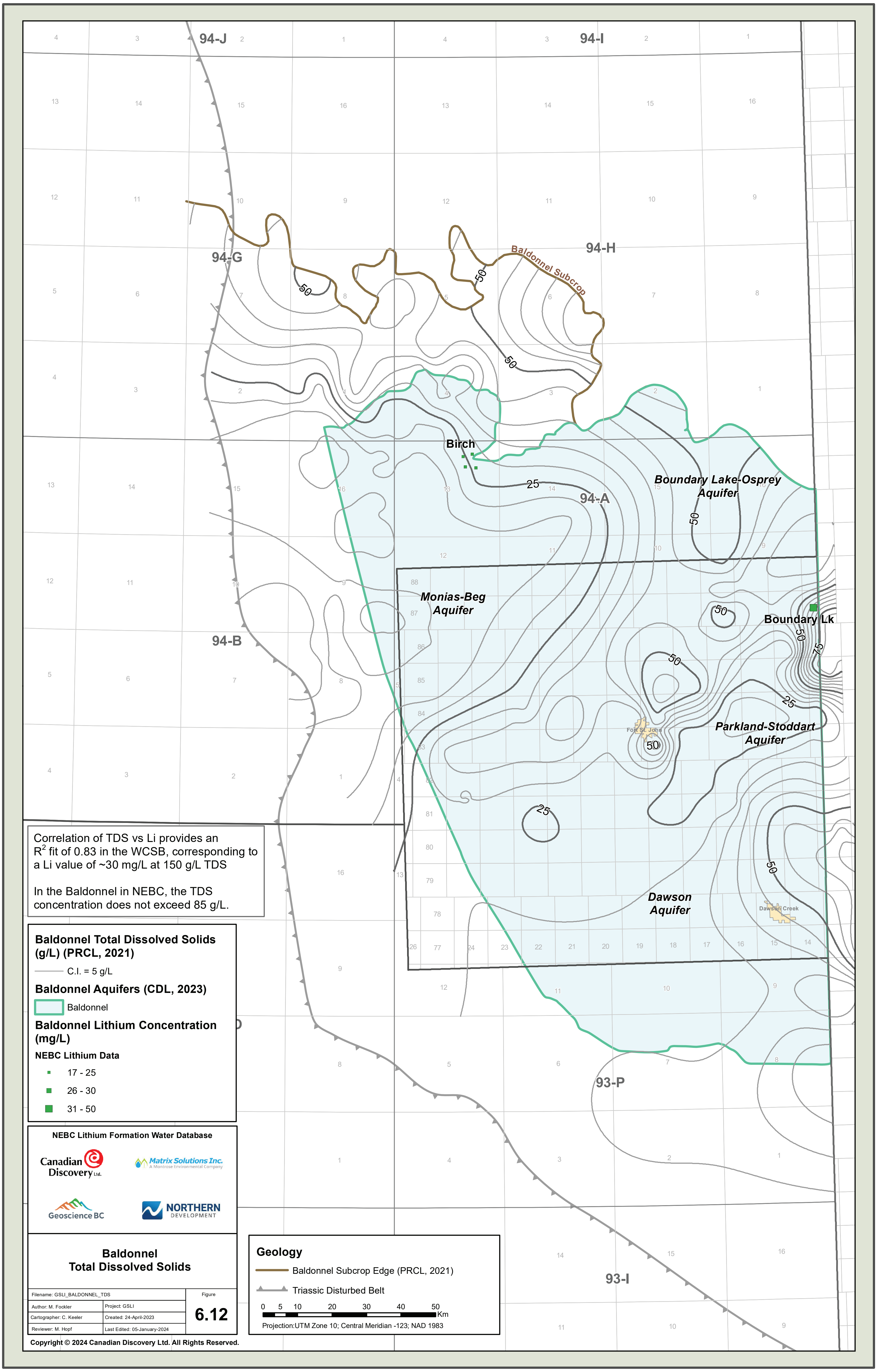

Correlation of TDS vs Li provides an R^2 fit of 0.83 in the WCSB, corresponding to a Li value of ~30 mg/L at 150 g/L TDS

In the Baldonnel in NEBC, the TDS concentration does not exceed 85 g/L.

Baldonnel
Total Dissolved Solids

Filename: GSLI_BALDONNEL_TDS		Figure
Author: M. Fockler	Project: GSLI	6.12
Cartographer: C. Keeler	Created: 24-April-2023	
Reviewer: M. Hopf	Last Edited: 05-January-2024	

© Canadian Discovery Ltd. *Figure 6.12*

volumes for an economic lithium extraction project is not a concern but pressure depletion and brine dilution in the reservoir become important factors. Other operations such as producing oil and gas pools and disposal water injection must also be considered when evaluating an area for lithium production and be included in the risk analysis.

There are several active Halfway, Doig and Baldonnel oil and gas pools near the areas of higher TDS concentrations, which could host economic concentrations of lithium. Producing brine and hydrocarbons separately from the same pool (i. e. two operators, one producing brine only and the other producing hydrocarbons along with associated water/brine) could exacerbate pressure depletion, which would reduce hydrocarbon production. In the case of brine-only production, the waste brine that remains after lithium extraction is not always pumped back into the producing reservoir, which would dilute the existing lithium concentration. Instead, the waste brine could be injected into a different formation. For the hydrocarbon producer, the additional pressure drawdown from the brine production from the aquifer could cause a significant decrease in production. The challenge for the regulator is to create regulations that determine who has tenure over the pore space with respect to hydrocarbon, lithium and geothermal production, or if tenure is shared.

Another area of concern for lithium brine extraction projects is injected fluids from the enhanced oil recovery (EOR) schemes that are in place in NEBC. Well spacing is a consideration, but a lithium producer must also consider the changes in the formation water chemistry that could occur as another operator injects fluids/gases into the reservoir. As well, the EOR scheme operator will have to consider the pressure impacts of having large volumes of fluid pumped out of a reservoir that already has a pressure depletion issue. If EOR and lithium operations do not have appropriate spacing, both producers will be negatively impacted.

Investigations need to be conducted on the drawdown radius associated with lithium-rich brine production and the production rates of brine to implement a buffer around producing oil and gas pools, a production cap on brine, or both. There is also the question of how regionally extensive these limits can be as reservoir quality can vary tremendously across the Halfway, Doig and Baldonnel fairways in NEBC.

Future Sampling Recommendations

None of the samples collected from the Triassic aquifers reached the current economic cutoff of 50 mg/L for lithium production. However, the correlation between TDS and lithium concentration suggests that there may be areas in the Halfway that could be prospective for lithium. The case is less compelling for the Baldonnel as the correlation between TDS and lithium suggests low lithium concentrations. Given the pace of technological advancements in extraction technologies, the Triassic aquifers (especially the Halfway) could have potential for brine-hosted lithium extraction in the future. With that in mind, further sampling is recommended in several areas.

For the Halfway-Doig, further sampling is recommended at Fireweed, Cache Creek, Buick Creek, Oak, Septimus, Wilder, and Monias. These are areas where TDS exceeds 150 g/L and/or net reservoir thickness mostly exceeds 15m *(figure 6.13)*.

While there are no specific areas recommended for further lithium sampling in the Baldonnel based on the low TDS values, continued sampling of all formations is recommended to increase the number of samples in the NEBC lithium database, to expand the geographical spread of lithium data, and to better understand lithium deposition and enrichment processes.

6.13 | Triassic Aquifers Lithium Summary Map

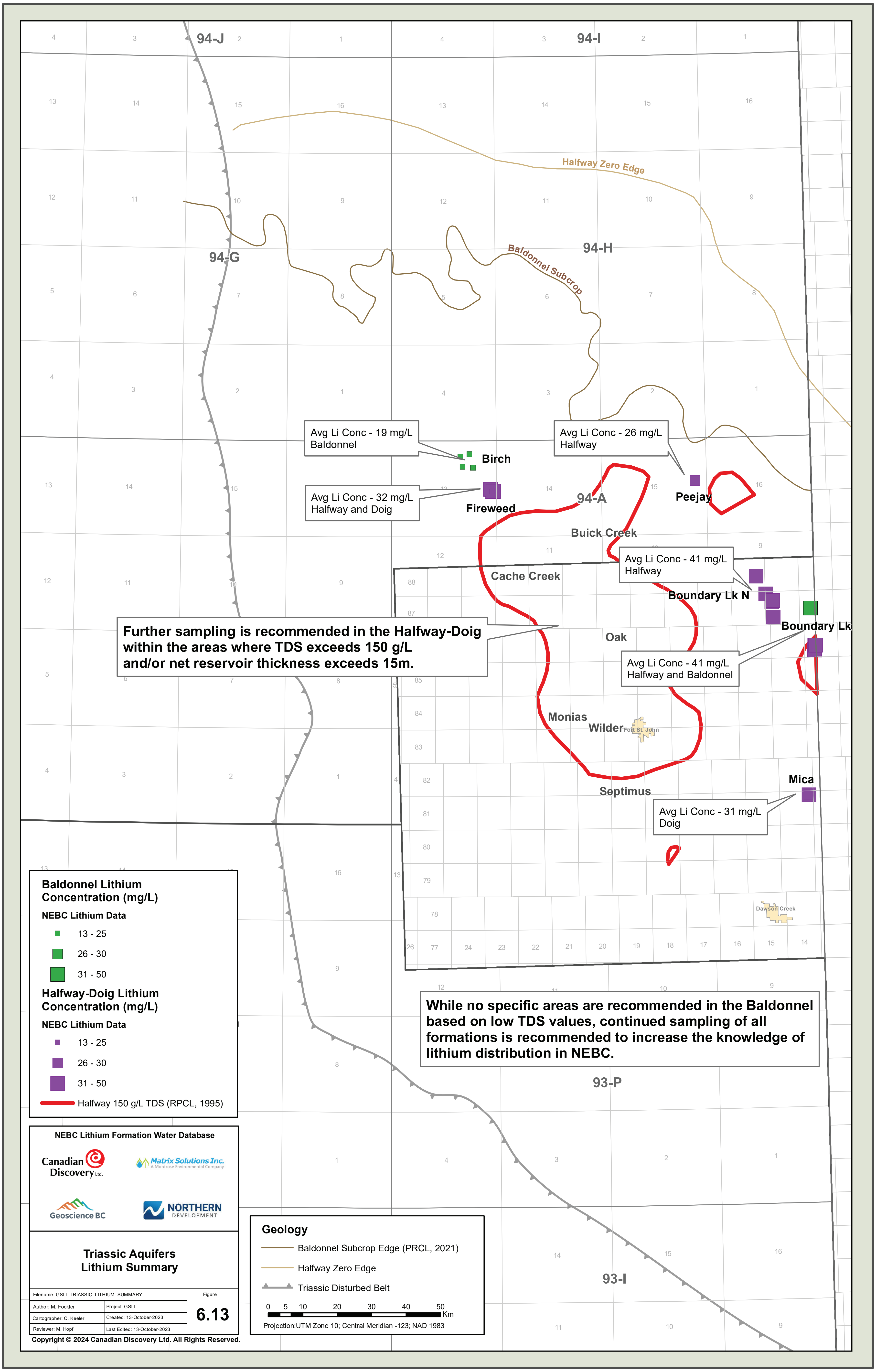

Figure 6.13

References

- Bachu, S. 1995. Synthesis and model of formation-water flow, Alberta Basin, Canada. American Association of Petroleum Geologists Bulletin, v. 79, p. 1159–1178.
- Bird, T.D., Barclay, J. E., Campbell, R. I., Lee, P. J., 1994. Triassic gas reservoirs of the Western Canada Sedimentary Basin Part-1: Geological Play analysis and resource assessment, Geological Survey of Canada, Bulletin 483, p. 96
- British Columbia Ministry of Energy, Mines and Petroleum Resources. Oil and Gas Division Resource Development and Geoscience Branch. Conventional Natural Gas Play Atlas, Northeast British Columbia. 2006. Petroleum Geology Publication 2006-01.
- Canadian Discovery Ltd. 2006. Strategy 2005: Geology and Metrics for 108 Plays (S2K5)
- Canadian Discovery Ltd. (CDL) and Geoscience BC, 2022. Northeast BC Geological Carbon Capture and Storage Atlas. https://www.geosciencebc.com/projects/2022-001/
- Davies, G.R. 1997. The Triassic of the Western Canada Sedimentary Basin: Tectonic and stratigraphic framework, paleogeography, paleoclimate and biota. Bulletin of Canadian Petroleum Geology, V. 45, P 434-460.
- Donaldson, W.S. Canadian Discovery. 2022. 2022 Western Canada Year in Review: Critical Minerals Development, 2023. https://digest.canadiandiscovery.com/pdf?query=[{%22name%22:%22excludeComingSoon%22,%22value%22:%22true%22}]&id=8627&url=/private/CDD/articles/2023_02_Feb14_2021_StrategicMinerals.pdf
- Eccles, D.R. and Berhane, H. 2011. Geological Introduction to Lithium-Rich Formation Water with Emphasis on the Fox Creek Area of West-Central Alberta (NTS 83F and 83K). ERCB/AGS Open File Report 2011-10.
- Ellis B. S., Szymanowski D., Magna T., Neukampf J., Dohmen R., Bachmann O., Ulmer P., Guillong M. 2018. Post-eruptive mobility of lithium in volcanic rocks, Nature Communications 9, Article Number: 3228 (2018).
- Kingston, A., Jiang, C., Wang, X. and Hobbs, T. 2023. Chemical compositions of flowback and produced water from the Duvernay shale and Montney tight reservoir developments in Western Canada: potential for lithium resources from wastewater, Geological Survey of Canada, Open File 8974.
- LithiumBank, 2023. LithiumBank Reports US$2.7 Billion Pre Tax NPV From Preliminary Economic Assessment on a 31,350 TPA LHM Operation at Boardwalk Lithium Brine Project, Alberta, Canada. https://www2.gov.bc.ca/assets/gov/farming-natural-resources-and-industry/natural-gas-oil/petroleum-geoscience/oil-gas-reports/og_report_2006-1_nebc_atlas_part1.pdf
- Petrel Robertson Ltd. (PRCL). 2021. Wastewater Disposal in the Maturing Montney Play Fairway of NEBC. Geoscience BC Report 2021-14: https://www.geosciencebc.com/projects/2019-004.
- Rakhit Petroleum Consulting Ltd. (RPCL), 1995. The Hydrogeological Atlas of the Western Canada Sedimentary Basin. HGAT.
- Standard Lithium, 2021. Standard Lithium Announces Positive Preliminary Economic Assessment and Update of Inferred Mineral Resource at South-West Arkansas Lithium Project. https://www.standardlithium.com/investors/news-events/press-releases/detail/99/standard-lithium-announces-positive-preliminary-economic
- Wust, R. A. J., Tu, S., Nassichuk, B., Bozart, T., Tucker, J., Cui, A., 2018. Chemostratigraphy, petrography, and SEM investigations of the Lower Triassic Montney Formation in Alberta: Implications for a new and revised diagenetic and depositional model. Bulletin of Canadian Petroleum Geology, V. 66, No 2, Pg. 436-471.

OTHER FORMATIONS

Other Formations Overview

At this time, it is generally accepted in industry and in the literature that lithium brine concentrations need to be above 50 mg/L to be considered economic (Standard Lithium, 2021; LithiumBank, 2023). In this study, the Devonian, Mississippian, Permian, low-lithium Triassic (that is, excluding the Montney and Triassic aquifers previously discussed in *chapters 5 and 6*) and Cretaceous formations are grouped together in this combined chapter because lithium concentrations from the samples obtained are well below the current economic threshold. These formations are shown on the stratigraphic chart on *figure 7.1*. Also, these samples are so limited in number that further sampling is needed across a broad geographical area to get a more realistic idea of the lithium potential in these formations throughout NEBC *(figure 7.2)*. *Table 7.1* provides average, median, minimum and maximum values of all analyzed major ions and trace elements in the program, including total dissolved solids (TDS).

7.1 Stratigraphic Chart

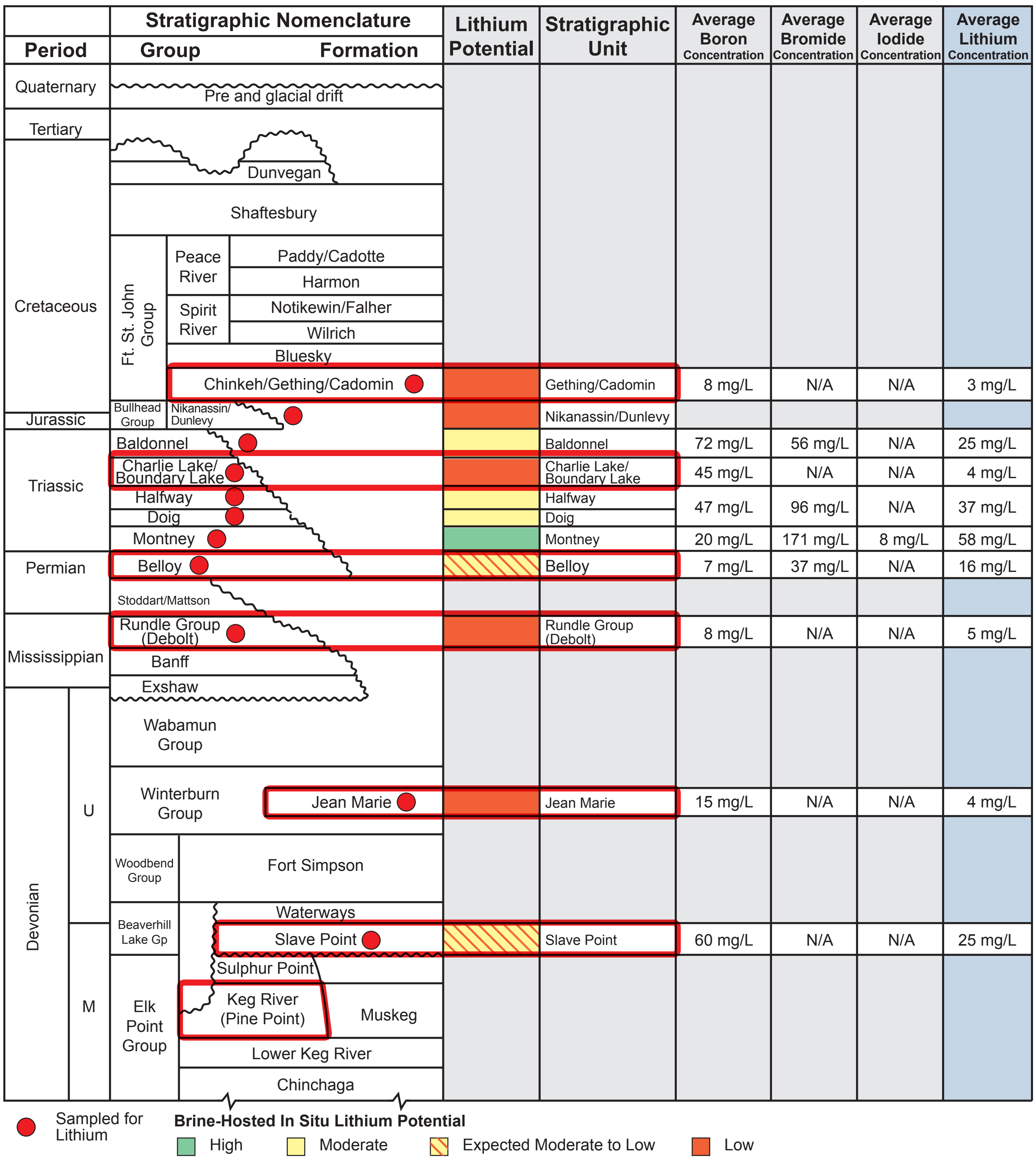

Lithium Potential	Stratigraphic Unit	Average Boron Concentration	Average Bromide Concentration	Average Iodide Concentration	Average Lithium Concentration
🟧	Gething/Cadomin	8 mg/L	N/A	N/A	3 mg/L
🟧	Nikanassin/Dunlevy				
🟨	Baldonnel	72 mg/L	56 mg/L	N/A	25 mg/L
🟧	Charlie Lake/ Boundary Lake	45 mg/L	N/A	N/A	4 mg/L
🟨	Halfway	47 mg/L	96 mg/L	N/A	37 mg/L
🟨	Doig				
🟩	Montney	20 mg/L	171 mg/L	8 mg/L	58 mg/L
▨	Belloy	7 mg/L	37 mg/L	N/A	16 mg/L
🟧	Rundle Group (Debolt)	8 mg/L	N/A	N/A	5 mg/L
🟧	Jean Marie	15 mg/L	N/A	N/A	4 mg/L
▨	Slave Point	60 mg/L	N/A	N/A	25 mg/L

● Sampled for Lithium

Brine-Hosted In Situ Lithium Potential
🟩 High 🟨 Moderate ▨ Expected Moderate to Low 🟧 Low

Modified from Bachu (1995) and this study

© Canadian Discovery Ltd. *Figure 7.1*

There are 46 samples in this group including duplicate tests; the maximum lithium concentration is 30 mg/L, the average is 7 mg/L, and the lowest concentration is 1 mg/L. It was noted during analysis that some of the sample TDS values did not align with regional mapped TDS values. The latter are obtained from CDL datasets that are a combination of public and proprietary data. Three samples that were taken from a produced water tank were not used in the analyses as they appear to be contaminated. There are several other data points with anomalously low TDS values compared to regional mapped values that were also removed from the analyses. These samples were taken from oil and gas fields that have been under waterflood since the 1960s. It is reasonable to assume that the injected water has diluted the formation waters and that these formations should be sampled away from water injection areas. As some formations have no lithium data at all due to sampling and testing issues, the economic lithium brine viability of the Boundary Lake and Charlie Lake formations cannot be ruled out.

The TDS to lithium concentration correlation developed in *the Overview chapter* suggests that the Permian Belloy and Middle Devonian Carbonates could have sufficient TDS values to host lithium concentrations above the economic threshold. A brief geological summary and a discussion of the aquifer reservoir quality are presented. An explanation of why no further analyses were done on the remaining formations is discussed.

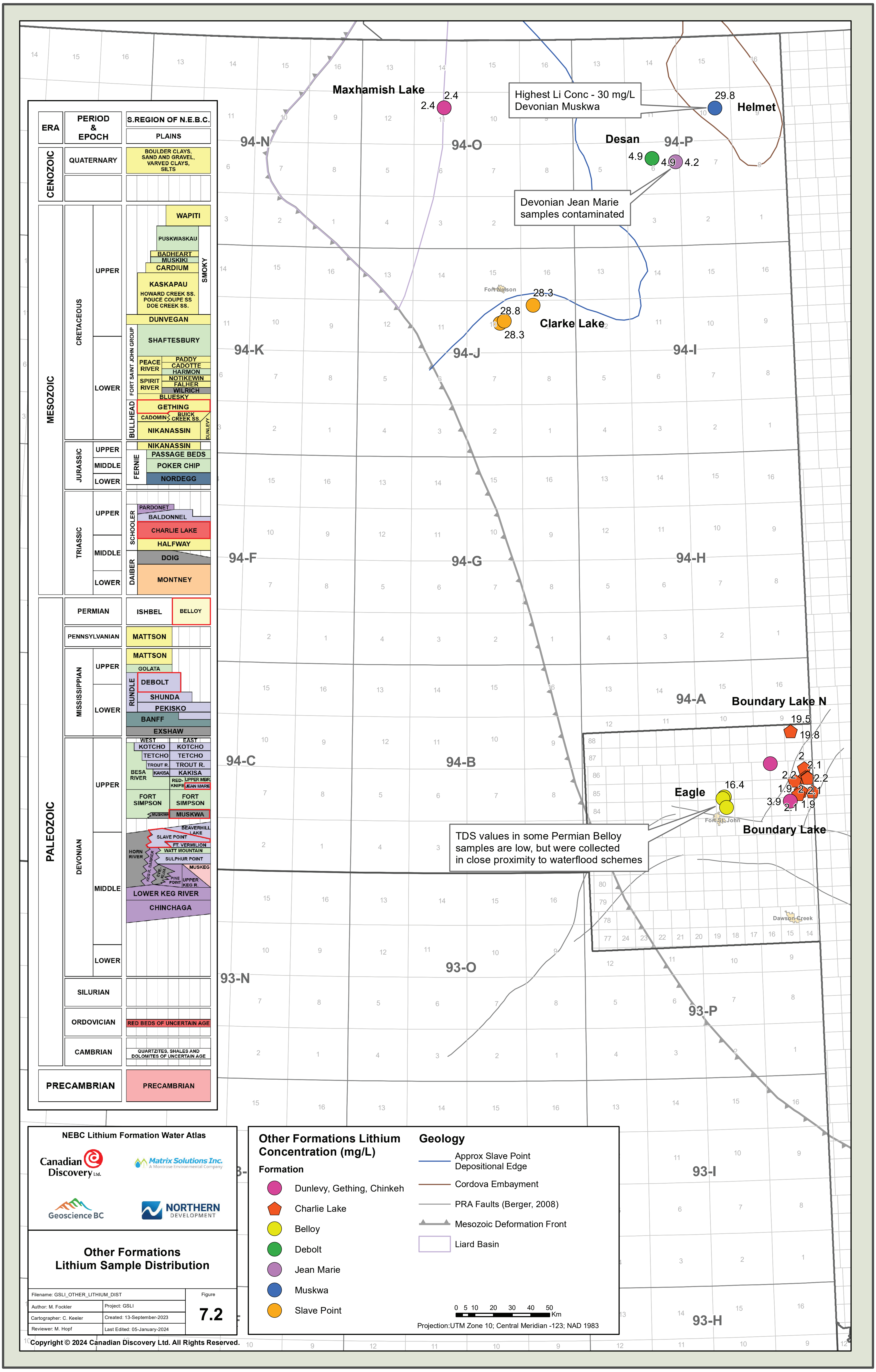

© Canadian Discovery Ltd.

Figure 7.2

Table 7.1: Statistics by Age for Analyzed Major Ions and Trace Elements

Major Ions and Trace Elements (Dissolved) (mg/L)	Montney				Triassic Aquifers				Triassic - Others			
	Average	Median	Min	Max	Average	Median	Min	Max	Average	Median	Min	Max
Potassium	2,227	2,205	125	3,910	1,074	1,026	230	1,960	804	910	521	980
Sodium	59,122	66,870	3,780	91,200	42,845	53,450	8,851	65,600	31,500	36,800	18,500	39,200
Calcium	15,508	16,430	841	23,320	2,182	2,420	33	5,800	2,127	2,267	1,520	2,595
Magnesium	1,550	1,495	182	2,850	511	534	15	1,100	413	409	400	430
Chloride	132,821	140,750	6,870	199,200	73,370	90,600	9,140	124,000	50,423	61,640	27,200	62,430
Aluminum	7	5	0.03	20	9	2	2	20	1	1	0.02	2
Antimony	3	1	0.01	10	2	0.50	0.50	5	0.17	0	0	0.50
Arsenic	6	2	0.01	30	5	1	1	10	1	1	1	1
Barium	245	10	0.05	1260	0.30	0.27	0.10	0.82	0.11	0.11	0.11	0.11
Beryllium	1	1	0	5	0.23	0.05	0.05	0.50	0.02	0	0	0.05
Boron	20	17	0.50	177	53	43	34	200	173	173	173	173
Bromide	171	169	17	306	82	65	27	152				
Cadmium	8	0.05	0	40	0.23	0.05	0.05	0.50	0.02	0	0	0.05
Chromium	0.40	0.50	0.01	1	0.24	0.05	0.05	0.50	0.02	0.01	0.01	0.05
Cobalt	0.59	1	0.01	1	0.46	0.10	0.10	1	0.04	0	0	0.10
Copper	0.56	1	0.01	1	0.46	0.10	0.10	1	0.04	0	0	0.10
Iodide	8	8	0	18								
Lead	8	2	0.01	20	9	2	2	20	1	1	0	2
Lithium	58	65	2	100	33	34	17	44	20	20	20	20
Molybdenum	0.66	1	0	1	0.46	0.10	0.10	1	0.03	0	0	0.10
Nickel	0.88	0.20	0.01	2	0.92	0.20	0.20	2	0.07	0	0	0.20
TDS (Calculated)	**211,607**	**228,119**	**14,128**	**309,457**	**122,516**	**151,861**	**21,774**	**196,029**	**88,070**	**105,374**	**51,412**	**107,425**

Major Ions and Trace Elements (Dissolved) (mg/L)	Cretaceous				Permian				Devonian-Mississippian			
	Average	Median	Min	Max	Average	Median	Min	Max	Average	Median	Min	Max
Potassium	104	102	67	175	598	467	162	1,490	379	119	31	1,105
Sodium	8,566	10,500	3,700	13,900	21,166	16,900	5,330	50,800	13,558	9,377	6,150	35,250
Calcium	523	173	29	1,280	1,580	1,330	436	3,810	2,185	1,658	129	8,390
Magnesium	114	74	24	230	301	253	88	708	308	209	159	867
Chloride	12,442	17,860	2,760	20,800	39,820	30,900	10,700	103,000	23,648	14,440	12,000	64,000
Aluminum	2	2	2	2	2	2	2	2	2	2	0.10	2
Antimony	0.50	0.50	0.50	0.50	0.50	0.50	0.50	0.50	0.36	0.50	0	0.50
Arsenic	1	1	1	1	1	1	1	1	0.87	1	0.01	1.49
Barium	49	5	1	119	6	6	0.07	11	590	392	1.07	1890
Beryllium	0.05	0.05	0.05	0.05	0.05	0.05	0.05	0.05	0.04	0.05	0	0.05
Boron	8	8	4	11	6	6	6	6	25	8	5	61
Bromide	65	65	65	65	37	35	0	73				
Cadmium	0.05	0.05	0.05	0.05	0.05	0.05	0.05	0.05	0.04	0.05	0	0.05
Chromium	0.05	0.05	0.05	0.05	0.05	0.05	0.05	0.05	0.05	0.05	0.01	0.09
Cobalt	0.10	0.10	0.10	0.10	0.10	0.10	0.10	0.10	0.07	0.10	0	0.10
Copper	0.10	0.10	0.10	0.10	0.10	0.10	0.10	0.10	0.11	0.10	0.01	0.33
Iodide												
Lead	2	2	2	2	2	2	2	2	1	2	0	2
Lithium	3	3	2	4	16	16	16	16	16	5	4	30
Molybdenum	0.10	0.10	0.10	0.10	0.10	0.10	0.10	0.10	0.08	0.10	0	0.10
Nickel	0.20	0.20	0.20	0.20	0.20	0.20	0.20	0.20	0.15	0.20	0.01	0.20
TDS (Calculated)	**23,641**	**31,190**	**9,297**	**36,773**	**63,658**	**50,181**	**16,865**	**159,975**	**41,117**	**27,098**	**20,344**	**107,775**

Table 7.1

7.3 Other Formations Lithium Concentrations by Formation

a. Lithium Concentration by Age

b. Lithium Concentration by Age (Detail)

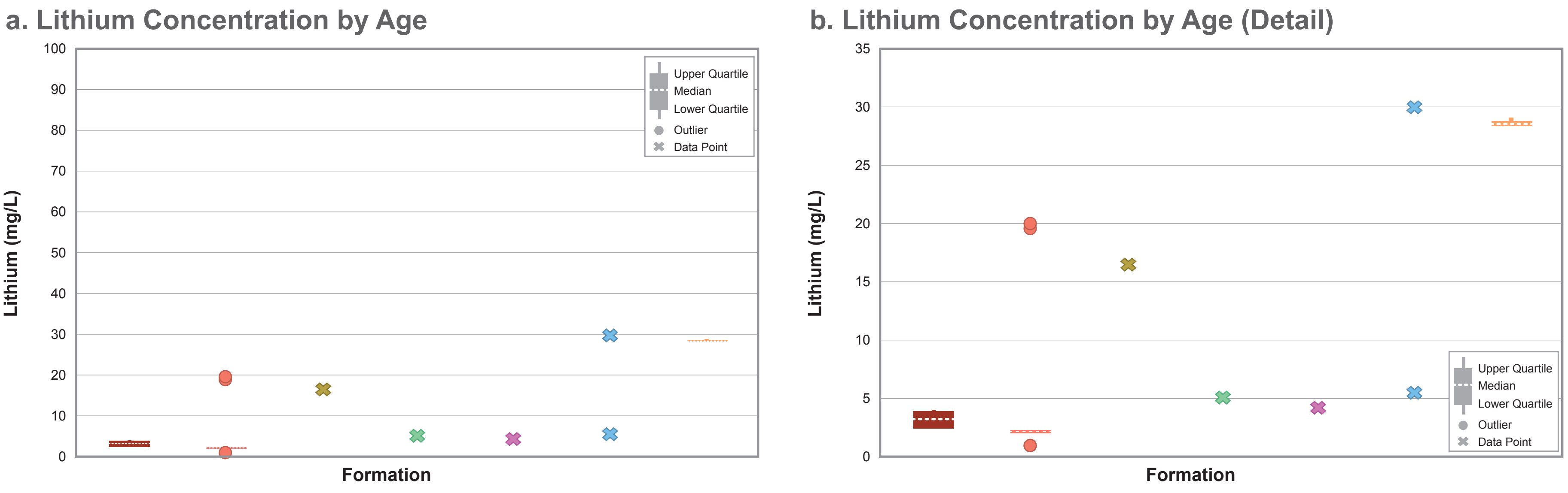

	Gething Chinkeh	Charlie Lake	Belloy	Debolt	Jean Marie	Muskwa	Slave Point
Count	4	17	1	2	1	2	3
Average	3	4	16	5	4	18	28
Median	3	2	-	-	-	-	28
Min	2	1	16	5	4	5	28
Max	4	20	16	5	4	30	29

	Gething Chinkeh	Charlie Lake	Belloy	Debolt	Jean Marie	Muskwa	Slave Point
Count	4	17	1	2	1	2	3
Average	3	4	16	5	4	18	28
Median	3	2	-	-	-	-	28
Min	2	1	16	5	4	5	28
Max	4	20	16	5	4	30	29

c. Lithium Concentration vs TDS

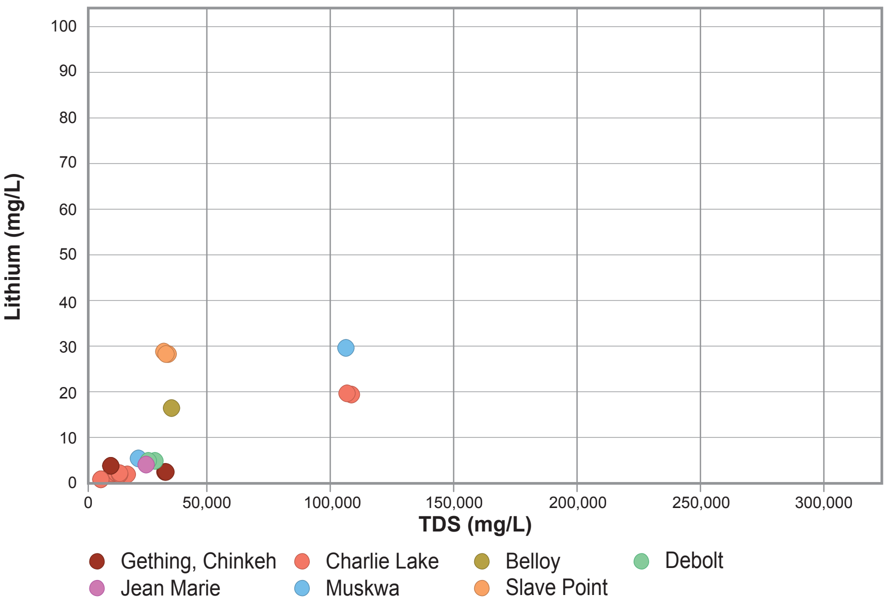

Lithium data sources from the current study

© Canadian Discovery Ltd.

Figure 7.3

Lithium Data Distribution

Cretaceous Chinkeh and Devonian Muskwa samples were collected from the Helmet Field close to the Northwest Territories border *(figure 7.2)*. Cretaceous Gething and Triassic Charlie Lake samples were collected from the Boundary Lake North and Boundary Lake fields. Permian Belloy samples were collected from the Eagle Field on the Peace River Arch. *Figures 7.3a and b* shows the range of sampled concentrations by formation with lithium concentrations ranging from 1 to 30 mg/L. The highest lithium values were tested in the Muskwa, where both samples came from the same well and had values of 30 mg/L. The lowest concentration, 1 mg/L, was recorded from the Charlie Lake at Boundary Lake. The crossplot of lithium concentration vs TDS values *(figure 7.3c)* is consistent with the correlation between TDS and lithium concentration in the *Montney chapter* where in general, higher lithium concentrations correspond to higher TDS values. For the *Other Formations*, TDS and lithium concentration values are relatively low suggesting that formation waters are generally fresher than those seen in the Montney.

Sample Collection and Testing Issues

Certain samples from the Triassic Boundary Lake and Charlie Lake, Permian Belloy and Devonian Jean Marie and Muskwa samples collected have abnormally low TDS values compared to regional mapped TDS values. Some of these samples were taken from wells in close proximity to areas under waterflood. It is assumed that formation water has been diluted with injection water; the values, therefore, do not reflect true formation water and were not used in this study.

The Cases for Lithium Economic Viability

The following sections discuss the *Other Formations* sampled and provide a brief geological summary for context and a brief assessment of the TDS and aquifer quality.

TDS as a Proxy for Lithium Concentration

As there is a limited number of samples in the various formations, and the geographical extent of those samples is limited, the TDS to lithium concentration correlation developed in the Montney chapter was used to high-grade or low-grade formations. The correlation established that a TDS value of 150,000 mg/L (150 g/L) suggests a lithium concentration of about 30 mg/L. The 150,000 mg/L contour from regional TDS mapping is used to approximate where lithium concentrations could be economically viable in the future. While the current industry established threshold is generally accepted at 50 mg/L, it is anticipated that technologies in this emerging industry will progress and this threshold will be reduced in the foreseeable future.

7.4 Belloy Schematic Cross-Section

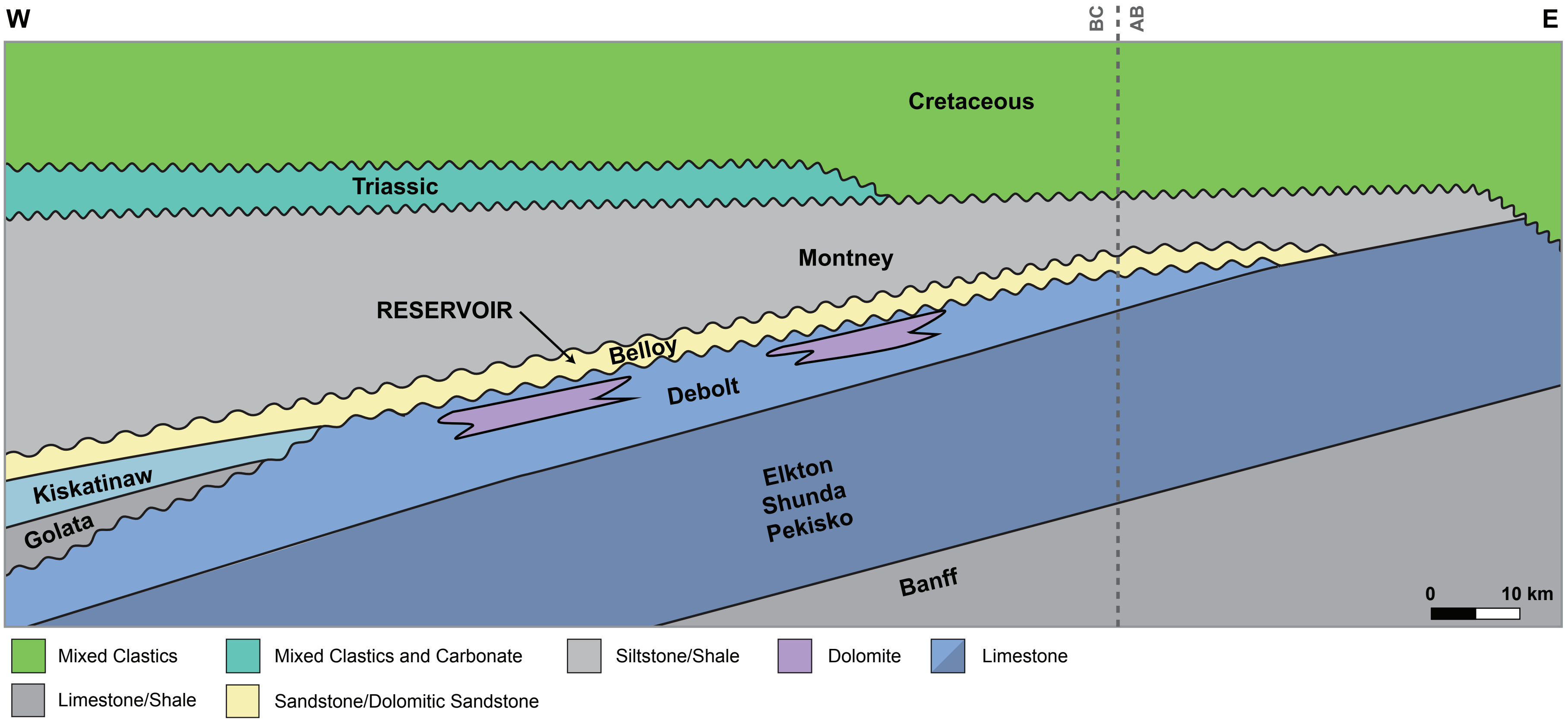

Modified from CDL, 2023

Figure 7.4

Possibly Economic

Permian Belloy

The Permian Belloy Formation is an excellent reservoir and a proven aquifer as it is the target of many oilfield disposal wells. The Belloy is best developed in the Peace River Embayment/Fort St. John Graben. It comprises several stacked regressive (sea level fall) sequences, grading from siltstones and fossiliferous carbonates typical of outer shelf to distal carbonate platform settings in the west, eastward to shoreface and tidal to fluvial (river) channel sandstones and dolostones *(figure 7.4)*. Reservoir quality is best developed on the embayment margins, where the section consists primarily of cleaner, better-sorted sandstones.

The Belloy may have the capacity to host economic amounts of in situ lithium. A band of 150+ g/L TDS is mapped in the eastern part of the Peace River block where the net reservoir is up to 40m thick (RPCL, 1995, CDL., 2022) *(figure 7.5)*. As the Belloy is known to be an excellent aquifer, water production should not be a problem. Further sampling should be undertaken in the most saline part of the formation, where the best reservoir quality exists, and in areas not affected by waterflooding.

Furthermore, the Lower Montney directly overlies the Belloy over much of the study area. The Lower Montney appears to have higher volumes of illite than the rest of the Montney. It is possible that the some of the lithium liberated into formation waters when smectite converted to illite could have migrated to the Belloy. More sampling of the Lower Montney has been recommended in the Montney chapter. Operators should consider sampling the Belloy as well.

7.5 | Belloy TDS and Net Reservoir Map

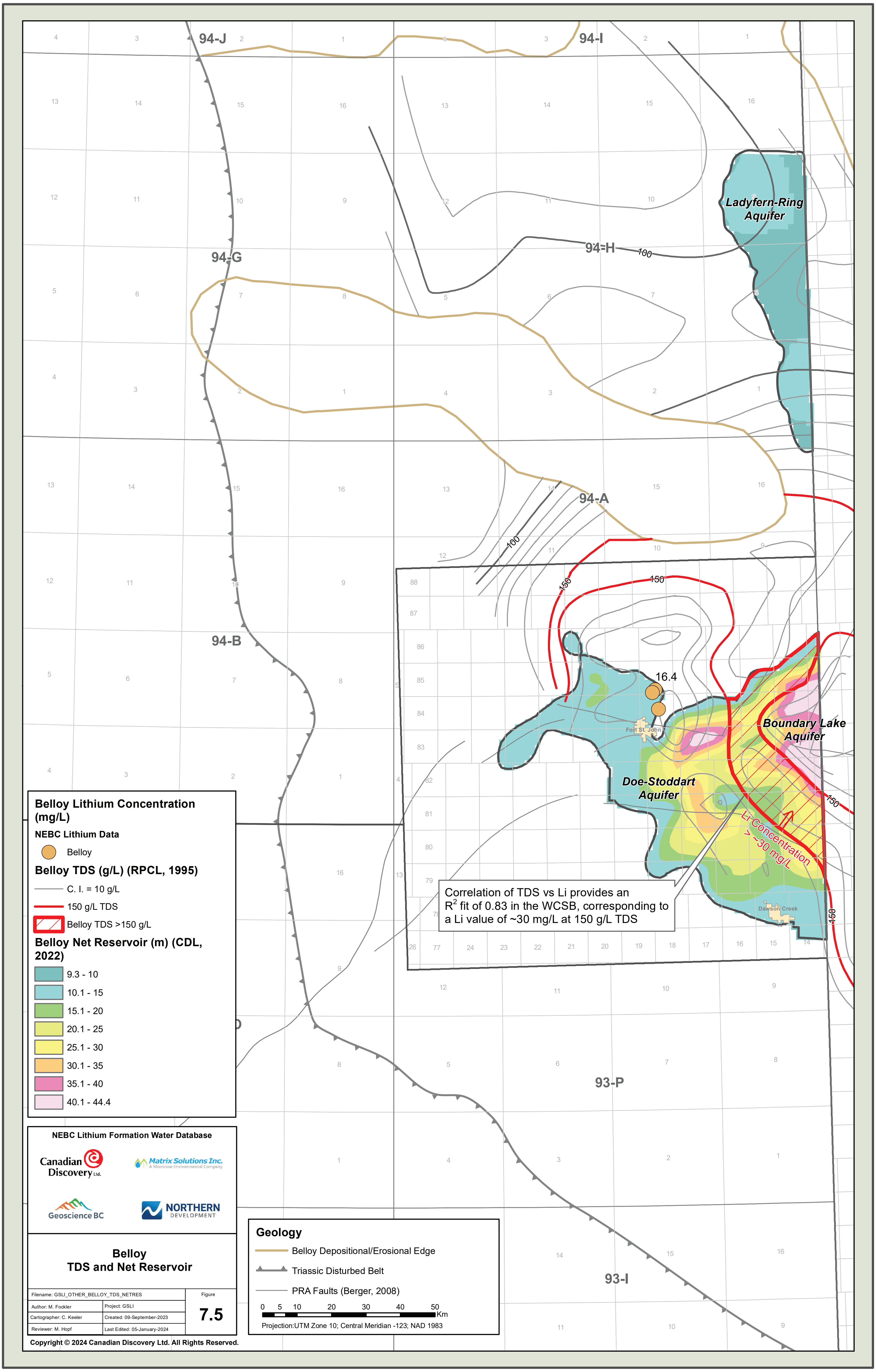

© Canadian Discovery Ltd.

Figure 7.5

7.6 Middle Devonian Carbonates Schematic Cross-Section

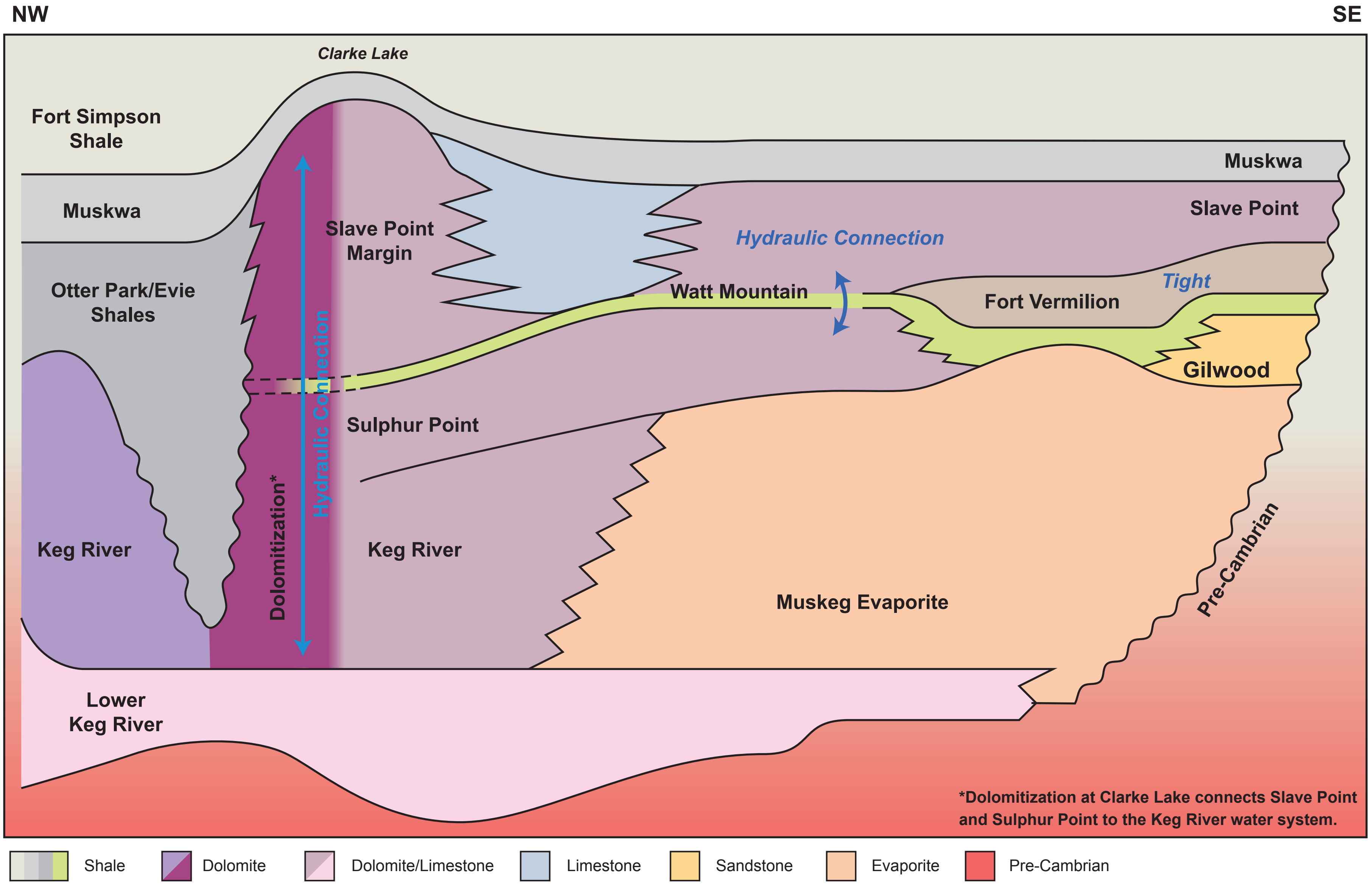

Source: Canadian Discovery, 2023

© Canadian Discovery Ltd.

Figure 7.6

Middle Devonian Carbonates

The Middle Devonian Slave Point and Keg River formations can also be excellent aquifers. They are two of the three successions that comprise the Middle Devonian carbonate complex in northern-most NEBC, namely the Slave Point, Sulphur Point and Keg River *(figure 7.6)*. The Slave Point was deposited in the early stages of a basin-wide transgression (sea level rise), which ultimately drowned the Middle Devonian carbonate platforms of NEBC and Alberta (NEBC Play Atlas, 2006). Slave Point strata form a thick and complex carbonate platform, comprising several stacked shallowing-upward cycles. Slave Point gas reservoirs are hosted within dolomitized reefal buildups, which grew on platform- and embayment-margin banks and have good reservoir characteristics.

In terms of the correlation between TDS and lithium concentration, the Slave Point and Keg River may have the capacity to host lithium concentrations considered to be economically viable in the future. In the Slave Point, there is an area where TDS ranges from 150 to 160+ g/L in the northeastern-most reaches of the study area, and net reservoir ranges up to 140m thick along the shelf edge *(figure 7.7)* (RPCL, 1995, CDL, 2022). As this area has an active aquifer, water production should not be an issue as long as porosity and permeability are developed. Further sampling should be undertaken in the most saline part of the formation, and where the best reservoir quality exists.

The Keg River may also host near economic concentrations of lithium as TDS exceeds 150 g/L in the southern part of the South Aquifer and over much of the same area as the Slave Point farther north *(figure 7.8)*.

Less Likely to be Economic

Cretaceous Dunlevy, Gething and Chinkeh

Regional TDS mapping shows the formation waters are relatively fresh over the study for the Gething, Dunlevy and Chinkeh formations (RPCL, 1995). The low lithium concentrations tested in the wells sampled for this study are consistent with low regional mapped TDS values and suggest a low in situ lithium potential for these formations. It is possible that there are areas where there could be an aeolian-derived volcanic felsic component in the Cretaceous sediments that was blown in from volcanism associated with the subduction of the Pacific plate beneath the North American plate (the Laramide orogeny) to the west. Cretaceous sampling is so sparse that lithium potential from a felsic volcanic component cannot be excluded.

Triassic Charlie Lake

Triassic Charlie Lake sampling is so sparse and geographically limited that lithium potential cannot be excluded. All the Charlie Lake samples were collected along the northeastern edge of the Peace River block, and are well under 50 mg/L of lithium. As there is no regional TDS mapping for the Charlie Lake, the correlation between TDS and lithium concentration cannot be used. Furthermore, the Charlie Lake was deposited in widespread, low-relief depositional environments in an arid climate, and therefore, reservoir units tend to be thin and discontinuous, which is not conducive to massive water production.

7.7 | Slave Point TDS and Net Reservoir Map

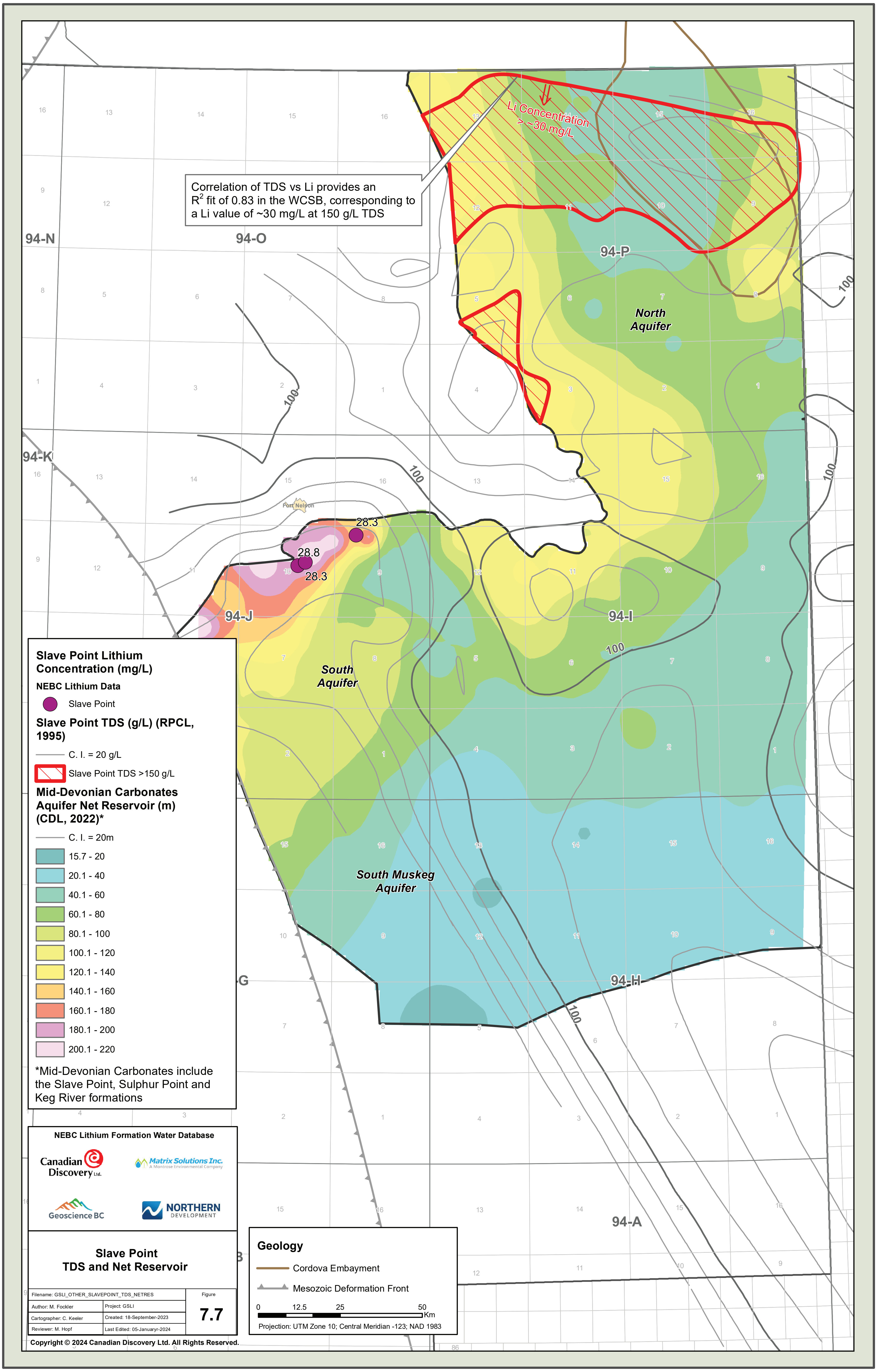

Correlation of TDS vs Li provides an R^2 fit of 0.83 in the WCSB, corresponding to a Li value of ~30 mg/L at 150 g/L TDS

© Canadian Discovery Ltd.

Figure 7.7

7.8 | Keg River TDS and Net Reservoir Map

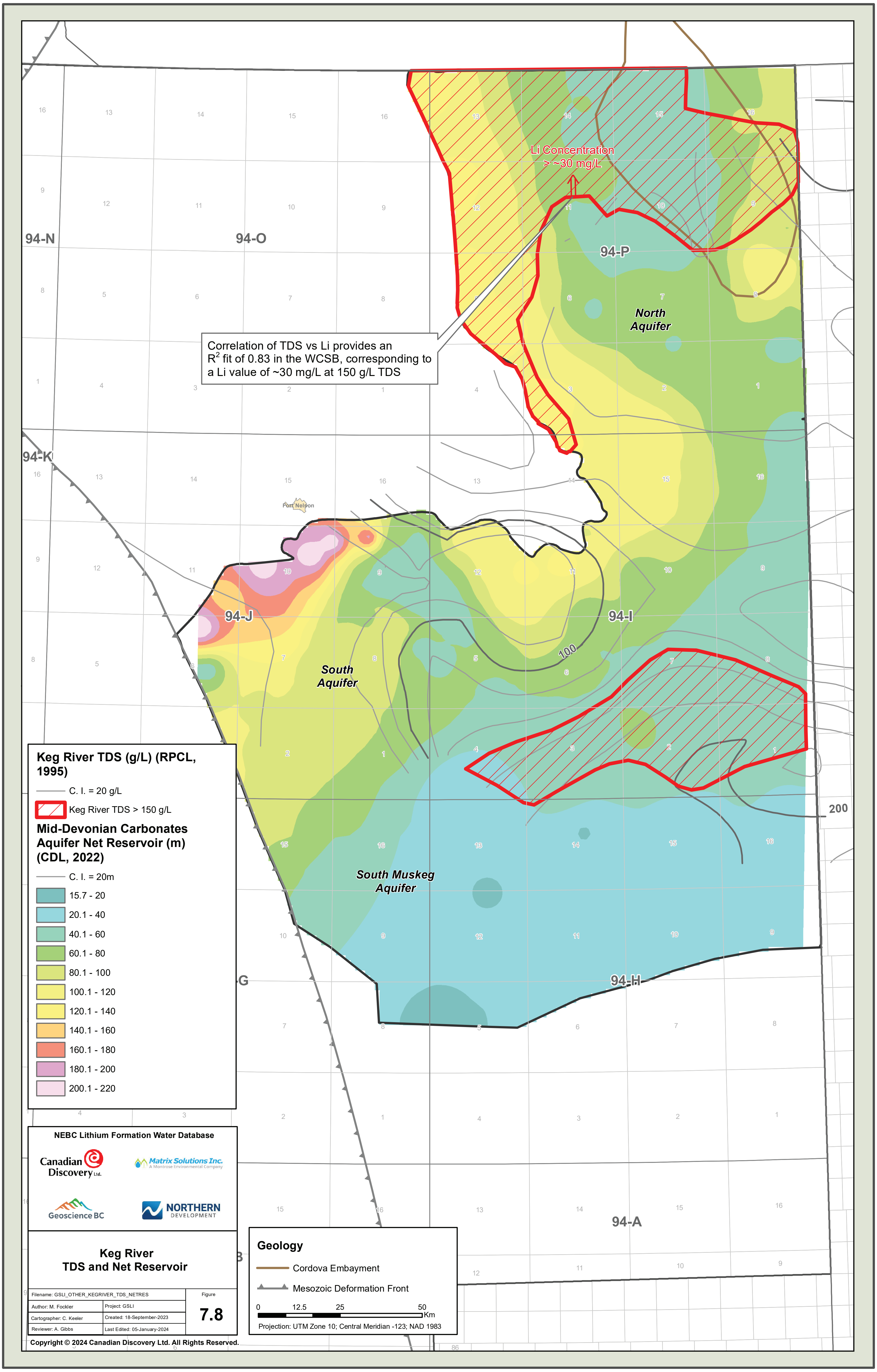

Figure 7.8

7.9 Other Formations Water Chemistry Crossplots

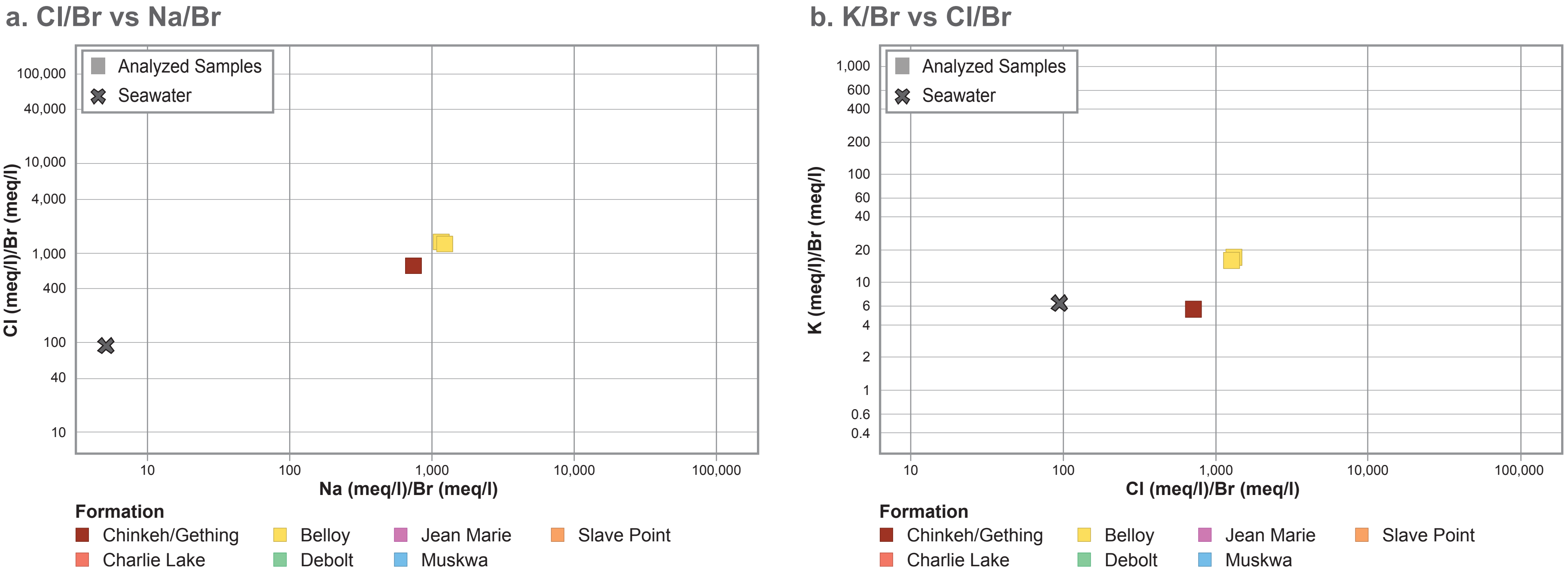
a. Cl/Br vs Na/Br

b. K/Br vs Cl/Br

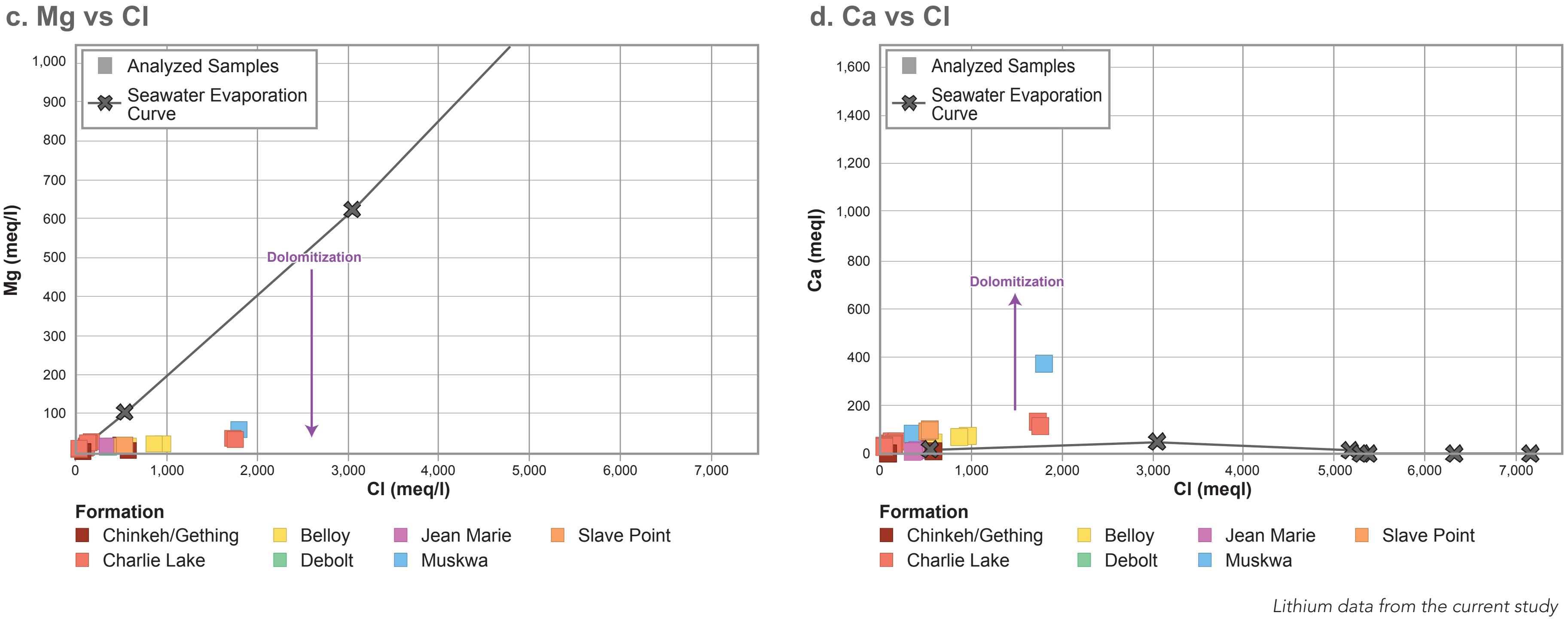
c. Mg vs Cl

d. Ca vs Cl

Lithium data from the current study

Figure 7.9

Mississippian Debolt

The Mississippian Debolt Formation is a well-known aquifer throughout NEBC. Regional TDS values are well below the 150 g/L threshold used in this study to indicate possible economic lithium viability. North of the Peace River block in 94-A, maximum TDS values of 120 g/L are mapped. At Desan in northern NEBC where the two Mississippian samples were taken, formation waters are even fresher with a mapped TDS value of about 20 g/L (RPCL, 1995). The low regional mapped TDS values do not bode well for economic concentrations of lithium in the Debolt.

Devonian Jean Marie

The Jean Marie has several points against it being economically viable for lithium. It is both underpressured and under-saturated with respect to water. Water flow rates are expected to be low. At Desan in northern NEBC, where the one contaminated Jean Marie sample was taken, formation waters are fresh with a mapped TDS value of about 20 g/L (RPCL, 1995).

Water Chemistry Trends

To be consistent with the previous chapters, the water chemistry graphs are presented for the other formations data in *figures 7.9 and 7.10*. As with the Montney and the Triassic aquifers, statistical analyses were run on several ions to see if there is any correlation to lithium. Chloride (Cl) and bromide (Br) are used to normalize data, as they tend to be conservative ions that remain in solution once dissolved and are not easily removed from the system by water-rock interactions. The general takeaway from these graphs is that lithium concentrations, along with the concentrations of other ions and ratios, are very low compared to the Montney.

Future Sampling Recommendations

Based on the TDS correlation with respect to lithium and previous net reservoir mapping, the Belloy and Middle Devonian Carbonates, specifically the Slave Point and Keg River, may have lithium potential and should be sampled in the most saline part of the formations, and where the best reservoir quality exists *(figure 7.11)*. Sampling in the Belloy should avoid any areas affected by waterflooding.

Total dissolved solids are low in all Cretaceous formations, and no specific areas are recommended for future sampling. However, Cretaceous sampling is so sparse that lithium potential from a felsic volcanic component in the sediments cannot be excluded.

Sampling all formations is recommended to increase not only the number of samples in the NEBC lithium database, but also the geographical spread of the data.

7.10 Other Formations Water Chemistry Lithium Crossplots

a. Li vs K

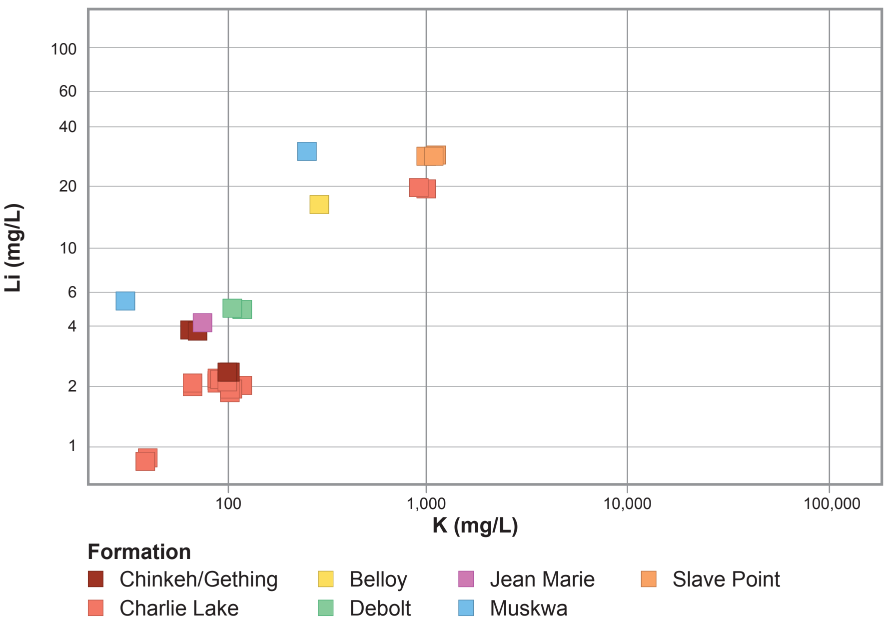

b. Li vs SO$_4$

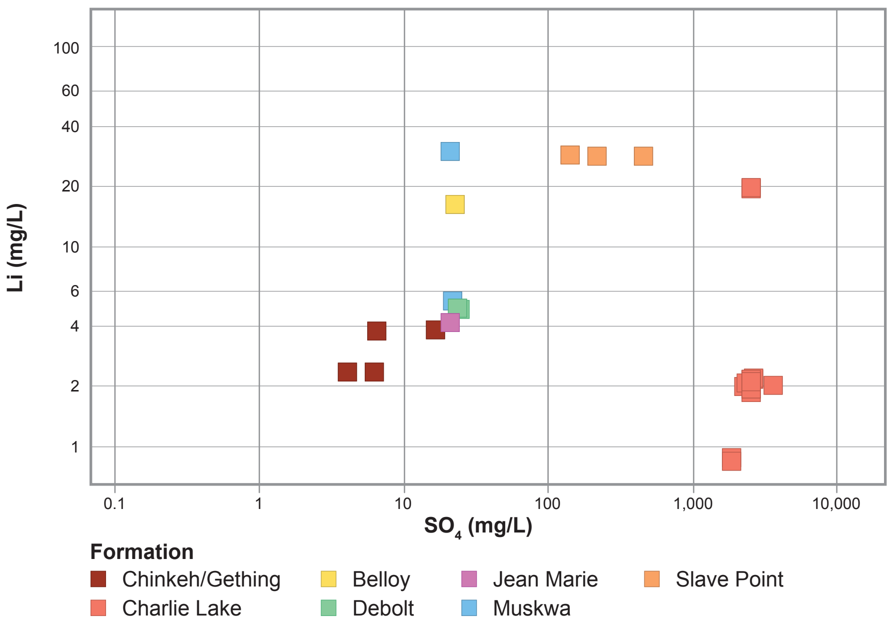

c. Li vs Mg

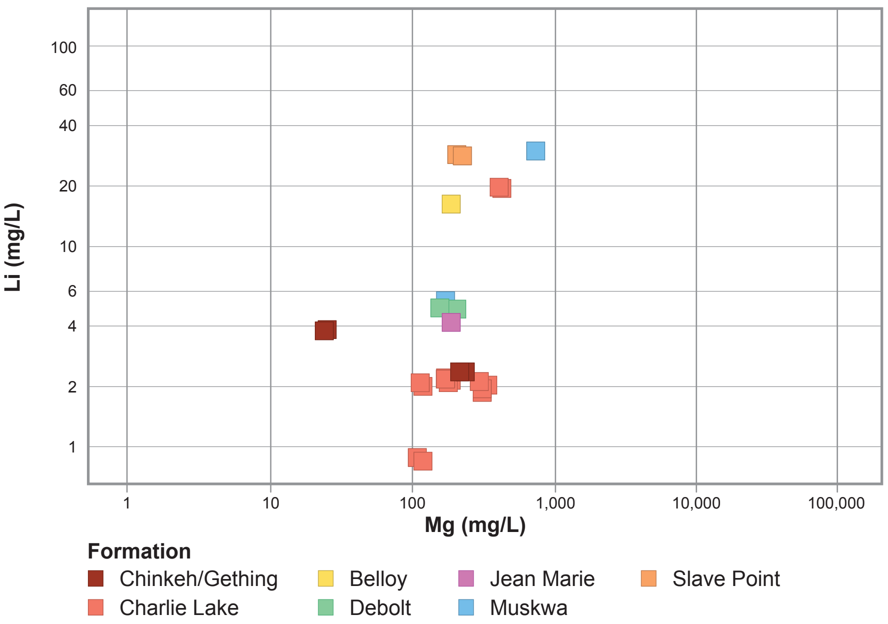

d. Li vs Ca

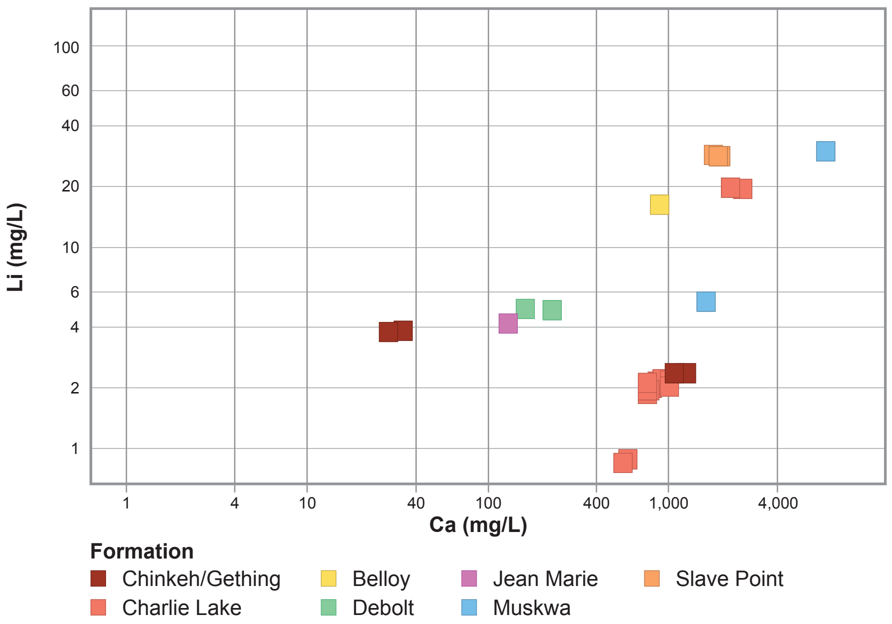

e. Li vs Br

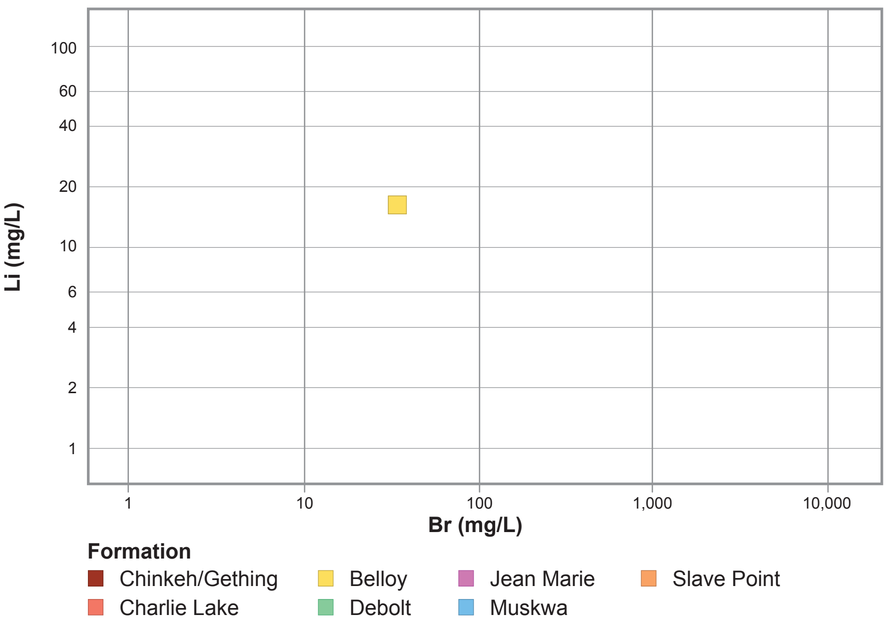

f. Li vs Cl

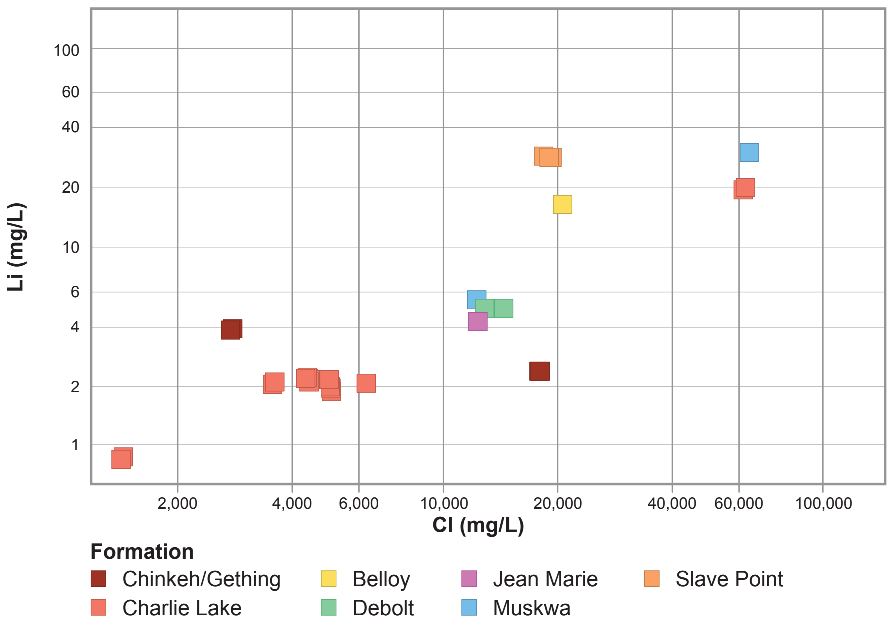

g. Li vs Sr

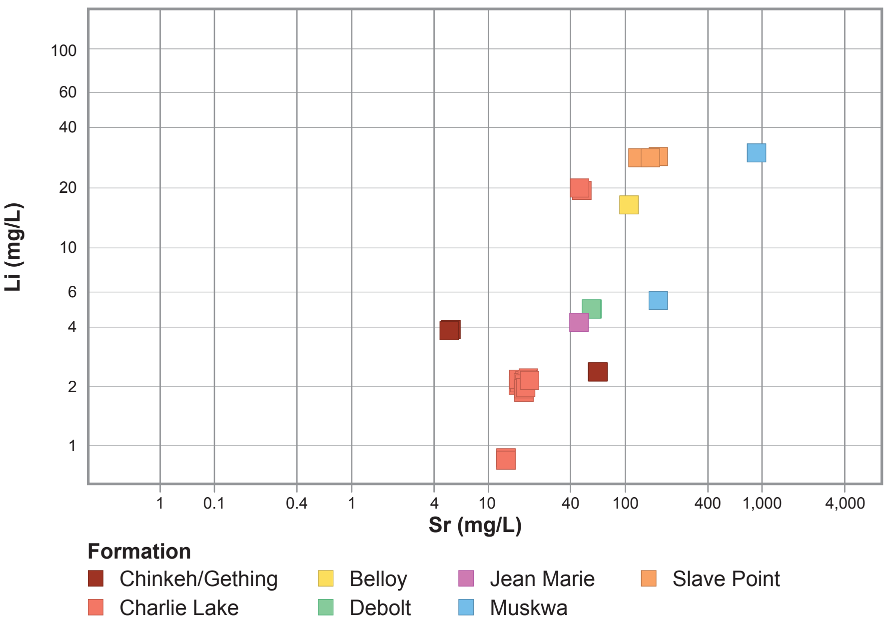

Lithium data from the current study

Figure 7.10

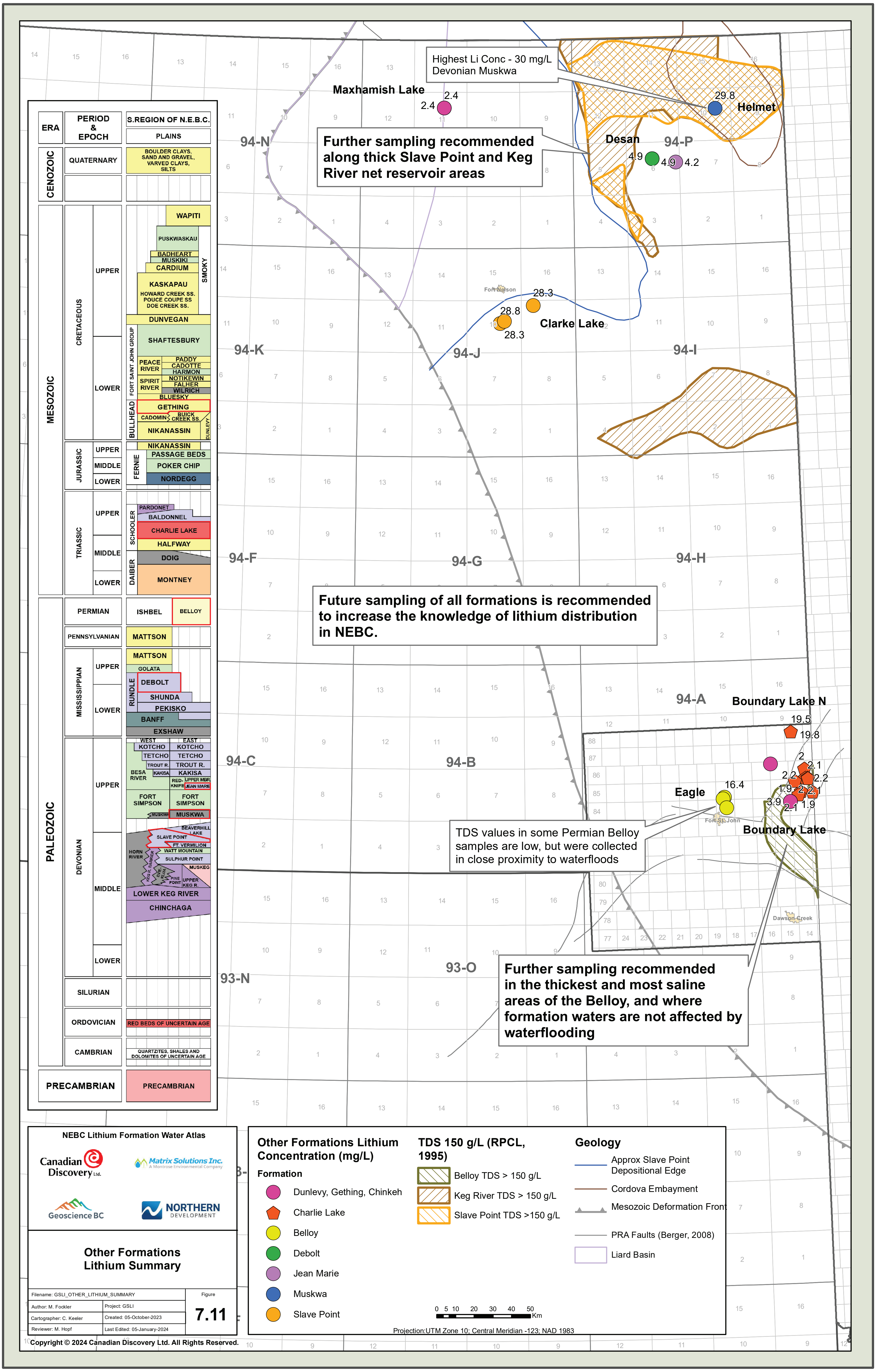

Further sampling recommended along thick Slave Point and Keg River net reservoir areas

Future sampling of all formations is recommended to increase the knowledge of lithium distribution in NEBC.

TDS values in some Permian Belloy samples are low, but were collected in close proximity to waterfloods

Further sampling recommended in the thickest and most saline areas of the Belloy, and where formation waters are not affected by waterflooding

© Canadian Discovery Ltd. *Figure 7.11*

References

- Bachu, S. 1995. Synthesis and model of formation-water flow, Alberta Basin, Canada. American Association of Petroleum Geologists Bulletin, v. 79, p. 1159–1178.
- Berger, Z., Boast, M., and Mushayandebvu, M., 2008. The contribution of integrated HRAM studies to exploration and exploitation of unconventional plays in North America. Part 1. The Peace River Arch. Canadian Society of Petroleum Geologists, Reservoir, v.35, no.10, p.42-47.
- British Columbia Ministry of Energy, Mines and Petroleum Resources, 2006. Oil and Gas Division Resource Development and Geoscience Branch. Conventional Natural Gas Play Atlas, Northeast British Columbia. 2006. Petroleum Geology Publication 2006-01.
- Brown, Teresa, 2016. British Geological Survey, Page 39, Mineral Profile: Lithium. https://nora.nerc.ac.uk/id/eprint/534440/1/lithium_profile.pdf
- Canadian Discovery Ltd. (CDL) and Geoscience BC, 2023. Northeast BC Geological Carbon Capture and Storage Atlas. https://www.geosciencebc.com/projectsto/2023-004
- LithiumBank, 2023. LithiumBank Reports US$2.7 Billion Pre Tax NPV From Preliminary Economic Assessment on a 31,350 TPA LHM Operation at Boardwalk Lithium Brine Project, Alberta, Canada. https://www.lithiumbank.ca/news/2023/ithiumankeports27illionreaxromrelimin20230525071202#:~:text=The%20Li%2Dbrine%20resources%20were,resource%20has%20units%20of%20grams
- Rakhit Petroleum Consulting Ltd. (RPCL), 1995. The Hydrogeological Atlas of the Western Canada Sedimentary Basin. HGAT.
- Standard Lithium, 2021. Standard Lithium Announces Positive Preliminary Economic Assessment and Update of Inferred Mineral Resource at South-West Arkansas Lithium Project. https://www.standardlithium.com/investors/news-events/press-releases/detail/99/standard-lithium-announces-positive-preliminary-economic

Water Chemistry Data

This Appendix is digital only, provided in Excel format, and includes the following:

- This studies water chemistry data
- The GSC water chemistry data used in this study
- The AGS water chemistry data used in this study

Data provided by Canadian Discovery Ltd., the GSC and the AGS.

APPENDIX B

SAMPLING METHODS AND ANALYTICAL PROCEDURES

Introduction

Sampling and data collection methods for the program were standardized where feasible and used to verify that the data obtained were of appropriate quality. This objective was addressed through the following key operational implementations:

1. The assembly and quality checking of well data pre-populated for each infrastructure type *(see 2., below)* and sample location prior to sampling. This task also captured key metadata fields of importance to the project, which were subsequently checked with specific operators for accuracy
2. The use of standardized sampling procedures
3. The use of a nationally accredited laboratory that has significant expertise in analyzing oilfield brines with specific applications to lithium and other metal concentration assessments.
4. Adherence to standardized QA/QC methodologies
5. Documented Chain of Custody procedures

These items are elaborated upon in the following sections.

Metadata Collection

Metadata parameters are considered those which are not explicitly analyzed but collected prior to and as part of the program activities. This includes sampling locations, sample collection dates, stratigraphic and depth intervals, infrastructure types utilized for sampling, as well as additional details on specific conditions of sampling. These parameters were organized into three main categories corresponding to their order of collection.

1. Pre-field metadata
2. Field-collected metadata
3. Post-field quality check and assurance data

The full list of metadata parameters is displayed in *table B.1*. All metadata parameters were collected as available. In cases where certain information was not available, a best effort was made to illustrate and document the circumstances involved as well as missing information or uncertainties.

Sampling Methodology and Procedures

A standardized sampling procedure was devised and implemented for the program, which considered variations on four key infrastructure types for sampling. These infrastructure types include wellhead sampling, sampling at an oil separator, sampling at a treater, and sampling of an onsite production stream or tankage under certain circumstances. The sample collection method from each of these infrastructure types followed Lico et al. (1982) as a benchmark industry standard. In general, the preference is to sample from isolated, "in-test" separators; however, in practice this can present challenges depending on infrastructure and production configuration and is not always feasible. Infrastructure configuration challenges account for the highest degree of variability and unforeseen challenges in attaining the full number of originally proposed samples. This was due to many operations in Northeastern BC configured in a "wet-metered" configuration with little or no means of fluid separation or isolating production from individual wells or zones. Measures were taken to adapt the sampling procedures to include additional sampling options where necessary and justified under certain conditions to attain a reasonable sample coverage. These samples are clearly identified in the results data.

Of utmost importance during sampling is safety. There is an inherent risk in oilfield sampling which necessitates rigorous safety requirements. The following descriptions are illustrative of the procedural sampling methodologies for data integrity and do not include the full industry standard safety procedures for the purposes of this report. All oilfield sampling programs must comply with Worksafe BC requirements and limits (OHS Guidelines – WorkSafeBC), as well as operator-specific safety standards and procedures.

Wellhead Sampling

Sampling at the wellhead is the process of collecting a fluid sample from a sampling port at the wellhead production assembly. For this project, an oilfield wellhead is defined as any mechanism fitted onto a well that has structural and pressure-containing interface capabilities, which involve at least one valve to isolate the well from the atmosphere. The surface pressure control is provided by a master valve, which is installed on the production tubing located above the casing bowl. Wellheads can have multiple isolation valves and chokes to control fluid flow. Wellheads are typically attached to a surface casing bowl welded/attached to the surface casing or surface conductor pipe, which has been cemented in place to ensure adequate well structural integrity.

Wellhead sampling is conducted after the necessary safety precautions are observed, such as testing and releasing wellhead pressure and properly opening infrastructure isolation valves.

Separator Sampling

Test separators are used in oil and gas fields to measure the flow rates of various wells and collect water and hydrocarbon samples from one or more wells at a satellite location. Test separators for this sampling program were either 2-phase or 3-phase. Two-phase means that oil and water are separated from gas, whereas 3-phase means that oil, water, and gas are each separated. For both 3-phase and 2-phase, a sampling valve on the separator tank was accessed and safely opened to produce a fluid sample. Where feasible, the owner and operator confirmed that the wells flowing to the separator were "into test" at least 24 hours prior to sample collection to flush the lines and ensure no risk of contamination from other wells. In some cases, the only way to collect a representative sample due to infrastructure and production configuration constraints was to collect a comingled fluid sample. Where this was the case, the samples are explicitly documented as such and have been identified as representing only one formation production interval despite being sourced from a group of wells.

Treater Sampling

A heater treater uses heat, delivered by a burner and fire tube, to heat the fluid inside a tank. This accelerates the process of separation. Similar to a 2-phase separator, the valves and piping will send the gas to either sales or flare, and the oil will be sent downstream. Produced water is also separated at this tank and is sent downstream for disposal. A sampling valve is usually present on treaters to gain access to production fluids which can be collected along the oil production stream.

On-Site Production Stream or Tankage

Where present, onsite tankage may provide an additional means of sampling although these may comprise commingled fluids and will need to be assessed for their degree of representation of discrete zones of interest. In these cases, sampling ports at the base of the tanks may provide access to the fluids inside and must be assessed on a case-by-case scenario in coordination with the well owner/operator. This infrastructure is considered as a last resort option for sample collection given that the formation waters will have equilibrated to surface pressure and temperature conditions, and therefore may introduce some additional margin of error as chemical constituents equilibrate in such tanks.

Sample Collection

Once infrastructure access to fluids is attained, sample collection is undertaken. The sampling procedure observed for this program conforms to the methods outlined in Lico et al. (1982), which is regarded as the foundational reference for oilfield formation water and brine sampling. Water is collected in an intermediate 9 L carboy and approximately 8 L of water or emulsion is collected if there is an oil/water mixture. The sample is capped and contained in the sealed carboy and allowed to sit for a period of time to assess whether the emulsion begins to separate on its own. Sample temperature is taken immediately after collection. Once the emulsion separates adequately, the spigot at the base of the carboy (where the denser formation water will separate out) is used to fill individual 1 L laboratory-provided standard oilfield sampling bottles. Typically, three to four 1 L bottles were collected for the project, one primary unfiltered and unpreserved sample, one secondary or duplicate raw sample and one sample filtered through two filters, a prefilter and a 0.45 µm filter and preserved with nitric acid. Additionally, another duplicate unfiltered and unpreserved sample was collected for a selected percentage of wells. In this fashion, a backup sample was captured in the event of damage or integrity issues in transit as well as to have a backup separate sample available for analysis if results were flagged for inconsistencies. The duplicate samples were collected in accordance with the QA/QC procedures described in their respective section of this summary. The filtered and preserved samples were collected to check for possible sample quality degradation in the raw unfiltered sample. Following the review of initial results and discussions with AGAT Laboratories Petroleum Testing Services, the collection of a filtered sample was discontinued. The filtered sample results did not exhibit a material difference from unfiltered samples and required the use of specialized equipment that added significant cost, logistical constraints, and prohibitive sampling time requirements for operator accommodation. This was consistent with AGAT's experience in the analysis of brine samples and allowed for more effective operator coordination and scheduling for the project. Details of the difference between the filtered and unfiltered sample results are captured in the Relative Percent Difference analysis included in *Appendix C*.

Nationally Accredited Laboratory

The program selected AGAT Laboratories Petroleum Testing Services for this project, with laboratories and branch locations in Fort St. John and Fort Nelson, BC, and an Oilfield Water Laboratory in Calgary, AB. A full suite of water chemistry analyses, including lithium-ion concentration was established to capture routine brine chemistry for characterization, along with the full suite of dissolved metal parameters of interest to this study. The routine analysis includes pH, electrical conductivity, Ca, Mg, Na, K, Fe, SO_4, Cl, Mn, carbonate, bicarbonate, NO_3, NO_2, NO_{3+}, NO_{2-}, N, alkalinity, hardness, calculated total dissolved solids (TDS), Dissolved Organic Carbon (DOC), Br and I. The dissolved metals analysis includes analysis for Al, Sb, As, Ba, Be, Bi, B, Cd, Ca, Cr, Co, Cu, Fe, Pb, Li, Mg, Mn, Mo, Ni, K, Se, Si, Ag, Na, S, Sr, Sn, Tl, Ti, U, V and Zn and has explicitly been selected to run on an ICP-OES instrument (in contrast to standard ICP-MS instruments) to mitigate requirements for analytical dilution and better accuracy and precision for dissolved lithium and other sensitive parameters. The project also partnered with the GSC, which has agreed to provide scientific input and share analytical costs in support of a parallel yet separate study, which will further analyze the collected samples for a suite of isotopic parameters.

QA/QC Controls and Procedures

In accordance with Matrix standard practices, QC protocols were followed for the sampling program. These QC measures included the collection and analysis of duplicate samples, as well as a review of the results for the laboratory QC samples. Samples were collected as blind samples and assigned a unique sample number for submission to the laboratory. This ensures that the sample location is not identified by the laboratory and results cannot be biased.

Duplicate samples were taken for each formation sampled, at a regular frequency, to monitor the reproducibility (precision) and variability of the sampling method and laboratory analysis. All duplicate samples analyzed were judged to be acceptable, with all relative percent difference values less than 30% and checked for acceptable charge balances within a 10% error. Duplicates were taken for each sampled formation or at every seventh collected sample (whichever applied, dependant on the number of samples collected).

Table B.1 Metadata Collection Parameters

Phase	Data Type	Metadata Parameter
Pre-Field Metadata and Confirmation	Location	Unique Well Identifier (UWI)
		Global Positioning System coordinates easting
		Global Positioning System coordinates northing
		Ground elevation, meters above sea level (masl)
		Operator company
		Producing field name
	Formation	Formation sampled (formation name)
		Formation member name (if available)
		Geological age (eg. Devonian)
		GeoScout downhole temperatue (degrees Celsius)
		Production zone, if known
	Well & Infrastructure	Well type: Oil / Gas
		Well Safety: Sweet or sour?
		Well type comment: Fracked well, flowback or other condition of produced water
	Completion	Well completion depth top (elevation masl)
		Well completion depth base (elevation masl)
		Most recent well intervention type and date - workover, fracking, etc.
	Production & Fluids	Certainty of singular prod zone (ranked: 1-low to 10-high)
		Water Cut (percentage if known ex: 75%)
		Additives - yes/no
		Additive information - concentration, location added, type (descaler, oxygen scavenger, biocide, unknown, proprietary, etc.)
		Pressure of producing well?
		Production hours of well (in test or other production condition or parameter)
Field Collected	Sampling & Infrastructure	Sample ID(s) (Pre-populated; coincides with chain of custody)
		Confirm if sample is sour (Y/N)
		Operator Company
		Supporting operator: last name, first name
		Collection date, time
		Number of sample bottles
		Infrastructure type sampled (ex: separator, wellhead etc.)
		Infrastructure additional comment (single or multi-well, in test condition and running time)
		Sample temperature at collection (degrees Celsius)
		Degree of emulsification (appx. Percentage ex: 10%)
		Description of sample - clear/cloudy, colour, emulsion, product, smell, gassy, turbid, etc.
		Field note / additional comments
Post Field Metadata Quality Checks	Collection and Transmittal Details	Chain of custody (COC) number
		Date shipped
		Transit time
		Lab arrival date & time
		Date sample processed and analyzed
		Observations about sample when analyzed, if applicable

Table B.1

An additional QA/QC control identified and considered for the project was the creation of a synthetic reference standard(s) for specific Li concentrations. Although this was viewed as a potentially useful tool, costs to create synthetic standards were prohibitive and were not within the project budgetary constraints.

Evaluation Criteria For Quality Control Measures

Matrix completed the initial review of all analytical data received from the laboratory. The criteria for evaluation of the field duplicate samples take into account the detection limit (DL), the reliable detection limit (RDL; 5 times the DL), the absolute difference between the duplicate values, and/or the relative percent difference (RPD) calculated for each set of duplicate parameter analyses (Zeiner, 1994). As well, the criteria take into consideration the expected chemistry of the sample based on historical cation values of the producing fields and the concentration of the specific parameter (Zeiner, 1994).

The results of the field duplicate sample analyses are indicated in the Data Quality columns of the formation waters database and the results of the duplicate analyses are also included in the results table.

The RPD is calculated as follows (Eaton et al., 2017):

$$RPD = \frac{\text{(Absolute difference between the two duplicate results)}}{\text{(Mean of the two duplicate results)}} \times 100$$

AGAT Laboratories Petroleum Testing Services also employed QC measures to ensure that the data released is as accurate and precise as possible. Upon receipt of the analytical report, Matrix checked to ensure that the data passed the laboratory's QC measures for duplicates and expected fluid cation chemistries as compared to historical field production. Matrix also evaluated the ion balance reported by the laboratory to ensure that it was within acceptable ranges of between 90 and 110 for brine samples. If a discrepancy was found, the laboratory was contacted and asked to provide a rationale for the discrepancy and, if necessary, a recheck of the result was requested or the samples was reanalyzed for the parameters of concern.

Chain of Custody Procedures

A standard chain of custody documentation procedure was used to capture sampling and relinquishing transactions of each sample in transit to the laboratory. This included all information, such as sampling time, bottle numbers, analytical requirements, and transit times as part of the sample submissions. Copies of the signed forms were documented for each step.

References

- Eaton, A.D. et al. (Eds.). 2017. Standard Methods for the Examination of Water and Wastewater. 23rd Edition. The American Public Health Association, the American Waterworks Association, and the Water Environment Federation. ISBN: 978 0 87553 287 5. Washington, DC, USA. June 15, 2017.
- Lico MS, Kharaka YK, Carothers WW, Wright VA. 1982. Methods for collection and analysis of geopressured geothermal and oil field waters. Geological Survey, Menlo Park, CA (USA)
- Zeiner S.T. 1994. Realistic criteria for the evaluation of field duplicate sample results. Reprinted from the proceedings of Superfund XV. Washington, DC, USA. November 29 to December 1, 1994.

Water Chemistry Screening

Due to the limited number of samples collected for this study, routine water chemistry has been incorporated into each chapter to provide a higher resolution understanding of water chemistry trends for each formation. The water chemistry data were obtained from geoLOGIC's Fluid Analysis module in geoSCOUT. These water chemistry samples are commonly recovered during drilling, testing, completion and production operations and may consist primarily of true formation water or of contaminants such as mud filtrates or completion fluid. As a result, various screening methods are required to distinguish reliable analyses of true formation waters from erroneous analyses and samples contaminated with drilling and completion/stimulation fluids. *Table 1* summarizes the baseline criteria used to screen the water chemistry data.

Additional screening was applied where necessary to further remove anomalous data. Additional screening may have included:

- Plotting data on a Na/Cl vs Mg (HCO_3 + SO_4) plot to flag data that fall off the expected formation water to meteoric dilution trend
- Analyzing individual Stiff diagrams. Occasionally tests with contamination will make it through the baseline screening, however the Stiff diagram may be able to clearly determine sample contamination
- TDS mapping. Any data with anomalously higher or lower TDS compared to neighbouring wells were removed during the mapping process

For the *Montney Chapter 5*, additional steps were taken to deal with the potential influence of frac fluid on water analyses. These steps are outlined in that chapter.

Table C.1: Screening Criteria Used for Water Chemistry Data from geoSCOUT

Acceptance Criteria	What is Removed
Ion Charge Balance calculated as mol cations/ mol anions >0.9 and < 1.1	Erroneous Analyses
pH <4.5	Acid Water/Completion Fluid
Ca/Cl > 0.3 And pH < 5.7	Acid Water/Completion Fluid
Na/Ca < 1.2	Acid Water/Completion Fluid
Na/Ca < 5 And Na/Mg< 10 And pH < 6	Acid Water/Completion Fluid
Na/Cl < 0.4 and pH <6.8	Acid Water/Completion Fluid
SO_4/Cl > 10	Corrosion Inhibitor
Water Density <0.95 and >0	Alcohols
Na/K < 20	KCl Mud Filtrate
Na/Cl > 5	Gel Chem Mud Filtrate
Na/Cl > 3.5 and SO_4/Cl > 1.5	Gel Chem Mud Filtrate

© Canadian Discovery Ltd. *Table C.1*

Table C.2: Water Quality Control Sample Results from Field Samples - All Duplicates

Sample Point	Sample Date	MSI Sample Number	Ca (mg/L)	Mg (mg/L)	Na (mg/L)	K (mg/L)	C (mg/L)	SO_4 (mg/L)	TDS (mg/L)	Li (mg/L)	Br (mg/L)
04-29-087-14W6/0	01-Jun-22	31224220601111	2,948	651	54,430	1,047	92,500	2,150	153,925	41.60	---
04-29-087-14W6/0	01-Jun-22	31224220601112	2,917	646	54,640	1,041	93,500	2,150	153,155	41.80	---
Detection Limit (DL)			1	0.50	3.50	5.60	7	3	1	0.10	1
Reliable Detection Limit (RDL)**			5	2.50	17.50	28	35	15	5	0.50	---
Absolute Difference*			31	5	210	6	1,000	0	770	0.20	---
Absolute Relative Percent Difference (RPD)*			1.06	0.77	0.39	0.57	1.08	0	0.50	0.48	---
Duplicate Sample Results Evaluation			Good	Good	Good	Good	Good	Good	Good	Good	---
06-29-087-14W6	01-Jun-22	31224220601117	2,977	703	53,570	954	92,300	2,120	152,772	40.70	---
06-29-087-14W6	01-Jun-22	31224220601118	2,829	694	54,540	950	92,000	2,160	153,318	40.50	---
Detection Limit (DL)			1	0.50	3.50	5.60	7	3	1	0.10	1
Reliable Detection Limit (RDL)**			5	2.50	17.50	28	35	15	5	0.50	---
Absolute Difference*			148	9	970	4	300	40	546	0.20	---
Absolute Relative Percent Difference (RPD)*			5.10	1.29	1.79	0.42	0.33	1.87	0.36	0.49	---
Duplicate Sample Results Evaluation			Good	Good	Good	Good	Good	Good	Good	Good	---
14-14-088-15W6/00	01-Jun-22	31224220601119	2,928	660	51,700	1,035	93,500	2,070	152,058	42.40	---
14-14-088-15W6/00	01-Jun-22	31224220601120	2,896	651	53,640	1,035	92,000	2,070	152,461	41.90	---
Detection Limit (DL)			1	0.50	3.50	5.60	7	3	1	0.10	1
Reliable Detection Limit (RDL)**			5	2.50	17.50	28	35	15	5	0.50	---
Absolute Difference*			32	9	1,940	0	1,500	0	403	0.50	---
Absolute Relative Percent Difference (RPD)*			1.10	1.37	3.68	0	1.62	0	0.26	1.19	---
Duplicate Sample Results Evaluation			Good	Good	Good	Good	Good	Good	Good	Good	---
08-08-086-13W6/00	02-Jun-22	31224220602101	2,908	729	56,880	967	103,000	2,880	168,178	40.50	---
08-08-086-13W6/00	02-Jun-22	31224220602102	3,140	772	55,610	1,025	100,000	2,660	163,994	39.50	---
Detection Limit (DL)			1	0.50	3.50	5.60	7	3	1	0.10	1
Reliable Detection Limit (RDL)**			5	2.50	17.50	28	35	15	5	0.50	---
Absolute Difference*			232	43	1,270	58	3,000	220	4,184	1	---
Absolute Relative Percent Difference (RPD)*			7.67	5.73	2.26	5.82	2.96	7.94	2.52	2.50	---
Duplicate Sample Results Evaluation			Good	Good	Good	Good	Good	Good	Good	Good	---
13-16-087-13W6/02	02-Jun-22	31224220602103	458	145	23,800	692	37,900	2,350	65,760	43.70	---
13-16-087-13W6/02	02-Jun-22	31224220602104	446	136	23,900	655	36,900	2,370	64,822	43.50	---
Detection Limit (DL)			1	0.50	3.50	5.60	7	3	1	0.10	1
Reliable Detection Limit (RDL)**			5	2.50	17.50	28	35	15	5	0.50	---
Absolute Difference*			12	9	100	37	1,000	20	938	0.20	---
Absolute Relative Percent Difference (RPD)*			2.65	6.41	0.42	5.49	2.67	0.85	1.44	0.46	---
Duplicate Sample Results Evaluation			Good	Good	Good	Good	Good	Good	Good	Good	---
01-17-086-13W6/00	02-Jun-22	31224220602107	3,384	853	50,800	981	94,500	2,230	152,977	42	---
01-17-086-13W6/00	02-Jun-22	31224220602108	3,490	874	52,300	1,026	97,700	2,250	157,874	42.20	---
Detection Limit (DL)			1	0.50	3.50	5.60	7	3	1	0.10	1
Reliable Detection Limit (RDL)**			5	2.50	17.50	28	35	15	5	0.50	---
Absolute Difference*			106	21	1,500	45	3,200	20	4,897	0.20	---
Absolute Relative Percent Difference (RPD)*			3.08	2.43	2.91	4.48	3.33	0.89	3.15	0.48	---
Duplicate Sample Results Evaluation			Good	Good	Good	Good	Good	Good	Good	Good	---
04-16-086-13W6/02	02-Jun-22	31224220602109	4,100	868	57,380	1,086	103,000	2,020	168,686	38.70	---
04-16-086-13W6/02	02-Jun-22	31224220602110	4,230	868	56,180	1,080	103,000	2,220	167,813	39.20	---
Detection Limit (DL)			1	0.50	3.50	5.60	7	3	1	0.10	1
Reliable Detection Limit (RDL)**			5	2.50	17.50	28	35	15	5	0.50	---
Absolute Difference*			130	0	1,200	6	0	200	873	0.50	---
Absolute Relative Percent Difference (RPD)*			3.12	0	2.11	0.55	0	9.43	0.52	1.28	---
Duplicate Sample Results Evaluation			Good	Good	Good	Good	Good	Good	Good	Good	---

Continued on next page

Continued from previous page

Table C.2: Water Quality Control Sample Results from Field Samples - All Duplicates

Sample Point	Sample Date	MSI Sample Number	Ca (mg/L)	Mg (mg/L)	Na (mg/L)	K (mg/L)	C (mg/L)	SO$_4$ (mg/L)	TDS (mg/L)	Li (mg/L)	Br (mg/L)
12-31-087-14W6/00	05-Jun-22	31224220305113	3,000	628	53,400	987	95,900	2,100	156,175	41	---
12-31-087-14W6/00	05-Jun-22	31224220305114	2,870	585	54,200	930	95,100	2,080	153,344	41	---
Detection Limit (DL)			1	0.50	3.50	5.60	7	3	1	0.10	1
Reliable Detection Limit (RDL)**			5	2.50	17.50	28	35	15	5	0.50	---
Absolute Difference*			130	43	800	57	800	20	2,831	0	---
Absolute Relative Percent Difference (RPD)*			4.43	7.09	1.49	5.95	0.84	0.96	1.83	0	---
Duplicate Sample Results Evaluation			Good	Good	Good	Good	Good	Good	Good	Good	---
06-24-086-14W6/00	07-Jul-22	31224220707120	834	117	2,280	67.30	3,550	2,260	9,294	2.02	---
06-24-086-14W6/00	07-Jul-22	31224220707121	828	115	2,290	67.30	3,600	2,300	9,409	2.09	---
Detection Limit (DL)			1	0.50	3.50	5.60	7	3	1	0.10	1
Reliable Detection Limit (RDL)**			5	2.50	17.50	28	35	15	5	0.50	---
Absolute Difference*			6	2	10	0	50	40	115	0.07	---
Absolute Relative Percent Difference (RPD)*			0.72	1.72	0.44	0	1.40	1.75	1.23	3.41	---
Duplicate Sample Results Evaluation			Good	Good	Good	Good	Good	Good	Good	Good	---
07-01-086-14W6/00	07-Jul-22	31224220707122	919	169	2,810	98	4,410	2,550	11,193	2.18	---
07-01-086-14W6/00	07-Jul-22	31224220707123	930	172	2,820	98.80	4,420	2,600	11,290	2.19	---
Detection Limit (DL)			1	0.50	3.50	5.60	7	3	1	0.10	1
Reliable Detection Limit (RDL)**			5	2.50	17.50	28	35	15	5	0.50	---
Absolute Difference*			11	3	10	0.80	10	50	97	0.01	---
Absolute Relative Percent Difference (RPD)*			1.19	1.76	0.36	0.81	0.23	1.94	0.86	0.46	---
Duplicate Sample Results Evaluation			Good	Good	Good	Good	Good	Good	Good	Good	---
06-06-086-14W6	07-Jul-22	31224220707124	867	186	2,870	90.20	4,470	2,500	11,209	2.15	---
06-06-086-14W6	07-Jul-22	31224220707125	869	183	2,860	91.50	4,430	2,500	11,184	2.09	---
Detection Limit (DL)			1	0.50	3.50	5.60	7	3	1	0.10	1
Reliable Detection Limit (RDL)**			5	2.50	17.50	28	35	15	5	0.50	---
Absolute Difference*			2	3	10	1.30	40	0	25	0.06	---
Absolute Relative Percent Difference (RPD)*			0.23	1.63	0.35	1.43	0.90	0	0.22	2.83	---
Duplicate Sample Results Evaluation			Good	Good	Good	Good	Good	Good	Good	Good	---
03-06-086-14W6	07-Jul-22	31224220707126	937	169	2,780	91.50	4,390	2,610	11,267	2.22	---
03-06-086-14W6	07-Jul-22	31224220707127	1,010	175	2,780	93.30	4,340	2,560	11,254	2.18	---
Detection Limit (DL)			1	0.50	3.50	5.60	7	3	1	0.10	1
Reliable Detection Limit (RDL)**			5	2.50	17.50	28	35	15	5	0.50	---
Absolute Difference*			73	6	0	1.80	50	50	13	0.04	---
Absolute Relative Percent Difference (RPD)*			7.50	3.49	0	1.95	1.15	1.93	0.12	1.82	---
Duplicate Sample Results Evaluation			Good	Good	Good	Good	Good	Good	Good	Good	---
16-10-085-14W6/00	07-Jul-22	31224220707129	783	304	3,520	105	5,080	2,510	12,647	1.87	---
16-10-085-14W6/00	07-Jul-22	31224220707130	787	307	3,550	106	5,070	2,540	12,735	1.94	---
Detection Limit (DL)			1	0.50	3.50	5.60	7	3	1	0.10	1
Reliable Detection Limit (RDL)**			5	2.50	17.50	28	35	15	5	0.50	---
Absolute Difference*			4	3	30	1	10	30	88	0.07	---
Absolute Relative Percent Difference (RPD)*			0.51	0.98	0.85	0.95	0.20	1.19	0.69	3.67	---
Duplicate Sample Results Evaluation			Good	Good	Good	Good	Good	Good	Good	Good	---
13-03-085-14W6/00	07-Jul-22	31224220707131	778	304	3,490	104	5,050	2,550	12,586	1.96	---
13-03-085-14W6/00	07-Jul-22	31224220707132	772	294	3,560	101	5,020	2,530	12,640	2.13	---
Detection Limit (DL)			1	0.50	3.50	5.60	7	3	1	0.10	1
Reliable Detection Limit (RDL)**			5	2.50	17.50	28	35	15	5	0.50	---
Absolute Difference*			6	10	70	3	30	20	54	0.17	---
Absolute Relative Percent Difference (RPD)*			0.77	3.34	1.99	2.93	0.60	0.79	0.43	8.31	---
Duplicate Sample Results Evaluation			Good	Good	Good	Good	Good	Good	Good	Good	---

Continued on next page

Continued from previous page

Table C.2: Water Quality Control Sample Results from Field Samples - All Duplicates

Sample Point	Sample Date	MSI Sample Number	Ca (mg/L)	Mg (mg/L)	Na (mg/L)	K (mg/L)	C (mg/L)	SO_4 (mg/L)	TDS (mg/L)	Li (mg/L)	Br (mg/L)
11-30-084-14W6/00	07-Jul-22	31224220707133	34.30	24.90	3,700	66.60	2,790	16.60	9,324	3.86	---
11-30-084-14W6/00	07-Jul-22	31224220707134	28.50	24.30	3,730	71.50	2,760	6.40	9,297	3.79	---
Detection Limit (DL)			1	0.50	3.50	5.60	7	3	1	0.10	1
Reliable Detection Limit (RDL)**			5	2.50	17.50	28	35	15	5	0.50	---
Absolute Difference*			5.80	0.60	30	4.90	30	10.20	27	0.07	---
Absolute Relative Percent Difference (RPD)*			18.47	2.44	0.81	7.10	1.08	---	0.29	1.83	---
Duplicate Sample Results Evaluation			Good	Good	Good	Good	Good	Good	Good	Good	---
05-33-085-13W6	07-Jul-22	31224220707135	599	110	996	40.70	1,440	1,860	5,161	0.88	---
05-33-085-13W6	07-Jul-22	31224220707136	574	117	962	39.80	1,420	1,850	5,081	0.85	---
Detection Limit (DL)			1	0.50	3.50	5.60	7	3	1	0.10	1
Reliable Detection Limit (RDL)**			5	2.50	17.50	28	35	15	5	0.50	---
Absolute Difference*			25	7	34	0.90	20	10	80	0.03	---
Absolute Relative Percent Difference (RPD)*			4.26	6.17	3.47	2.24	1.40	0.54	1.56	3.47	---
Duplicate Sample Results Evaluation			Good	Good	Good	Good	Good	Good	Good	Good	---
a-018-J/094-O-11/00	12-Jul-22	31224220711101	1,280	230	10,500	104	17,860	4	31,190	2.36	---
a-018-J/094-O-11/00	12-Jul-22	31224220711103	1,100	216	11,000	102	18,000	6.30	31,621	2.38	---
Detection Limit (DL)			1	0.50	3.50	5.60	7	3	1	0.10	1
Reliable Detection Limit (RDL)**			5	2.50	17.50	28	35	15	5	0.50	---
Absolute Difference*			180	14	500	2	140	2.30	431	0.02	---
Absolute Relative Percent Difference (RPD)*			15.13	6.28	4.65	1.94	0.78	---	1.37	0.84	---
Duplicate Sample Results Evaluation			Good	Good	Good	Good	Good	Good	Good	Good	---
d-51-G	26-Jul-22	31224220726144	8,390	867	35,250	255	62,900	23	107,775	30.20	---
d-51-G	26-Jul-22	31224220726145	7,450	724	32,400	250	64,000	21.10	104,935	29.80	---
Detection Limit (DL)			1	1	1	1	1	1	1	1	1
Reliable Detection Limit (RDL)**			5	5	5	5	5	5	5	5	---
Absolute Difference*			940	143	2,850	5	1,100	1.90	2,840	0.40	---
Absolute Relative Percent Difference (RPD)*			11.87	17.98	8.43	1.98	1.73	8.62	2.67	1.33	---
Duplicate Sample Results Evaluation			Good	Good	Good	Good	Good	Good	Good	Good	---
a-01-K	26-Jul-22	31224220726146	230	209	10,160	119	14,440	24.40	27,098	4.90	---
a-01-K	26-Jul-22	31224220726147	164	159	9,150	108	12,840	23.60	24,299	4.92	---
Detection Limit (DL)			1	0.50	3.50	5.60	7	3	1	0.10	1
Reliable Detection Limit (RDL)**			5	2.50	17.50	28	35	15	5	0.50	---
Absolute Difference*			66	50	1,010	11	1,600	0.80	2,799	0.02	---
Absolute Relative Percent Difference (RPD)*			33.50	27.17	10.46	9.69	11.73	3.33	10.89	0.41	---
Duplicate Sample Results Evaluation			Poor	Good	Good	Good	Good	Good	Good	Good	---
b-83-H	26-Jul-22	31224220726148	180	234	10,230	86.60	12,600	21.20	25,305	4.14	---
b-83-H	26-Jul-22	31224220726149	129	190	8,860	76	12,360	20.50	23,588	4.20	---
Detection Limit (DL)			1	0.50	3.50	5.60	7	3	1	0.10	1
Reliable Detection Limit (RDL)**			5	2.50	17.50	28	35	15	5	0.50	---
Absolute Difference*			51	44	1,370	10.60	240	0.70	1,717	0.06	---
Absolute Relative Percent Difference (RPD)*			33.01	20.75	14.35	13.04	1.92	3.36	7.02	1.44	---
Duplicate Sample Results Evaluation			Poor	Good	Good	Good	Good	Good	Good	Good	---
13-21-088-14W6/00	08-Sep-22	31224220908512	2,595	430	39,200	980	61,640	2,483	107,425	19.50	---
13-21-088-14W6/00	08-Sep-22	31224220908514	2,267	400	36,800	910	62,430	2,471	105,374	19.80	---
Detection Limit (DL)			1	0.50	3.50	5.60	7	3	1	0.10	1
Reliable Detection Limit (RDL)**			5	2.50	17.50	28	35	15	5	0.50	---
Absolute Difference*			328	30	2,400	70	790	12	2,051	0.30	---
Absolute Relative Percent Difference (RPD)*			13.49	7.23	6.32	7.41	1.27	0.48	1.93	1.53	---
Duplicate Sample Results Evaluation			Good	Good	Good	Good	Good	Good	Good	Good	---

Continued on next page

Continued from previous page

Table C.2: Water Quality Control Sample Results from Field Samples - All Duplicates

Sample Point	Sample Date	MSI Sample Number	Ca (mg/L)	Mg (mg/L)	Na (mg/L)	K (mg/L)	C (mg/L)	SO_4 (mg/L)	TDS (mg/L)	Li (mg/L)	Br (mg/L)
05-25-080-16W6	09-Sep-22	31224220909523	9,660	1,300	56,200	1,540	127,500	350.40	196,601	77.70	---
05-26-080-16W6	09-Sep-22	31224220909525	11,000	1,410	60,800	1,690	119,900	331	195,177	81.10	---
Detection Limit (DL)			1	0.50	3.50	5.60	7	3	1	0.10	1
Reliable Detection Limit (RDL)**			5	2.50	17.50	28	35	15	5	0.50	---
Absolute Difference*			1,340	110	4,600	150	7,600	19.40	1,424	3.40	---
Absolute Relative Percent Difference (RPD)*			12.97	8.12	7.86	9.29	6.14	5.69	0.73	4.28	---
Duplicate Sample Results Evaluation			Good	Good	Good	Good	Good	Good	Good	Good	---
12-09-080-16W6	09-Sep-22	31224220909527	23,300	2,080	79,600	2,560	171,700	159	279,414	75.90	---
12-09-080-16W6	09-Sep-22	31224220909529	20,100	1,830	69,700	2,250	182,500	163	276,580	71.60	---
Detection Limit (DL)			1	0.50	3.50	5.60	7	3	1	0.10	1
Reliable Detection Limit (RDL)**			5	2.50	17.50	28	35	15	5	0.50	---
Absolute Difference*			3,200	250	9,900	310	10,800	4	2,834	4.30	---
Absolute Relative Percent Difference (RPD)*			14.75	12.79	13.26	12.89	6.10	2.48	1.02	5.83	---
Duplicate Sample Results Evaluation			Good	Good	Good	Good	Good	Good	Good	Good	---
01-10-080-16W6	12-Sep-22	31224220912516	23,300	2,700	77,400	2,490	181,700	191	287,785	71.20	---
01-10-080-16W6	12-Sep-22	31224220912518	20,600	2,030	76,950	2,210	185,620	195.70	287,621	70.70	---
Detection Limit (DL)			1	0.50	3.50	5.60	7	3	1	0.10	1
Reliable Detection Limit (RDL)**			5	2.50	17.50	28	35	15	5	0.50	---
Absolute Difference*			2,700	670	450	280	3,920	4.70	164	0.50	---
Absolute Relative Percent Difference (RPD)*			12.30	28.33	0.58	11.91	2.13	2.43	0.06	0.70	---
Duplicate Sample Results Evaluation			Good	Good	Good	Good	Good	Good	Good	Good	---
05-15-080-19W6	30-Sep-22	31224220930797	19,500	1,340	79,000	3,020	190,400	7.40	293,277	80.40	---
05-15-080-19W6	30-Sep-22	31224220930795	19,300	1,300	79,300	2,840	195,100	6.80	297,857	73.10	---
Detection Limit (DL)			1	0.50	3.50	5.60	7	3	1	0.10	1
Reliable Detection Limit (RDL)**			5	2.50	17.50	28	35	15	5	0.50	---
Absolute Difference*			200	40	300	180	4,700	0.60	4,580	7.30	---
Absolute Relative Percent Difference (RPD)*			1.03	3.03	0.38	6.14	2.44	---	1.55	9.51	---
Duplicate Sample Results Evaluation			Good	Good	Good	Good	Good	Good	Good	Good	---
13-08-080-19W6	18-Oct-22	31224221018784	20,900	1,550	19,600	2,940	74,760	0	119,760	90.40	---
13-08-080-19W6	18-Oct-22	31224221018785	20,800	1,600	20,400	2,880	73,530	0	119,220	89.70	---
Detection Limit (DL)			1	0.50	3.50	5.60	7	3	1	0.10	1
Reliable Detection Limit (RDL)**			5	2.50	17.50	28	35	15	5	0.50	---
Absolute Difference*			100	50	800	60	1,230	0	540	0.70	---
Absolute Relative Percent Difference (RPD)*			0.48	3.17	4	2.06	1.66	---	0.45	0.78	---
Duplicate Sample Results Evaluation			Good	Good	Good	Good	Good	Good	Good	Good	---
06-36-081-14W6	18-Jan-23	31224230118001	5,400	1,100	62,500	1,930	124,000	1,020	196,029	29.80	144
06-36-081-14W6	18-Jan-23	31224230118003	5,800	1,100	65,600	1,880	117,000	995	192,453	31.10	152
Detection Limit (DL)			1	0.50	3.50	5.60	7	3	1	0.10	1
Reliable Detection Limit (RDL)**			5	2.50	17.50	28	35	15	5	0.50	5
Absolute Difference*			400	0	3,100	50	7,000	25	3,576	1.30	8
Absolute Relative Percent Difference (RPD)*			7.14	0	4.84	2.62	5.81	2.48	1.84	4.27	5
Duplicate Sample Results Evaluation			Good	Good	Good	Good	Good	Good	Good	Good	Good
a-042-H/094-A-13	19-Jan-23	31224230119010	2,140	496	53,600	1,830	87,700	1,924	148,195	32.60	66
a-042-H/094-A-13	19-Jan-23	31224230119012	2,350	503	54,800	1,960	87,400	1,874	149,386	35.20	57
Detection Limit (DL)			1	0.50	3.50	5.60	7	3	1	0.10	1
Reliable Detection Limit (RDL)**			5	2.50	17.50	28	35	15	5	0.50	5
Absolute Difference*			210	7	1,200	130	300	50	1,191	2.60	9
Absolute Relative Percent Difference (RPD)*			9.35	1.40	2.21	6.86	0.34	2.63	0.80	7.67	15
Duplicate Sample Results Evaluation			Good	Good	Good	Good	Good	Good	Good	Good	Good

Continued on next page

Continued from previous page

Table C.2: Water Quality Control Sample Results from Field Samples - All Duplicates

Sample Point	Sample Date	MSI Sample Number	Ca (mg/L)	Mg (mg/L)	Na (mg/L)	K (mg/L)	C (mg/L)	SO$_4$ (mg/L)	TDS (mg/L)	Li (mg/L)	Br (mg/L)
b-042-H/094-A-13	19-Jan-23	31224230119013	2,110	494	53,100	1,920	87,400	1,854	147,209	25	58
b-042-H/094-A-13	19-Jan-23	31224230119015	2,074	512	54,200	1,900	90,200	1,857	151,035	33.70	71
Detection Limit (DL)			1	0.50	3.50	5.60	7	3	1	0.10	1
Reliable Detection Limit (RDL)**			5	2.50	17.50	28	35	15	5	0.50	5
Absolute Difference*			36	18	1,100	20	2,800	3	3,826	8.70	13
Absolute Relative Percent Difference (RPD)*			1.72	3.58	2.05	1.05	3.15	0.16	2.57	29.64	20
Duplicate Sample Results Evaluation			Good	Good	Good	Good	Good	Good	Good	Good	Good
c-019-I/094-A-13	19-Jan-23	31224230119016	73.60	27.40	11,100	312	13,700	944	28,432	20.10	27
c-019-I/094-A-13	19-Jan-23	31224230119018	63.60	17	10,560	296	13,400	922.80	27,507	19.70	50
Detection Limit (DL)			1	0.50	3.50	5.60	7	3	1	0.10	1
Reliable Detection Limit (RDL)**			5	2.50	17.50	28	35	15	5	0.50	5
Absolute Difference*			10	10.40	540	16	300	21.20	925	0.40	23
Absolute Relative Percent Difference (RPD)*			14.58	46.85	4.99	5.26	2.21	2.27	3.31	2.01	60
Duplicate Sample Results Evaluation			Good	Poor	Good	Good	Good	Good	Good	Good	Poor
c-013-J/094-A-13	19-Jan-23	31224230119019	47.60	19	8,988	232	10,200	920.40	23,035	19.80	50
c-013-J/094-A-13	19-Jan-23	31224230119021	33.40	18.50	8,966	230	10,300	900.50	22,978	19.50	63
Detection Limit (DL)			1	0.50	3.50	5.60	7	3	1	0.10	1
Reliable Detection Limit (RDL)**			5	2.50	17.50	28	35	15	5	0.50	5
Absolute Difference*			14.20	0.50	22	2	100	19.90	57	0.30	13
Absolute Relative Percent Difference (RPD)*			35.06	2.67	0.25	0.87	0.98	2.19	0.25	1.53	23
Duplicate Sample Results Evaluation			Poor	Good	Good	Good	Good	Good	Good	Good	Good
d-051-J/094-A-13	19-Jan-23	31224230119022	41	15.10	8,851	234	9,490	758.70	21,971	17.70	115
d-051-J/094-A-13	19-Jan-23	31224230119024	39	14.80	9,074	239	9,140	680.10	21,774	17.40	51
Detection Limit (DL)			1	0.50	3.50	5.60	7	3	1	0.10	1
Reliable Detection Limit (RDL)**			5	2.50	17.50	28	35	15	5	0.50	5
Absolute Difference*			2	0.30	223	5	350	78.60	197	0.30	64
Absolute Relative Percent Difference (RPD)*			5	2.01	2.49	2.11	3.76	10.93	0.90	1.71	77
Duplicate Sample Results Evaluation			Good	Good	Good	Good	Good	Good	Good	Good	Poor
d-065-H/094-A-15	31-Jan-23	31224230131037	1,820	495	27,800	713	47,200	2,340	80,369	26.20	93
d-065-H/094-A-15	31-Jan-23	31224230131039	1,800	477	28,100	725	47,300	2,370	80,814	25.20	90
Detection Limit (DL)			1	1	1	1	1	1	1	1	1
Reliable Detection Limit (RDL)**			5	5	5	5	5	5	5	5	5
Absolute Difference*			20	18	300	12	100	30	445	1	3
Absolute Relative Percent Difference (RPD)*			1.10	3.70	1.07	1.67	0.21	1.27	0.55	3.89	3
Duplicate Sample Results Evaluation			Good	Good	Good	Good	Good	Good	Good	Good	Good
06-31-086-15W6	01-Feb-23	31224230201067	173	73.80	13,900	175	20,800	374	36,773	<0.10	65
06-31-086-15W6	01-Feb-23	31224230201069	0	0	0	0	0	0	0	<0.10	0
Detection Limit (DL)			1	0.50	3.50	5.60	7	3	1	0.10	1
Reliable Detection Limit (RDL)**			5	2.50	17.50	28	35	15	5	0.50	5
Absolute Difference*			173	73.80	13,900	175	20,800	374	36,773	---	65
Absolute Relative Percent Difference (RPD)*			---	---	---	---	---	---	---	---	---
Duplicate Sample Results Evaluation			Poor	Poor	Poor	Poor	Poor	Poor	Poor	Good	Poor
01-23-081-18W6	20-Jan-23	31224230120028	21,000	1,814	75,530	3,023	185,530	1,245	288,164	58.70	306
01-23-081-18W6	20-Jan-23	31224230120030	22,300	2,080	74,400	2,390	175,000	72	276,439	67.50	169
Detection Limit (DL)			1	0.50	3.50	5.60	7	3	1	0.10	1
Reliable Detection Limit (RDL)**			5	2.50	17.50	28	35	15	5	0.50	5
Absolute Difference*			1,300	266	1,130	633	10,530	1,173	11,725	8.80	137
Absolute Relative Percent Difference (RPD)*			6	13.66	1.51	23.39	5.84	178.13	4.15	13.95	58
Duplicate Sample Results Evaluation			Good	Good	Good	Good	Good	Poor	Good	Good	Poor

Continued on next page

Continued from previous page

Table C.2: Water Quality Control Sample Results from Field Samples - All Duplicates

Sample Point	Sample Date	MSI Sample Number	Ca (mg/L)	Mg (mg/L)	Na (mg/L)	K (mg/L)	C (mg/L)	SO_4 (mg/L)	TDS (mg/L)	Li (mg/L)	Br (mg/L)
multi-well produced water tank at surface location A-067-K 094-P-07	15-Mar-23	31224230315101	27.10	12.50	592	6.80	848	0	1,670	0.30	2.7
multi-well produced water tank at surface location A-067-K 094-P-07	15-Mar-23	31224230315102	25.90	12.10	578	6.30	844	0	1,648	0.31	2.3
Detection Limit (DL)			1	0.50	3.50	5.60	7	3	1	0.10	1
Reliable Detection Limit (RDL)**			5	2.50	17.50	28	35	15	5	0.50	5
Absolute Difference*			1.20	0.40	14	0.50	4	0	22	0.01	0.4
Absolute Relative Percent Difference (RPD)*			4.53	3.25	2.39	---	0.47	---	1.33	---	---
Duplicate Sample Results Evaluation			Good	Good	Good	Good	Good	Good	Good	Good	Good

Notes

–	- not applicable
*	- non-detectable concentrations are assessed at 95% of the detection limit
**	- the reliable detection limit (RDL) or practical detection limit (PDL) is defined as 5 times the DL
Good	- evaluation indicates acceptable reproducibility
Poor	- evaluation indicates poor reproducibility

Evaluation of Duplicate Analyses:

- reproducibility is unacceptable if RPD is > 30% for inorganic waters and > 40% for soils and organics
- if RPD is not applicable (---), reproducibility is evaluated based on Absolute Difference (unacceptable if > 2 x RDL)
- if Absolute Difference is not applicable (---), reproducibility is evaluated based on the parameter concentration (unacceptable if > 2 x RDL)
- pH is evaluated based on Absolute Difference (unacceptable if > 0.5)

RPD

$$\text{RPD} = \frac{\text{Difference between the two duplicate results} \times 100}{\text{Mean of the two duplicate results}}$$

Table C.2

Table C.3: Water Quality Control Sample Results - Filtered vs Unfiltered Results

Filtered (Y/N)	Sample Point	Sample Date	MSI Sample Number	Ca (mg/L)	Mg (mg/L)	Na (mg/L)	K (mg/L)	Cl (mg/L)	SO_4 (mg/L)	TDS (mg/L)	Li (mg/L)
Y	06-29-087-14W6	01-Jun-22	31224220601117	2,977	703	53,570	954	92,300	2,120	152,772	40.7
N	06-29-087-14W6	01-Jun-22	31224220601118	2,829	694	54,540	950	92,000	2,160	153,318	40.5
Detection Limit (DL)				1	0.5	3.5	5.6	7	3	1	0.1
Reliable Detection Limit (RDL)**				5	2.5	17.5	28	35	15	5	0.5
Absolute Difference*				148	9	970	4	300	40	546	0.2
Absolute Relative Percent Difference (RPD)*				5	1	2	0	0	2	0	0
Duplicate Sample Results Evaluation				Good	Good	Good	Good	Good	Good	Good	Good
Y	06-24-086-14W6/00	07-Jul-22	31224220707120	834	117	2,280	67.3	3,550	2,260	9,294	2.02
N	06-24-086-14W6/00	07-Jul-22	31224220707121	828	115	2,290	67.3	3,600	2,300	9,409	2.09
Detection Limit (DL)				1	0.5	3.5	5.6	7	3	1	0.1
Reliable Detection Limit (RDL)**				5	2.5	17.5	28	35	15	5	0.5
Absolute Difference*				6	2	10	0	50	40	115	0.07
Absolute Relative Percent Difference (RPD)*				1	2	0	0	1	2	1	3
Duplicate Sample Results Evaluation				Good	Good	Good	Good	Good	Good	Good	Good
Y	07-01-086-14W6/00	07-Jul-22	31224220707122	919	169	2,810	98	4,410	2,550	11,193	2.18
N	07-01-086-14W6/00	07-Jul-22	31224220707123	930	172	2,820	98.8	4,420	2,600	11,290	2.19
Detection Limit (DL)				1	0.5	3.5	5.6	7	3	1	0.1
Reliable Detection Limit (RDL)**				5	2.5	17.5	28	35	15	5	0.5
Absolute Difference*				11	3	10	0.8	10	50	97	0.01
Absolute Relative Percent Difference (RPD)*				1	2	0	1	0	2	1	0
Duplicate Sample Results Evaluation				Good	Good	Good	Good	Good	Good	Good	Good
Y	06-06-086-14W6	07-Jul-22	31224220707124	867	186	2,870	90.2	4,470	2,500	11,209	2.15
N	06-06-086-14W6	07-Jul-22	31224220707125	869	183	2,860	91.5	4,430	2,500	11,184	2.09
Detection Limit (DL)				1	0.5	3.5	5.6	7	3	1	0.1
Reliable Detection Limit (RDL)**				5	2.5	17.5	28	35	15	5	0.5
Absolute Difference*				2	3	10	1.3	40	0	25	0.06
Absolute Relative Percent Difference (RPD)*				0	2	0	1	1	0	0	3
Duplicate Sample Results Evaluation				Good	Good	Good	Good	Good	Good	Good	Good
Y	03-06-086-14W6	07-Jul-22	31224220707126	937	169	2,780	91.5	4,390	2,610	11,267	2.22
N	03-06-086-14W6	07-Jul-22	31224220707127	1,010	175	2,780	93.3	4,340	2,560	11,254	2.18
Detection Limit (DL)				1	0.5	3.5	5.6	7	3	1	0.1
Reliable Detection Limit (RDL)**				5	2.5	17.5	28	35	15	5	0.5
Absolute Difference*				73	6	0	1.8	50	50	13	0.04
Absolute Relative Percent Difference (RPD)*				7	3	0	2	1	2	0	2
Duplicate Sample Results Evaluation				Good	Good	Good	Good	Good	Good	Good	Good
Y	16-10-085-14W6/00	07-Jul-22	31224220707129	783	304	3,520	105	5,080	2,510	12,647	1.87
N	16-10-085-14W6/00	07-Jul-22	31224220707130	787	307	3,550	106	5,070	2,540	12,735	1.94
Detection Limit (DL)				1	0.5	3.5	5.6	7	3	1	0.1
Reliable Detection Limit (RDL)**				5	2.5	17.5	28	35	15	5	0.5
Absolute Difference*				4	3	30	1	10	30	88	0.07
Absolute Relative Percent Difference (RPD)*				1	1	1	1	0	1	1	4
Duplicate Sample Results Evaluation				Good	Good	Good	Good	Good	Good	Good	Good

Continued on next page

Continued from previous page

Table C.3: Water Quality Control Sample Results - Filtered vs Unfiltered Results

Filtered (Y/N)	Sample Point	Sample Date	MSI Sample Number	Ca (mg/L)	Mg (mg/L)	Na (mg/L)	K (mg/L)	Cl (mg/L)	SO_4 (mg/L)	TDS (mg/L)	Li (mg/L)
Y	13-03-085-14W6/00	07-Jul-22	31224220707131	778	304	3,490	104	5,050	2,550	12,586	1.96
N	13-03-085-14W6/00	07-Jul-22	31224220707132	772	294	3,560	101	5,020	2,530	12,640	2.13
			Detection Limit (DL)	1	0.5	3.5	5.6	7	3	1	0.1
			Reliable Detection Limit (RDL)**	5	2.5	17.5	28	35	15	5	0.5
			Absolute Difference*	6	10	70	3	30	20	54	0.17
			Absolute Relative Percent Difference (RPD)*	1	3	2	3	1	1	0	8
			Duplicate Sample Results Evaluation	Good	Good	Good	Good	Good	Good	Good	Good
Y	11-30-084-14W6/00	07-Jul-22	31224220707133	34.3	24.9	3,700	66.6	2,790	16.6	9,324	3.86
N	11-30-084-14W6/00	07-Jul-22	31224220707134	28.5	24.3	3,730	71.5	2,760	6.4	9,297	3.79
			Detection Limit (DL)	1	0.5	3.5	5.6	7	3	1	0.1
			Reliable Detection Limit (RDL)**	5	2.5	17.5	28	35	15	5	0.5
			Absolute Difference*	5.8	0.6	30	4.9	30	10.2	27	0.07
			Absolute Relative Percent Difference (RPD)*	18	2	1	7	1	–	0	2
			Duplicate Sample Results Evaluation	Good	Good	Good	Good	Good	Good	Good	Good
Y	05-33-085-13W6	07-Jul-22	31224220707135	599	110	996	40.7	1,440	1,860	5,161	0.88
N	05-33-085-13W6	07-Jul-22	31224220707136	574	117	962	39.8	1,420	1,850	5,081	0.85
			Detection Limit (DL)	1	0.5	3.5	5.6	7	3	1	0.1
			Reliable Detection Limit (RDL)**	5	2.5	17.5	28	35	15	5	0.5
			Absolute Difference*	25	7	34	0.9	20	10	80	0.03
			Absolute Relative Percent Difference (RPD)*	4	6	3	2	1	1	2	3
			Duplicate Sample Results Evaluation	Good	Good	Good	Good	Good	Good	Good	Good

Notes

–	▪ not applicable
*	▪ non-detectable concentrations are assessed at 95% of the detection limit
**	▪ the reliable detection limit (RDL) or practical detection limit (PDL) is defined as 5 times the DL
Good	▪ evaluation indicates acceptable reproducibility
Poor	▪ evaluation indicates poor reproducibility

Evaluation of Duplicate Analyses:

- reproducibility is unacceptable if RPD is > 30% for inorganic waters and > 40% for soils and organics
- if RPD is not applicable (---), reproducibility is evaluated based on Absolute Difference (unacceptable if > 2 x RDL)
- if Absolute Difference is not applicable (---), reproducibility is evaluated based on the parameter concentration (unacceptable if > 2 x RDL)
- pH is evaluated based on Absolute Difference (unacceptable if > 0.5)

RPD

$$\text{RPD} = \frac{\text{Difference between the two duplicate results}}{\text{Mean of the two duplicate results}} \times 100$$

Table C.3

APPENDIX D

WHOLE ROCK, SEDIMENT AND MINERAL LITHIUM CONCENTRATIONS

Whole Rock, Sediment and Mineral Lithium Concentrations

Table D1 shows the lithium concentrations in rocks, sediments and minerals. The lithium concentrations are provided according to the 25th and 75th percentile of the dataset found in published sources (Dugamin et al., 2023).

Table D.1: Whole Rock, Sediment and Mineral Lithium Concentrations

		Lithium Concentration (ppm)		Reference
		Q_1	Q_3	
Intrusive Series	Peridotite	1	3	Aulbach and Rudnick, 2009
	Xenolith	1	60	Su et al., 2014
	Lherzolite - Harzburgite	2	4	Rudnick and Ionov, 2007
	Gabbro	2	80	Horstman, 1957; Wedepohl, 1984
	Diorite	40		James and Palmer, 2000; Teng et al., 2004
	Syenite	5	30	Horstman, 1957; Estrade et al., 2014; Moreno et al., 2014; Wang et al., 2018
	Peralkaline granite	20	70	Teng et al., 2009; Moreno et al., 2014; Estrade et al., 2014; Estrade et al., 2015
	Granite	20	200	Horstman, 1957; Wedepohl, 1984; Shearer et al., 1987; MacDonald et al., 1992; Bea et al., 1994; Raimbault et al., 1995; Dostal and Chatterjee, 1995; Hecht et al., 1997; Förster et al., 1999; James and Palmer, 2000; Neiva, 2002; Teng et al., 2004; Frindt et al., 2004; Selway et al., 2005; Teng et al., 2006; Stilling et al., 2006; Müller et al., 2006; Haapala et al., 2007; Zaraisky et al., 2009; Teng et al., 2009; Sokolova et al., 2011; Canosa et al., 2012; Estrade et al., 2014; Guo et al., 2015; Romer et al., 2014; Mahdy et al. 2015; Sun et al., 2016; Xie et al., 2016; Chicharro et al., 2016; Simons et al., 2017; Wu et al., 2017; Ballouard et al., 2017; Li et al., 2018; Zhu et al., 2018; Wang et al., 2018; Zhang et al., 2021
	I and S type granite	20	160	Teng et al., 2004
	Peraluminous granites	80	280	Horstman, 1957; MacDonald et al., 1992; Bea et al., 1994; Dostal and Chatterjee, 1995; Raimbault et al., 1995; Förster et al., 1999; Ramirez and Grundvig, 2000; Neiva, 2002; Müller et al., 2006; Sokolova et al., 2011; Canosa et al., 2012; Chicharro et al., 2016; Xie et al., 2016; Wu et al., 2017; Ballouard et al., 2017
	Cornubian batholith granite	110	2,500	Simons et al., 2017
	Pegmatite	30	1,100	Selway et al., 2005; Teng et al., 2006; Stilling et al., 2006; Liu et al., 2010; Canosa et al., 2012; Godfrey et al., 2013; Estrade et al., 2014; Maneta and Baker, 2019
Volcanic Series	Basalt	5	20	Horstman, 1957; Chan et al., 1993; James and Palmer, 2000; Chan et al., 2006; Godfrey et al., 2013
	Andesite	30	60	Horstman, 1957; Wedepohl, 1984
	Rhyolite	20	70	Horstman, 1957; Haapala et al., 2007
	Rhyolitic glass	4	30	Ellis et al., 2022
	Glassy tephra and tephra	15	130	Hofstra et al., 2013; Castor et al., 2020
Metamorphic Series	Tuff	30	600	Horstman, 1957; Hofstra et al., 2013; Benson et al., 2017; Castor et al., 2020
	Greenschist	5	50	Chan et al., 2006; El Korh et al., 2019
	Micaschist	3	60	Wedepohl, 1984; El Korh et al., 2019
	Gneiss	10	20	Gao et al., 1998; Teng et al., 2008; Godfrey et al., 2013
	Blueschist	0.3	100	Marschall et al., 2007; El Korh et al., 2019
	Quartzite	30	60	Liu et al., 2010
	Serpentinite	0.3	4	El Korh et al., 2019
	Amphibolite	1	35	Horstman, 1957; Liu et al., 2010; Godfrey et al., 2013; El Korh et al., 2019
	Eclogite	0.2	10	Marschall et al., 2007; El Korh et al., 2019

Source: Dugamin et al., 2023

Continued on next page

Continued from previous page

Table D.1: Whole Rock, Sediment and Mineral Lithium Concentrations

		Lithium Concentration (ppm)		Reference
		Q$_1$	Q$_3$	
Sediments	Bentonite	20	170	Horstman, 1957; Tardy et al., 1972
	Detrital clay	70	80	Huh et al., 1998
	Halite (Continental environment)	<2		Fontes and Matray, 1993
	Halite (Marine environment)	<0.25		Fontes and Matray, 1993
	Aragonite in evaporite	20		Huh et al., 1998
	Limestone	0.4	8	Hoefs and Sywall, 1997; Chan et al., 1997, Huh et al., 1998; Chan et al., 2006; Weynell et al., 2017
	Loess	15	40	Teng et al., 2004
	Marine clay	30	110	Teng et al., 2004
	Pelagic clay	40	70	Ishikawa and Nakamura, 1993; Bouman et al., 2004; Chan et al., 2006
	Sand	10	40	Horstman, 1957; Wedepohl, 1984; Bouman et al., 2004; Chan et al., 2006
	Shale	50	60	Wedepohl, 1984; James and Palmer, 2000
	Post Archaean Australian Shales	40	90	Teng et al., 2004
	Tainiolite	12,100		Morissette, 2012
Minerals	Albite	10	100	Maneta and Baker, 2019; El Korh et al., 2019
	Anorthite (An 30-50)	5	40	Panienka, 2012
	Anorthite (An 60-90)	5	10	Panienka, 2012
	K-feldspar	5	1,100	Selway et al., 2005; Maneta and Baker 2019; Zhang et al., 2021
Clays	Kaolinite	10	340	Horstman, 1957; Tardy et al., 1972
	Hectorite	3,200	6,000	Tardy et al., 1972; Morissette, 2012; Castor et al., 2020
	Montmorillonite	30	1,200	Horstman, 1957; Tardy et al., 1972
	Illite-Smectite (Caldera)	1,500	6,000	Castor et al., 2020
Phyllo-Silicates	Illite	35	120	Tardy et al., 1972
	Muscovite	480	2,300	Selway et al., 2005; Teng et al., 2006; Maneta and Baker, 2019
	Chlorite	15	40	Wilkinson et al., 2015; El Korh et al., 2019
	Biotite	200	1,200	Zhang et al., 2021
Other Silicates	Olivine	2	4	Rudnick and Ionov, 2007; Aulbach and Rudnick, 2009; Su et al., 2014
	Pyroxene	2	20	Seitz and Woodland, 2000
	Amphibole	1	110	Liu et al., 2010; El Korh et al., 2019
	Serpentine	25	30	Wedepohl, 1984; James and Palmer, 2000
Li-Ore Minerals	Lepidolite	10,000	30,000	Černý et al., 2005; Godfrey et al., 2013; Bradley et al., 2017
	Spodumene	22,330	37,300	Teng et al., 2006; Liu et al., 2010
	Li-Phosphate	34,000	90,000	Bradley et al., 2017

Source: Dugamin et al., 2023

Table D.1

APPENDIX E

DUGAMIN ET AL., 2023 REFERENCES LIST

Dugamin et al., 2023 References List

Dugamin et al., 2023 provided a comprehensive list of references pertaining to all things lithium. Some of the papers have been cited in this study, but not all.

- Dugamin, E. J., Cathelineau, M., Boiron, M. C., Richard, A., Despinois, F. 2023. Lithium enrichment processes in sedimentary formation waters.

References

- Alexeev, S.V., Alexeeva, L.P., Vakhromeev, A.G., 2020. Brines of the Siberian Platform (Russia): geochemistry and processing prospects. Appl. Geochem. 117, 104588.
- Andrew, A.S., Whitford, D.J., Berry, M.D., Barclay, S.A., Giblin, A.M., 2005. Origin of salinity in produced waters from the palm valley gas field, northern territory, Australia. Appl. Geochem. 20 (727), 747.
- Arn´orsson, S., Gunnlaugsson, E., Svavarsson, H., 1983. The chemistry of geothermal waters in Iceland. III. Chemical geothermometry in geothermal investigations. Geochim. Cosmochim. Acta 47, 567–577.
- Bagheri, R., Nadri, A., Raeisi, E., Eggenkamp, H.G.M., Kazemi, G.A., Montaseri, A., 2014a. Hydrochemical and isotopic (δ18O, δ2H, 87Sr/86Sr, δ37Cl and δ81Br). Evidence for the origin of saline formation water in a gas reservoir. Chem. Geol. 384, 62 75.
- Bagheri, R., Nadri, A., Raeisi, E., Kazemi, G.A., Eggenkamp, H.G.M., Montaseri, A., 2014b. Origin of brine in the Kangan gasfield: isotopic and hydrogeochemical approaches. Environ. Earth Sci. 72, 1055–1072.
- Banks, D.A., Yardley, B.W.D., 1992. Crush-leach analysis of fluid inclusions in small natural and synthetic samples. Geochim. Cosmochim. Acta 56, 245–248.
- Barnaby, R.J., Oetting, G.C., Gao, G., 2004. Strontium isotopic signatures of oil-field waters: Applications for reservoir characterisation. Am. Assoc. Pet. Geol. Bull. 88, 1677–1704.
- Bea, F., Pereira, M.D., Corretg´e, L.G., Fershtater, G.B., 1994. Differentiation of strongly peraluminous, perphosphorus granites: the Pedrobernardo pluton, Central Spain. Geochim. Cosmochim. Acta 58, 2609–2627.
- Benson, T.R., Coble, M.A., Rytuba, J.J., Mahood, G.A., 2017. Lithium enrichment in intracontinental rhyolite magmas leads to Li deposits in caldera basins. Nat. Commun. 8, 1–9.
- Bibienne, T., Magnan, J.F., Rupp, A., Laroche, N., 2020. From mine to mind and mobiles: Society's increasing dependence on lithium. Elements 16, 265–270.
- Birkle, P., García, B.M., Padr´on, C.M.M., 2009a. Origin and evolution of formation water at the Jujo-Tecominoac´an oil reservoir, Gulf of Mexico. Part 1: Chemical evolution and water-rock interaction. Appl. Geochem. 24, 543 554.
- Birkle, P., García, B.M., Padr´on, C.M.M., Eglington, B.M., 2009b. Origin and evolution of formation water at the Jujo–Tecominoac´an oil reservoir, Gulf of Mexico. Part 2: Isotopic and field-production evidence for fluid connectivity. Appl. Geochem. 24, 555–573.
- Blondes, M.S., Shelton, J.L., Engle, M.A., Trembly, J.P., Doolan, C.A., Jubb, A.M.,Chenault, J.C., Rowan, E.L., Haefner, R.J., Mailot, B.E., 2020. Utica shale play oil and gas brines: Geochemistry and factors influencing wastewater management. Environ. Sci. Technol. 54, 13917–13925.
- Bodine, M., Jones, B., 1990. Normative analysis of groundwaters from the Rustler Formation associated with the Waste Isolation pilot Plant (WIPP), Southeastern New Mexico. Geochem. Soc. Spec. Publicat. 2, 213–269.
- Boiron, M.C., Cathelineau, M., Richard, A., 2010. Fluid flows and metal deposition near basement/cover unconformity: lessons and analogies from Pb–Zn–F–Ba systems for the understanding of Proterozoic U deposits. Geofluids 10, 270–292.
- Bradley, D.C., Stillings, L.L., Jaskula, B.W., Munk, L., McCauley, A.D., 2017. Lithium, Chapter K. Schulz, K.J., DeYoung, Jr. J.H., Seal II, R.R., Bradley, D.C. (eds.). Critical mineral resources of the United States – Economic and environmental geology and prospects for future supply U.S. Geol. Surv. Prof. Pap. 1802, K1–K21.
- Breiter, K., 2012. Nearly contemporaneous evolution of the A- and S-type fractionated granite in the Kruˇsn´e hory/Erzgebirge Mts., Central Europe. Lithos 151, 105–121.
- Brenner-Tourtelot, E.F., Glanzman, R.K., 1978. Lithium-bearing rocks of the horse spring formation, Clark County, Nevada. Energy 3, 255–262.

- Canosa, F., Martin-Izard, A., Fuertes-Fuente, M., 2012. Evolved granitic systems as a source of rare-element deposits: the Ponte Segade case (Galicia, NW Spain). Lithos 153, 165–176.
- Carpenter, A.B., 1978. Origin and chemical evolution of brines in sedimentary basins. In: SPE annual fall Technical Conference and Exhibition, Houston, Texas, October 1978. Paper SPE-7504-MS.
- Carpenter, A.B., Trout, M.L., Pickett, E.E., 1974. Preliminary report on the origin and chemical evolution of lead-and zinc-rich oil field brines in Central Mississippi. Econ. Geol. 69, 1191–1206.
- Castor, S.B., Henry, C.D., 2020. Lithium-Rich Claystone in the McDermitt Caldera, Nevada, USA: Geologic, Mineralogical, and Geochemical Characteristics and possible Origin. Minerals 10, 68.
- Cathelineau, M., Boiron, M.C., Jakomulski, H., 2021. Triassic evaporites: a vast reservoir of brines mobilised successively during rifting and thrusting in the Pyrenees. J. Geol. Soc. 178 (6) https://doi.org/10.1144/jgs2020-259.
- Chan, L.H., Edmond, J.M., Thompson, G., 1993. A lithium isotope study of hot springs and metabasalts from mid-ocean ridge hydrothermal systems. J. Geophys. Res. Solid Earth 98, 9653–9659.
- Chan, L.H., Kastner, M., 2000. Lithium isotopic compositions of pore fluids and sediments in the Costa Rica subduction zone: implications for fluid processes and sediment contribution to the arc volcanoes. Earth Planet. Sci. Lett. 183, 275–290.
- Chan, L.H., Leeman, W.P., Plank, T., 2006. lithium isotopic composition of marine sediments. Geochem. Geophys. Geosyst. 7.
- Chan, L.H., Sturchio, N.C., Katz, A., 1997. Lithium isotope study of the Yellowstone hydrothermal system. EOS Trans. Am. Geophys. Union 78, F802.
- Cheng, X., Zhang, D., Jolivet, M., Yu, X., Du, W., Liu, R., Guo, Z., 2018. Cenozoic structural inversion from transtension to transpression in Yingxiong Range, western Qaidam Basin: New insights into strike-slip superimposition controlled by Altyn Tagh and Eastern Kunlun Faults. Tectonophysics 723, 229–241.
- Chicharro, E., Boiron, M.C., Lopez-Garcia, J.A., Barfod, D.N., Villaseca, C., 2016. Origin, ore forming fluid evolution and timing of the Logros´an Sn- (W) ore deposits (Central Iberian Zone, Spain). Ore Geol. Rev. 72, 896–913.
- Coffey, D.M., Munk, L.A., Ibarra, D.E., Butler, K.L., Boutt, D.F., Jenckes, J., 2021. Lithium storage and release from lacustrine sediments: implications for lithium enrichment and sustainability in continental brines. Geochem. Geophys. Geosyst. 22.
- Collins, A., 1975. Geochemistry of Oilfield Waters, First ed. Elsevier, Amsterdam. Comision Nacional de Hidrocarburos (Mexico), 2015. Gulf of Mexico-deep water-south sector. Salinas Basin. Petrol. Geol. Synth. CNH-Mexicodoc 47p.
- Craig, H., 1961. Isotopic Variations in Meteoric Waters. Science 133, 1702–1703.
- Craig, H., Gordon, L.I., 1965. Deuterium and Oxygen 18 variations in the ocean and the marine atmosphere. In: Tongiorgi, E. (Ed.), Proceedings of a Conference on Stable Isotopes in Oceanographic Studies and Paleotemperatures, Spoleto, July 26–27. Lab. Geol.Nucl. Sci, Pisa, Italy, pp. 9–130.
- Cuevas, J., de la Villa, R.V., Ramirez, S., Petit, S., Meunier, A., Leguey, S., 2003. Chemistry of Mg smectites in lacustrine sediments from the Vicalvaro sepiolite deposit, Madrid Neogene Basin (Spain). Clay Clay Miner. 51, 457–472.
- Davisson, M.L., Criss, R.E., 1996. Na-Ca-Cl relations in basinal fluids. Geochim. Cosmochim. Acta 60, 2743–2752.
- Demir, I., Seyler, B., 1999. Chemical Composition and Geologic history of Saline Waters in Aux Vases and Cypress Formations, Illinois Basin. Aquat. Geochem. 5, 281–311 cheng.
- Dostal, J., Chatterjee, A.K., 1995. Origin of topaz-bearing and related peraluminous granites of the late Devonian Davis Lake pluton, Nova Scotia, Canada: crystal versus fluid fractionation. Chem. Geol. 123, 67–88.
- Dresel, P.E., Rose, A.W., 2010. Chemistry and origin of oil and gas well brines in Western Pennsylvania: Pennsylvania, Geological Survey. In: 4th Ser. OFOG, 10–01.0 48.
- Dugamin, E.J., 2022. Facteurs controllant les concentrations en m´etaux dans les eaux de formation des bassins s´edimentaires. PhD thesis,. Lorraine University, p. 343p.
- Dugamin, E.J., Richard, A., Cathelineau, M., Boiron, M.C., Despinois, F., Brisset, A., 2021. Groundwater in sedimentary basins as potential lithium resource: a global prospective study. Sci. Rep. 11, 1–10.
- Ellis, B.S., Szymanowski, D., Harris, C., Tollan, P.M.E., Neukampf, J., Guillong, M., Cortes- Calderon, E.A., Bachmann, O., 2022. Evaluating the potential of Rhyolitic Glass as a Lithium Source for Brine Deposits. Econ. Geol. 117, 91–105.
- Engle, M.A., Reyes, F.R., Varonka, M.S., Orem, W.H., Ma, L., Ianno, A.J., Schell, T.M., Xu, P., Carroll, K.C., 2016. Geochemistry of formation waters from the Wolfcamp and “Cline” shales: Insights into brine origin, reservoir connectivity, and fluid flow in the Permian Basin, USA. Chem. Geol. 425, 76–92.

- Ericksen, G.E., Salas, O.R., 1987. Geology and resources of Salars in the Central Andes. In: U.S. Geological Survey Open-File Report, pp. 88–210.
- Evans, R.K., 2014. Lithium. In: Gunn, G. (Ed.), Critical Minerals Handbook. Wiley and Sons, pp. 230–260.
- Fontes, J.C., Matray, J.M., 1993. Geochemistry and Origin of Formation Brines from the Paris Basin, France 1. Brines associated with Triassic salts. Chem. Geol. 109, 149–175.
- Förster, H.J., Tischendorf, G., Trumbull, R.B., 1999. Late-Collisional Granites in the Variscan Erzgebirge, Germany. J. Petrol. 40, 1613–1645.
- Fouillac, C., Michard, G., 1981. Sodium/lithium ratios in water applied to geothermometry of geothermal reservoirs. Geothermics 10, 55–70.
- Fournier, R.O., 1979. A revised equation for the Na/K geothermometer. Trans. Geotherm. Res. Coun. 3, 221–224.
- Franco, M.G., Arnold, Y.J.P., Santamans, C.D., Steinmetz, R.L.L., Tassi, F., Venturi, S., Jofr´e, C.B., Caffe, P.J., C´ordoba, F.E., 2020. Chemical and isotopic features of Li-rich brines from the Salar de Olaroz, Central Andes of NW Argentina. J. S. Am. Earth Sci. 103, 102742.
- Friedman, I., Smith, R.L., 1958. The deuterium content of water in some volcanic glasses. Geochim. Cosmochim. Acta 15, 218–228.
- Frindt, S., Haapala, I., Pakkanen, L., 2004. Anorogenic Gross Spitzkoppe granite stock in central western Namibia: part I. Petrology and geochemistry. Am. Mineral. 89, 841–856.
- Giggenbach, W.F., 1988. Geothermal solute equilibria. Derivation of Na-K-Mg-Ca geoindicators. Geochim. Cosmochim. Acta 52, 2749–2765.
- Hanor, J.S., 1987. Origin and migration of subsurface sedimentary brines. SEPM Short Course 21, 247.
- Hoefs, J., Sywall, M., 1997. Lithium isotope composition of Quaternary and Tertiary biogene carbonates and a global lithium isotope balance. Geochim. Cosmochim. Acta 61, 2679–2690.
- Horstman, E.L., 1957. The distribution of lithium, rubidium and caesium in igneous and sedimentary rocks. Geochim. Cosmochim. Acta 12, 1–28.
- Hoyer, M., Kummer, N.A., Merkel, B., 2015. Sorption of lithium on bentonite, kaolin and zeolite. Geosciences 5, 127–140.
- Hudec, M.R., Jackson, M.P., Peel, F.J., 2013a. Influence of deep Louann structure on the evolution of the northern Gulf of Mexico Salt Influence. Am. Assoc. Pet. Geol. Bull. 97, 1711–1735.
- Hudec, M.R., Norton, I.O., Jackson, M.P., Peel, F.J., 2013b. Jurassic evolution of the Gulf of Mexico salt basin. Am. Assoc. Pet. Geol. Bull. 97, 1683–1710.
- Huh, Y., Chan, L.H., Zhang, L., Edmond, J.M., 1998. Lithium and its isotopes in major world rivers: implications for weathering and the oceanic budget. Geochim. Cosmochim. Acta 62, 2039–2051.
- Hulen, J.B., Kaspereit, D., Norton, D.L., Osborn, W., Pulka, F.S., Bloomquist, R., 2002. Refined conceptual modeling and a new resource estimate for the Salton Sea geothermal field, Imperial Valley, California. Geotherm. Res. Coun. Trans. 26, 22–25.
- Jahani, S., Callot, J.P., Letouzey, J., Frizon de Lamotte, D., 2009. The eastern termination of the Zagros Fold-and-Thrust Belt, Iran: Structures, evolution, and relationships between salt plugs, folding, and faulting. Tectonics 28.
- James, R.H., Allen, D.E., Seyfried Jr., W.E., 2003. An experimental study of alteration of oceanic crust and terrigenous sediments at moderate temperatures (51 to 350°C): Insights as to chemical processes in near-shore ridge-flank hydrothermal systems. Geochim. Cosmochim. Acta 67, 681–691.
- James, R.H., Palmer, M.R., 2000. Marine geochemical cycles of the alkali elements and boron: the role of sediments. Geochim. Cosmochim. Acta 64, 3111–3122.
- Jarrett, A., Edwards, D., Boreham, C., McKirdy, D., 2016. Petroleum geochemistry of the Amadeus Basin. In: Annual Geoscience Exploration Seminar (AGES) Proceedings. Alice Springs. Northern Territory Geological Survey Record 2016-001, pp. 37–42.
- Kharaka, Y.K., Hanor, J.S., 2003. Deep fluids in the continents: I. Sedimentary basins. In: Drever, J.L. (Ed.), Treatise on Geochemistry, 5, pp. 1–48.
- Kharaka, Y.K., Mariner, R.H., 1989. Chemical geothermometers and their application to formation waters from sedimentary basins. In: Naeser, N.D., McCulloh, T.H. (Eds.), Thermal History of Sedimentary Basins. Springer, New York, NY.
- Kharaka, Y.K., Maest, A.S., Carothers, W.W., Law, L.M., Lamothe, P.J., Fries, T.L., 1987. Geochemistry of metal-rich brines from Central Mississippi Salt Dome Basin, USA. Appl. Geochem. 2 (543), 561.
- Kloppmann, W., N´egrel, P., Casanova, J., Klinge, H., Schelkes, K., Guerrot, C., 2001. Halite dissolution derived brines in the vicinity of a Permian Salt Dome (N German Basin). Evidence from boron, strontium, oxygen, and hydrogen isotopes. Geochim. Cosmochim. Acta 65, 4087–4101.

- Knauth, L.P., Beeunas, M.A., 1986. Isotope geochemistry of fluid inclusions in Permian halite with implications for the isotopic history of ocean water and the origin of saline formation waters. Geochim. Cosmochim. Acta 50, 419–433.
- Kumar, A., Fukuda, H., Hatton, T.A., Lienhard, J.H., 2019. Lithium recovery from oil and gas Produced water: a need for a growing energy industry. Energy Lett. 4 (6), 1471–1474.
- Labbe, J.F., Daw, G., 2012. Panorama 2011 du March´e du Lithium. BRGM RP-61340-FR. Land, L.S., 1995. Na-Ca-Cl saline formation waters, Frio Formation (Oligocene), South Texas, USA: products of diagenesis. Geochim. Cosmochim. Acta 59, 2163–2174.
- Land, L.S., Kupecz, J.A., Mack, L.E., 1988. Louann salt geochemistry (Gulf of Mexico sedimentary basin, USA): a preliminary synthesis. Chem. Geol. 74, 25–35.
- Land, L.S., Macpherson, G.L., 1992. Origin of saline formation waters, Cenozoic section, Gulf of Mexico sedimentary basin. Am. Assoc. Pet. Geol. Bull. 76, 1344–1362.
- Land, L.S., Prezbindowski, D.R., 1981. The origin and evolution of saline formation water, lower cretaceous carbonates, south-Central Texas, USA. J. Hydrol. 54, 51–74.
- Lippmann, M., Truesdell, A., Frye, G., 1999. The Cerro Prieto and Salton Sea geothermal fields—Are they really alike. In: Proceedings of the 24th Workshop on Geothermal Reservoir Engineering. Stanford University, Stanford, California, pp. 25–27.
- Liu, X.M., Rudnick, R.L., Hier-Majumder, S., Sirbescu, M.L.C., 2010. Processes controlling lithium isotopic distribution in contact aureoles: a case study of the Florence County pegmatites, Wisconsin. Geochem. Geophys. Geosyst. 11–18.
- Liu, X., Wen, Z., Wang, Z., Song, C., He, Z., 2018. Structural characteristics and main controlling factors on petroleum accumulation in Zagros Basin, Middle East. J. Nat. Gas Geosci. 3, 273–281.
- L´opez Steinmetz, R.L., Salvi, S., 2021. Brine grades in Andean salars: when basin size matters a review of the lithium triangle. Earth Sc. Rev. 217, 103615.
- L´opez Steinmetz, R.L., Salvi, S., Garcia, G., Arnold, Y.P., Beziat, D., Franco, G., Constantini, G., Cordoba, F.E., Caffe, P.J., 2018. Northern Puna Plateau-scale survey of Li brine-type deposits in the Andes of NW Argentina. J. Geochem. Explor. 190, 26–38.
- L´opez Steinmetz, R.L., Salvi, S., Sarchi, C., Santamans, C., L´opez Steinmetz, L.C., 2020. Lithium and brine geochemistry in the salars of the Southern Puna, Andean Plateau of Argentina. Econ. Geol. 115, 1079–1096.
- Lowenstein, T.K., Hardie, L.A., Timofeeff, M.N., Demicco, R.V., 2003. Secular variation in seawater chemistry and the origin of calcium chloride basinal brines. Geology. 31, 857–860.
- Lüders, V., Plessen, B., Romer, R.L., Weise, S.M., Banks, D.A., Hoth, P., Dulski, P., Schettler, G., 2010. Chemistry and isotopic composition of Rotliegend and Upper Carboniferous formation waters from the north German Basin. Chem. Geol. 276 (198), 208.
- Ma, Z., Han, F., Chen, T., Yi, L., Lu, X., Chen, F., Liu, X., Yuan, W., 2021. The forming age and the evolution process of the brine lithium deposits in the qaidam basin based on geochronology and mineral composition. Front. Earth Sci. 9, 702223.
- Maneta, V., Baker, D.R., 2019. The potential of lithium in alkali feldspars, quartz, and muscovite as a geochemical indicator in the exploration for lithium-rich granitic pegmatites: a case study from the spodumene-rich Moblan pegmatite, Quebec, Canada. J. Geochem. Explor. 205, 106336.
- McCaffrey, M.A., Lazar, B.H.D.H., Holland, H.D., 1987. The evaporation path of seawater and the coprecipitation of Br (super-) and K (super+) with halite. J. Sediment. Res. 57, 928–937.
- Mempes, M., Cremasco, D., Hansberry, R., 2020. Geology and evolution of the Dukas structure, Amadeus Basin, Northern Territory. In: Annual Geoscience Exploration Seminar (AGES) Proceedings, 90. Alice Springs, Northern Territory.
- Mohr, S., Mudd, G., Giurco, D., 2010. Lithium Resources and Production: A Critical Global Assessment. Institute for Sustainable Futures (University of Technology, Sydney) and Department of Civil Engineering (Monash University).
- Moldovanyi, E.P., Walter, L.M., 1992. Regional trends in water chemistry, Smackover Formation, Southwest Arkansas: geochemical and physical controls. Am. Assoc. Pet. Geol. Bull. 76, 864–894.
- Monnier, L., Salvi, S., Melleton, J., Lach, P., Pochon, A., Bailly, L., Beziat, D., De Parseval, P., 2022. Mica trace-element signatures: Highlighting superimposed W-Sn mineralisations and fluid sources. Chem. Geol. 600, 120866.
- Moreno, J.A., Molina, J.F., Montero, P., Anbar, M.A., Scarrow, J.H., Cambeses, A., Bea, F., 2014. Unraveling sources of A-type magmas in juvenile continental crust: Constraints from compositionally diverse Ediacaran post-collisional granitoids in the Katerina Ring complex, southern Sinai, Egypt. Lithos 192, 56–85.
- Morton, R.A., Land, L.S., 1987. Regional variations in formation water chemistry, Frio formation (Oligocene), Texas Gulf Coast. Am. Assoc. Pet. Geol. Bull. 71, 191–206.
- Mount, V.S., 2014. Structural style of the Appalachian Plateau fold belt, north-Central Pennsylvania. J. Struct. Geol. 69, 284–303.

- Müller, A., Seltmann, R., Halls, C., Siebel, W., Dulski, P., Jeffries, T., Spratt, J., Kronz, A., 2006. The magmatic evolution of the Land's End pluton, Cornwall, and associated pre- enrichment of metals. Ore Geol. Rev. 28, 329–367.
- Munk, L.A., Hynek, S., Bradley, D.C., Boutt, D., Labay, K.A., Jochens, H., 2016. Lithium brines: a global perspective. Econ. Geol. 18, 339–365.
- Nate, S., Bilan, Y., Kurylo, M., Lyashenko, O., Napieralski, P., Kharlamova, G., 2021. Mineral Policy within the Framework of Limited critical Resources and a Green Energy transition. Energies 14, 2688.
- Qishun, F., Ma, H., Lai, Z., Tan, H., Li, T., 2010. Origin and evolution of oilfield brines from Tertiary strata in Western Qaidam Basin: constraints from 87Sr/86Sr, δD, δ18O, δ34S and water chemistry. Chin. J. Geochem. 29 (446), 54.
- Raimbault, L., Cuney, M., Azencott, C., Duthou, J.L., Joron, J.L., 1995. Geochemical evidence for a multistage magmatic genesis of Ta-Sn-Li mineralisation in the granite at Beauvoir, French Massif Central. Econ. Geol. 90, 548–576.
- Rine, M.J., 2015. Depositional Facies and Sequence Stratigraphy of Niagaran-Lower salina Reef Complex Reservoirs of the Guelph Formation, Michigan Basin. Master Theses. Western Michigan Unversity.
- Risacher, F., Alonso, H., Salazar, C., 1999. Geoquımica de aguas en cuencas cerradas, I, II, III Regiones, Chile. Ministerio de Obras Publicas, Direccion General de Aguas.
- Risacher, F., Fritz, B., 1991. Quaternary geochemical evolution of the salars of Uyuni and Coipasa, Central Altiplano, Bolivia. Chem. Geol. 90 (211), 31.
- Rogers, J.D., Boutwell, G., Watkins, C., Karadeniz, D., 2006. Chapter Three: Geology of the New Orleans Region. Independent Levee, Investigation Team, New Orleans Levee Systems, Hurricane Katrina.
- Sanders, L.L., 1991. Geochemistry of Formation Waters from the lower Silurian Clinton Formation (Albion Sandstone), Eastern Ohio. American Assoc. Petrol. Geol. Bull. 75, 1593–1608.
- Sanjuan, B., Gourcerol, B., Millot, R., Rettenmaier, D., Jeandel, E., Rombaut, A., 2022. Lithium-rich geothermal brines in Europe: an up-date about geochemical characteristics and implications for potential Li resources. Geothermics 101, 102385.
- Sanjuan, B., Millot, R., Dezayes, C., Brach, M., 2010. Main characteristics of the deep geothermal brine (5km) at Soultz-sous-Forˆets (France) determined using geochemical and tracer test data. Compt. Rendus Geosci. 342, 546–559.
- Scholz, F., Hensen, C., De Lange, G.J., Haeckel, M., Liebetrau, V., Meixner, A., Reitz, A., Romer, R.L., 2010. Lithium isotope geochemistry of marine pore waters–insights from cold seep fluids. Geochim. Cosmochim. Acta 74, 3459–3475.
- Seyfried Jr., W.E., Janecky, D.R., Mottl, M.J., 1984. Alteration of the oceanic crust: implications for geochemical cycles of lithium and boron. Geochim. Cosmochim. Acta 48, 557–569.
- Skeen, J.C., 2010. Basin Analysis and Aqueous Chemistry of Fluids in the Oriskany Sandstone, Appalachian Basin, USA. Graduate Theses, Dissertations, and Problem Reports, 2978.
- Smith, L.B., 2013. Shallow transgressive onlap model for Ordovician and Devonian organic- rich shales, New York State. In: SPE/AAPG/SEG Unconventional Resources Technology Conference. OnePetro.
- Sokolova, E.N., Smirnov, S.Z., Astrelina, E.I., Annikova, I.Y., 2011. Ongonite - elvan magmas of the Kalguty ore-magmatic system (Gorny Altai): composition, fluid regime, and genesis. Russ. Geol. Geophys. 52, 1378–1400.
- Starkey, H.C., 1982. The role of clays in fixing lithium. In: US Government Printing Office, 1278.
- Starkey, H.C., Mountjoy, W., 1973. Identification of a lithium-bearing smectite from Spor Mountain, Utah. J. Res. U. S. Geol. Surv. 1, 415–419.
- Stueber, A.M., Walter, L.M., 1991. Origin and chemical evolution of formation waters from Silurian-Devonian strata in the Illinois Basin, USA. Geochim. Cosmochim. Acta 55 (309), 325.
- Stueber, A.M., Walter, L.M., Huston, T.J., Pushkar, P., 1993. Formation waters from Mississippian-Pennsylvanian reservoirs, Illinois Basin, USA: Chemical and isotopic constraints on evolution and migration. Geochim. Cosmochim. Acta 57 (763), 84.
- Tan, H., Rao, W., Ma, H., Chen, J., Li, T., 2011. Hydrogen, oxygen, helium and strontium isotopic constraints on the formation of oilfield waters in the Western Qaidam Basin, China. J. Asian Earth Sc. 40, 651–660.
- Tardy, Y., Krempp, G., Trauth, N., 1972. Le lithium dans les min´eraux argileux des s´ediments et des sols. Geochim. Cosmochim. Acta 36, 397–412.
- Teng, F.Z., McDonough, W.F., Rudnick, R.L., Walker, R.J., Sirbescu, M.L.C., 2006. Lithium isotopic systematics of granites and pegmatites from the Black Hills, South Dakota. Am. Mineral. 91, 1488–1498.

- Thompson, J.M., Fournier, R.O., 1988. Chemistry and geothermometry of brine produced from the Salton Sea scientific drill hole, Imperial Valley, California. J. Geophys. Res. Solid Earth 93, 13165–13173.

- Torres-Ruiz, J., L´opez-Galindo, A., Gonz´alez-L´opez, J.M., Delgado, A., 1994. Geochemistry of Spanish sepiolite-palygorskite deposits: genetic considerations based on trace elements and isotopes. Chem. Geol. 112, 221–245.

- U.S. Geological Survey, 2021. Mineral Commodity Summaries. U.S. Geological Survey.

- Ulmishek, G.F., 2001. Petroleum Geology and Resources of the Nepa-Botuoba High, Angara- Lena Terrace, and Cis-Patom Foredeep, Southeastern Siberian Craton. US Department of the Interior, US Geological Survey, Russia.

- Verma, S.P., Santoyo, E., 1997. New improved equations for NaK, NaLi and SiO2 geothermometers by outlier detection and rejection. J. Volcanol. Geotherm. Res. 79, 9–23.

- Vigier, N., Decarreau, A., Millot, R., Carignan, J., Petit, S., France-Lanord, C., 2008. Quantifying Li isotope fractionation during smectite formation and implications for the Li cycle. Geochim. Cosmochim. Acta 72, 780–792.

- White, D.E., 1965. Saline waters of sedimentary rocks. In: Yound, A., Galley, G.E. (Eds.), Fluids in Subsurface Environments, 4. Am. Ass. Petrol. Geol. Mem, pp. 342–366.

- Williams, L.B., Hervig, R.L., 2005. Lithium and boron isotopes in illite-smectite: the importance of crystal size. Geochim. Cosmochim. Acta 69, 5705–5716.

- Williams, A.E., McKibben, M.A., 1989. A brine interface in the Salton Sea geothermal system, California: fluid geochemical and isotopic characteristics. Geochim. Cosmochim. Acta 53, 1905–1920.

- Wilson, T.P., Long, D.T., 1993a. Geochemistry and isotope chemistry of Ca-Na-CI brines in Silurian strata, Michigan Basin, USA. Appl. Geochem. 8, 507–524.

- Wilson, T.P., Long, D.T., 1993b. Geochemistry and isotope chemistry of Michigan Basin brines: Devonian formations. Appl. Geochem. 8, 81–100.

- Wu, M., Samson, I.M., Zhang, D., 2017. Textural and chemical constraints on the formation of disseminated granite-hosted W-Ta-Nb mineralisation at the Dajishan Deposit, Nanling Range, Southeastern China. Econ. Geol. 112, 855–887.

- Yaksic, A., Tilton, J.E., 2009. Using the cumulative availability curve to assess the threat of mineral depletion: the case of lithium. Res. Policy 34, 185–194.

- Zhang, P.X., 1987. The Salt Lakes of the Qaidam Basin. Science Press, Beijing.

- Zhang, L., Chan, L.H., Gieskes, J.M., 1998. Lithium isotope geochemistry of pore waters from Ocean Drilling Program Sites 918 and 919, Irminger Basin. Geochim. Cosmochim. Acta 62, 2437–2450.

- Zhang, R., Ghosh, R., Sen, M.K., Srinivasan, S., 2013. Time-lapse surface seismic inversion with thin bed resolution for monitoring CO2 sequestration: a case study from Cranfield, Mississippi. Int. J. Greenhouse Gas Control 18, 430–438.

APPENDIX F

MODERN SEAWATER AND EVAPORITE MINERALS ION CONCENTRATIONS

Modern Seawater and Evaporite Minerals Ion Concentrations

The concentrations of ions in seawater can vary drastically across the globe depending on where the water is sampled. Modern seawater concentrations used in this study are provided for various ions along with the seawater evaporation curve ion concentrations from Carpenter, 1978.

Table F.1: Modern Seawater and Evaporite Minerals Ion Concentrations

Ion	Sodium (mg/L)	Potassium (mg/L)	Calcium (mg/L)	Magnesium (mg/L)	Strontium (mg/L)	Chloride (mg/L)	Bromide (mg/L)	Bicarbonate (mg/L)	Sulphate (mg/L)	Lithium (mg/L)
Modern Seawater	10,500	380	400	1260	13	19,000	65	140	2,650	0.2
Seawater Evaporation Minerals										
Calcite ($CaCO_3$)						46,000	300			
Gypsum ($CaSO_4 \cdot 2H_2O$)	59,700	2,220	1,040	7,590		107,800	396		13,300	
Halite (NaCl)	94,300	5,600	307	19,600		183,300	1,010		27,700	
Epsomite ($MgSO_4 \cdot 7H_2O$)	55,200	15,800		50,500		187,900	2,670		76,200	
Sylvite (KCl)	48,200	17,700		56,100		190,500	2,970		82,200	
Carnalite ($KMgCl \cdot 6H_2O$)	22,100	25,900		72,900		224,000	4,770		56,100	
Bischofite ($MgCl_2 \cdot 6H_2O$)	8,960	18,800		92,600		254,000	6,060		54,200	

© Canadian Discovery Ltd.

Table F.1

References

- Carpenter, A. B., 1978. Origin and Chemical Evolution of Brines in Sedimentary Basins, Oklahoma Geological Survey Circular 79, 1978, p. 60 - 77.

Appendix G

MAPS, SHAPEFILES AND LIST OF FIGURES

All formation maps and shapefiles are provided digitally.

The following maps are provided:

- Study Area Sample Distribution and Transportation Infrastructure
- NEBC Lithium Study Summary
- Western Canada Lithium Concentration
- Western Canada Brine-Hosted Lithium Crown Majority Rights
- Alberta Lithium Concentrations by Geological Age
- Lithium Sample Distribution

Shapefiles provided for formations (if applicable):

- Total Dissolved Solids
- Potassium Concentration
- Net Reservoir
- Estimate Lithium Concentration
- Expected Lithium Concentration

The following maps are provided for each formation chapter:

- Total Dissolved Solids
- Potassium Concentration
- Net Reservoir
- Lithium Summary

The following maps are provided for the Montney Formation:

- Mg- and Ca-Enriched Areas
- Tmax
- Present Day Temperature
- Geothermal Gradient
- Estimated Lithium Concentration
- Expected Lithium Concentration
- Water Production First Year Monthly Average Rate

List of Figures

Chapter 1 Executive Summary

Chapter 2 Lithium Overview

Chapter 3 Study Overview

Chapter 4 Alberta and Saskatchewan Overview

Chapter 5 Montney

Chapter 6 Triassic Aquifers

Chapter 7 Other Formations